

**METABOLOMICS FOR CHARACTERIZATION OF
DIETARY ADHERENCE IN PHENYLKETONURIA
PATIENTS AND ELECTRONIC CIGARETTE SMOKE
EXPOSURE IN PLACENTAL CELLS**

**METABOLOMICS FOR CHARACTERIZATION OF
DIETARY ADHERENCE IN PHENYLKETONURIA
PATIENTS AND ELECTRONIC CIGARETTE SMOKE
EXPOSURE IN PLACENTAL CELLS**

By JENNIFER L. WILD, B. Arts Sc.

A Thesis Submitted to the School of Graduate Studies in Partial Fulfilment of
the Requirements for the Degree Master of Science

McMaster University © Copyright by Jennifer Wild, September 2017

MASTER OF SCIENCE (2017)

McMaster University

(Chemical Biology)

Hamilton, Ontario

TITLE: Metabolomics for Characterization of Dietary Adherence in Phenylketonuria Patients and Electronic Cigarette Smoke Exposure in Placental Cells

AUTHOR: Jennifer L. Wild, B. Arts Sc. (McMaster University)

SUPERVISOR: Dr. Philip Britz-McKibbin

PAGES: xx, 201

Abstract

Metabolomics is the systematic analysis of low-molecular weight compounds (metabolites) within biological systems that represent molecular endpoints of gene expression and environmental exposures. A major goal of metabolomics is achieving better understanding of the pathophysiology of complex disease processes while elucidating mechanisms of action of nutrients, toxins, and/or drugs. Multisegment injection-capillary electrophoresis-mass spectrometry (MSI-CE-MS) is a high-throughput microseparation platform that is ideal for the analysis of polar/ionic metabolites from volume-restricted biological samples. This thesis includes two major metabolomics projects using MSI-CE-MS that are aimed at contributing new advances in public health and chronic disease prevention. *Chapter II* presents an analysis of the metabolome from patients with phenylketonuria (PKU) — a genetic disease affecting phenylalanine (Phe) metabolism that requires lifelong dietary restriction to prevent irreversible intellectual disabilities. A targeted and nontargeted metabolomics approach using matching urine and plasma samples was conducted to confirm known markers of PKU and identify new markers associated with dietary adherence and disease progression. Along with increased excretion of Phe catabolites in urine, high plasma Phe was associated with decreased excretion of acylcarnitines and greater excretion of histidine catabolites, suggesting impaired fatty acid oxidation and micronutrient deficiencies, respectively. Overall, this may provide a strategy to

objectively monitor dietary adherence beyond standard dietary records or patient recall. *Chapter III* investigates the impact of electronic cigarette smoke exposure on the placental metabolome as a model cell line of fetal development. Evidence of altered amino acid metabolism, in addition to changes in acylcarnitines and metabolites associated with cellular proliferation, were observed in more susceptible first trimester placental cells and were attributed to flavouring agents irrespective of nicotine dosage. This work supports the hypothesis that flavoured e-cigarette formulations pose a significant health risk in comparison to unflavoured formulations and supports the need for further risk assessment and careful regulation of these products to prevent deleterious birth outcomes in pregnant mothers.

Acknowledgements

To begin, I would like to thank my supervisor, Dr. Philip Britz-McKibbin, for his support and guidance throughout my studies. I truly appreciate the optimism and enthusiasm in times of struggle and for allowing me to maintain my independence throughout this research. I would also like to thank my committee members Dr. Jim McNulty and Dr. Murray Potter for their invaluable feedback, questions, and encouragement, which allowed me to re-evaluate my work and perspective on numerous occasions. This work would not have been possible without my collaborators- Dr. Alison Holloway and her students. The excitement expressed during our discussions was truly refreshing and gave me the motivation I needed to push through. Thank you to Tammy Feher for being incredibly helpful with any questions I've had along the way and to the entire Department of Chemistry and Chemical Biology for their support.

I would like to express my gratitude towards my lab members who offered advice, sympathy, and friendship, truly making my experience in the lab a positive one: Alicia DiBattista, Meera Shanmuganathan, Karen Lam, Adriana Nori de Macedo, Nadine Wellington, Mai Yamamoto, Michelle Saoi, Ritchie Ly, Stellena Mathiapparanam, Sandi Azab, and Biban Gill. In particular, I'd like to thank Alicia for being a wonderful mentor from day one, for helping me with statistics and endless technical issues I had with the TOF, for letting me vent, and for being a great friend.

I can say with certainty that I would not have been able to get to where I am today without the love and support from my family, friends, and boyfriend. I am so incredibly grateful for my parents, Mary and Rich Wild, for their loving support throughout my university career and for encouraging me to always strive to be the best I could be. To my older sister, Erin Wild—thank you for being the best role model I could ever ask for and for inspiring me to always keep learning. To my ‘frens’ Alison Stewart, Lucia Lee, Sheilan Sinjari, and Christal Zhou—thank you for being incredible friends and making this past year so memorable. Finally, I would like to thank Jiwon Lee for being the best support system I could ever ask for, for being a shoulder to cry on, and for constantly reminding me to stay positive and keep moving forward. I love you all very much and am incredibly thankful to have each and every one of you in my life.

Table of Contents

Abstract.....	iii
Acknowledgements.....	v
Table of Contents.....	vii
List of Figures.....	x
List of Tables.....	xiii
List of Abbreviations and Symbols.....	xiv
Declaration of Academic Achievement.....	xx
CHAPTER I. INTRODUCTION	1
1.1 Metabolomics.....	2
1.1.1 Applications of Metabolomics.....	3
1.1.2 Analytical Techniques for Metabolomics: NMR and MS.....	9
1.1.3 Analytical Techniques for Metabolomics: Separation Methods.....	15
1.2 Capillary Electrophoresis-Mass Spectrometry.....	19
1.2.1 Electrokinetic Separation in CE.....	19
1.2.1.1 Electroosmotic Flow.....	21
1.2.1.2 Electrophoretic Mobility.....	24
1.2.2 Applications of CE-MS in Metabolomics.....	25
1.3 Metabolomics Workflow: From Data to Information.....	30
1.4 Thesis Overview and Objectives.....	36
1.5 References.....	40
CHAPTER II. METABOLOMIC STUDIES OF PHENYLKETONURIA PATIENTS FOR ASSESSMENT OF DIETARY ADHERENCE	49
2.1 Abstract.....	50
2.2 Introduction.....	51
2.2.1 Inborn Errors of Metabolism.....	51
2.2.2 Phenylketonuria.....	53
2.2.2.1 Pathogenesis and Clinical Symptoms of PKU.....	57
2.2.3 Current Treatment Options for PKU.....	59
2.2.3.1 Lifelong Dietary Management for Classic PKU.....	60
2.2.4 Metabolomic Studies of PKU.....	63
2.3 Experimental.....	65
2.3.1 Chemicals and Reagents.....	65
2.3.2 Instrumentation.....	66
2.3.3 Study Cohort Selection and Ethics Approval.....	67
2.3.4 Sample Collection and Preparation.....	68
2.3.5 Data Processing.....	69
2.3.6 Calibration and Method Validation.....	70
2.3.7 Statistical Data Analysis.....	71
2.4 Results and Discussion.....	72
2.4.1 Study Design and Cohort Characteristics for PKU Patients.....	72

2.4.2 Method Validation and Intermethod Comparison	73
2.4.3 Targeted Metabolite Profiling: Primary Markers of PKU	80
2.4.4 Nontargeted Metabolite Profiling: Beyond Altered Phe Catabolism .	87
2.4.4.1 Plasma Metabolome Analysis.....	87
2.4.4.2 Urine Metabolome Analysis	93
2.4.5 Evaluation of Metabolome Variation in Children with PKU	101
2.5 Conclusion	103
2.6 References.....	106
2.7 Supplementary Tables and Figures.....	114
CHAPTER III. EVALUATING THE IMPACT OF ELECTRONIC CIGARETTE SMOKE EXPOSURE ON THE PLACENTAL METABOLOME	116
3.1 Abstract.....	117
3.2 Introduction.....	118
3.2.1 Cigarette and Tobacco Usage	118
3.2.2 Electronic Cigarettes (‘E-Cigarettes’)..	120
3.2.3 E-Cigarette Liquid Formulations and Product Regulations.....	122
3.2.4 Biological Effects of E-Cigarettes	126
3.2.5 E-Cigarette Use in Canada.....	128
3.2.6 Role of the Placenta in Pregnancy	130
3.2.7 Smoking and Nicotine Exposure During Pregnancy	132
3.3 Materials and Methods.....	135
3.3.1 Chemicals and Reagents	135
3.3.2 Instrumentation: CE-MS and GC/MS.....	136
3.3.3 Culture and Preparation of Exposed Placental Cell Extracts.....	138
3.3.4 Metabolite Extraction and Sample Preparation	140
3.3.5 Data Processing.....	141
3.3.6 External Calibration Curve and Nicotine Quantification.....	142
3.3.7 Statistical Data Analysis	143
3.4 Results and Discussion	144
3.4.1 Nicotine Dosage and Alkaloid Impurities in E-Cigarette Liquids....	144
3.4.2 Characterization of Volatile Organics in E-Cigarette Liquids.....	148
3.4.3 Preparation and Validation of E-Cigarette Vapour Media	152
3.4.4 Placental Cell Exposure to E-Cigarette Vapour.....	153
3.4.4.1 First Trimester Placental Cell Exposure to Unflavoured E-Cigarette Vapour.....	162
3.4.3.2 First Trimester Placental Cell Exposure to Flavoured E-Cigarette Vapour.....	166
3.5 Conclusion	172
3.6 References.....	174
3.7 Supplementary Tables and Figures.....	184

CHAPTER IV. CONCLUSION AND FUTURE DIRECTIONS.....	187
4.1 Overview of Major Thesis Contributions	188
4.2 Evaluating the Impact of Nutrition on the PKU Metabolome	192
4.3 Targeted Evaluation of Vaporized Flavour Chemicals in E-Cigarettes ..	196
4.4 Overall Perspective	199
4.5 References.....	200

List of Figures

Figure 1.1	Schematic of a reflectron TOF-MS	14
Figure 1.2	Setup of a CE-ESI-MS system showing separation in the CE capillary and the coaxial sheath liquid interface coupling CE to ESI prior to sampling into the MS for detection	18
Figure 1.3	Separation of cationic, neutral, and anionic components in a sample by capillary electrophoresis	21
Figure 1.4	The relationship between the EOF and pH	23
Figure 1.5	Comparison of the parabolic/laminar flow profile for a pressure-driven system such as LC and the flat ‘plug’ EOF flow profile that is generated for solute transport in CE	23
Figure 1.6	Format for multisegment injection (MSI) of seven samples within a single capillary for CE-MS	27
Figure 1.7	Components of an accelerated data workflow for nontargeted metabolomic studies using MSI-CE-MS	31
Figure 2.1	The PAH-catalyzed reaction converting Phe to Tyr	53
Figure 2.2	Crystal structure of tetrameric human PAH	54
Figure 2.3	Overlay of CE current traces for 40 runs over 8 days by MSI-CE-MS for metabolomic analyses of plasma and urine samples with full-scan data acquisition in (A) positive and (B) negative ion mode	75
Figure 2.4	A control chart depicting relative peak area (RPA) of recovery standard 4-fluorophenylalanine (F-Phe)	75
Figure 2.5	Representative extracted ion electropherogram for (A) Phe and (B) Tyr, with the pooled QC sample in position 5 of 7 within the MSI injection sequence	76
Figure 2.6	2D scores plot from principal component analysis (PCA) of (A) 55 cationic and anionic metabolites detected in plasma filtrate and (B) 76 cationic and anionic metabolites detected in urine samples when using MSI-CE-MS	77
Figure 2.7	Bland-Altman % difference plot (A) and Passing-Bablok regression analysis (B) comparing Phe and Tyr concentrations as determined by MSI-CE-MS relative to UPLC-UV	79
Figure 2.8	Frequency distribution of plasma Phe concentrations (μM) measured by MSI-CE-MS for all samples and initial plasma samples upon	

	consent	81
Figure 2.9	Metabolism of Phe in humans	84
Figure 2.10	Extracted ion electropherograms for <i>N</i> -phenylacetylglutamine, <i>p</i> -cresol sulfate, phenylsulfate, phenyllactate, phenylpyruvate, and <i>o</i> -hydroxyphenylacetate for a representative pooled QC sample using MSI with a serial dilution trend filter	85
Figure 2.11	Box-and-whisker plots showing median fold-change and <i>p</i> -values for urinary Phe, <i>N</i> -phenylacetylglutamine, <i>o</i> -hydroxyphenylacetate, and phenylpyruvate when grouped by plasma Phe concentrations of 360 μ M as a cut-off to signify likely dietary compliance of PKU patients to ensure optimal therapeutic outcomes	86
Figure 2.12	Separation between PKU patients with low/moderate plasma Phe, high plasma Phe, and patients on an uncontrolled diet not taking specialized amino acid formula as depicted in a 2D scores plot when using PLS-DA	89
Figure 2.13	Box plots for plasma metabolites determined to be significantly different when grouped by plasma Phe concentrations	91
Figure 2.14	Separation between PKU patients with low/moderate and high Phe excretion in urine and PKU patients not taking a specialized amino acid formula who were not following a Phe-restricted diet as depicted in a 2D scores plot when using PLS-DA	95
Figure 2.15	Group separation between PKU patients consuming a specialized amino acid formula and following a Phe-restricted diet with low/moderate and high Phe excretion in urine shown in a 2D scores plot by PLS-DA	97
Figure 2.16	Box plots showing differences in urinary excretion of two histidine catabolites, imidazoleacetic acid and imidazolelactic acid, when group by low, moderate, or high urinary Phe	98
Figure 2.17	Histidine metabolism in mammals	99
Figure 2.18	Box plots showing differential urinary excretion of carnitine (C0) and acylcarnitines (C2 and C5) based on urinary Phe, grouped by low/moderate or high excretion, with PKU patients not consuming a specialized amino acid formula or following a restricted diet as a control	101
Figure 2.19	Plasma Phe concentrations throughout sample collection for three infants recently diagnosed with classic PKU under 2 y	102

Figure S2.1	Extracted ion electropherogram and ESI+ mass spectrum for imidazoleacetic acid and imidazolelactic acid in urine	114
Figure 3.1	Third-generation e-cigarette	122
Figure 3.2	The prevalence of Canadians who have used e-cigarettes has increased significantly since 2013, with usage being highest among youth (ages 15-19) and young adults (ages 20-24)	129
Figure 3.3	Extracted ion electropherogram of nicotine (163.1230:0.472) for a representative MSI-CE-MS run of e-cigarette liquids containing 0 and 12 mg/mL nicotine	146
Figure 3.4	Total ion chromatograms when using HS-GC/MS comparing the chemical profile of (A) Blacklisted and (B) Blue Balls e-cigarette liquid formulations with 0 mg/mL nicotine	151
Figure 3.5	An overlay of CE current traces from 42 runs performed over 8 days of analysis in positive and negative ion mode	156
Figure 3.6	Control chart depicting relative peak area (RPA) of recovery standard 4-fluorophenylalanine (F-Phe) over 50 HTR-8/SVneo cells, 15 BeWo cells, and 13 pooled QCs in positive ion mode	156
Figure 3.7	2D scores plot from principal component analysis (PCA) of 49 cationic and anionic metabolites detected in first trimester HTR-8/SVneo cells showing (A) uncorrected data and (B) PQN-corrected data in comparison to the adequate technical variation within the QC samples analyzed within each run	159
Figure 3.8	Hierarchical cluster analysis (HCA) 2D heatmap of PQN-corrected, autoscaled, and <i>log</i> -transformed metabolomic data showing the overall data structure for HTR-8/SVneo cells treated with 1% and 10% <i>v/v</i> e-cigarette vapour conditioned media and control maintenance media	160
Figure 3.9	PLS-DA 2D scores plot for HTR-8/SVneo cells exposed to (A) 10% <i>v/v</i> and (B) 1% <i>v/v</i> e-cigarette vape-conditioned media	161
Figure 3.10	Box plots showing the effect of treatment with 1% and 10% <i>v/v</i> BL12 vape-conditioned media in comparison to control cells	165
Figure 3.11	Box plots showing the effects of flavoured e-cigarette vapour at 1% and 10% <i>v/v</i> on GABA, Ile, Pro, and iso-C5 in comparison to control cells	168
Figure S3.1	Extracted ion electropherogram for nicotine calibration standards with concentrations ranging from 0.5 to 200 μ M in dH ₂ O	184

List of Tables

Table 1.1	Major strengths and limitations of CE-MS in metabolomics	28
Table 2.1	Most common disease-causing mutations associated with classic PKU	55
Table 2.2	Incidence of PKU by country	56
Table 2.3	Summary of cohort of 23 classic PKU patients grouped by age (adults <i>vs.</i> children) in this cross-sectional study with matching plasma and urine specimens collected	73
Table 2.4	Spearman’s rank correlation results between excreted urinary Phe and its association with its major catabolites <i>N</i> -phenylacetyl glutamine, phenylsulfate, phenyllactate, phenylpyruvate, and <i>o</i> -hydroxyphenylacetate	85
Table 2.5	Summary of PKU patients within each class examined for nontargeted plasma metabolome analysis	89
Table 2.6	Significant metabolites when comparing PKU patients with low, moderate, and high plasma Phe concentrations as determined by Kruskal-Wallis H tests	90
Table 2.7	Summary of classic PKU patients examined for nontargeted urinary metabolome studies with low/moderate urinary Phe excretion, high urinary Phe excretion, and PKU patients not taking an amino acid supplement with a poor/uncontrolled diet	94
Table 2.8	Significant metabolites when comparing PQN-normalized urine with low/moderate and high Phe excretion as determined by Mann-Whitney U tests	97
Table S2.1	Clinical characteristics of PKU patients	115
Table 3.1	E-liquid manufacturing and ingredient standards set by the Electronic Cigarette Trade Association (ECTA) of Canada	125
Table 3.2	Nicotine degradation products and minor tobacco alkaloids detected in e-liquid formulations with 12 mg/mL nicotine by MSI-CE-MS in positive ion mode	147
Table 3.3	List of compounds detected by MSI-CE-MS in Blacklisted and Blue Balls e-cigarette liquids	149
Table 3.4	List of compounds detected by HS-GC/MS in Blacklisted and Blue Balls e-cigarette liquids with nicotine concentrations of 0 and 12	

	mg/mL	150
Table 3.5	Nicotine content in original growth media (undiluted stock), as well as 10% and 1% v/v vape-conditioned media prepared for treatment of first and third trimester placental cells	153
Table 3.6	Significant metabolites altered in first trimester placental cells when comparing unexposed control cells, 1% v/v BL12 vape-conditioned media, and 10% v/v BL12 conditioned media as determined by Kruskal-Wallis H tests in order to evaluate the effect of nicotine on placental cells	164
Table 3.7	Significant metabolites when comparing cells treated with control maintenance media and 10% v/v BB0 vape-conditioned media as determined by Mann-Whitney U tests in order to compare the effects of flavouring agents in nicotine-free e-cigarette vapours	168
Table S3.1	Summary of 49 metabolites consistently detected in first trimester HTR-8/SVneo cells, including <i>m/z</i> , RMT, ionization mode (p = ESI+, n = ESI-), molecular formula, and compound ID	185

List of Abbreviations and Symbols

α spin state	Low energy spin state
β spin state	High energy (excited) spin state
ε	Dielectric constant
η	Viscosity
R_H	Hydrodynamic radius
t_m	Analyte migration time
μ_{app}	Apparent mobility
μ_{eo}	Mobility of the electroosmotic flow
μ_{ep}	Electrophoretic mobility
v_{eo}	Velocity of the electroosmotic flow
v_{ep}	Electrophoretic velocity
v_{app}	Apparent migration velocity
ζ	Zeta potential
(MH) ⁺	Protonated molecule
¹ H NMR	Proton NMR
ACC	Acetyl-CoA carboxylase
ACMGG	American College of Medical Genetics and Genomics
ADMET	Absorption, distribution, metabolism, excretion, and toxicology
ANOVA	Analysis of variance
Arg	<i>L</i> -Arginine
BB0	Blue Balls e-cigarette liquid, 0 mg/ml nicotine concentration
BB12	Blue Balls e-cigarette liquid, 12 mg/ml nicotine concentration
BeWo	<i>Homo sapiens</i> third trimester choriocarcinoma trophoblast cells
BGE	Background electrolyte
BH ₄	Tetrahydrobiopterin
BL0	Blacklisted e-cigarette liquid, 0 mg/ml nicotine concentration
BL12	Blacklisted e-cigarette liquid, 12 mg/ml nicotine concentration
BMI	Body mass index
C0	<i>L</i> -Carnitine
C2	Acetyl- <i>L</i> -carnitine
C3	Propionyl- <i>L</i> -carnitine
C5	Valeryl- <i>L</i> -carnitine
C6	Hexenoyl- <i>L</i> -carnitine
C8	Octanoyl- <i>L</i> -carnitine
C18	Octadecanoyl- <i>L</i> -carnitine
CE	Capillary Electrophoresis

CE-ESI-MS	Capillary Electrophoresis-Electrospray Ionization-Mass Spectrometry
CE-ESI-TOF-MS	Capillary Electrophoresis-Electrospray Ionization-Time-of-Flight-Mass Spectrometry
CE-MS	Capillary Electrophoresis-Mass Spectrometry
CF	Cystic fibrosis
CID	Collisional induced dissociation
Cl-Tyr	3-Chlorotyrosine
CNS	Central nervous system
CTAB	Cetrimonium bromide
CTRL	Control
CV	Coefficient of variance
CVD	Cardiovascular disease
DBS	Dried blood spots
dH ₂ O	Deionized water
DEHP	Bis(2-ethylhexyl)phthalate
<i>E</i>	Electric field
E-cigarette	Electronic cigarette
E-liquid	Electronic cigarette liquid
ECTA	Electronic Cigarette Trade Association
EDR	Extended dynamic range
EI	Electron Ionization
ENDS	Electronic nicotine delivery system
ENNDS	Electronic non-nicotine delivery system
EOF	Electroosmotic flow
ESI	Electrospray Ionization
ESI-MS	Electrospray Ionization-Mass Spectrometry
F-Phe	4-Flourophénylalanine
FDA	Food and Drug Administration
FDR	False discovery rate
FEMA	Flavor and Extracts Manufacturing Association
FIA-MS/MS	Flow Injection Analysis-Tandem Mass Spectrometry
FID	Flame Ionization Detection
FWHM	Full width at half maximum
GABA	γ -Aminobutyric acid
GC	Gas Chromatography
GC/MS	Gas Chromatography-Mass Spectrometry
GH	Growth hormone
Gln	<i>L</i> -Glutamine

GMP	Glycomacropeptide
GRAS	Generally recognized as safe
HCA	Hierarchical cluster analysis
HCMV	Human cytomegalovirus
HDL	High-density lipoprotein
HEPES	(4-(2-hydroxyethyl)-1-piperazineethanesulfonic acid)
HILIC	Hydrophilic Interaction Chromatography
HiREB	Hamilton Integrated Research Ethics Board
HMDB	Human Metabolome Database
HPA	Hyperphenylalaninemia
HPHC	Harmful and potentially harmful constituents
HPLC	High Performance Liquid Chromatography
HS-GC/MS	Headspace-Gas Chromatography-Mass Spectrometry
HTR-8/Svneo	<i>Homo sapiens</i> first trimester trophoblast cells
IEM	Inborn error of metabolism
IGF-1	Insulin-like growth factor 1
IL	Interleukin
Ile	<i>L</i> -Isoleucine
IS	Internal standard
Iso-C5	Isovaleryl- <i>L</i> -carnitine
IUGR	Intrauterine growth restriction
KE	Kinetic energy
<i>L</i>	Length
LAT-1	Large amino acid transporter 1
LC	Liquid Chromatography
LC-MS	Liquid Chromatography-Mass Spectrometry
LC-MS/MS	Liquid Chromatography-Tandem Mass Spectrometry
Leu	<i>L</i> -Leucine
LNAA	Large neutral amino acid
LOD	Limit of detection
LOQ	Limit of quantification
<i>m/z</i>	Mass-to-charge
MCP-1	Monocyte chemotactic protein 1
MEHP	Mono(2-ethylhexyl)phthalic acid
Met	<i>L</i> -Methionine
MFE	Molecular Feature Extractor
MFG	Molecular Formula Generator
MS	Mass Spectrometry
MS/MS	Tandem Mass Spectrometry

MSI-CE-MS	Multisegment Injection-Capillary Electrophoresis-Mass Spectrometry
MWCO	Molecular weight cut-off
NACE-MS	Non-Aqueous-Capillary Electrophoresis-Mass Spectrometry
nAChR	Nicotinic acetylcholine receptor
NaOH	Sodium hydroxide
NBS	Newborn screening
NH ₄ HCO ₃	Ammonium bicarbonate
NIST	National Institute of Standards and Technology
NMR	Nuclear Magnetic Resonance
NMS	Sodium-2-naphthalene sulfonate
NNN	<i>N</i> -nitrosonornicotine
NPKUA	National PKU Alliance
NRT	Nicotine replacement therapy
PAH	Phenylalanine hydroxylase
PAL	Phenylalanine ammonia-lyase
PC	Principal component
PCA	Principal component analysis
PEG	Polyethylene glycol
Phe	<i>L</i> -Phenylalanine
PKU	Phenylketonuria
PLS-DA	Partial least squares discriminant analysis
PON	Paraoxonase
ppm	Parts per million
PQN	Probabilistic quotient normalization
Pro	<i>L</i> -Proline
PSA	Prostate specific antigen
qPCR	Real-time polymerase chain reaction
QA	Quality assurance
QC	Quality control
QTOF	Quadrupole Time-of-Flight
R ²	Coefficient of determination
RF	Radio frequency
ROC	Receiver operating characteristic
RPA	Relative peak area
RPLC	Reversed-Phase-Liquid Chromatography
RPMI	Roswell Park Memorial Institute
RS	Recovery standard
SD	Standard deviation

SDS	Sodium dodecyl sulfate
Ser	<i>L</i> -Serine
TCA	Tricarboxylic acid
TMAO	Trimethylamine- <i>N</i> -oxide
TOF	Time-of-Flight
TOF-MS	Time-of-Flight-Mass Spectrometry
Trp	<i>L</i> -Tryptophan
Tyr	<i>L</i> -Tyrosine
UHPLC	Ultra-High-Performance-Liquid Chromatography
UPLC	Ultra-Performance-Liquid Chromatography
UV	Ultraviolet
Val	<i>L</i> -Valine
VEGF	Vascular endothelial growth factor
VIP	Variable importance in projection
VLCAD	Very-long-chain acyl-CoA dehydrogenase deficiency

Declaration of Academic Achievement

Dr. Philip Britz-McKibbin provided much guidance throughout both projects and thoroughly edited all chapters in this thesis.

Chapter II: The ethics application was completed with assistance by Dr. Murray Potter. Mika Hayashi assisted with data processing. I was responsible for study recruitment, sample preparation, analysis with MSI-CE-MS, data processing, and statistical analysis.

Chapter III: This study was completed in collaboration with Dr. Alison Holloway (Department of Obstetrics & Gynecology, McMaster University). Sarah Kleiboer and Sergio Ráez Villanueva prepared the e-cigarette vapour media and exposed BeWo and HTR-8/SVneo placental cells. The GC/MS headspace work for e-cigarette liquids was performed and analyzed by Leah Allen and Dr. Fan Fei from McMaster Regional Centre for Mass Spectrometry (MRCMS). I performed metabolite extraction, sample preparation, targeted/nontargeted metabolomics using MSI-CE-MS, data processing, and statistical analysis.

CHAPTER I.

INTRODUCTION

1.1 Metabolomics

The metabolome refers to the comprehensive set of low-molecular weight (<1500 Da) compounds (*i.e.*, metabolites) within an organism.¹ Metabolites are intermediates and by-products of metabolic reactions necessary for cellular metabolism, including maintenance, growth, and normal function of the cell.² The metabolome consists of primary and secondary metabolites, with the former being essential for cell function (*e.g.*, amino acids and fatty acids). Secondary metabolites are end-products of primary metabolites that are unessential for growth but serve important functions, such as communication or defence.^{2,3} The human metabolome includes endogenous metabolites formed as by-products of cellular metabolism as well as exogenous metabolites that are derived from environmental exposures, such as diet, drugs, and pollutants.⁴ The metabolome is considered to best reflect the molecular phenotype of an organism since metabolites represent "real-world" molecular endpoints of gene expression closely associated with phenotype.⁵ Metabolomics is, therefore, critical in deciphering the role of genes or enzymes of unknown function,⁶ as well as understanding the pathophysiology of complex human diseases.⁵ Metabolomics involves nontargeted metabolite profiling and strives to identify and quantify all metabolites that can be detected and identified in a complex biological specimen (*e.g.*, urine, plasma, cell extract, etc.).⁷ In contrast, metabolic profiling is a targeted approach that involves the analysis of a specific set of metabolites (*i.e.*,

compound class or members of a metabolic pathway), whereas metabolic fingerprinting involves the comparison of patterns of metabolites that change in response to a perturbation, such as disease, that does not require their identification. The integration of genomics, transcriptomics, proteomics, and metabolomics allows for a more holistic understanding of the complex interactions between genes and the environment.⁸ Importantly, changes in metabolite concentrations due to a perturbation (*e.g.*, smoke exposure, genetic mutation, and habitual diet) are often more readily measured in comparison to changes in gene expression, protein concentrations, or enzyme activity.⁹

1.1.1 Applications of Metabolomics

The metabolic phenotype or metabotype of an organism is a reflection of the interactions between genetic, epigenetic, and other confounding factors, such as sex, age, ethnicity, and diet.⁹ For this reason, the study of metabolomics has had a major impact in the fields of genetics, medicine, nutrition, and toxicology.⁵ Metabolites can be measured by temporal and spatial perturbations in the steady-state concentration or flux of metabolites when using stable-isotope labeled tracers.⁹ Urine and blood (*i.e.*, serum or plasma) are the most common biological fluids used in metabolomics as their collection is minimally invasive and they are frequently used in clinical medicine for diagnosis, prognosis, and treatment monitoring. In particular, urine analysis is advantageous as it provides insights into the complex interactions of host metabolism, microflora activity, environment, and lifestyle. For instance, drug screening often relies on urine

specimens to confirm therapeutic drug compliance and to detect potential misuse of illicit drugs of abuse (*e.g.*, synthetic opioids) given the unreliability of patient self-reporting.¹⁰

In addition, metabolomics can assist in applications such as improved disease diagnostics or dietary interventions optimal for individual patients.⁷ Disease processes alter metabolic pathways and, ultimately, specific metabolites that can serve as biochemical markers (*i.e.*, biomarkers) for early detection of treatable human diseases even prior to overt clinical symptoms.^{9,11} For example, metabolite profiling using tandem mass spectrometry (MS/MS) has revolutionized clinical medicine via multiplexed screening of a panel of biomarkers associated with dozens of inborn errors of metabolism (IEM).¹² An IEM is a rare disease that is characterized by a genetic mutation resulting in partial or complete loss of enzyme activity, leading to disruption of important metabolic pathways.¹² Metabolic dysfunction in IEM leads to a deleterious accumulation of substrate, formation of toxic intermediates, and/or deficiency of key downstream products of enzyme action. In this case, biomarkers for IEM are associated with accumulation/deficiency of metabolites in urine or blood, which are significantly elevated/decreased relative to healthy/nonaffected individuals.¹² Recently, a new class of biomarker has been discovered for early detection of galactosemia, an IEM in which galactose metabolism is severely impaired in affected infants, resulting in learning disabilities, cataracts, and neurological impairments if left untreated.¹³ In this case, significant elevations in *N*-galactated amino acids in

neonates with galactosemia offers a more robust biomarker for neonatal screening from dried blood spots (DBS) using multiplexed MS/MS technology as compared to conventional fluorescence-based enzyme assays, which are prone to false positives.

Drug discovery and safety is another growing field of interest in metabolomics, which can elucidate drug targets (*i.e.*, enzymes) and their underlying mechanisms of action, including potential non-specific or off-target activity that contribute to cytotoxicity.^{14,15} Metabolomic methods to identify genes or enzymes affected by a disease (*i.e.*, pathway analysis or metabolic flux analysis) are valuable for the identification of novel drug targets.¹⁶ Additionally, many inhibitors of enzyme activity are structurally related to the enzyme's natural substrate and/or co-factors. For example, nontargeted metabolomic analysis of human fibroblasts infected with human cytomegalovirus (HCMV) with liquid chromatography-mass spectrometry (LC-MS) showed elevations in citric acid cycle intermediates and acetylated amino acids.¹⁷ Analysis of metabolic flux using isotopic labeling implicated acetyl-CoA carboxylase (ACC) as a novel target for the treatment of HCMV by impairment of viral replication.¹⁶ Conventional methods used for chemical library testing rely on robotics or computational high-throughput screening technology to identify drug candidates, which is supplemented with absorption, distribution, metabolism, excretion, and toxicology (ADMET) analysis for prediction of favorable drug-like properties.¹⁸ Metabolomics streamlines this process as it can be used for the detection of

possible toxic by-products of drug metabolism and can be combined with *in vitro* cell-based approaches (e.g., cell culture assays).

Recently, “precision medicine” has been introduced as a strategy to improve disease treatment by taking into account individual genetic, metabolic, environmental, and lifestyle variability.¹⁹ Metabolic signatures of disease risk (*i.e.*, predictive biomarkers) for individual patients will allow for better understanding of the origins of health and disease, including biomarkers for assessing variation in drug response and risk assessment of disease recurrence (*i.e.*, cancer).²⁰ Furthermore, metabolomics can aid in determining an optimal balance between drug efficacy and toxicity. For example, treatment for schizophrenia targets dopamine, serotonin, and glutamate neurotransmitter systems, however there is a large variation in individual response to treatment and side effects, which is poorly understood.²¹ Metabolomics has been applied to better understand pathways that are altered by antipsychotic drugs in individuals with schizophrenia. One study examined the effects of atypical antipsychotics (e.g., olanzapine, risperidone, aripiprazole) on phospholipids and fatty acid concentrations, noting the possibility of liver lipases as possible side targets of these drugs.²² Also, methotrexate is an anti-folate drug used for the treatment of rheumatoid arthritis and many cancers.²³ Methotrexate inhibits dihydrofolate reductase, which leads to attenuation in the *de novo* synthesis of purine nucleotides.²⁴ However, due to the high toxicity of methotrexate therapy with significant variability in individual responses, there is a need to evaluate treatment

efficacy through continuous monitoring.²³ A ¹H NMR method identified 11 serum metabolites, including uric acid, uracil, hypoxanthine, and trimethylamine-*N*-oxide (TMAO), which vary significantly with methotrexate response in individuals with early rheumatoid arthritis; these metabolites may serve as promising biomarkers to evaluate the efficacy of methotrexate treatment in patients.

The field of nutritional metabolomics is a powerful way for evaluating the impact of habitual dietary patterns on an individual's health status.²⁵ Habitual diet is typically measured through dietary records,²⁶⁻²⁸ where individuals quantitatively and qualitatively record everything they eat and drink over a defined time period.²⁹ Other, less accurate, measures of dietary intake include dietary recalls, in which an interviewer prompts the participant to recall all food consumed within a period of time, and food frequency questionnaires, in which the participant responds to standardized questions regarding their food intake. However, there are major issues in clinical studies evaluating dietary intake based on food frequency questionnaires, diet records, or recalls since they are unreliable and subject to selective reporting bias, especially in the case of obese and elderly individuals who tend to underestimate caloric intake.³⁰⁻³³ For example, in studies examining the relationship between diet and obesity, there is a high incidence of underreporting foods high in calories, fats, and carbohydrates.^{30,33} In this context, biomarkers of specific food intake (*i.e.*, cruciferous vegetables, citrus fruits, red meat) can provide a reliable indicator of an individual's habitual dietary patterns,

while avoiding self-reporting bias issues when relying on diet records.³⁰ Thus, the use of biomarkers allows a more objective and accurate measurement of dietary intake as it takes into account nutrient bioavailability and individual metabolism.³¹ Furthermore, while diet is one of the major modifiable lifestyle factors contributing to the alarming increase in prevalence of obesity, diabetes, and cardiovascular disease (CVD) worldwide,³⁰ the relationship between diet, metabolic health, and chronic disease risk is not well understood.³⁴ In the case of metabolic diseases with strict nutrition requirements to avoid deleterious health outcomes, the combination of nutritional metabolomics and standardized dietary records would be an asset for physicians/dieticians in making appropriate diet/treatment interventions for patients based on the individual's metabotype.^{35,36}

Exposomics describes the response of organisms and biological systems to the totality of environmental exposures over a lifetime.^{37,38} Specific environmental exposures, such as chemical pollutants, tobacco smoke, and environmental toxins, have independent yet often synergistic effects on an individual's chronic disease risk. In the case of tobacco smoke, metabolomics analysis of urine allows the differentiation of smokers and non-smokers based on differences in endogenous metabolites in addition to the presence of tobacco-specific metabolites, such as nicotine, cotinine, and *trans*-hydroxycotinine.³⁹ For example, a number of intermediate metabolites in the glutathione pathway are lower in the urine of smokers in comparison to non-smokers, which is consistent with previous studies on cigarette smoke exposure leading to oxidative stress

response and glutathione depletion. Indeed, the long-term impact of deleterious environmental exposures at early stages of life is often unknown when evaluating risk assessment; therefore, there is growing interest to explore the cumulative effect of multiple exposures on health outcomes, including pre-natal exposures during fetal development.³⁸⁻⁴⁰

1.1.2 Analytical Techniques for Metabolomics: NMR and MS

Metabolomic analysis is challenging due to the wide chemical diversity of metabolites in terms of differences in their physiochemical properties (*i.e.*, molecular weight, polarity, hydrophobicity, solubility, volatility, and stability) and their wide dynamic range spanning over six order of magnitude (pM to mM).^{41,42} As a result, metabolomics relies on complementary hyphenated instrumental methods in order to expand coverage of the human metabolome.⁴³ The validation of these methods is of utmost importance to ensure adequate precision, accuracy, and robustness for routine analysis without interferences or matrix effects.⁴² However, there is no single analytical platform that can resolve, detect, and identify all metabolites that may exist in real-world biological samples – the vast majority of which comprise unknown compounds that lack chemical standards or reference spectral databases.⁵

Nuclear magnetic resonance (NMR) and, increasingly, high-resolution mass spectrometry (MS) are major instrumental platforms used in discovery-based metabolomics research. ¹H NMR is widely used in metabolomics since the vast majority of known metabolites contain hydrogen (abundance > 99.98%) and

analysis is rapid due to the short relaxation time of the ^1H nucleus.^{42,44} Routine analysis with one dimensional ^1H NMR spectra enables simultaneous detection of all hydrogen-containing low-molecular weight metabolites above a concentration of $10\ \mu\text{M}$.⁴⁵ Typical ^1H NMR spectra of biological fluids are very complex due to the presence of hundreds of endogenous and exogenous metabolites, which result in many overlapping resonance peaks. The majority of studies using NMR as a profiling technique use pattern recognition techniques (*i.e.*, PCA) together with spectral binning to classify samples as normal or abnormal. While NMR cannot detect below micromolar concentrations, it is advantageous as it is non-invasive, non-destructive, rapid, and requires minimal sample preparation without chromatographic separation.^{5,44} Further, the peak area corresponding to a compound in the NMR spectrum is directly related to the concentration of the nuclei of study, which allows for direct quantification in complex matrices.⁴⁶ NMR also allows the analysis of liquid biological samples, intact tissues, or tissues *in vivo*. For these reasons, NMR is often used for high-throughput metabolic fingerprinting and profiling while also offering a more robust platform than MS for large-scale studies over years in duration.⁴⁵ The major drawbacks of NMR, however, include poor sensitivity that limits metabolome coverage, large sample requirements, and high infrastructure costs.⁵ While data processing was a limitation of NMR-based metabolomics in the past, Bayesil software developed by the Wishart research group enables rapid ($< 5\ \text{min}$) processing of NMR spectra with spectral fitting to biofluid-specific libraries.⁴⁷ Further, full characterization is

not possible using ^1H NMR for some metabolites (*i.e.*, proton deficient functional groups), such as with ether sulfate conjugates of hydroxyl groups present in drug metabolites, phosphates, or *N*-oxides.^{48,49}

MS is increasingly applied in metabolomic studies since it offers greater sensitivity and selectivity, notably when coupled to high efficiency separation techniques.⁷ In addition, it provides useful qualitative structural information and excellent quantitative performance, especially when using stable-isotope internal standards to correct for potential matrix effects.^{42,50} In MS, metabolites are ionized in the source of the mass spectrometer, separated as gas-phase ions by a mass analyzer according to their mass-to-charge (m/z) ratio, and detected by a transducer that measures electrical charge reflecting ion abundance.⁴² After detection, signals are generated for ions and displayed as a mass spectrum showing their relative abundance (*i.e.*, ion counts) as a function of their m/z .⁵⁰ The most common ionization methods used in MS-based metabolomics are electron ionization (EI) and electrospray ionization (ESI). EI is a hard ionization technique typically used for the analysis of volatile compounds in the gas-phase when using GC/MS; however, new interface designs have been developed in LC-MS to allow for direct EI.⁵¹ Ionization with EI occurs when a neutral molecule of a metabolite collides with a high-energy electron beam (70 eV), creating a parent ion and multiple fragment ions. As the process occurs in the gas-phase, it is inert to matrix interferences unlike atmospheric pressure ionization methods widely used in LC-MS. As a “hard” ionization technique, extensive fragmentation of the molecular

ion occurs, which provides a molecular fingerprint for unknown compound identification by comparing with mass spectral libraries (*e.g.*, NIST).⁵² In contrast, ESI is a “soft” ionization technique in which samples are introduced into the MS as a fine spray of charged droplets following direct infusion of liquid or liquid-based effluent after separation.⁵⁰ A drying gas evaporates the solvent, increasing the charge density of the droplets. Charged ions are then accelerated towards the inlet of the mass analyzer under an applied voltage, where they are focused electrokinetically via ion optics prior to mass analysis. ESI is the preferred ionization technique for polar/ionic compounds and is routinely used following LC and CE separations.^{39,53} However, ionization efficiency in ESI is highly dependent on the physicochemical properties of a metabolite, which can vary over three orders of magnitude.⁵⁴ Moreover, ESI is prone to ion suppression and enhancement effects that are matrix dependent, especially if sample workup and/or separation conditions are not optimized prior to ionization.⁵⁵

Mass resolution and accuracy in MS are dependent on the type of mass analyzer used and are important for the confident determination of a likely molecular formula for an unknown ion based on its m/z and isotope pattern. Mass resolution is the ability to distinguish separation between two equal intensity peaks of different m/z and is defined by $\frac{m}{\Delta m}$, where m is the mass and Δm is the peak width, which is typically measured by an ion’s signal at full width at half maximum (FWHM).⁵⁶ Mass accuracy is the ratio of the error in the m/z measurement to the true m/z and is assessed in parts per million (ppm). Time-of-

flight (TOF) mass analyzers are often used in metabolomics as they are ideal to couple with high efficiency separation techniques due to their fast scanning data acquisition, high mass resolution and accuracy, unlimited mass range, and good robustness.^{7,57} A mass reflectron in TOF-MS utilizes an ion mirror to compensate for differences in kinetic energies (KE) of ions leaving the source to enhance mass resolution (**Figure 1.1**).⁵⁸ Ions are generated in the source and accelerated under an electric field, where they are subsequently allowed to travel within a "field-free" drift tube under vacuum. Following mass calibration, the TOF-MS measures the ion's characteristic drift time and ion abundance, which is converted into a signal within a mass spectrum (*i.e.*, m/z versus ion count).⁵⁷ The KE of an ion is dependent on its charge and the electric field strength ($KE = zeV$, where $z =$ charge, and $eV =$ electric field strength). Ions are separated within the drift tube according to their m/z (**A**) with flight time being dependent on m/z and total distance travelled within the flight tube:⁵⁸

$$t_d = d \cdot \frac{\sqrt{m/z}}{\sqrt{2e \cdot V}} \quad (1)$$

where, t_d is the ion's flight time, d is the distance from the ion source to the detector, e is the charge on an electron, and V is the accelerating potential. Thus, the m/z of an ion is directly proportional to its flight time, where lighter ions with the same charge state (*i.e.*, small m/z) travel the fastest and reach the detector first prior to larger and more bulky ions.

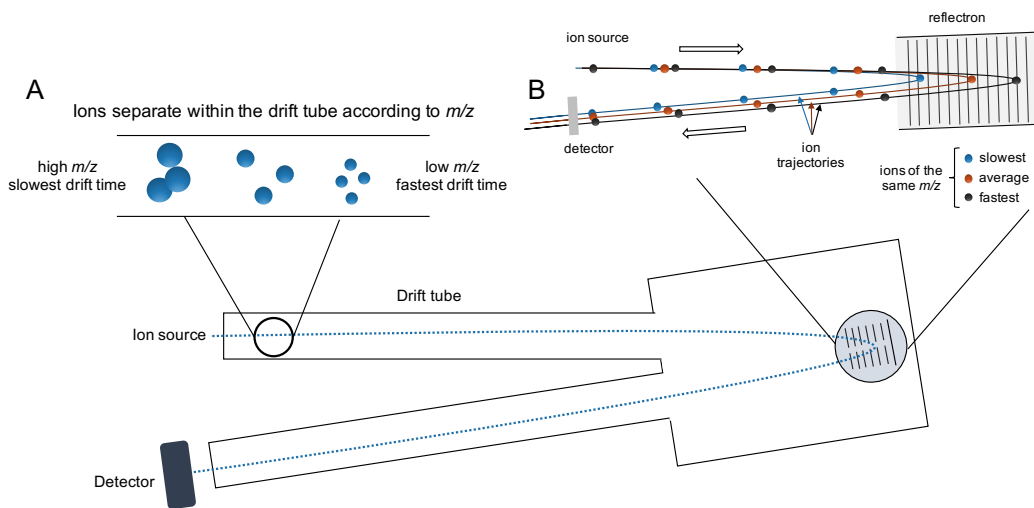


Figure 1.1. Schematic of reflectron TOF-MS. Ions separate within the drift tube according to their m/z (A). The reflectron compensates for variations in ion flight with ions of the same m/z , allowing them to reach the detector at the same time (B). Figure adapted from (58).

Tandem MS (MS/MS) requires the coupling of multiple mass analyzers in series, which allows for multiple steps of mass selection for improved selectivity and structural elucidation. For instance, a quadrupole time-of-flight (QTOF)-MS system incorporates a low resolution quadrupole mass analyzer (Q1) as a primary mass filter to select a precursor ion prior to collisional-induced dissociation (CID) within a collisional/reaction cell (Q2) filled with an inert neutral gas, such as Ar.^{59,60} High-resolution product ion scanning (*i.e.*, fragmentation spectra) is then acquired by a TOF, which serves as the third mass analyzer (Q3).⁵⁰ Unknown compound identification often requires CID experiments at an optimal collisional energy (*e.g.*, 10, 20, 40 V) when using MS/MS to generate characteristic product ion spectrum with residual precursor ion still detected. Recent advances in fragmentation algorithms now allows for *in-silico* prediction of MS/MS spectra

for rapid identification of unknown compounds, which is important when commercial standards do not exist or when reference libraries are incomplete.⁶¹

1.1.3 Analytical Techniques for Metabolomics: Separation Methods

Coupling MS with an electrophoretic or chromatographic separation method enhances the performance of metabolomic analysis of complex biological samples as it reduces matrix effects and ion suppression, allows for isomeric resolution, and provides additional qualitative information for unknown identification, such as retention or migration time.⁶² Gas chromatography-mass spectrometry (GC/MS) is the method of choice for the analysis of volatile, non-polar, and thermally stable metabolites.⁴² A vast majority of metabolites analyzed by GC/MS (*i.e.*, polar metabolites), however, require chemical derivatization to improve their volatility and retention properties. Pre-column chemical derivatization can complicate chromatographic separation and quantification due to the formation of multiple or incomplete derivatization products. For instance, several metabolite classes containing more than one functional group will form multiple products following derivatization with reactive silylating agents, which complicates data analysis.^{42,63} GC/MS based metabolomics typically uses EI as the ionization method, which allows metabolite identification based on matching with extensive EI-MS spectral libraries and/or *de novo* structural elucidation of fragmentation spectra.⁴²

LC-MS often avoids chemical derivatization and it is better suited for resolving a wider range of non-volatile polar and nonpolar compounds with less

complicated sample workup as compared to GC/MS. Separation selectivity by LC-MS is dependent on the stationary phase used as the analytical column; reversed-phase LC-MS (RPLC-MS) using C₈ or C₁₈ as stationary phases is widely used for the resolution of complex mixtures of non-polar metabolites, such as lipids.⁶⁴ RPLC-MS suffers from poor retention of highly polar/ionic metabolites as they are not retained by the stationary phase and elute with the solvent front.^{42,65} In this case, separation for polar/ionic compounds can be realized by ion pair-RPLC⁶⁶ or alternatively by hydrophilic interaction chromatography (HILIC) using polar stationary phases with weak ion-exchange properties (*e.g.*, silica) together with acetonitrile-rich elution solvents.^{42,65} The coupling of LC with MS allows for improved selectivity, sensitivity, and reproducibility by reducing matrix effects and isobaric interferences that also complements unknown identification by MS/MS.⁶⁷

Capillary electrophoresis-mass spectrometry (CE-MS) is a complementary microseparation platform to GC/MS and LC-MS in metabolomics since a large fraction of metabolites found in biological samples, such as urine, are hydrophilic/ionic metabolites, including amino acids, organic acids, nucleotides, and nucleosides, in addition to secondary metabolites as their intact glucuronide or sulfate conjugates.^{63,68,69} CE separations are based on differences in the electrophoretic mobility (μ_{ep}) of an ion (*i.e.*, charge density) in free solution under an electric field. Hyphenation of CE to MS typically uses a coaxial sheath liquid interface, where solvent is delivered to the end of the capillary as a terminal

electrolyte reservoir at a rate of 5 to 10 $\mu\text{L}/\text{min}$ to form a stable spray under an applied voltage (3-5 kV). This makes up for the low flow rate at the capillary outlet in CE (10-100 nL/min), which is not sufficient for microspray formation alone.⁷⁰ Additionally, this interface provides a closed electrical contact with the BGE and electrode for stable spray formation in ESI (**Figure 1.2**).^{54,70,71} The nebulizer gas flow outside of the Taylor cone also assists in the formation and desolvation of charged droplets in the electrospray process. A major advantage of the coaxial sheath liquid interface is that it allows for independent optimization from separation conditions, while also providing a homogenous solvent composition for spray formation during the separation, unlike gradient elution programs used in LC-MS. Importantly, CE-MS analyses are typically fast with high separation efficiency, do not require extensive workup of highly saline biological samples, and are highly cost-effective due to limited use of organic solvents/reagents while using inexpensive bare fused-silica capillaries rather than LC columns. Additionally, CE requires only small sample volumes ($< 5 \mu\text{L}$), which makes it an ideal technique for analyzing volume-restricted biological samples (*e.g.*, DBS cut-outs containing about 3 μL of whole blood)⁷² while also allowing for “single cell” metabolomic studies.⁷³ However, a major constraint in CE-MS is that concentration sensitivity is limited as a result of small injection volumes (5-10 nL) and post-capillary dilution effects due to the coaxial sheath liquid interface leading to additional dilution of the CE effluent during ionization.⁷⁰ Alternatively, various sheathless interfaces have been developed to

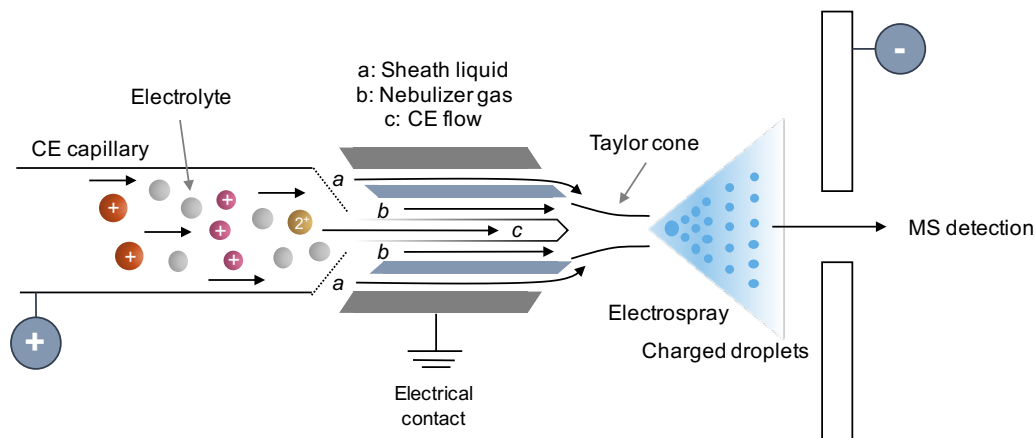


Figure 1.2. Setup of a CE-ESI-MS system showing separation in the CE capillary and the coaxial sheath liquid interface coupling CE to ESI prior to sampling into the MS for detection. Figure adapted from (54).

improve concentration sensitivity in CE-MS, but have not yet been widely adopted yet due to their high costs and/or poor robustness.⁷⁴ Additionally, separations in CE are prone to large migration time variability due to changes in the electroosmotic flow (EOF) when using bare/uncoated fused-silica capillaries, however this can be readily overcome by use of internal standard(s) for normalization of migration (*i.e.*, relative migration time) or the use of dynamic warping algorithms for time alignment during data processing.⁷⁵ Overall, CE-MS has limited metabolome coverage in terms of resolution and detection of nonpolar/neutral metabolites in comparison to RPLC-MS. New advances in non-aqueous CE-MS (NACE-MS) may allow for analysis of non-polar yet ionized long-chain fatty acids and phospholipids, however it is not routinely used nor has it been rigorously validated.⁷⁶

1.2 Capillary Electrophoresis-Mass Spectrometry

CE involves the electrophoretic separation of charged ions within a narrow-bore open-tubular fused-silica capillary in free solution, where the background electrolyte (BGE) composition largely determines selectivity (*e.g.*, pH, ionic strength, organic additives).⁷⁷ The capillaries used for CE separations are also coated with polyimide to prevent capillary breakage while ensuring thermal stability. Capillaries range from 10 to 130 cm in length with inner diameters between 25 to 100 μm . The small inner diameter and high surface-volume ratio of the capillary allows for efficient heat dissipation upon application of high voltages (30 kV maximum). CE is a high efficiency microseparation technique (number of theoretical plates, $N \approx 10^6$) with the ability to resolve a wide range of metabolite classes within complex sample mixtures that also functions as an effective desalter to prevent ion suppression in ESI-MS.

1.2.1 Electrokinetic Separation in CE

Separation of metabolites in CE is dependent on two electrokinetic separation principles: the bulk EOF of the solution and the discrete electrophoretic mobility (μ_{ep}) of a solute (*i.e.*, metabolite). The silanol groups on the capillary wall are partially de-protonated and are predominately negatively charged as a function of solution pH (pH > 5). The negatively charged silanol surface attracts positive ions from the buffer, forming an electric double layer of cations.⁷⁸ When a voltage is applied, the mobile or diffuse layer migrates toward the cathode, resulting in a net

flow of solution (EOF) in that direction. In general, a faster EOF occurs under alkaline conditions when using low ionic strength buffers in low viscosity solvents at high temperature. The electrophoretic mobility is dependent of the velocity of an ion under an applied electric field. Importantly, μ_{ep} is dependent on the effective charge density of an ion (*i.e.*, molecular volume and pK_a) under a defined background electrolyte (BGE) and ambient conditions, such as pH, ionic strength, temperature, and solvent viscosity. While the EOF transports all analytes equally in a sample towards a fixed detector (or ion source), differences in μ_{ep} impact selectivity in CE, where cations migrate prior to neutral compounds, which co-migrate with the EOF, and anionic species migrate counter to the EOF as depicted in **Figure 1.3**. Each ion has an apparent mobility (μ_{app}), which is determined by the apparent migration velocity (v_{app}) and the electric field strength (E). μ_{app} can be determined experimentally from the apparent migration time of the analyte (t_m) and separation conditions used in CE, including voltage and capillary length:⁷⁷

$$\mu_{app} = \frac{v_{app}}{E} = \frac{L_d \cdot L_c}{V \cdot t_m} \quad (2)$$

where, L_d is the length of the capillary from the inlet to the detector, V is the applied voltage, and L_c is the total length of the capillary.

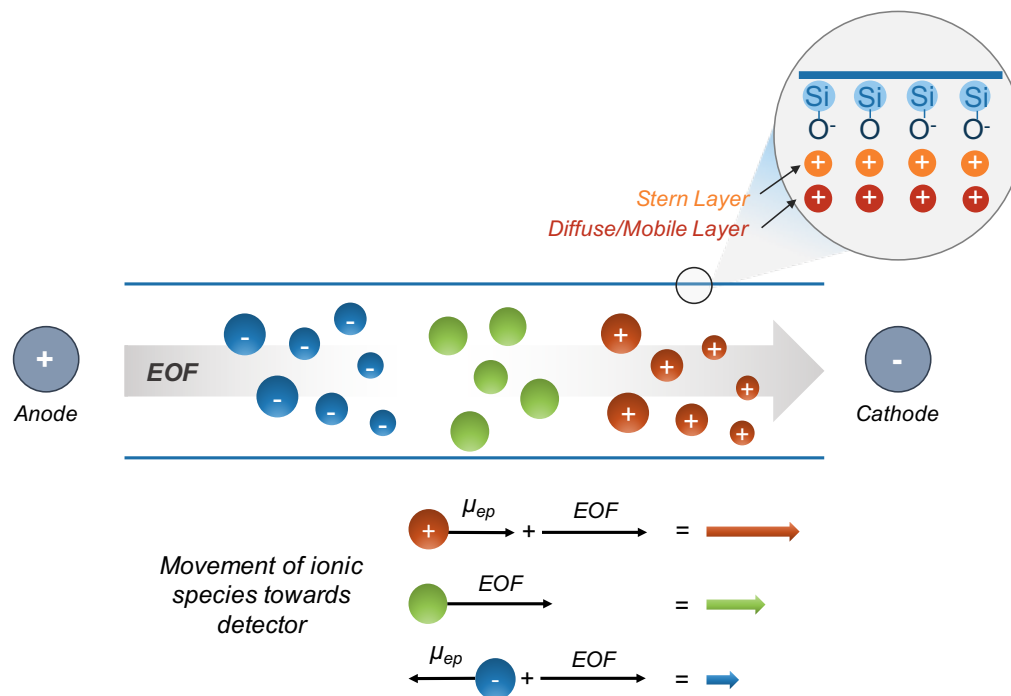


Figure 1.3. Separation of cationic, neutral, and anionic components in a sample by capillary electrophoresis. The EOF is a bulk flow of solution towards the cathode and detector that is a result of the doubly charged cationic layer at the capillary wall. The differences in electrophoretic mobility results in cationic species reaching the detector first (positive μ_{ep}), followed by neutral ($\mu_{ep} = 0$) and anionic species (negative μ_{ep}).

1.2.1.1 Electroosmotic Flow

The EOF is the bulk flow of solution that is generated upon application of voltage across a buffer-filled fused-silica capillary. The surface of the capillary walls possesses a net negative charge due to the deprotonation of silanol functional groups at high pH ($pK_a \approx 6.3$).⁷⁹ The capillary wall attracts a double layer of cationic species within the BGE solution; the innermost layer of cations is adsorbed to the capillary wall (Stern layer), while the outermost layer is a diffuse layer of mobile cations.^{80,81} The cations in the outer layer migrate towards the

cathode, transporting bulk solution with a mobility of μ_{eo} , as described by the Smoluchowski equation:

$$\mu_{eo} = \frac{\varepsilon \cdot \zeta}{4\pi \cdot \eta} \quad (3)$$

where, ε is the dielectric constant of the buffer, η is the viscosity of the buffer, and ζ is the zeta potential of the capillary surface.⁸⁰ ζ reflects the effective charge near the capillary surface and arises as a result of the electric potential difference between the Stern layer and the bulk solution.⁸¹ The magnitude and sign of ζ and, subsequently, the EOF can be altered by changes in buffer pH, the presence of organic modifiers (*i.e.*, organic solvent, surfactants), and ionic strength. Under acidic buffer conditions (pH < 4), the silanol groups are protonated, which effectively suppresses the EOF as highlighted in **Figure 1.4**. In contrast, the addition of cationic surfactants in the buffer (*e.g.*, CTAB) reverses the effective charge with formation of a lipid bilayer on the capillary surface thereby also reversing the direction of the EOF. As a result, the EOF is highly sensitive to properties of the capillary surface and composition of the BGE, which ultimately impacts the apparent migration time for polar/ionic metabolites in CE.

Due to the narrow internal diameter of the capillary, the velocity distribution of EOF is nearly uniform resulting in a flat or ‘plug flow’ (**Figure 1.5**). Pressure-driven systems, such as HPLC or GC, have non-uniform velocities across the column creating a parabolic flow profile.⁷⁹ The flat plug flow profile characteristic of the EOF reduces the effect of band broadening (*i.e.*, resulting in

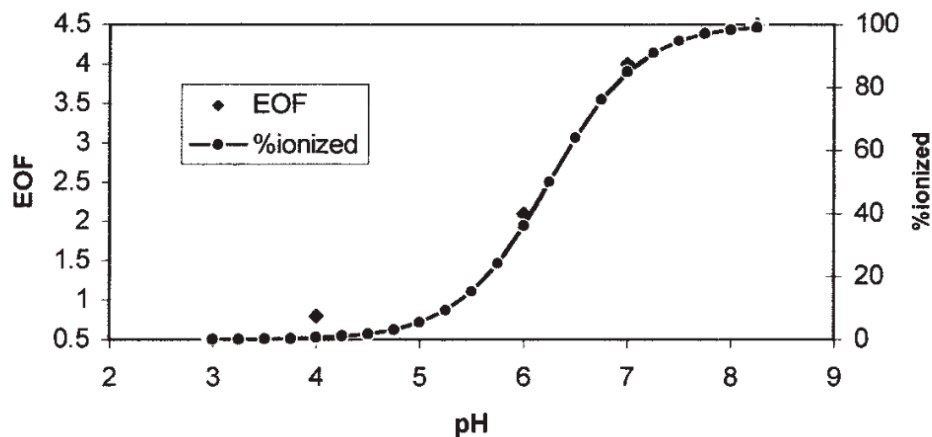


Figure 1.4. The relationship between the EOF and pH. At pH <3, the EOF is effectively suppressed.⁷⁹

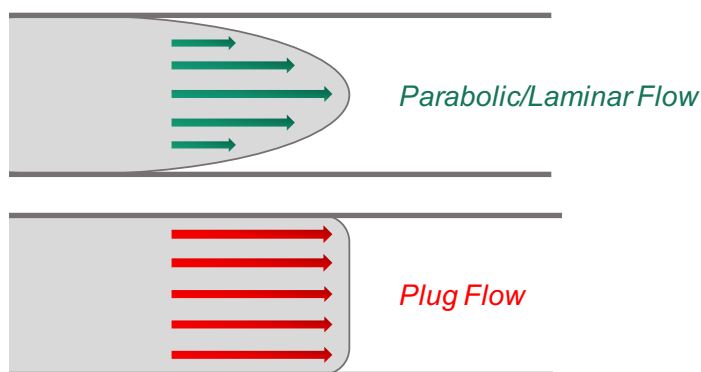


Figure 1.5. Comparison of the parabolic/laminar flow profile for a pressure-driven system such as LC and the flat ‘plug’ EOF flow profile that is generated for solute transport in CE. The plug flow profile of the EOF in CE allows for higher efficiency separations and reduces the band broadening effect observed in LC or GC.

sharper peaks) that is observed in pressure-driven systems due to increased frictional forces present near the column walls.^{78,80} This is a major reason for the higher efficiency separation in CE since band broadening is primarily determined by longitudinal diffusion, whereas HPLC is also subject to additional processes, such as Eddy diffusion and mass transfer.

1.2.1.2 Electrophoretic Mobility

The electrophoretic mobility μ_{ep} ($\text{cm}^2 \text{V}^{-1} \text{s}^{-1}$) is a fundamental property of an analyte under defined experimental conditions.⁷⁷ μ_{ep} depends on both analyte physiochemical properties and BGE conditions that impact the effective charge and molecular size/shape of an analyte. Overall, μ_{ep} is proportional to the net charge of the analyte (q) and inversely proportional to its hydrated hydrodynamic radius (R_H) and solution viscosity when assuming a spherical and uniformly charged ion based on the following equation:⁷⁹

$$\mu_{ep} = \frac{v_{ep}}{E} = \frac{q}{6\pi\eta R_H} \quad (4)$$

The effective charge density of an ion is thus the key parameter that controls both the direction and magnitude of μ_{ep} ; cations and anions will have positive and negative μ_{ep} , respectively, whereas neutral analytes will co-migrate with the EOF with a μ_{ep} of 0 (cations > neutral > anions). Neutral compounds can be resolved in CE, however, when using charged surfactants (*e.g.*, SDS) as pseudo-stationary phases in the BGE due to dynamic solute partitioning during electromigration, which is referred to as micellar electrokinetic chromatography (MEKC)—a widely used mode of separation in CE.⁷⁹ However, most surfactants are not compatible with ESI-MS since they are non-volatile and thus contribute to deleterious ion suppression.⁸² Overall, separation in CE is highly dependent on buffer pH. At high pH (alkaline/neutral), the EOF is strong and transports all ionic

species towards the detector, where selectivity is determined by differences in their μ_{ep} . Under acidic conditions, the EOF is suppressed, which results in the migration of negatively charged species ($\mu_{ep} > \mu_{eo}$) towards the anode where they exit at the capillary inlet. Under these counter-flow conditions, only cationic species can be fully resolved since they co-migrate with the EOF in the same direction. For the separation of strong anions ($pK_a < 2$) such as sulfate, sulfite, and chloride, an acidic BGE under reversed polarity can be applied for improved selectivity.⁸³ This results in the electrokinetic rejection of cations and weak acids in complex biological samples (*e.g.*, urine), allowing for selective detection of strong anions by CE with indirect UV detection without spectral interferences.

1.2.2 Applications of CE-MS in Metabolomics

The high separation efficiency, small sample requirements, and low operating costs makes CE-MS an attractive platform in metabolomics.⁶⁸ Additionally, higher sample throughput with improved data fidelity can be achieved when using multisegment injection (MSI)-CE-MS, where serial sample plugs are injected sequentially between buffer segments prior to separation.^{84,85} After a voltage is applied, ions are then able to migrate as a series of resolved zones under steady-state conditions prior to ESI-MS as shown in **Figure 1.6**. MSI-CE-MS also allows for the design of novel data workflows to encode mass spectral information temporally for biomarker discovery when performing non-targeted metabolite profiling. For instance, a dilution trend filter can be used as a

robust screening tool for peak picking in metabolomics by rejecting background ions and spurious signals via injection of a representative pooled sample that is serially diluted with a blank as a control. Authentic features are those that are not present in the blank, show a linear response with dilution, and can be measured with adequate precision ($CV < 40\%$). Furthermore, quality assurance (QA) can be achieved by inclusion of a pooled quality control (QC) sample in the injection configuration within each run when using MSI-CE-MS.⁸⁵ This allows the monitoring of long-term system drift and overall technical precision while applying batch correction algorithms during large-scale studies where there is evidence of bias.⁸⁶ Thus, MSI-CE-MS offers a multiplexed separation platform for high-throughput metabolite profiling while implementing versatile data workflows to reduce false discoveries with QC/QA.

Soga *et. al.* first reported the use of CE-MS for the comprehensive analysis of anionic metabolites in bacterial samples in 2002.⁸⁷ While its use in metabolomics has since grown significantly, CE-MS-based metabolomics still represents a small fraction of metabolomic studies as compared to more established methods based on GC/MS and LC-MS.⁸⁸ For instance, in 2016, there were over 1,730 publications in metabolomics (Web of Science search query with *metabolom** or *metabonom** in title) with about 56% of all reports utilizing NMR or MS-based detection. Of these, only 2.4% utilized CE-MS as opposed to GC/MS (22.6%), LC-MS (38.6%), and NMR (36.4%). The major benefits and

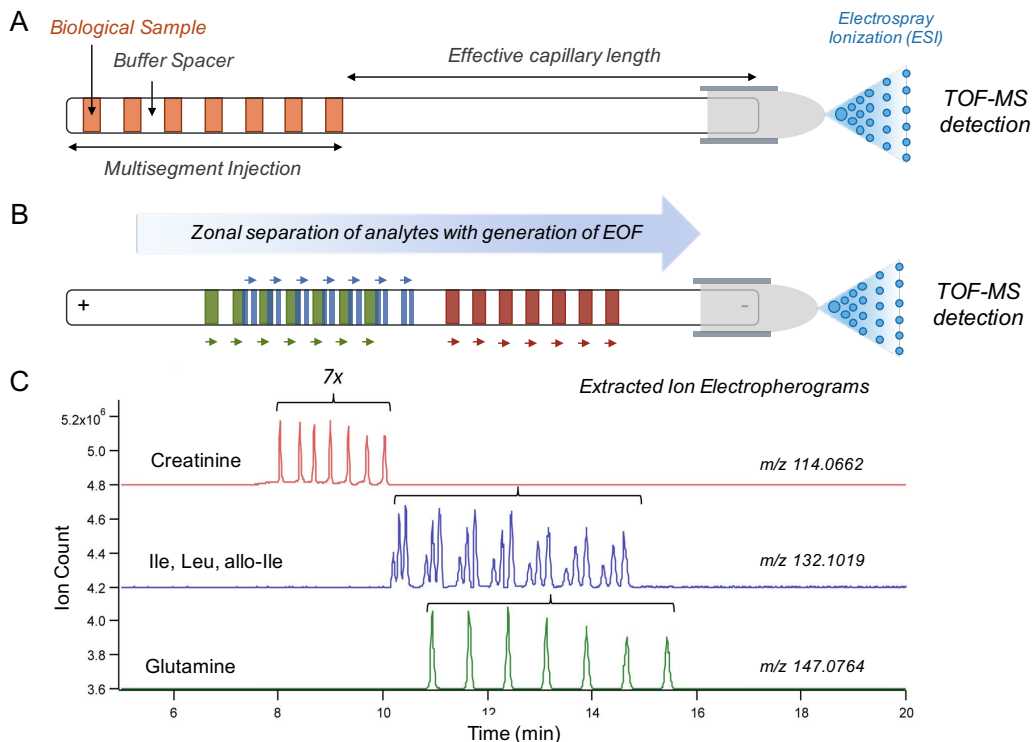


Figure 1.6. Format for multisegment injection (MSI) of seven samples within a single capillary for CE-MS (A).⁸⁴ Ions migrate in a series of zones with the generation of the EOF before ionization and detection by TOF-MS (B). The use of MSI-CE-MS allows the quantification of co-migrating and isomeric metabolites (C). Figure modified from (84).

limitations of CE-MS are summarized in **Table 1.1**, including recent technological advances to overcome major constraints.⁸⁹⁻⁹³ Primary limitations in CE-MS for metabolomics include poor concentration sensitivity, method robustness, and precision for apparent migration times. Furthermore, there are few commercial vendors that offer service support and there is a lack of customized software packages for processing CE-MS metabolomics data.⁹⁴ Also, very few studies published in the literature have performed rigorous and long-term validation studies using CE-MS, including intermethod comparisons or external validation as part of proficiency or round-robin testing.⁹⁵ Recently, Boizard *et al.*

Table 1.1. Major strengths and limitations of CE-MS in metabolomics.

<i>Strengths</i>	<ul style="list-style-type: none"> • Low sample volume (< 5 μL) that is ideal for mass-limited samples • Low operating costs (<i>i.e.</i>, capillary/buffers) • Ideal for polar/ionic compounds in highly saline biological samples • Limited sample pretreatment required
<i>Limitations</i>	<ul style="list-style-type: none"> • Poor concentration sensitivity • Migration time/EOF variation • Difficulty with metabolite identification • Problems with long-term method robustness
<i>Recent Advances</i>	<ul style="list-style-type: none"> • Improvement of throughput by up to 10^1 with MSI⁸⁴ • Sensitivity improvements with sheathless/low-flow interfaces^{89,90} • Expanded metabolome coverage with nonaqueous-CE⁷⁶ • On-line preconcentration to increase sample volume loading⁹¹ • Improved EOF control/migration time precision with column coating strategies⁹² • Chemical derivatization to improve solute ionization and separation performance for low abundance metabolites by introduction of a charged/hydrophobic group⁹³

*al.*⁹⁵ used a CE-MS-based analysis pipeline to illustrate its long-term stability in measuring the urinary metabolome using the same sample over a period of 4 years. CE-MS-based metabolomic analysis of urine samples has also been applied to the discovery of novel biomarkers of cigarette smoking,⁹⁶ targeted screening for glutaric acid acidurias,⁹⁷ discovery of potential predictive markers for cancers as well as therapy efficiency,^{98,99} and for the screening/quantitation of drugs of abuse.¹⁰⁰ The development of MSI-CE-MS greatly increases sample throughput without added infrastructure costs that is ideal for application in large-scale clinical or epidemiological studies. DiBattista *et. al.*¹³ demonstrated an accelerated data workflow for unambiguous identification and quantification of biomarkers of IEMs from neonatal DBS extracts when using MSI-CE-MS that was compared with validated methods based on stable isotope dilution-direct

infusion MS/MS within an accredited clinical laboratory facility. In this case, duplicate injections of three presumptive IEM samples were analyzed with a pooled QC sample representing a healthy neonatal control. This strategy was validated for detection of known IEM biomarkers for the routine analysis of > 20 IEM, including phenylketonuria (PKU). Additionally, nontargeted metabolite profiling of DBS identified new putative biomarkers of galactosemia that may allow for low cost multiplexed MS/MS screening without the need for colorimetric enzyme bioassays. Nontargeted metabolite profiling was also recently applied using MSI-CE-MS in volume-restricted sweat samples from screen-positive infants for cystic fibrosis (CF).⁸⁶ Several discriminating metabolites associated with CF-affected infants were identified, including asparagine and glutamine. Unexpectedly, two exogenous metabolites, pilocarpic acid, a hydrolysis product of the sweat stimulating drug pilocarpine, and mono(2-ethylhexyl)phthalic acid (MEHP), a metabolite of the plasticizer bis(2-ethylhexyl)phthalate (DEHP), were secreted at significantly lower concentrations in comparison to age-matched nonaffected infants. These results suggest that CF infants have a higher risk for paraoxanase (PON 1) deficiency, which is an enzyme associated with lipid metabolism, xenobiotic detoxification, and bacterial biofilm regulation, shedding new insights into the underlying pathophysiology of CF.

1.3 Metabolomics Workflow: From Data to Information

The primary goal of metabolomics is the comprehensive analysis of all metabolites that are detectable in a biological sample in order to derive systematic understanding of an organism on a molecular level. Nontargeted metabolite profiling enables the identification of unexpected compounds of clinical or biological significance, which can be applied for improved screening, diagnosis, and/or treatment monitoring of individual patients.¹⁰¹ However, pre-analytical steps associated with experimental design, cohort selection, sample collection/storage and sample workup, as well as post-analytical steps involving peak picking, time alignment, statistical analysis, metabolite identification, and biochemical interpretation, are all essential components within a metabolomics workflow.¹⁰² **Figure 1.7** provides an overview of an accelerated data workflow developed for biomarker discovery in metabolomics when using MSI-CE-MS. The experimental design used for hypothesis testing is critical to control for different and often confounding variables within a study that can contribute to bias or false discoveries (*e.g.*, age, sex, BMI, co-morbidity).¹⁰³ This includes the implementation of standardized protocols for sample collection, preparation, and storage, especially in small underpowered pilot studies. Moreover, rigorous method validation and daily preventative maintenance/mass calibration routines for instrumentation are also required, including stringent QC/QA to minimize bias when performing large-scale metabolomics studies over long periods of time.¹⁰³ Method validation is a critical step as it ensures the method is reproducible,

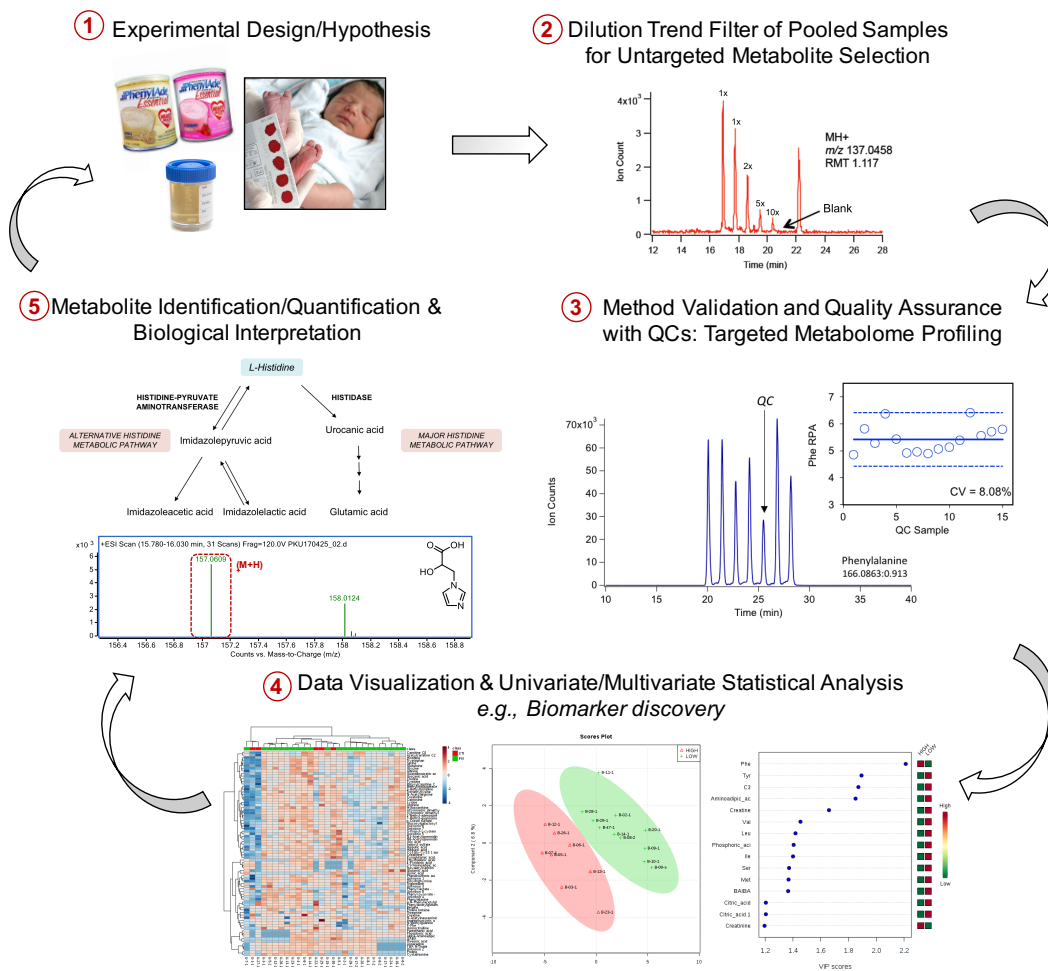


Figure 1.7. Components of an accelerated data workflow for nontargeted metabolomic studies using MSI-CE-MS. Experimental design (1) is critical for controlling different variables within a study, and includes standardized sample collection and preparation. A dilution trend filter (2) can be used for an untargeted primary screen of unique sample-derived metabolites, while excluding spurious signals and background ions. Method validation and quality assurance (3) by analyzing QC samples within each run over the entire study duration ensures that the method is reproducible, accurate, and robust. Data visualization and hypothesis testing (4) is then carried out after pre-processing (*i.e.*, normalization, scaling, transformation) using multivariate and univariate statistics, which is followed by the qualitative/quantitative identification of biologically significant metabolites and related metabolic pathways associated with the study design (5). Adapted from (85).

accurate, and robust, such that measured changes in metabolic responses are not due to technical variations or systematic bias. This is achieved by analyzing representative QC samples intermittently over the entire duration of the study.

The QC also provides selection criteria for molecular features when performing nontargeted metabolite profiling based on acceptable technical precision ($CV < 40\%$).¹⁰³

Following data acquisition, data pre-processing involves the application of various processes to the raw data prior to statistical analysis, including correction, normalization, scaling, and transformation. Batch-correction provides a way to adjust raw data in order to reduce variability and correct for systematic error as reflected by changes in response for QC samples analyzed over time.⁸⁶ Normalization is useful to correct for variations in sample composition, sample recovery, and/or sample injection volume, such as with creatinine normalization to correct for differences in hydration status in human urine.^{104,105} Also, normalization of ion responses for all measured metabolites in CE-MS is often performed when using an internal standard (IS) and/or recovery standard (RS) that are added to all samples at a fixed concentration in order to correct for differences in on-column injection volumes between samples.¹⁰⁶ In the case of skewed data distributions, a logarithmic transformation is also frequently applied to a data matrix as required for application of parametric statistical tests. Additionally, autoscaling is a common data pretreatment method in metabolomics during explorative analysis (*i.e.*, mean-centered data divided by its standard deviation for each metabolite) in order to provide equal weight when comparing metabolite responses that vary over a wide dynamic range irrespective of their abundance.¹⁰⁷ Additional data transformations may be required depending on the

type of biological specimen, the biological question to be answered, and the underlying origin(s) of variance, such as normalization of metabolite response to dried mass for wet tissue biopsies.

Statistical analysis, which involves univariate and multivariate statistical tests, is a major step in the data workflow in metabolomics, allowing sample classification, correlation between features, and identification of significant features, all of which are important for biological/biochemical interpretation.¹⁰⁷ Univariate statistical methods test the significance of individual features between different groups. With data that is distributed normally, Student's *t*-test and one-way analysis of variance (ANOVA) are widely used. Non-normal data require nonparametric statistical tests such as the Mann-Whitney U test to compare the difference between two groups. Receiver operating characteristic (ROC) curves are also utilized to assess the performance of a biomarker for differentiating between two states (*i.e.*, healthy versus disease) by observing how a critical threshold affects sensitivity and specificity.^{108,109} In addition to ROC curves, scatter plots, histograms, and box plots are used to visualize and evaluate data trends terms of their overall statistical significance after adjusting for covariates (*e.g.*, age and sex).¹⁰⁹ Multivariate statistical methods are classified as unsupervised or supervised, where unsupervised methods classify the data without knowledge of sample classification.⁷ Supervised methods, however, have known classifications (*i.e.*, disease state versus healthy subjects) and are useful for identification and ranking of biomarkers. Principal component analysis (PCA), an

unsupervised multivariate method used for reduction of data dimensionality and filtering noise in order to cluster samples based on the underlying variance of the data, is often used as a starting point for data exploration. PCA transforms the data into ranked principal components (PCs) which are latent variables that explain the directionality of maximum data variance. The first principal component (PC1) possesses the highest variance within the data set, with each subsequent orthogonal PC representing the next greatest variance. The PCA scores plot can give an overview of the data in terms of trends/pattern recognition, grouping, and outlier detection.¹⁰⁷ Furthermore, PCA is useful for comparing the technical variance of the method based on clustering of repeat QC samples relative to the much greater biological variance of study groups examined. Statistical parameters such as effect size and average fold-change should be reported along with the probability (*p*-value) with confidence intervals (*e.g.*, 95% confidence). Hierarchical cluster analysis (HCA) is another unsupervised multivariate method that clusters data based on the differences between pairs of samples/features.⁷ Small distances between pairs suggest that the samples have greater similarity in terms of their overall metabolic phenotype. The partial least squares discriminant analysis (PLS-DA) is a supervised multivariate statistical method that plots the regression of the data matrix (*x*-axis) against a classification matrix (*y*-axis). The goal of a PLS-DA model is to optimize the separation between sample classes, while identifying features responsible for class separation.^{106,107} As the number of hypothesis tests increase (*i.e.*, with the number

of features), the frequency of type I errors (*i.e.*, false positives) also increases—this is known as the multiple testing problem.¹¹⁰ In metabolomics, multiple hypothesis testing should be applied by using appropriate adjustments, such as false discovery rate (FDR) or more conservative Bonferroni correction.

The final step in the metabolomics workflow is the interpretation of the data based on known metabolic pathways, which allows further understanding and characterization of specific metabolic stressors. This is often challenging as many biomarkers do not have well-understood biochemical pathways and/or roles in disease pathophysiology. Furthermore, the interpretation of the significance of changes in a large number of metabolites is also difficult, however visualization can be carried out using metabolic pathway maps.¹¹¹ Initial validation of putative biomarkers must be carried out prior to translation as a way to reduce false discoveries; pre-validation can be carried out by measuring putative biomarkers in an independent set of samples (*i.e.*, replication) in a different patient population using the same analytical platform and/or by cross-validation by re-analyzing same samples using a different platform. For validation of biomarkers using a more targeted data workflow, the analytical figures of merit of the assay must be determined to demonstrate adequate linearity, sensitivity, limit of detection, robustness, and reproducibility of measurement in samples without complicated sample workup. Importantly, the biomarker must offer a measurable clinical benefit in terms of improving patient health outcomes (*e.g.*, higher positive predictive value, reduced mortality or morbidity), or reducing healthcare costs.¹¹²

For example, TMAO, a metabolite of dietary choline, phosphatidylcholine, and *L*-carnitine, has been extensively validated by several research groups independently as a biomarker for cardiovascular disease, including atherosclerosis.¹¹³ Further investigation into the clinical value of TMAO also confirmed its contributory role in the development of renal dysfunction.¹¹⁴ Sarcosine is another biomarker for predicting aggressive prostate cancer in high risk patients, however its biological mechanisms and clinical utility are still being evaluated relative to conventional prostate specific antigen (PSA).¹¹³

1.4 Thesis Overview and Objectives

Metabolomics is a powerful way to elucidate the effect of many single or multiple stressors on human health, including perturbations induced by genetic mutations, dietary patterns, and/or environmental exposures. One of the main priorities of metabolomics is to better understand the pathophysiology associated with human diseases, including the role of potentially modifiable lifestyle factors, such as smoking and habitual diet. A better understanding of these mechanisms is essential for improved disease prevention on a population level, in addition to predicting an individual's susceptibility to environmental stressors. Metabolomics has the potential to improve the screening and diagnostics of IEM, where early detection relies on analysis of sensitive yet specific disease-associated biomarkers.¹¹⁵ In the case of PKU, which is a potentially debilitating genetic disease affecting phenylalanine metabolism that leads to lifelong cognitive

impairment if left untreated, new advances for dieticians to objectively measure adherence to a low protein diet will greatly improve clinical outcomes. However, birth outcomes are not only dependent on dietary patterns and genetics, but also on lifelong chemical exposures especially during critical stages of fetal development. In this case, metabolomics offers a novel approach to reveal the sub-acute toxicity effects of low level exposure to vapour from electronic cigarettes (“e-cigarettes”) using first trimester placental cells as a relevant cell model system for prenatal exposures.

The work in this thesis aims to address two major projects in metabolomics associated with public health with a focus on chronic disease prevention relevant to pediatric medicine. *Chapter II* focuses on the impact of diet and nutrition on the urinary and plasma metabolome of PKU patients. In PKU, a severe accumulation of circulating Phe coupled to a deficiency in Tyr leads to irreversible neurotoxic effects such as cognitive impairments, reduced melanin production, and growth deficiencies.^{116,117} This can be readily prevented with lifelong dietary restriction of Phe using specialized medical foods that promote normal growth without undernutrition. The major research objectives associated with this project were to perform targeted/nontargeted metabolomics to confirm known and reveal unknown biomarkers associated with severe PKU and explore its relationship to dietary adherence for individual patients. The first component of this project focused on (a) the validation of the MSI-CE-MS method in measuring clinically monitored and relevant biomarkers of PKU (Phe and Tyr) in

comparison to the reference method for amino acid analysis based on UPLC-UV. In addition, (b) the targeted analysis of several known Phe catabolites associated with PKU was performed, including gut microflora-derived metabolites of aromatic amino acids, demonstrating a correlation of these metabolites to Phe concentrations measured in both plasma and urine. Finally, (c) the nontargeted analysis was applied to identify novel biomarkers associated with PKU, which highlighted that urinary acylcarnitines and catabolites of histidine were strongly correlated to excreted concentrations of Phe. This may provide a way in which to monitor consequences of dietary inadherence, such as macronutrient (*e.g.*, essential fatty acids) and micronutrient/vitamin deficiencies (*e.g.*, folic acid), or hormonal changes. Metabolomics research examining PKU pathophysiology is extremely limited and there is little work focused on the complex interactions of the PKU diet, which includes protein restriction and supplementation with amino acid formula, or other treatment options that impact the metabolome.

Chapter III focuses on the examination of the metabolic effects of e-cigarettes on placental trophoblast cells at different stages of development. E-cigarettes are advertised as a harm reduction alternative to tobacco cigarettes and users inhale vaporized liquids containing propylene glycol and/or glycerol, nicotine in concentrations ranging from 0-24 mg/mL, and a wide range of flavouring agents and chemical additives. Relative to tobacco smoke, e-cigarette aerosol has been demonstrated to be less cytotoxic *in vivo*; however, long-term biological effects simulating sub-acute exposure to vaporized flavour additives

within these solutions is unknown. It has been demonstrated that some flavour additives commonly found in e-cigarette solutions (*e.g.*, diacetyl and cinnamaldehyde) are associated with severe implications on human health, such as the development of respiratory disease.¹¹⁸ E-cigarettes represent a serious potential threat to public health as a result of advertising and unawareness coupled with sparse research efforts in the field. In particular, research into chronic exposure to flavoured e-cigarettes is urgently needed for high risk populations during critical periods of development (*i.e.*, adolescents and during pregnancy). In order to better elucidate the potential effects of e-cigarettes, exposure of first and third trimester trophoblast cells to unflavoured and flavoured e-cigarette liquid vapour was carried out as a function of nicotine dosage. The major achievements of this project included: (a) the characterization of e-cigarette liquid formulations with different analytical methods with a focus on volatile components in addition to polar/ionic components; (b) the validation of the preparation of exposed cell growth media; and (c) the targeted and nontargeted analysis of placental cell exposure to (i) unflavoured/simple, (ii) nicotine-containing, and (iii) flavoured e-cigarette liquids. Overall, this work offers valuable insight on the potential harm of e-cigarettes on fetal development. Furthermore, the identification of metabolites that are significantly altered in placental cells, such as acylcarnitines and metabolites of fatty acid oxidation, will aid in identifying enzyme targets and metabolic pathways that may be affected by components in e-cigarette vapour. As it is known that e-cigarette liquids and their vapours are incredibly complex, this

work provides a basis for further analysis into specific flavouring additives and their deleterious effects on placental function. Furthermore, this work strives to apply metabolomics using a unique data workflow by MSI-CE-MS to evaluate the effects of potentially modifiable lifestyle factors (*i.e.*, diet, smoking) on human health, with emphasis on genetic diseases in children in support of universal newborn screening programs, and public health as related to an alarming increase in e-cigarette smoking prevalence among young adults.

1.5 References

1. Matsuda, F. Technical challenges in mass spectrometry-based metabolomics. *Mass Spectrom.* 2016, **5**: S0052-S0059.
2. Bentley, R. Secondary metabolite biosynthesis: the first century. *Crit. Rev. Biotech.* 1999, **19**: 1-40.
3. Nielsen, J. Systems biology of metabolism. *Annu. Rev. Biochem.* 2017, **86**: 245-275.
4. Scalbert, A.; Brennan, L.; Fiehn, O.; Hankemeier, T.; Kristal, B.S.; van Ommen, B.; Pujos-Guillot, E.; Verheij, E.; Wishart, D.; Wopereis, S. Mass-spectrometry-based metabolomics: limitations and recommendations for future progress with particular focus on nutrition research. *Metabolomics.* 2009, **5**: 435-458.
5. Monton, M.R.N.; Soga, T. Metabolome analysis by capillary electrophoresis-mass spectrometry. *J. Chromatogr. A.* 2007, **1168**: 237-246.
6. Prosser, G.A.; Larrouy-Maumus, G.; de Carvalho, L.P.S. Metabolomic strategies for the identification of new enzyme functions and metabolic pathways. *EMBO Rep.* 2014, **15**: 657-669.
7. Dettmer, K.; Aronov, P.A.; Hammock, B.D. Mass spectrometry-based metabolomics. *Mass Spectrom. Rev.* 2007, **26**: 51-78.
8. Rochfort, S. Metabolomics reviewed: a new “omics” platform technology for systems biology and implications for natural product research. *J. Nat. Prod.* 2005, **68**: 1813-1820.
9. Gowda, G.A.N.; Zhang, S.; Gu, H.; Asiago, V.; Shanaiah, N.; Raftery, D. Metabolomics-based methods for early disease diagnostics: A review. *Expert Rev. Mol. Diagn.* 2008, **8**: 617-633.
10. Tsai, I.-L.; Weng, T.-I.; Tseng, Y.J.; Tan, H.K.-L.; Sun, H.-J.; Kuo, C.-H. Screening and confirmation of 62 drugs of abuse and metabolites in urine by

- ultra-high-performance liquid chromatography-quadrupole time-of-flight mass spectrometry. *J. Anal. Toxicol.* 2013, **37**: 642-651.
11. Wishart, D.S. Emerging applications of metabolomics in drug discovery and precision medicine. *Nat. Rev. Drug Discov.* 2016, **15**: 473-484.
 12. Gowda, G.A.N.; Raftery, D. Biomarker discovery and translation in metabolomics. *Curr. Metabolomics* 2013, **1**: 227-240.
 13. DiBattista, A.; McIntosh, N.; Lamoureux, M.; Al-Dirbashi, O.Y.; Chakraborty, P.; Britz-McKibbin, P. Temporal signal pattern recognition in mass spectrometry: A method for rapid identification and accurate quantification of biomarkers for inborn errors of metabolism with quality assurance. *Anal. Chem.* 2017, published online ahead of print, doi:10.1021/acs.analchem.7b01727.
 14. Roede, J.R.; Park, Y.; Li, S.; Strobel, F.H.; Jones, D.P. Detailed mitochondrial phenotyping by high resolution metabolomics. *PLoS One* 2012, **7**: e33020.
 15. Strigun, A.; Wahrheit, J.; Beckers, S.; Heinzle, E.; Noor, F. Metabolic profiling using HPLC allows classification of drugs according to their mechanisms of action in HL-1 cardiomyocytes. *Toxicol. Appl. Pharmacol.* 2011, **25**: 183-191.
 16. Rabinowitz, J.D.; Purdy, J.G.; Vastag, L.; Shenk, T.; Koyuncu, E. Metabolomics in drug target discovery. *Cold Spring Harb. Symp. Quant. Biol.* 2011, **76**: 235-246.
 17. Vastag, L.; Koyuncu, E.; Grady, S.L.; Shenk, T.E.; Rabinowitz, J.D. Divergent effects of human cytomegalovirus and herpes simplex virus-1 on cellular metabolism. *PLoS Pathog.* 2011, **7**: e1002124.
 18. Cuperlovic-Culf, M.; Culf, A.S. Applied metabolomics in drug discovery. *Expert Opin. Drug Discov.* 2016, **11**: 759-770.
 19. Tolstikov, V.; Akmaev, V.R.; Sarangarajan, R.; Narain, N.R.; Kiebish, M.A. Clinical metabolomics: a pivotal tool for companion diagnostic development and precision medicine. *Expert Rev. Molec. Diagnost.* 2017, **17**: 411-413.
 20. Beger, R.D.; Dunn, W.; Schmidt, M.A.; Gross, S.S.; Kirwan, J.A.; Cascante, M.; Brennan, L.; Wishart, D.S.; Oresic, M.; Hankemeier, T.; Broadhurst, D.I.; Lane, A.N.; Suhre, K.; Kastenmüller, G.; Sumner, S.J.; Thiele, I.; Fiehn, O.; Kaddurah-Daouk, R. Metabolomics enables precision medicine: “A White Paper, Community Perspective”. *Metabolomics* 2016, **12**: 149-163.
 21. Kaddurah-Daouk, R.; Kristal, B.S.; Wienshilboum, R.M. Metabolomics: A global biochemical approach to drug response and disease. *Annu. Rev. Pharmacol. Toxicol.* 2008, **48**: 653-683.
 22. Kaddurah-Daouk, R.; McEvoy, J.; Baillie, R.A.; Lee, D.; Yao, J.K.; Doraiswamy, P.M.; Krishnan, K.R. Metabolomic mapping of atypical antipsychotic effects in schizophrenia. *Mol. Psychiatry.* 2007, **12**: 934-945.
 23. Wang, Z.; Chen, Z.; Yang, S.; Wang, Y.; Yu, L.; Zhang, B.; Rao, Z.; Gao, J.; Tu, S. ¹H NMR-based metabolomic analysis for identifying serum

- biomarkers to evaluate methotrexate treatment in patients with early rheumatoid arthritis. *Exp. Ther. Med.* 2012, **4**: 165-171.
24. Fairbanks, L.D.; Rückmann, K.; Qui, Y.; Hawrylowicz, C.M.; Richards, D.F.; Swaminathan, R.; Kirschbaum, B.; Simmonds, H.A. Methotrexate inhibits the first committed step of purine biosynthesis in mitogen-stimulated human T-lymphocytes: a metabolic basis for efficacy in rheumatoid arthritis? *Biochem. J.* 1999, **342**: 143-152.
 25. Koulman, A.; Volmer, D.A. Perspectives for metabolomics in human nutrition: An overview. *Nutr. Bull.* 2008, **33**: 324-330.
 26. Newby, P.K.; Maras, J.; Bakun, P.; Muller, D.; Ferrucci, L.; Tucker, K.L. Intake of whole grains, refined grains, and cereal fiber measured with 7-d diet records and associations with risk factors for chronic disease. *Am. J. Clin. Nutr.* 2007, **86**: 1745-1753.
 27. Bray, G.A.; Flatt, J.-P.; Volaufova, J.; DeLany, J.P.; Champagne, C.M. Corrective responses in human food intake identified from an analysis of 7-d food-intake records. *Am. J. Clin. Nutr.* 2008, **88**: 1504-1510.
 28. Buzzard, I.M.; Faucett, C.L.; Jeffrey, R.W.; McBane, L.; McGovern, P.; Baxter, J.S.; Shapiro, A.C.; Blackburn, G.L.; Chlebowski, R.T.; Elashoff, R.M.; Wynder, E.L. Monitoring dietary change in low-fat diet intervention study: Advantages of using 24-hour dietary recalls vs food records. *J. Am. Diet Assoc.* 1996, **96**: 574-579.
 29. Klesges, R.C.; Eck, L.H.; Ray, J.W. Who underreports dietary intake in a dietary recall? Evidence from the second national health and nutrition examination survey. *J. Consult. Clin. Psychol.* 1995, **63**: 438-444.
 30. Swinburn, B.A.; Caterson, I.; Seidell, J.C.; James, W.P.T. Diet, nutrition and the prevention of excess weight gain and obesity. *Public Health Nutr.* 2004, **7**: 122-146.
 31. O’Gorman, A.; Gibbons, H.; Brennan, L. Metabolomics in the identification of biomarkers of dietary intake. *Comput. Struct. Biotechnol. J.* 2013, **4**: e201301004.
 32. Seale, J.L.; Klein, G.; Friedman, J.; Jensen, G.L.; Mitchell, D.C.; Smiciklas-Wright, H. Energy expenditure measured by doubly labeled water, activity recall, and diet records in the rural elderly. *Nutrition* 2002, **18**: 568-573.
 33. Heitmann, B.L.; Lissner, L. Dietary underreporting by obese individuals—is it specific or non-specific? *BMJ* 1995, **45**: 583-599.
 34. Hebert, J.R.; Clemow, L.; Pbert, L.; Ockene, I.S.; Ockene, J.K. Social desirability bias in dietary self-report may compromise the validity of dietary intake measures. *Int. J. Epidemiol.* 1995, **24**: 389-398.
 35. Pallister, T.; Jennings, A.; Mohny, R.P.; Yarand, D.; Mangino, M.; Cassidy, A.; MacGregor, A.; Spector, T.D.; Menni, C. Characterizing blood metabolomics profiles associated with self-reported food intakes in female twins. *PLoS One* 2016, **11**: e0158568.
 36. Bhupathiraju, S.N.; Hu, F.B. One (small) step towards precision nutrition by use of metabolomics. *Lancet Diabetes Endocrinol.* 2017, **5**: 154-155.

37. Bundy, J.G.; Davey, M.P.; Viant, M.R. Environmental metabolomics: a critical review and future perspectives. *Metabolomics* 2009, **5**: 3-21.
38. Renz, H.; Holt, P.G.; Inouye, M.; Logan, A.C.; Prescott, S.L.; Sly, P.D. An exposome perspective: Early-life events and immune development in a changing world. *J. Allergy Clin. Immunol.* 2017, **140**: 24-40.
39. Garcia-Perez, I.; Lindon, J.C.; Minet, E. Application of CE-MS to a metabonomics study of human urine from cigarette smokers and non-smokers. *Bioanalysis* 2014, **6**: 2733-2749.
40. Barrera-Gómez, J.; Agier, L.; Portengen, L.; Chadeau-Hyam, M.; Giorgis-Allemand, L.; Siroux, L.; Robinson, O.; Vlaanderen, J.; González, J.R.; Nieuwenhuijsen, M.; Vineis, P.; Vrijheid, R.; Slama, R.; Basagaña, X. A systematic comparison of statistical methods to detect interactions in exposome-health associations. *Environ. Health* 2017, **16**: 74-86.
41. Birkenmeyer, C.; Luedemann, A.; Wagner, C.; Erban, A.; Kopka, J. Metabolome analysis: the potential of *in vivo* labeling with stable isotopes for metabolite profiling. *Trends Biotechnol.* 2005, **23**: 28-33.
42. Dunn, W.B.; Ellis, D.I. Metabolomics: Current analytical platforms and methodologies. *Trends Anal. Chem.* 2005, **24**: 285-294.
43. Ullsten, S.; Danielsson, R.; Bäckström, D.; Sjöberg, P.; Bergquist, J. Urine profiling using capillary electrophoresis-mass spectrometry and multivariate data analysis. *J. Chromatogr. A* 2006, **1117**: 87-93.
44. Kruk, J.; Doskocz, M.; Jodłowska, E.; Zacharzewska, A.; Łakomiec, J.; Czaja, K.; Kujawski, J. NMR techniques in metabolomics studies: A quick overview on examples of utilization. *Appl. Magn. Res.* 2017, **48**: 1-21.
45. Serkova, N.J.; Niemann, C.U. Pattern recognition and biomarker validation using quantitative ¹H-NMR-based metabolomics. *Expert Rev. Mol. Diagn.* 2006, **6**: 717-731.
46. Veenstra, T.D. Metabolomics: the final frontier? *Genome Med.* 2012, **4**: 40-42.
47. Ravanbakhsh, S.; Liu, P.; Bjordahl, T.C.; Mandal, R.; Grant, J.R.; Wilson, M.; Eisner, R.; Sinelnikov, I.; Hu, X.; Luchinat, C.; Greiner, R.; Wishart, D.S. Accurate, fully-automated NMR spectral profiling for metabolomics. *PLoS ONE* 2015, **10**: e0124219.
48. Shockcor, J.P.; Unger, S.E.; Wilson, I.D.; Foxall, P.J.D.; Nicholson, J.K.; Lindon, J.C. Combined HPLC, NMR spectroscopy, and ion-trap mass spectrometry with application to the detection and characterization of xenobiotic and endogenous metabolites in human urine. *Anal. Chem.* 1996, **68**: 4431-4435.
49. Villas-Bôas, S.G.; Mas, S.; Åkesson, M.; Smedsgaard, J.; Nielsen, J. Mass spectrometry in metabolome analysis. *Mass Spectrom. Rev.* 2005, **24**: 613-646.
50. Ho, C.S.; Lam, C.W.K.; Chan, M.H.M.; Cheung, R.C.K.; Law, L.K.; Lit, L.C.W.; Ng, K.F.; Suen, M.W.M.; Tai, H.L. Electrospray ionization mass

- spectrometry: Principles and clinical applications. *Clin. Biochem. Rev.* 2003, **24**: 3-12.
51. Palma, P.; Famiglioni, G.; Trufelli, H.; Pierini, E.; Termopoli, V.; Cappiello, A. Electron ionization in LC-MS: recent developments and applications of the direct-EI LC-MS interface. *Anal. Bioanal. Chem.* 2011, **399**: 2683-2693.
 52. Kind, T.; Fiehn, O. Advances in structure elucidation of small molecules using mass spectrometry. *Bioanal. Rev.* 2010, **2**: 23-60.
 53. Gowda, G.A.N.; Djukovic, D. Overview of mass spectrometry-based metabolomics: Opportunities and challenges. *Methods Mol. Biol.* 2014, **1198**: 3-12.
 54. Chalcraft, K.R.; Lee, R.; Mills, C.; Britz-McKibbin, P. Virtual quantification of metabolites by capillary electrophoresis-electrospray ionization-mass spectrometry: Predicting ionization efficiency without chemical standards. *Anal. Chem.* 2009, **81**: 2506-2515.
 55. Panuwet, P.; Hunter Jr., R.E.; D'Souza, P.E.; Chen, X.; Radford, S.A.; Cohen, J.R.; Marder, M.E.; Kartavenka, K.; Ryan, P.B.; Barr, D.B. Biological matrix effects in quantitative tandem mass spectrometry-based analytical methods: Advancing biomonitoring. *Crit. Rev. Anal. Chem.* 2016, **46**: 93-105.
 56. Murray, K.M.; Boyd, R.K.; Eberlin, M.N.; Longley, G.J.; Li, L.; Naito, Y. Definitions of terms relating to mass spectrometry (IUPAC recommendations 2013). *Pure Appl. Chem.* 2013, **85**: 1515-1609.
 57. Wiley, W.C.; McLaren, I.H. Time-of-flight mass spectrometer with improved resolution. *Rev. Sci. Instrum.* 1955, **26**: 1150-1157.
 58. Henderson, W.; McIndoe, J.S. Mass spectrometry of inorganic and organometallic compounds: Tools – Techniques – Tips. West Sussex, England: John Wiley & Sons, 2005.
 59. de Hoffmann, E. Tandem mass spectrometry: a primer. *J. Mass Spec.* 1996, **31**: 129-137.
 60. Chernushevich, I.G.; Loboda, A.V.; Thomson, B.A. An introduction to quadrupole-time-of-flight mass spectrometry. *J. Mass Spectrom.* 2001, **36**: 849-865.
 61. Blaženović, I.; Kind, T.; Torbašinović, H.; Obrenović, S.; Mehta, S.S.; Tsugawa, H.; Wermuth, T.; Schauer, N.; Jahn, M.; Biedendieck, R.; Jahn, D.; Fiehn, O. Comprehensive comparison of in silico MS/MS fragmentation tools of the CASMI contest: database boosting is needed to achieve 93% accuracy. *J. Cheminform.* 2017, **9**: 32.
 62. Zhentian, L.; Huhman, D.V.; Sumner, L.W. Mass spectrometry strategies in metabolomics. *J. Biol. Chem.* 2011, **286**: 25435-25442.
 63. Zhang, A.; Sun, H.; Wang, P.; Han, Y.; Wang, X. Modern analytical techniques in metabolomics analysis. *Analyst* 2012, **137**: 293-300.
 64. Cajka, T.; Fiehn, O. Comprehensive analysis of lipids in biological systems by liquid chromatography-mass spectrometry. *Trends Anal. Chem.* 2014, **61**: 192-206.

65. Theodoridis, G.; Gika, H.G.; Wilson, I.D. LC-MS-based methodology for global metabolite profiling in metabonomics/metabolomics. *Trends Anal. Chem.* 2008, **27**: 251-260.
66. Petritis, K.N.; Chaimbault, P.; Elfakir, C.; Dreux, M. Ion-pair reversed-phase liquid chromatography for determination of polar underivatized amino acids using perfluorinated carboxylic acids as ion pairing agent. *J. Chromatogr. A* 1999, **833**: 147-155.
67. Xiao, J.F.; Zhou, B.; Ransom, H.W. Metabolite identification and quantitation in LC-MS/MS-based metabolomics. *Trends Anal. Chem.* 2012, **32**: 1-14.
68. Ramautar, R.; Somsen, G.W.; de Jong, G.J. CE-MS in metabolomics. *Electrophoresis* 2009, **30**: 276-291.
69. Ullsten, S.; Danielsson, R.; Bäckström, D.; Sjöberg, P.; Bergquist, J. Urine profiling using capillary electrophoresis-mass spectrometry and multivariate data analysis. *J. Chromatogr. A* 2007, **1117**: 87-93.
70. Zhang, W.; Hankemeier, T.; Ramautar, R. Next-generation capillary electrophoresis-mass spectrometry approaches in metabolomics. *Curr. Opin. Biotech.* 2017, **43**: 1-7.
71. Kirby, D.P.; Thorne, J.M.; Götzinger, W.K.; Karger, B.L. A CE/ESI-MS interface for stable, low-flow operation. *Anal. Chem.* 1996, **68**: 4451-4457.
72. Ramautar, R.; Toraño, J.S.; Somsen, G.W.; de Jong, G.J. Evaluation of CE methods for global metabolic profiling of urine. *Electrophoresis* 2010, **31**: 2319-2327.
73. Zenobi, R. Single-cell metabolomics: analytical and biological perspectives. *Science* 2013, **342**: 1243-1259.
74. Maxwell, E.J.; Chen, D.D. Twenty years of interface development for capillary electrophoresis-electrospray ionization-mass spectrometry. *Anal. Chim. Acta.* 2008, **627**: 25-33.
75. Ramautar, R.; Somsen, G.W.; de Jong, G.J. CE-MS in metabolomics. *Electrophoresis* 2009, **30**: 276-291.
76. Yang, Q.; Benson, L.M.; Johnson, K.L.; Naylor, S. Analysis of lipophilic peptides and therapeutic drugs: on-line-nonaqueous capillary electrophoresis-mass spectrometry. *J. Biochem. Biophys. Methods* 1999, **38**: 103-121.
77. Wätzig, H.; Günter, S. Capillary electrophoresis- a high performance analytical separation technique. *Clin. Chem. Lab. Med.* 2003, **41**: 724-738.
78. Moini, M. Capillary electrophoresis mass spectrometry and its application to the analysis of biological mixtures. *Anal. Bioanal. Chem.* 2002, **373**: 466-480.
79. Whatley, H. "Basic Principles and Modes of Capillary Electrophoresis" *Clinical and Forensic Applications of Capillary Electrophoresis*. Eds. Petersen, J.R.; Mohammad, A.A. Totowa, NJ: Humana Press, 2001: 21-58, doi: 10.1007/978-1-59259-120-6.

80. Copper, C.L. Capillary electrophoresis. Part I. Theoretical and experimental background. *J. Chem. Ed.* 1998, **75**: 343-347.
81. Kirby, B.J.; Hasselbrink, E.F., Jr. Zeta potential of microfluidic substrates: 1. Theory, experimental techniques, and effects on separations. *Electrophoresis* 2004, **25**: 187-202.
82. Rundlett, K.L.; Armstrong, D.W. Mechanism of signal suppression by anionic surfactants in capillary electrophoresis-electrospray ionization mass spectrometry. *Anal. Chem.* 1996, **68**: 3493-3497.
83. de Macedo, A.N.; Jiwa, M.I.Y.; Macri, J.; Belostotsky, V.; Hill, S.; Britz-McKibbin, P. Strong anion determination in biological fluids by capillary electrophoresis for clinical diagnosis. *Anal. Chem.* 2013, **85**: 11112-11120.
84. Kuehnbaum, N.L.; Kormendi, A.; Britz-McKibbin, P. Multisegment injection-capillary electrophoresis-mass spectrometry: A high-throughput platform for metabolomics with high data fidelity. *Anal. Chem.* 2013, **85**: 10664-10669.
85. Kuehnbaum, N.L.; Gillen, G.B.; Kormendi, A.; Lam, K.P.; DiBattista, A.; Gibala, M.J.; Britz-McKibbin, P. Multiplexed separation for biomarker discovery in metabolomics: Elucidating adaptive responses to exercise training. *Electrophoresis* 2015, **36**: 2226-2236.
86. de Macedo, A.N.; Mathiapparanam, S.; Brick, L.; Keenan, K.; Gonska, T.; Pedder, L.; Hill, S.; Britz-McKibbin, P. The sweat metabolome of screen-positive Cystic Fibrosis infants: revealing mechanisms beyond impaired chloride transport. *ACS Cent. Sci.* 2017, **3**: 904-913.
87. Soga, T.; Ueno, Y.; Naraoka, H.; Ohashi, Y.; Tomita, M.; Nishioka, T. Simultaneous determination of anionic intermediates for *Bacillus subtilis* metabolic pathways by capillary electrophoresis electrospray ionization mass spectrometry. *Anal. Chem.* 2002, **74**: 2233-2239.
88. Ramautar, R.; Somsen, G.W.; de Jong, G.J. CE-MS for metabolomics: Developments and applications in the period 2014-2016. *Electrophoresis* 2017, **38**: 190-202.
89. Ramautar, R.; Busnel, J.M.; Deelder, A.M.; Mayboroda, O.A. Enhancing the coverage of the urinary metabolome by sheathless capillary electrophoresis-mass spectrometry. *Anal. Chem.* 2012, **84**: 885-892.
90. Gulersonmez, M.C.; Lock, S.; Hankemeier, T.; Ramautar, R. Sheathless capillary electrophoresis-mass spectrometry for anionic metabolic profiling. *Electrophoresis* 2016, **37**: 1007-1014.
91. Osbourn, D.M.; Weiss, D.J.; Lunte, C.E. On-line preconcentration methods for capillary electrophoresis. *Electrophoresis* 2000, **21**: 2768-2779.
92. Nowak, P.M.; Woźniakiewicz, M.; Gładysz, M.; Janus, M.; Kościelniak, P. Improving repeatability of capillary electrophoresis—a critical comparison of ten different capillary inner surfaces and three criteria of peak identification. *Anal. Bioanal. Chem.* 2017, **409**: 4383-4393.

93. D'Agostino, L.A.; Lam, K.P.; Lee, R.; Britz-McKibbin, P. Comprehensive plasma thiol redox status determination for metabolomics. *J. Prot. Res.* 2011, **10**: 592-603.
94. Sugimoto, M.; Hirayama, A.; Ishikawa, T.; Robert, M.; Baran, R.; Uehara, K.; Kawai, K.; Soga, T.; Tomita, M. Differential metabolomics software for capillary electrophoresis-mass spectrometry data analysis. *Metabolomics* 2010, **6**: 27-41.
95. Boizard, F.; Brunchault, V.; Moulos, P.; Breuil, B.; Klein, J.; Lounis, N.; Caubet, C.; Tellier, S.; Bascands, J.L.; Decramer, S.; Schanstra, J.P.; Buffin-Meyer, B. A capillary electrophoresis coupled to mass spectrometry pipeline for long term comparable assessment of the urinary metabolome. *Sci. Rep.* 2016, **6**: 34453-34469.
96. Garcia-Perez, I.; Lindon, J.C.; Minet, E. Application of CE-MS to a metabonomics study of human urine from cigarette smokers and non-smokers. *Bioanalysis* 2014, **6**: 2733-2749.
97. Fernández-Bravo, J.; de Andrés, F.; Zougagh, M.; Rios, Á. Selective screening of glutaric acid acidurias by capillary electrophoresis-mass spectrometry. *J. Pharm. Biomed. Anal.* 2017, **145**: 40-45.
98. Chen, J.L.; Fan, J.; Lu, X.J. CE-MS based on moving reaction boundary method for urinary metabolomics analysis of gastric cancer patients. *Electrophoresis* 2014, **35**: 1032-1039.
99. Yu, L.; Jiang, C.; Huang, S.; Gong, X.; Wang, S.; Shen, P. Analysis of urinary metabolites for breast cancer patients receiving chemotherapy by CE-MS coupled with on-line concentration. *Clin. Biochem.* 2013, **46**: 1065-1073.
100. Kohler, I.; Schappler, J.; Rudaz, S. Highly sensitive capillary electrophoresis-mass spectrometry for rapid screening and accurate quantitation of drugs of abuse in urine. *Anal. Chim. Acta.* 2013, **780**: 101-109.
101. Gehlenborg, N.; O'Donoghue, S.I.; Baliga, N.S.; Goesmann, A.; Hibbs, M.A.; Kitano, H.; Kohlbacher, O.; Neuweger, H.; Schneider, R.; Tenenbaum, D.; Gavin, A.C. Visualization of omics data for systems biology. *Nat. Methods* 2010, **7**: S56-S68.
102. Weckwerth, W.; Morgenthal, K. Metabolomics: from pattern recognition to biological interpretation. *Drug Discov. Today* 2005, **10**: 1551-1558.
103. Dunn, W.B.; Wilson, I.D.; Nicholls, A.W.; Broadhurst, D. The importance of experimental design and QC samples in large-scale and MS-driven untargeted metabolomic studies of humans. *Bioanalysis* 2012, **4**: 2249-2264.
104. Armstrong, L.E. Hydration assessment techniques. *Nutr. Rev.* 2005, **63**: S40-S54.
105. Chetwynd, A.J.; Abdul-Sada, A.; Holt, S.G.; Hill, E.M. Use of a pre-analysis osmolality normalization method to correct for variable urine concentrations and for improved metabolomic analyses. *J. Chromatogr. A* 2016, **1431**: 103-110.

106. Gromski, P.S.; Muhamadali, H.; Ellis, D.I.; Xu, Y.; Correa, E.; Turner, M.L.; Goodacre, R. A tutorial review: Metabolomics and partial least squares-discriminant analysis – a marriage of convenience or a shotgun wedding. *Anal. Chim. Acta* 2015, **879**: 10-23.
107. van den Berg, R.A.; Hoefsloot, H.C.; Westerhuis, J.A.; Smilde, A.K.; van der Werf, M.J. Centering, scaling, and transformations: improving the biological information content of metabolomics data. *BMC Genomics* 2006, **7**: 142.
108. Xia, J.; Sinelnikov, I.V.; Han, B.; Wishart, D.S. MetaboAnalyst 3.0—making metabolomics more meaningful. *Nuc. Acids Res.* 2015, **43**: W251-W257.
109. Vinaixa, M.; Samino, S.; Saez, I.; Duran, J.; Guinovart, J.J.; Yanes, O. A guideline to univariate statistical analysis for LC/MS-based untargeted metabolomics-derived data. *Metabolites* 2012, **2**: 775-795.
110. Broadhurst, D.I.; Kell, D.B. Statistical strategies for avoiding false discoveries in metabolomics and related experiments. *Metabolomics* 2006, **2**: 171-196.
111. Gowda, G.A.N.; Raftery, D. Biomarker discovery and translation in metabolomics. *Curr. Metabolomics* 2013, **1**: 227-240.
112. Drucker, E.; Krapfenbauer, K. Pitfalls and limitations in translation from biomarker discovery to clinical utility in predicative and personalized medicine. *EPMA J* 2013, **4**: 7.
113. Crutchfield, C.A.; Thomas, S.N.; Sokoll, L.J.; Chan, D.W. Advances in mass spectrometry-based clinical biomarker discovery. *Clin. Proteom.* 2016, **13**: 1.
114. Tang, W.H.W.; Wang, Z.; Kennedy, D.J.; Wu, Y.; Buffra, J.A.; Agatista-Boyle, B.; Li, X.S.; Levison, B.S.; Hazen, S.L. Gut microbiota-dependent trimethylamine *N*-oxide (TMAO) pathway contributes to both development of renal insufficiency and mortality risk in chronic kidney disease. *Circ. Res.* 2015, **116**: 448-455.
115. Miller, M.J.; Kennedy, A.D.; Eckhart, A.D.; Burrage, L.C.; Wulff, J.E.; Miller, L.A.D.; Milburn, M.V.; Ryals, J.A.; Beaudet, A.L.; Sun, Q.; Sutton, V.R.; Elsea, S.H. Untargeted metabolomic analysis for the clinical screening of inborn errors of metabolism. *J. Inherit. Metab. Dis.* 2015, **38**: 1029-1039.
116. Williams, R.A.; Mamotte, C.D.S.; Burnett, J.R. Phenylketonuria: An inborn error of phenylalanine metabolism. *Clin. Biochem. Rev.* 2008, **29**: 31-41.
117. Imperlini, E.; Orrù, S.; Corbo, C.; Daniele, A.; Salvatore, F. Altered brain protein expression profiles are associated with molecular neurological dysfunction in the PKU mouse model. *J. Neurochem.* 2014, **129**: 1002-1012.
118. Allen, J.G.; Flanigan, S.S.; LeBlanc, M.; Vallarino, J.; MacNaughton, P.; Stewart, J.H.; Christiani, D.C. Flavoring chemicals in e-cigarettes: Diacetyl, 2,3-pentanedione, and acetoin in a sample of 51 products, including fruit-, candy-, and cocktail-flavoured e-cigarettes. *Environ. Health Perspect.* 2016, **124**: 733-739.

CHAPTER II.

METABOLOMIC STUDIES OF PHENYLKETONURIA

PATIENTS FOR ASSESSMENT OF DIETARY ADHERENCE

2.1 Abstract

Phenylketonuria (PKU) is an inherited metabolic disease caused by a deficiency of the enzyme phenylalanine hydroxylase (PAH), which is required for the conversion of phenylalanine (Phe) from dietary protein sources to tyrosine (Tyr). Management of PKU primarily involves lifelong dietary restriction of Phe while consuming a low protein diet that is essential to prevent irreversible cognitive impairment and severe mental disabilities early in life. Metabolomics offers a systematic approach to identify pathognomonic markers of PKU associated with clinical outcomes, as well as monitor dietary adherence during treatment monitoring. In this work, the urine and plasma metabolome of a cohort of classic PKU patients ($n = 23$) was characterized using multisegment injection-capillary electrophoresis-mass spectrometry (MSI-CE-MS) in order to confirm known disease biomarkers associated with Phe catabolism, as well as identify new markers associated with disease progression and dietary compliance. An intermethod comparison of MSI-CE-MS was first validated for accurate quantification of plasma Phe and Tyr from PKU patients relative to UPLC-UV, which demonstrated good mutual agreement with bias under 10%. We also confirmed that plasma Phe concentrations were strongly correlated with the excretion of urinary Phe as well as several host derived Phe catabolites and gut microflora by-products, such as *N*-phenylacetylglutamine, phenylpyruvate, and phenylsulfate. Nontargeted metabolite profiling by MSI-CE-MS based on

circulating plasma Phe levels and Phe excretion in urine was also carried out to identify novel biomarkers associated with PKU disease status. Multivariate and univariate analysis of single-spot urine samples classified by Phe excretion showed significant decreases in carnitine and short- and medium-chain acylcarnitines, which suggested that accumulation of Phe and phenylacetate is associated with inhibition of fatty acid β -oxidation. Additionally, two histidine catabolites in urine were strongly correlated with Phe excretion, which may reflect micronutrient/vitamin deficiencies caused by poor dietary adherence. Overall, analysis of the urine metabolome from PKU patients has demonstrated its potential clinical utility for therapeutic treatment monitoring, as it is noninvasive, it includes several clinically relevant pathognomonic markers of PKU, and it may allow for evaluation of dietary compliance and/or nutritional deficiencies that is especially problematic in older children and adults.

2.2 Introduction

2.2.1 Inborn Errors of Metabolism

Inborn errors of metabolism (IEM) are rare genetic diseases causing partial or complete loss of enzyme activity, which can have severe implications in birth outcomes for affected children, including death or lifelong disabilities.^{1,2} The predominant mechanism in the majority of IEM is protein misfolding and loss of function as a result of various types of genetic mutations.³ The folding of proteins into their three-dimensional native conformations is necessary for full

functionality; mutations in the amino acid sequence may lead to reduced thermodynamic stability due to changes in hydrophobic interactions between side chains.^{1,3} Molecular chaperones are responsible for regulating protein assembly and for stabilizing protein conformations from natural (*e.g.*, heat shock or oxidative stress) and acquired (*e.g.*, genetic mutations) stress.⁴ Early diagnosis and treatment of IEM is critical to avoid the onset of adverse health outcomes.⁵ Universal newborn screening (NBS) was first implemented in the early 1960s with the successful detection of PKU.⁶ Robert Guthrie first introduced a bacterial inhibition assay for the screening of PKU that employed dried blood spots (DBS) on filter paper as a simple method for specimen collection and transport. Population-based screening of newborns for PKU has contributed to significant socioeconomic benefits due to early detection and prevention of lifelong developmental disabilities with long-term healthcare savings as compared to symptomatic diagnosis.^{7,8} Prior to the introduction of tandem mass spectrometry (MS/MS), PKU and congenital hyperthyroidism were widely screened in infants at birth using conventional biochemical assays.⁹ However, the advent of MS/MS technology within accredited clinical laboratories now allows for selective, sensitive, and high-throughput screening of biomarkers associated with dozens of IEM at incremental costs in a multiplexed manner unlike classic immunoassay and enzyme kinetic assays.⁸⁻¹⁰

2.2.2 Phenylketonuria

PKU is an autosomal recessive disorder due to a functional deficiency of hepatic phenylalanine hydroxylase (PAH), the enzyme responsible for catalyzing the hydroxylation of *L*-phenylalanine (Phe) to *L*-tyrosine (Tyr).^{11,12} Human PAH is a homo-tetrameric enzyme that requires binding of iron (II), together with molecular oxygen (O₂) and a redox-active co-factor, tetrahydrobiopterin (BH₄), to the active site as shown in the reaction scheme in **Figure 2.1**.¹³ In humans, PAH is the initial rate-limiting step in the degradation of Phe from dietary protein. Mammalian PAH is composed of four identical 50 kDa subunits (**Figure 2.2**), each of which possesses an *N*-terminal regulatory domain (residues 1-110), a catalytic domain (residues 111-410), and a *C*-terminal oligomerization domain (residues 411-452).^{10,14} Binding of Phe to the regulatory domain leads to conformational changes involving the dimer-tetramer equilibrium, triggering the activation of PAH.^{15,16}

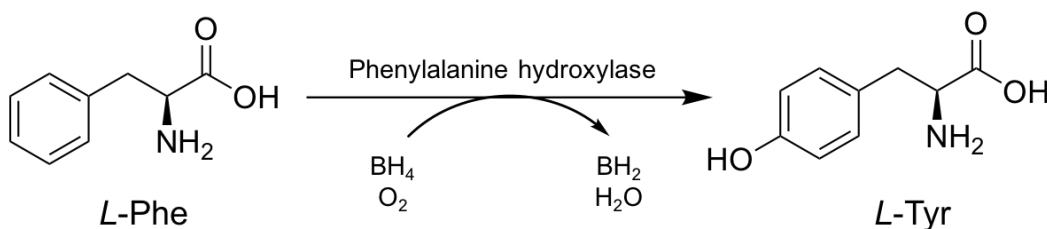


Figure 2.1. The PAH-catalyzed reaction converting Phe to Tyr in the presence of iron, molecular oxygen, and tetrahydrobiopterin (BH₄).¹¹

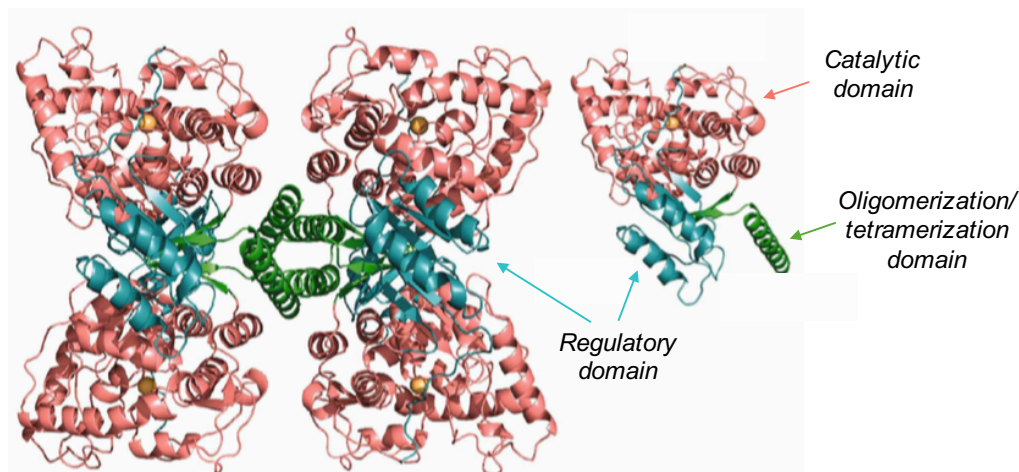


Figure 2.2. Crystal structure of tetrameric human PAH.¹⁷ Each subunit consists of three domains: the N-terminal regulatory domain, the catalytic domain, and the C-terminal oligomerization domain.

Clinically relevant mutations of PAH lead to protein misfolding, resulting in a severe accumulation of Phe, as well as a risk for Tyr deficiency if not supplemented in the diet. There are over 600 known PKU-causing mutations — the majority of which are missense mutations (62%) or small/large deletions (13%) on the PAH gene, which is located on chromosome 12q23 (**Table 2.1**).^{17,18} While some mutations are variants of unknown significance (13%) or benign variants (13%), the majority of mutations are pathogenic or likely pathogenic (74%),¹⁹ affecting PAH enzymatic activity, oligomerization, thermal stability, and/or folding. These mutations are associated with reduced activity (*i.e.*, residual activity range of 2% to 70%) or complete abolishment of PAH activity (*i.e.*, < 2% residual activity), which is most commonly associated with classic PKU.¹⁸⁻²¹ The PKU phenotype is a complex trait with Mendelian inheritance that shows a broad range of symptoms that manifest among affected individuals. Moderate to severe

Table 2.1. Most common disease-causing mutations associated with classic PKU.²²⁻²⁶

<i>PAH Mutation</i>	<i>Mutation Type</i>	<i>Frequency</i>	<i>Phenotype</i>
R408W	Missense	9.22%	Affects catalytic domain, severe structure mutation, decreased stability, folding defect ²³
IVS10-11G>A	Splice	7.24%	Loss of catalytic activity due to conformational change ²⁴
I65T	Missense	5.60%	Affects regulatory domain, impaired hydrophobic packing at dimer interface ^{25,26}
R261Q	Missense	4.91%	Affects catalytic domain, impaired dimer/tetramer formation ²⁵
P281L	Missense	4.01%	Affects catalytic domain, active site mutation ²⁶

phenotypes (*i.e.*, classic PKU) are a result of severe mutations that are present homozygously or heterozygously with a mild mutation, whereas higher residual enzymatic activity of PAH as a result of a mild mutation usually leads to a milder disease phenotype.^{27,28} Phenotypic variability between individuals with the same genotype is thought to be a result of between subject differences in gene products involved in protein stability, such as molecular chaperones.²⁸ PKU is diagnosed based on repeat measurement of elevated Phe in plasma shortly after birth following a screen-positive result by MS/MS in NBS. In this case, Phe is grossly elevated well above a population mean of about 60 μM for healthy infants with unrestricted feeding (*e.g.*, breast feeding or formula).²⁹ An upper cut-off of Phe above the 99th percentile of a normal infant population is often used to reduce false negatives and maximize detection of PKU in affected infants; however, this is periodically reviewed and adjusted.³⁰ Classic or severe PKU makes up the majority of PKU cases requiring prompt treatment, and is defined by plasma Phe > 1,200 μM , whereas mild PKU is classified by Phe concentrations ranging from

600 to 1,200 μM .¹⁷ Additionally, non-PKU hyperphenylalaninemia (HPA) is defined for screen-positive infants with plasma Phe concentrations that are between an upper reference limit of 120-150 μM and 600 μM . Non-PKU HPA is related to mild mutations affecting PAH, however do not lead to major elevations of Phe or Phe metabolites and thus do not require treatment. Malignant PKU is caused by defects in the synthesis or recycling of the PAH co-factor, BH_4 , and can usually be discriminated from PKU with a BH_4 loading test.³¹ **Table 2.2** highlights that the prevalence of PKU varies widely by country and ethnicity, however it is highest in Turkey (1:2,600) and Ireland (1:4,500).¹¹ Also, it is most prevalent among Caucasians (1:10,000 births), whereas it has a much lower incidence among Japanese.^{11,29}

Table 2.2. Incidence of PKU by country.^{11,12,32}

<i>Country</i>	<i>Incidence</i>
Turkey	1:2,600
Ireland	1:4,500 ¹¹
Israel (Yemenite Jewish)	1:5,300
Scotland	1:5,300
Czechoslovakia	1:7,000
Australia	1:10,000
Hungary	1:11,000
Denmark	1:12,000
France	1:13,500
United Kingdom	1:14,300
Norway	1:14,500
Canada	1:15,000 ¹²
United States	1:15,000 ³²
China	1:17,000
Italy	1:17,000
Japan	1:125,000

2.2.2.1 Pathogenesis and Clinical Symptoms of PKU

The accumulation of Phe from PKU leads to irreversible brain damage resulting in intellectual impairment and poor cognitive function in affected children.¹⁷ Phe is an essential amino acid that is derived exclusively from diet and/or proteolysis (*i.e.*, protein turn-over).³¹ Clinical symptoms also include eczema and hypopigmentation of the skin and hair due to reduced melanin production, as well as growth deficiencies and behavioural problems such as hyperactivity, aggressiveness and anxiety.^{17,33,34} Severely elevated levels of Phe and its catabolites leads to neurotoxicity due to oxidative stress, mitochondrial dysfunction, altered cerebral protein/neurotransmitter synthesis, and impaired lipid metabolism.³⁵ There is evidence of increased protein and lipid oxidative damage, increased production of reactive oxygen species, and decreased antioxidant levels in PKU patients as a result of accumulation of Phe and its catabolites. Another mechanism contributing to the neurotoxicity in classic PKU is related to a deficiency in essential amino acids in the brain as a result of saturation of the large amino acid transporter 1 (LAT-1) by Phe.^{17,36} The LAT-1 transporter is responsible for delivering the large neutral amino acids (LNAA) across the blood-brain barrier.³⁶ LAT-1 has the highest affinity to Phe in comparison to the other LNAAs; elevated blood Phe therefore leads to increased uptake of Phe into the brain compromising transport of other LNAAs. For instance, Tyr is a precursor of melanin, *L*-thyroxine, and the catecholamine neurotransmitters dopamine, norepinephrine, and epinephrine.¹¹ The latter

neurotransmitters rely on tyrosine hydroxylase activity to form the key intermediate, 3,4-dihydroxy-*L*-phenylalanine (DOPA), that is inhibited by elevated Phe.³⁷ Also, saturation of LAT-1 leads to reduced availability of the other LNAAs, which impairs cerebral protein synthesis and monoaminergic neurotransmitter synthesis.³⁸ Impaired transport of tryptophan (Trp) across the blood-brain barrier leads to reduced brain serotonin synthesis.³⁹ Serotonin and dopamine are involved in post-natal brain development and maturation, which may explain some of the cognitive disabilities in classic PKU patients. Recent work has shown decreased cerebral glucose metabolism and deficiencies of proteins involved in glycolysis and the tricarboxylic acid (TCA) cycle in PKU mouse models.²¹ Impaired lipid metabolism is suggested to be a factor in the hypomyelination commonly associated with PKU patients; many lipoproteins, such as cholesterol, high-density lipoprotein (HDL), low-density lipoprotein (LDL), and long-chain polyunsaturated fatty acids, are lower in individuals with PKU.³⁵ The pathogenesis of PKU is still not fully understood; however, it is proposed that the combination of metabolic alterations as a result of high Phe leads to brain damage and cognitive impairment in PKU. In this context, new advances in nontargeted metabolite profiling of PKU patients may contribute to a better understanding of the pathophysiology of PKU, as well as differences in disease progression and treatment responses of individual patients with the same genotype.

2.2.3 Current Treatment Options for PKU

The early detection of PKU by universal NBS programs and immediate dietary restriction of Phe prevents the onset of severe symptoms. However, population screening needs to be integrated with treatment monitoring since lifelong dietary restriction of Phe and amino acid supplementation is essential to ensure normal growth and development during infancy and throughout childhood.¹¹ Other treatment options with varying success include Phe restriction together with LNAA therapy, as well as supplementation with the enzyme's natural co-factor, BH₄, or enzyme replacement therapy using PEGylated phenylalanine ammonia-lyase (PAL) for classic PKU patients. The synthetic form of BH₄, sapropterin hydrochloride (Kuvan), acts as a chaperone that assists in the folding/stabilization of mutant PAH, and is most effective in non-PKU HPA patients or patients with mutations causing defects in BH₄ synthesis/recycling.⁴⁰ While Kuvan may allow for less restrictive dietary adherence, it is expensive (*i.e.*, up to \$166,000 USD per year)⁴¹ and, importantly, only 40% of mild-to-moderate PKU cases are found to be responsive to Kuvan treatment.⁴² PAL, an enzyme found abundantly in yeast, plants, and fungi, is responsible for the biotransformation of Phe into *trans*-cinnamic acid and ammonia.⁴³ The conjugation of PAL with polyethylene glycol (PEG) improves drug stability, efficacy, and safety, at the expense of a reduction in PAL activity by 75%.^{44,45} Treatment with PAL is currently undergoing phase 3 clinical trials to assess its efficacy for reducing circulating Phe in PKU patients (*i.e.*, $\geq 30\%$ to be

considered therapeutically effective);⁴³ however, it is limited by its high costs, the need for daily subcutaneous injections, and potential adverse effects (*e.g.*, immune reactions and infection) that require careful therapeutic monitoring.⁴⁴ There is, therefore, a critical need for new treatment strategies that are both cost effective and efficacious for treatment of classic PKU, which ultimately supports normal growth and development during childhood without burdensome lifelong dietary restrictions.

2.2.3.1 Lifelong Dietary Management for Classic PKU

Following confirmatory diagnosis of mild or classic PKU (blood Phe > 360 μM),²⁶ dietary restriction of Phe is initiated promptly to promote normal growth and neurodevelopment.¹¹ Dietary management is not recommended for mild PKU or HPA with blood Phe levels between 120 and 360 μM , however they are still monitored closely to ensure Phe levels do not increase with higher protein intake. The goal of dietary restriction is to maintain blood Phe concentrations within safe limits (120-360 μM), however diet should still allow adequate protein intake to prevent undernutrition.^{26,45} Phe restriction, when supplemented with reduced or Phe-free amino acid mixtures, is very effective in preventing symptoms of PKU. However, the specific diet for individual PKU patients vary based on the estimated tolerance for Phe, which is influenced by residual PAH activity, as well as other genetic factors (*i.e.*, mutation), age, sex, growth, general health, and disease severity.⁴⁷ Frequent monitoring of the patient's diet and plasma Phe levels

is thus required to ensure treatment success. Within the first year of life, blood Phe levels are typically monitored weekly, with special care to monitor during periods of rapid growth and/or introduction of solid food.²⁶ In children between 1 and 12 years, monitoring is decreased to biweekly or monthly. Foods high in protein (*e.g.*, dairy, meat, fish, eggs, legumes, nuts/grains) are excluded from the diet and Phe-free protein is sourced from commercial medical foods and/or infant formula. The PKU formula, which is enriched in amino acids (excluding Phe), minerals, vitamins, and other nutrients, provides > 80% of the individual's protein and energy needs for classic PKU patients.⁴⁷ Furthermore, supplementation with LNAAs (*e.g.*, Leu, His, Trp, Tyr, Met) has shown to reduce brain Phe concentrations, with improved neuropsychological outcomes in treated PKU patients.⁴⁸ Medical foods which have been modified to be low-protein and/or Phe-free are an important calorie source for PKU patients given their dietary restrictions.²⁶

Glycomacropeptide (GMP), which is derived from cheese whey and occurs naturally in bovine milk, is a source of naturally Phe-free protein.^{45,49} It is a 64-amino acid glycoposphopeptide that contains no aromatic amino acids in its primary structure (*i.e.*, Phe, Tyr, Trp) with a high fraction of isoleucine (Ile) and threonine (Thr) residues.⁴⁹ With the addition of other LNAAs, GMP offers an alternative protein-source to the synthetic amino acid formulations widely used in PKU medical foods and formula. GMP supplements have been reported to be more palatable than conventional formulas in addition to improving the efficiency

of protein utilization, nitrogen retention, and long-term bone health.⁵⁰ Also, the use of GMP within the diet of PKU patients may improve dietary compliance; however, the metabolic and nutritional impacts of GMP are still being investigated.⁴⁹ However, GMP often still contains low residual levels of Phe from whey protein impurities that requires testing for quality assurance.⁵¹ Indeed, short term studies have shown no significant changes in plasma Phe levels with an increase in blood Tyr.^{51,52} Daly *et. al.*⁴⁹ reported loss of blood Phe control (increased blood Phe and decreased Tyr) with 6-month pilot treatment of GMP in 22 PKU patients. The mixed results suggest that careful monitoring of individuals consuming GMP-containing medical foods should be carried out, including better process control and manufacturing standards in GMP products. The introduction of more palatable medical foods, including high purity GMP-based medical foods, has improved dietary adherence of PKU patients, especially into adulthood. These medical foods, however, are more expensive in comparison to non-modified foods and costs are not likely to be fully covered, if at all, by third-party insurance payers.²⁶ Many PKU patients struggle with maintaining their blood Phe concentrations within the range of 120 to 360 μM , as recommended by the American College of Medical Genetics and Genomics (ACMGG).⁵³ A study by the National PKU Alliance (NPKUA) showed that, of 625 survey participants, less than half (46.7%) reported blood Phe under 360 μM . Additionally, dietary adherence for adults is much lower than that of young children and adolescents, with children being 3-times more likely to keep blood Phe levels within the

recommended range. For example, blood Phe over 360 μM was reported in 25.5% of individuals under 18 years ($n = 329$), in comparison to 61.5% of adults ($n = 286$).⁵³ One of the major challenges associated with dietary compliance is poor insurance coverage of medical formula and low-protein food products.³⁰ In the United States, 50% of states provide no coverage or only partial coverage of medical formula for PKU and other orphan diseases; for individuals without coverage, the cost of formula/medical foods or the insurance deductible cost for those with coverage may be too high for the patient to afford. Several socioeconomic barriers exist such as unemployment, few adult PKU clinics, transportation-related issues, and lack of familial support which collectively contribute to poor accessibility and dietary adherence. Since current treatments are limited by high costs and variable efficacy, there is an urgent need for better strategies to improve health outcomes in affected PKU patients.

2.2.4 Metabolomic Studies of PKU

In clinical metabolomics, the nontargeted profiling of metabolites in complex biological samples has offered new insights into the mechanisms of disease, including biomarker discovery, as required for improved screening, diagnosis, and/or treatment monitoring.⁵⁴⁻⁵⁶ A major hurdle, however, is understanding the physiological roles of metabolites and their pathways in affected patients. To date, there have been few metabolomic studies of PKU, which have primarily focused on targeted profiling of known compounds associated with the disease, such as

catabolites of Phe and Tyr. For instance, targeted metabolomics using GC/MS and LC-MS/MS reported that PKU children following a Phe-restricted diet with low dietary intake of saturated/unsaturated fatty acids had lower serum free carnitine (C0) and acylcarnitine (C2, C3, C6, C18) levels as compared to healthy controls.⁵⁷ Recently, a study by Blasco *et. al.*⁵⁸ conducted a cross-platform (GC/MS, NMR, amino acid analyzer) metabolomics study comprising 118 known metabolites detected in matching urine and plasma samples from a small cohort of PKU patients. Using univariate and multivariate statistical analysis, the authors demonstrated a negative correlation between Arg, α -aminobutyric acid, and Phe, in contrast to a positive correlation between Arg, succinic acid, Gln, and Tyr. This work also confirmed the pathophysiology of PKU due to elevated circulating Phe concentrations contributed to aberrant metabolic pathways associated with protein synthesis, central energy metabolism, and oxidative stress. Recently, Ney *et. al.*⁵⁹ used metabolomics to assess metabolites and neurotransmitters derived from Tyr and Trp in PKU patients consuming a standard Phe-free fortified diet as compared to a GMP medical food product. This study noted reduced bioavailability and altered metabolism of Tyr and Trp in PKU patients consuming a standard amino acid formulation as a result of changes in intestinal microflora activity. However, long-term dietary studies are still required to fully validate the efficacy of specialized Phe-restricted protein products on improving primary clinical outcomes (*i.e.*, growth and cognitive function) among classic PKU patients. Given the highly variable phenotype that is dependent on the complex interactions of

genes, diet, and gut microbiota, there is an urgent need to better characterize the metabolome of PKU patients that may also objectively assess dietary compliance or identify poor responders to intervention.

Herein, we examined the plasma and urine metabolome using multisegment injection-capillary electrophoresis-mass spectrometry (MSI-CE-MS)^{60,61} from a representative cohort of 23 classic PKU patients spanning various ages, disease severity, and nutritional status. This cross-sectional study confirmed that plasma Phe was strongly correlated with urinary excretion of a Phe, as well as a wide range of Phe catabolites, such as phenylsulfate, phenylpyruvate and *N*-phenylacetylglutamine. Nontargeted metabolite profiling by MSI-CE-MS was also carried out to identify novel biomarkers associated with PKU disease status when using complementary univariate and multivariate statistical methods. Overall, the goal of this project was to expand understanding of the metabolic phenotype of classic PKU patients who exhibit highly different circulating Phe levels due to poor dietary compliance.

2.3 Experimental

2.3.1 Chemicals and Reagents

All chemicals were obtained from Sigma-Aldrich Inc. (St. Louis, MO, USA). All aqueous buffers and stock solutions were prepared with deionized water (dH₂O) using a Thermo Scientific Barnstead EasyPure II LF ultrapure water system and stored in plastic, transport tubes. Amino acid standard mixtures,

internal standards, and the sodium azide solutions were stored at 4° C, whereas aqueous background electrolytes (BGE) and sheath liquid solutions were stored at room temperature.

2.3.2 Instrumentation

Therapeutic monitoring of PKU patients based on circulating concentrations of Phe and Tyr was performed by a validated amino acid analyzer based on a Waters Acquity UPLC system with UV detection using a MassTrak kit for amino acids. MSI-CE-MS experiments were performed using an Agilent G7100A CE system interfaced with a coaxial sheath liquid Jet Stream electrospray ion (ESI) source with heated gas to an Agilent 6230 time-of-flight-mass-spectrometer (TOF-MS). The nebulizer gas in the ESI source and the drying gas for MS were nitrogen gas, and the damping/collision gas was helium gas. The sheath liquid for positive ion mode was 60% MeOH/H₂O with 0.1% formic acid and was 50% MeOH/H₂O for negative ion mode conditions. Purine and HP-921 were added into the sheath liquid (0.02%) for reference mass calibration (m/z 121.050873 and m/z 922.009798, respectively). The instrument was run in 2GHz extended dynamic range (EDR) mode. An uncoated fused-silica capillary with an internal diameter of 50 μ m and total capillary length of 120 cm was conditioned by flushing with methanol, 1 M sodium hydroxide (NaOH), deionized H₂O (dH₂O), and background electrolyte (BGE) at high pressure for 30 min each. The BGE used for positive-ion mode (detection of cationic metabolites) was 1 M formic

acid with 15% acetonitrile (ACN) at pH 1.8, whereas the BGE for negative-ion mode (detection of anionic metabolites) was 50 μ M ammonium bicarbonate (NH_4HCO_3) at pH 8.5. For MSI, the samples were injected hydrodynamically (100 mbar, 5 s) between spacer segments of BGE (100 mbar, 40 s), for a total injection time of approximately 5 min.⁶⁰ A QC sample was included in a randomized position in the MSI injection sequence. After sample injection, an applied voltage of 30 kV was applied to begin separation for a total run time of 45 to 60 min. All runs were performed with the capillary temperature maintained at 25°C. Between runs, the capillary was flushed with BGE for 10 min. At the beginning of each day, an amino acid standard mixture run and QC run (6 injections of the QC sample with a dH_2O blank) were performed to assess instrument performance prior to running plasma/urine samples. Capillaries were rinsed with dH_2O (10 min) and air (10 min) for overnight storage.

2.3.3 Study Cohort Selection and Ethics Approval

25 PKU patients were recruited to participate in a 1 year cross-sectional study. The majority of PKU patients had an initial diagnosis of classic PKU based on elevated plasma Phe ($> 1,200 \mu\text{M}$) with the exception of 2 cases having mild PKU or HPA. Participants were approached and recruited by convenience during regular clinical visits to McMaster Children's Hospital. The study protocol was approved by the Hamilton Integrated Research Ethics Board (HiREB project #1459, July 2016). Signed informed consent was acquired from all participants.

Most participants provided a random single-spot urine sample at each appointment as well as provided access to food records, patient information, and non-fasting plasma specimens as part of routine therapeutic monitoring during clinical visits. All identifiers except age, sex, clinical diagnosis, treatment regime, and formula information were removed and replaced with a study number to protect participant privacy.

2.3.4 Sample Collection and Preparation

Random single-spot urine samples were collected mid-stream in sterile containers during clinical visits and stored at 4°C prior to the addition of preservative solution (1 mM sodium azide) with recovery standards (RS) 100 µM 4-fluorophenylalanine (F-Phe) and 100 µM HEPES.⁶² Urine samples were thawed on ice, vortexed for 30 s, and particulate matter was precipitated by centrifugation at 1,500 *g* for 5 min. Urine was then diluted five-fold in dH₂O with 20 µM 3-chlorotyrosine (Cl-Tyr) and 50 µM naphthalene monosulfonic acid (NMS) as internal standards (IS). Blood samples were collected in heparin-coated tubes and plasma was separated. Blood plasma remaining after clinical testing was aliquoted and stored at -80°C prior to analysis. For infant/child PKU patients who had frequent clinical appointments, repeat plasma samples were collected over an 8 month period. Plasma was diluted four-fold with dH₂O containing 20 µM Cl-Tyr, 20 µM F-Phe, 20 µM NMS, and 5 mM ¹³C-glucose as IS/RS and vortexed for 30 s. Plasma proteins were filtered by ultracentrifugation using a 3 kDa MWCO

Nanosep centrifugal device (Pall Life Sciences, Washington, NY, USA) at 14,500 *g* for 15 min.

2.3.5 Data Processing

After extraction of raw data with Mass Hunter Workstation Qualitative Analysis software (Agilent Technologies Inc.), nontargeted metabolite profiling was performed using Molecular Feature Extractor (MFE) and Molecular Formula Generator (MFG) within Qualitative Analysis. A dilution trend filter was first applied when using MSI-CE-MS based on a serial 7-plug sample injection of a pooled urine or a pooled plasma sample (1x, 2x, 4x, 8x) from the PKU cohort together with a blank (dH₂O).⁶⁰ This strategy allowed for identification of authentic, yet reliable, molecular features originating from samples while rejecting spurious or background signals that comprise a majority of signals generated during spray formation in ESI-MS.⁶⁰ Urine and plasma samples were subsequently analyzed using MSI-CE-MS with a pooled QC sample included in a randomly selected injection position. All samples were run in positive and negative ion mode conditions over a period of 1 week. Urine and plasma metabolites were tentatively identified from a compiled personal database library and/or searching an online metabolomic databases including METLIN (<http://metlin.scripps.edu>) and the Human Metabolome Database (<http://hmdb.ca>). In urine, 58 cationic and 18 anionic metabolites were consistently detected with adequate precision in the QC samples (CV < 40%, *n* = 5) in the majority of classic PKU cases (present in > 75% of samples). In plasma, 36 cationic and 19 anionic

metabolites were detected in the pooled QC with adequate precision ($CV < 40\%$, $n = 15$) and consistently measured in $> 75\%$ of samples. Unique metabolites annotated by their characteristic accurate mass (m/z) and relative migration time (RMT) as their molecular ion (MH^+ or $M-H^-$) were extracted based on a target peak list selected from the dilution trend filter after excluding redundant signals derived from co-migrating adducts or in-source fragments. Peaks were smoothed (Savitzky-Golay quadratic/cubic function, 15 points) and integrated in profile mode using a 10 ppm mass window. Ion responses and migration times were normalized to an IS (*i.e.*, Cl-Tyr for positive ion mode and NMS for negative ion mode) to improve method precision.

2.3.6 Calibration and Method Validation

External calibration curves for Phe and Tyr were prepared in triplicate ($n = 3$) using MSI-CE-MS by serial dilution in dH_2O with 20 μM Cl-Tyr and 20 μM F-Phe as IS. Linearity was measured over a 400-fold concentration range (0.5 μM to 200 μM). Linear least-squares regression was used to calculate the calibration equation for Phe ($y = 0.148x - 0.205$) and Tyr ($y = 0.182x - 0.177$). Good linearity ($R^2 > 0.996$) was observed for each calibration curve. The LOD was estimated based on a signal-to-noise ratio (S/N) of ≈ 3 to be 0.1 μM and 0.3 μM for Phe and Tyr, respectively. MedCalc (MedCalc® Software) was used for intermethod comparison analysis (Bland-Altman percent difference, Passing-

Bablok regression) of plasma Phe and Tyr concentrations measured independently by MSI-CE-MS and UPLC-UV.

2.3.7 Statistical Data Analysis

Extracted ion electropherograms were prepared in Igor Pro 5.0 (Wavemetrics Inc., Lake Oswego, OR, USA). Linear regression was performed in Excel 2007 (Microsoft Inc., Redmond, WA, USA). SPSS Statistics (IBM, v. 23) and MetaboAnalyst 3.0 (McGill University) were used for data normalization/transformation and univariate/multivariate statistical tests. Features with > 75% missing values were removed from the data set. Missing values (*i.e.*, no signal integrated) were estimated by half of the minimum value. Urinary metabolites were corrected using probabilistic quotient normalization (PQN) to correct for differences in urine dilution.⁶³ Urinary and plasma metabolites were assessed for normality using the Shapiro-Wilk test. Nonparametric tests were used on nontransformed data that did not show normality with *log*-transformation. Group differences between normally distributed metabolites were assessed using *t*-tests and one-way ANOVA, whereas non-normally distributed data was assessed using Mann Whitney U or Kruskal-Wallis H tests as appropriate. Correlation analysis was assessed using a Spearman's ranks test. For multivariate statistical analysis, data were *log*-transformed, mean-centered, and scaled by dividing by the standard deviation of each variable (*i.e.*, auto-scaling). Also, partial least squares-discriminant analysis (PLS-DA) was used to identify metabolites that discriminate between circulating Phe status (*i.e.*, low versus high) among PKU patients, with

feature selection determined by variable importance in projection (VIP) scores (MetaboAnalyst 3.0) to rank significant features associated with disease severity.

2.4 Results and Discussion

2.4.1 Study Design and Cohort Characteristics for PKU Patients

A representative cohort of 23 classic PKU patients (defined as Phe > 1,200 μM upon initial diagnosis) and 2 mild PKU/HPA (Phe from 160 to 360 μM) patients provided urine and/or blood plasma samples in this cross-sectional metabolomics study. A summary of the characteristics of the PKU cohort (classic PKU) is highlighted in **Table 2.3**, with individual information for each patient reported in **Supplementary Table S2.1**. Overall, the cohort was comprised of infants, children, and adults (aged from 0.2 to 50 years) with plasma Phe concentrations ranging from 30 to over 1,500 μM . Individuals with mild PKU/HPA ($n = 2$) were excluded from the study in order to focus analysis on classic PKU patients recommended to follow Phe-restricted diets. Adult patients (> 18 y) were found to have, on average, three-fold higher plasma Phe concentrations as compared to children and were two times more likely to have plasma Phe concentrations greater than the recommended ACMGG cut-off of 360 μM . Furthermore, there was a significantly greater frequency of poor dietary adherence among adults since they were less likely to be consuming specialized Phe-free amino acid formula/medical foods. This confirms previous work reporting higher blood Phe concentrations and poor dietary compliance in adult

Table 2.3. Summary of the cohort of 23 classic PKU patients grouped by age (adult vs. children) recruited in this cross-sectional study with matching plasma and urine specimens collected.

<i>Criterion</i>		<i>Children</i> 0 – 18 y	<i>Adults</i> > 18 y
<i>Age (years)</i>	<i>n</i>	14	9
	Mean (SD)	7.2 (4.3)	32.1 (9.3)
	Min – Max	0.2 – 14.0	23.0 – 50.0
<i>Sex</i>	Male, <i>n</i> (%)	9 (64%)	3 (33%)
	Female, <i>n</i> (%)	5 (36%)	6 (67%)
<i>Plasma Phe (μM)</i> ¹	Missing, <i>n</i> (%)	1 (7.1%)	4 (44.4%)
	< 360 μM, <i>n</i> (%)	9 (64.3%)	1 (11.1%)
	> 360, <i>n</i> (%)	4 (28.6%)	4 (44.4%)
	Average (SD)	263.2 μM (173.7)	862.4 μM (500.4)
<i>Treatment</i>	Formula ² , <i>n</i> (%)	14 (100%)	4 (44.4%)
	Kuvan, <i>n</i> (%)	4 (28.6%)	1 (11.1%)
<i>Dietary Adherence</i> ³	Poor, <i>n</i> (%)	0 (0%)	6 (66.6%)
	Excellent, <i>n</i> (%)	9 (64.3%)	1 (11.1%)

¹ Significantly different plasma Phe concentration between children and adult PKU patients ($p < 0.05$)

² Phe-free amino acid supplementation

³ Dietary adherence was evaluated using diet records and ranked as 'poor' if it was noted that they were not following a controlled diet and/or food intake showed high Phe consumption.

PKU patients in comparison to children.^{53,64} Additionally, one adult patient (50 y) was not screened by NBS at birth and did not benefit from early detection and treatment. The PKU cohort is thus highly heterogeneous, which introduces challenges in data interpretation due to large biological variability in circulating Phe status that are confounded by factors such as age, dietary compliance and disease progression.

2.4.2 Method Validation and Intermethod Comparison

MSI-CE-MS was applied as a high-throughput platform for nontargeted metabolite profiling of plasma filtrates ($n = 19$) and single-spot/random urine ($n = 16$) specimens collected from 23 classic PKU cases over a recruitment period of 8 months, with 12 patients providing matching plasma and urine samples. Repeat

plasma samples were also collected over time among a subset of recently diagnosed PKU infants. In this case, multiplexed CE separations together with high-resolution MS allows for rapid screening of diverse classes of polar/ionic metabolites in conjunction with accelerated data workflows for biomarker discovery with quality assurance.⁵⁵ For instance, serial sample injections enable analysis of seven randomized sample plugs within a single run, including a pooled urine or plasma filtrate specimen to serve as a quality control (QC). **Figure 2.3** depicts an overlay of CE current traces from a total of 40 runs for 272 samples using (A) acidic BGE/positive ion and (B) alkaline BGE/negative ion modes for analysis of cationic and anionic metabolites, respectively. This provides a simple means to monitor for instrument stability and robustness during data acquisition over 8 days when using MSI-CE-MS. Overall, there was good reproducibility in CE current traces between days with CVs < 3%. Additionally, quality assurance measures also included the use of control charts for monitoring the recovery standard (F-Phe, 20 μ M) within all samples analyzed (including pooled QC specimens) by MSI-CE-MS in positive ion mode as shown in **Figure 2.4**. Overall, the apparent ion response ratio measured for F-Phe in positive ion mode (total $n = 136$) displays normal random variation in plasma (CV = 4.7%) and urine (CV = 6.5%) within acceptable limits with only one outlier exceeding outer limits of confidence. The apparent ion response ratio for F-Phe measured in negative ion mode showed similar trends for plasma (CV = 20.6%) and urine (CV = 24%) with all data points within the limits of confidence. This provides confidence when

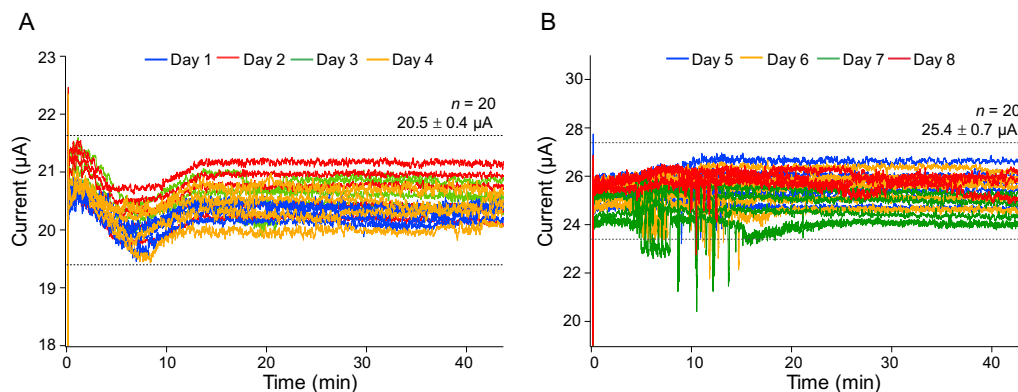


Figure 2.3. Overlay of CE current traces for 40 runs over 8 days by MSI-CE-MS for metabolomic analyses of plasma and urine samples with full-scan data acquisition in (A) positive and (B) negative ion mode detection. There was good reproducibility in CE current traces in positive and negative ion mode with CVs of 1.8% and 2.6%. Upper and lower action limits (dashed line) for excluding runs were determined by $\pm 3SD$.

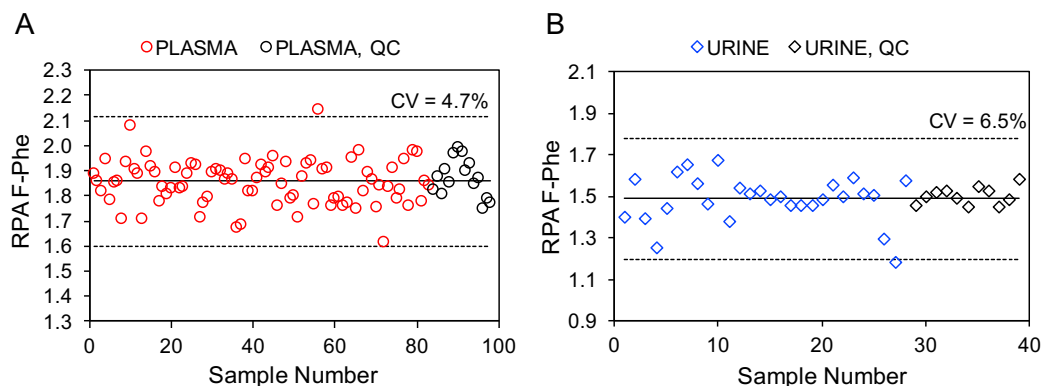


Figure 2.4. A control chart depicting relative peak area (RPA) of recovery standard 4-fluorophenylalanine (F-Phe) over 83 blood plasma samples (red), 28 urine samples (blue), and pooled plasma (15) and urine (10) QC samples (black) for a total of 136 injections. The solid line represents the average RPA, and the dotted lines represent the upper and lower action limits ($\pm 3SD$).

evaluating the reliability in both sample preparation and instrument performance (*i.e.*, technical precision) in order to reduce bias that contributes to false discoveries in metabolomics.⁶⁵ **Figure 2.5** shows extracted ion electropherograms (positive ion mode) for Phe and Tyr in plasma filtrate samples, in which the QC is located in position 5 of the 7-serial sample injection format for this run. Control

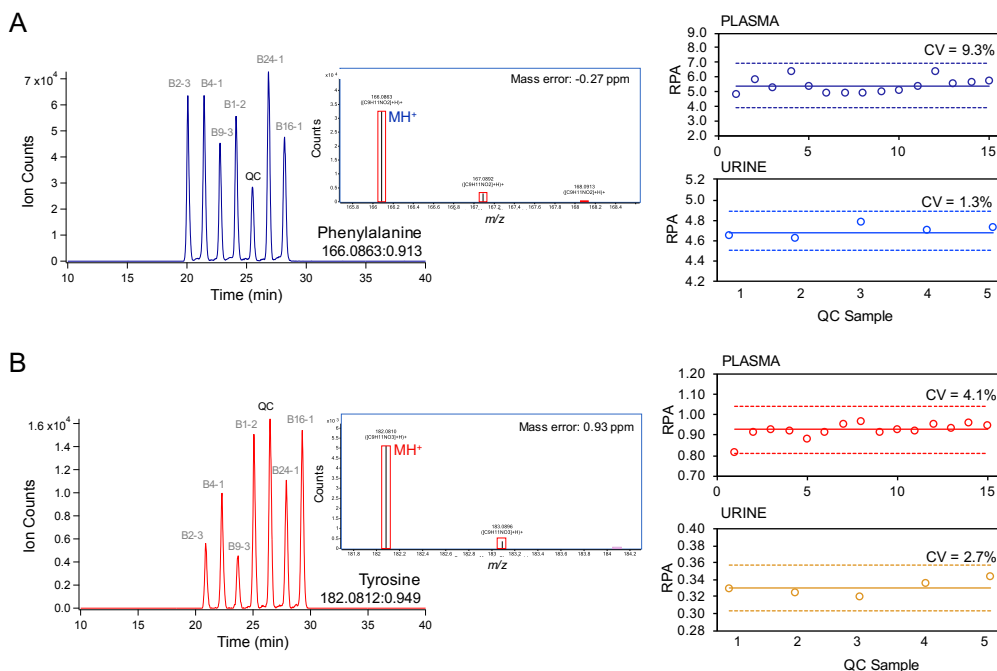


Figure 2.5. Representative extracted ion electropherograms for (A) Phe and (B) Tyr, with the pooled QC sample in position 5 of 7 within the MSI injection sequence. The TOF-MS spectra are shown as insets, with mass errors < 5 ppm. Control charts highlighting the analytical performance based on the integrated peak areas of Phe/Tyr relative to an internal standard (CI-Tyr) within the QC for plasma ($n = 15$) and urine ($n = 5$) are shown on the right. CVs are < 10%, which shows excellent precision. The mean is represented as a solid line, whereas the upper and lower action limits ($\pm 3D$) are dashed lines.

charts for the QC sample within each run show excellent technical precision, as shown for Phe and Tyr with CVs < 10%. Similarly, **Figure 2.6** highlights the low technical variation as reflected by the tight clustering of the QC group as compared to total biological variation among classic PKU patients, as shown in a principal component analysis (PCA) 2D scores plot for plasma (A) and urine (B). In this case, the median CV for all features within the data matrix ($n_{\text{plasma}} = 55$ over 30 runs; $n_{\text{urine}} = 76$ over 10 runs) was 14.0% and 14.5% for plasma and urine, respectively, which demonstrates acceptable technical variation within both sets

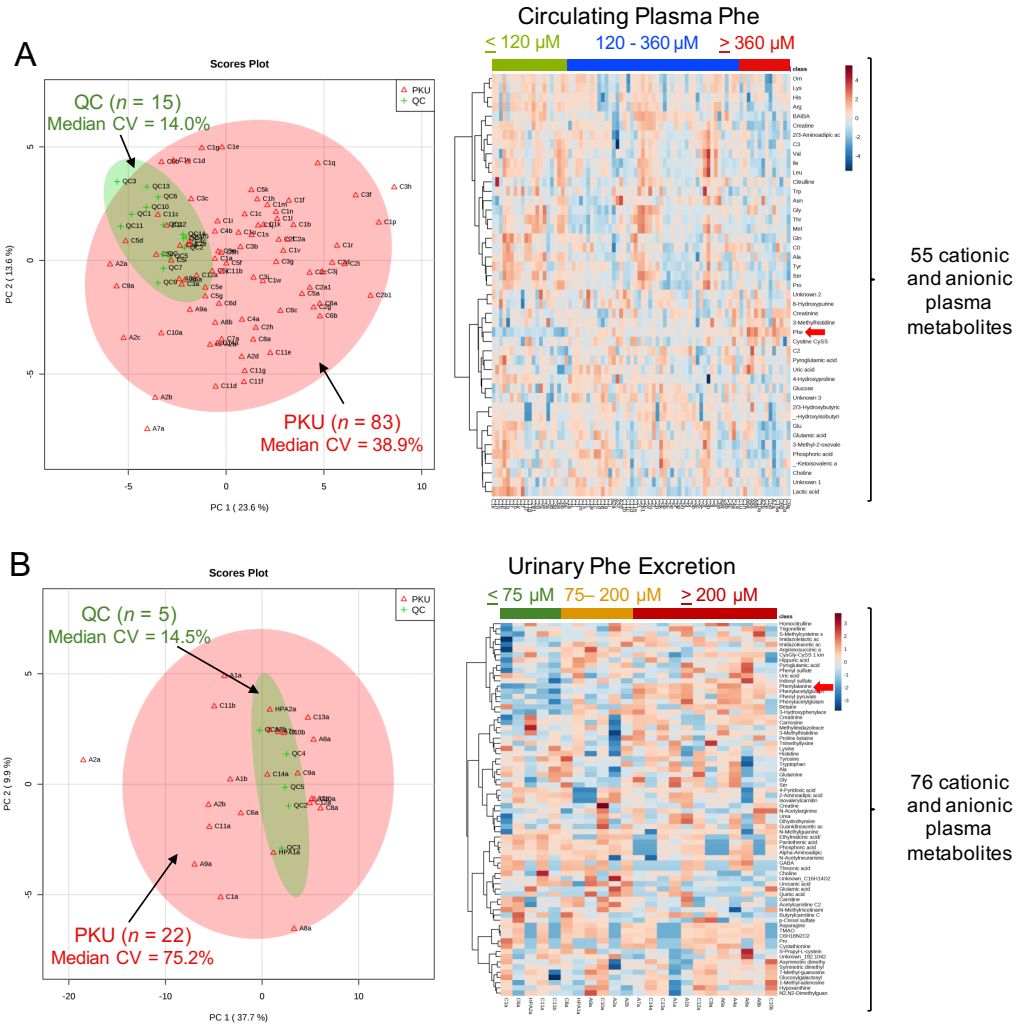


Figure 2.6. 2D scores plot from principal component analysis (PCA) of (A) 55 cationic and anionic metabolites detected in plasma filtrate and (B) 76 cationic and anionic metabolites detected in urine samples when using MSI-CE-MS showing the low technical variation of the QC samples analyzed within every run in comparison to all PKU patients. Urine samples were classified based on cut-offs determined from correlation of matched urine/plasma samples: ‘low’ (urinary Phe < 75 μM), ‘moderate’ (75 < urinary Phe < 200 μM), or ‘high’ (urinary Phe > 200 μM). All data was *log*-transformed and autoscaled. An overview of the overall data structure is shown with 2D heatmaps with hierarchical cluster analysis (HCA).

of biological samples. The 2D heat maps with HCA provide an overview of the data structure for plasma and urine samples. In plasma (A), major differences in certain LNAAs (e.g., Gln, Ala, His, Thr, and Tyr), creatine, and other metabolites

were evident between samples with low (*i.e.*, < 120 μM) and high (*i.e.*, > 360 μM) circulating Phe. In urine samples (**B**), samples with high Phe are clustered away from low Phe, with visual differences between Phe-related metabolites.

Measured plasma Phe concentrations among PKU patients ranged from 30 to over 1,500 μM (median = 275 μM ; IQR = 342 μM) whereas Tyr concentrations ranged from 30 to 200 μM (median = 60 μM , IQR = 48 μM). Plasma Phe and Tyr concentrations were not normally distributed as determined by a Shapiro-Wilk test (p -value < 0.001, $n = 88$). Also, measured plasma Phe and Tyr concentrations demonstrated a weak, negative correlation with each other, as determined with a Spearman's rank test ($r_s = -0.243$, $p < 0.05$). In order to evaluate the accuracy of MSI-CE-MS for reliable measurement of known biomarkers of PKU, an intermethod comparison with UPLC-UV was performed as shown in **Figure 2.7**. Overall, random distributions of plasma concentrations were evident about a mean when comparing MSI-CE-MS relative to UPLC-UV data with an average bias of -14.8% and +9.8% for Phe and Tyr, respectively, as illustrated in Bland-Altman % difference plots (**A**). The Bland-Altman plot identified only one sample as an extreme outlier for plasma Phe that exceeded the confidence interval range for limits of agreement. A strong correlation ($p < 0.00001$) was observed between the two methods based on Spearman's ranks coefficients of 0.979 (Phe) and 0.948 (Tyr), which was also reflected by slopes close to unity when using Passing-Bablok regression analysis (**B**). Passing-Bablok regression also showed a small degree of bias for Phe and Tyr (-22% and -12%, respectively) with greater

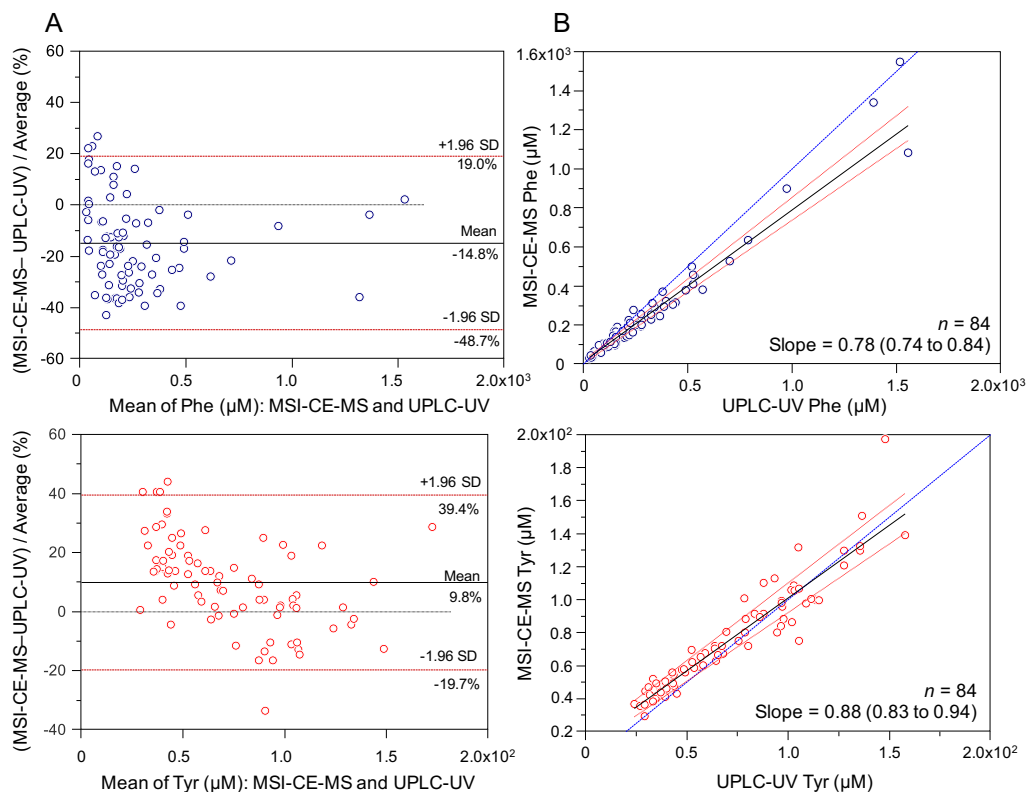


Figure 2.7. Bland-Altman % difference plot (A) and Passing-Bablok regression analysis (B) comparing Phe (blue, top) and Tyr (red, bottom) concentrations as determined by MSI-CE-MS relative to UPLC-UV. In A, the mean % difference (-14.8% and +9.8%) is shown as a solid black line, the upper and lower limits of agreement (± 1.96 SD; 19.0% and -48.7% Phe; -19.7% and 39.4% Tyr) are red dotted lines, and the zero line is a black dotted line. In B, the slope and y-intercept are indicated with the 95% confidence interval. The regression line is a solid black line, the 95% confidence interval lines are dotted red lines, and the unity line is a dashed blue line.

deviation of MSI-CE-MS from UPLC-UV values at higher concentrations.

Overall, the extent of the bias (10-15%) between the two methods was similar to the technical variation measured by QC runs (median CV = 14%) for metabolomics data, as well as for Phe and Tyr (CV < 10%) when using MSI-CE-MS as shown in **Figure 2.5**. It can be concluded that MSI-CE-MS provides consistent measurements of plasma Phe and Tyr concentrations that are mutually agreeable with validated UPLC-UV protocols. As a result, MSI-CE-MS offers a

reliable and higher-throughput platform for therapeutic monitoring of PKU patients relative to UPLC-UV methods that rely on a single sample injection format with long total analysis times (> 45 min) as required for gradient elution and column reconditioning.⁵⁵

2.4.3 Targeted Metabolite Profiling: Primary Markers of PKU

Plasma Phe concentrations were highly variable among classic PKU patients as summarized in **Figure 2.8**, however, no other known biomarkers of PKU derived from aberrant Phe catabolism were detected in plasma samples with MSI-CE-MS. The majority of subjects with PKU (about 58% from PKU cases) fall within or below the optimal therapeutic cut-off range of 120–360 μM , most of whom were children (median age = 6.0 y), which is now considered a lifelong maintenance range for Phe as recently recommended by ACMGG.^{26,53} However, some earlier guidelines had proposed a more relaxed upper threshold concentration of 600–900 μM for adults and adolescents over the age of 12 y.⁶⁶ In our study, there were 4 PKU patients with plasma Phe exceeding 600 μM , and 2 who had grossly elevated levels of Phe (> 1 mM). Upon closer examination, both individuals were adult PKU patients (> 30 y) and, at the time of sample collection, they were not taking a specialized Phe-free amino acid formula or following a Phe-restricted diet as determined from patient/diet records. The relationship between patient age and plasma Phe concentrations in individuals with PKU was also evaluated with a Spearman's rank correlation analysis, which

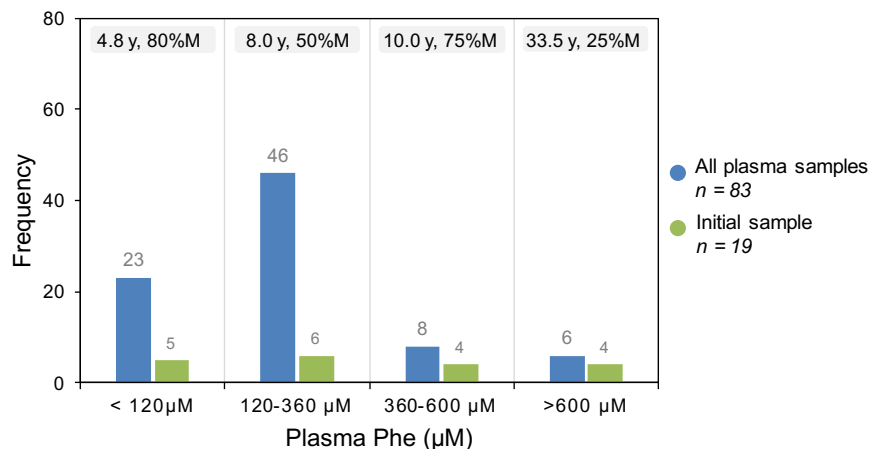


Figure 2.8. Frequency distribution of plasma Phe concentrations (μM) measured by MSI-CE-MS for all samples (blue) and initial plasma samples upon consent (green). The frequency is listed in grey above each bar, whereas the median age and sex distribution (%M) is listed for each grouping at the top of the graph. The majority of samples fall within or below the goal therapeutic range of 120 to 360 μM . Age was a significant factor ($p < 0.05$) associated with higher Phe concentrations, whereas sex was not significant different for Phe status.

demonstrated a moderate positive correlation ($r_s = 0.671$, $p < 0.01$, $n = 19$). It has been demonstrated that dietary adherence/irregularities becomes more problematic as PKU patients age,^{53,66,67} with higher plasma Phe concentrations more often reported among adults in comparison to children likely due to parental control.⁵⁶ However, several studies have shown adverse health effects in the adult PKU patient population with prolonged Phe $> 600\text{-}900 \mu\text{M}$, including a decrease in cerebral protein synthesis and higher oxidative stress,⁶⁸⁻⁷⁰ which has prompted a change in current dietary policies relevant to adult PKU patients.

In this work, urine metabolite responses were normalized by probabilistic quotient normalization (PQN). While random single-spot urine samples are far more convenient to collect than 24-h urine specimens, disadvantages include greater variation caused by differences in individual hydration status, which

ultimately impacts urinary metabolite concentrations.⁷¹ Normalization of metabolite concentrations/responses to urinary creatinine is often used to correct for variations in hydration status, assuming normal kidney function and protein intake.⁷³ Creatinine is a by-product of muscle metabolism (formed from creatine and phosphocreatine in the muscle) and is excreted in the urine by glomerular filtration.^{71,73} However, the rate of creatinine excretion is variable across different patient demographics, such as differences in age, sex, and protein intake.^{71,74} As this study involves the comparison of adults and children with classic PKU who are recommended to follow protein-restricted diets, creatinine excretion is thus not appropriate.⁷¹ For this reason, probabilistic quotient normalization (PQN) was used to overcome the limitations of urinary creatinine while reducing biological variance caused by random differences in hydration status. In this case, PQN calculates a ‘probable’ dilution factor from the median distribution of quotients of sample responses relative to a reference response (*i.e.*, pooled QC urine sample) for each molecular feature.⁶³

Urinary Phe concentrations (corrected with PQN) ranged from 25 to 800 μM (median = 206 μM ; IQR = 293 μM). As expected, plasma Phe concentrations were strongly correlated to matching urinary excretion of Phe when using a Spearman’s rank correlation analysis ($r_s = 0.895$, $n = 21$, $p < 0.0001$). A strong positive correlation was also observed for urinary Phe without PQN correction ($r_s = 0.836$, $p < 0.0001$). Phe is derived from two sources: intake of dietary protein and turnover of endogenous protein to recycle free amino acid pools.⁷⁵

Approximately 25% of free Phe is incorporated into proteins, whereas the majority of remaining Phe (~ 70%) undergoes hydroxylation to Tyr.⁷⁵ Thus, alternative metabolic pathways are needed to alleviate excess Phe in PKU, which occur enzymatically via decarboxylation and transamination (**Figure 2.9**).¹⁵ Decarboxylation and transamination of Phe accounts for less than 6% of Phe metabolism in otherwise healthy individuals.⁷⁶ As a result, PKU is characterized by the accumulation and higher urinary excretion of several Phe-derived catabolites normally present at low concentration levels in healthy individuals.⁷⁷ In our work, *N*-phenylacetylglutamine, phenylsulfate, and *o*-hydroxy phenylacetate were detected consistently in over 90% of samples, whereas phenylpyruvate and phenyllactate were detected in 57 and 37% due to their lower abundance, respectively. However, phenylacetate was not detected in any of the urine samples from classic PKU cases since it undergoes conjugation (as its activated acyl-coenzyme A ester) with glutamine to form the major urinary metabolite, *N*-phenylacetylglutamine. Phenylsulfate is derived from gut microbial metabolism and sulfation of Tyr, along with *p*-cresol sulfate, which were both detected in urine.⁷⁸ Aside from Phe, *N*-phenylacetylglutamine was most abundant of Phe catabolites in urine, as observed by the extracted ion electropherogram overlay for a pooled urine QC in **Figure 2.10**. A Spearman's rank order correlation was next performed to determine the relationship between urinary Phe and Phe-derived metabolites. As expected, circulating plasma Phe and urinary Phe excretion showed strong, positive correlations with *N*-phenylacetylglutamine,

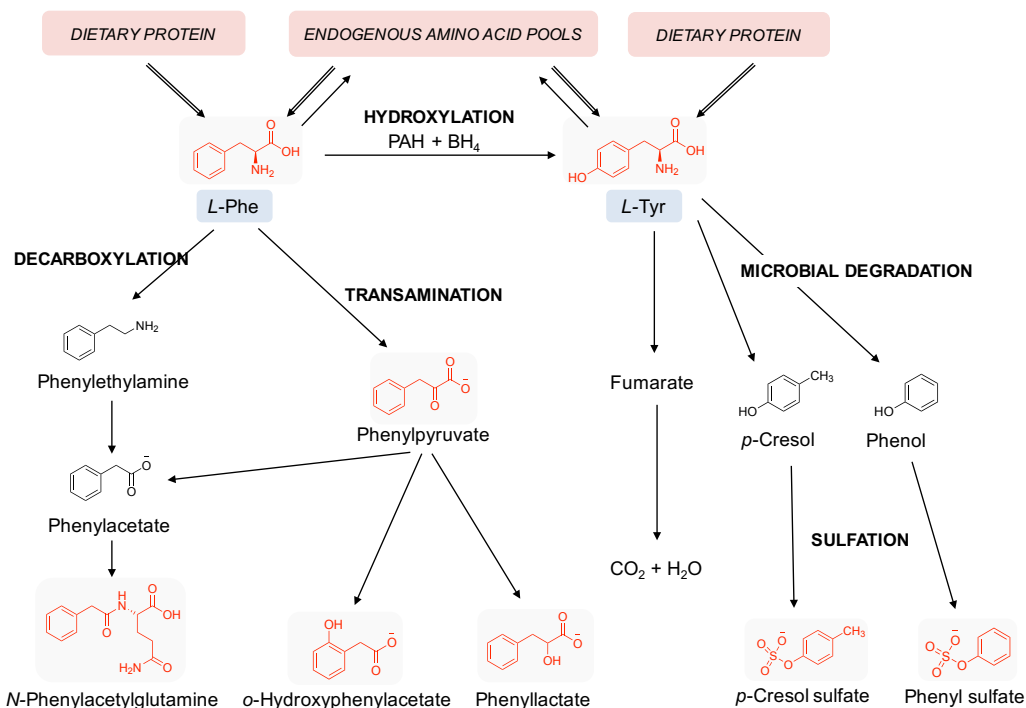


Figure 2.9. Metabolism of Phe in humans. *L*-Phe is introduced through dietary protein sources and is recycled through amino acid pools. Hydroxylation of *L*-Phe by PAH in the presence of BH₄ and molecular O₂ produces *L*-Tyr. *L*-Phe is also metabolized through decarboxylation and transamination to produce various catabolites, which are excreted in urine, where red indicates detected metabolites from PKU patients. Figure modified from (11).

phenylsulfate, phenylpyruvate, and *o*-hydroxyphenylacetate, which were all statistically significant ($p < 0.003$), with the exception of phenyllactate and *p*-cresol sulfate (**Table 2.4**). In addition, when comparing individual PKU patients with significantly elevated plasma Phe (*i.e.*, plasma Phe $> 360 \mu\text{M}$, $n = 10$) to optimal therapeutic levels (*i.e.*, plasma Phe $< 360 \mu\text{M}$, $n = 7$), urinary Phe, *o*-hydroxyphenylacetate, *N*-phenylacetylglutamine, and phenylpyruvate were significantly elevated ($p < 0.05$) (**Figure 2.11**), whereas phenylsulfate was not significantly different.

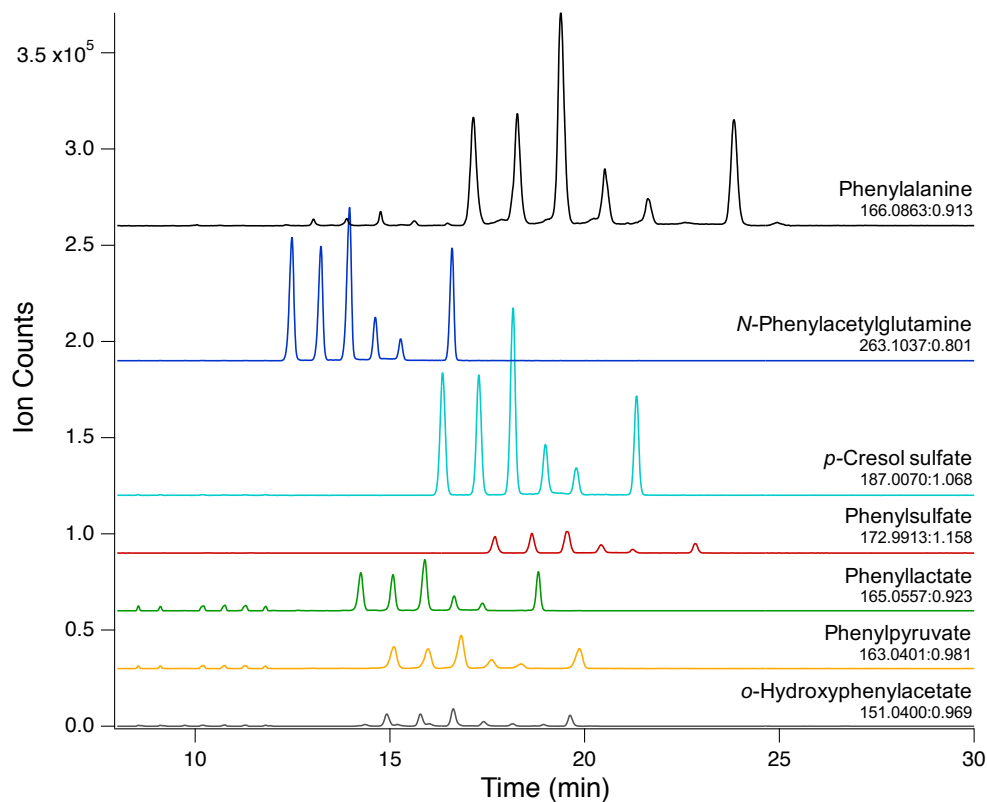


Figure 2.10. Extracted ion electropherogram overlay for Phe, *N*-phenylacetylglutamine, *p*-cresol sulfate, phenylsulfate, phenyllactate, phenylpyruvate, and *o*-hydroxyphenylacetate for a representative pooled urine QC sample using MSI-CE-MS with a serial dilution trend filter. Phe was detected in positive ion mode with ion responses scaled down by a factor of 2, whereas all other anionic metabolites were detected in negative ion mode.

Table 2.4. Spearman's rank correlation results between excreted urinary Phe and its association with its major catabolites *N*-phenylacetylglutamine, phenylsulfate, phenyllactate, phenylpyruvate, and *o*-hydroxyphenylacetate.

Phe Catabolite	m/z:RMT:mode	<i>n</i>	Correlation Coefficient (r_s)	<i>p</i> -value
Phenylpyruvate	163.0401:0.981:n	16	0.862	1.8E-5
<i>N</i> -Phenylacetylglutamine	263.1037:0.801:n	26	0.787	2.0E-6
Phenylsulfate	172.9913:1.158:n	31	0.563	1.0E-3
<i>o</i> -Hydroxyphenylacetate	151.0400:0.969:n	28	0.543	3.0E-3
Phenyllactate	165.0557:0.923:n	11	0.347	<i>N.S.</i>

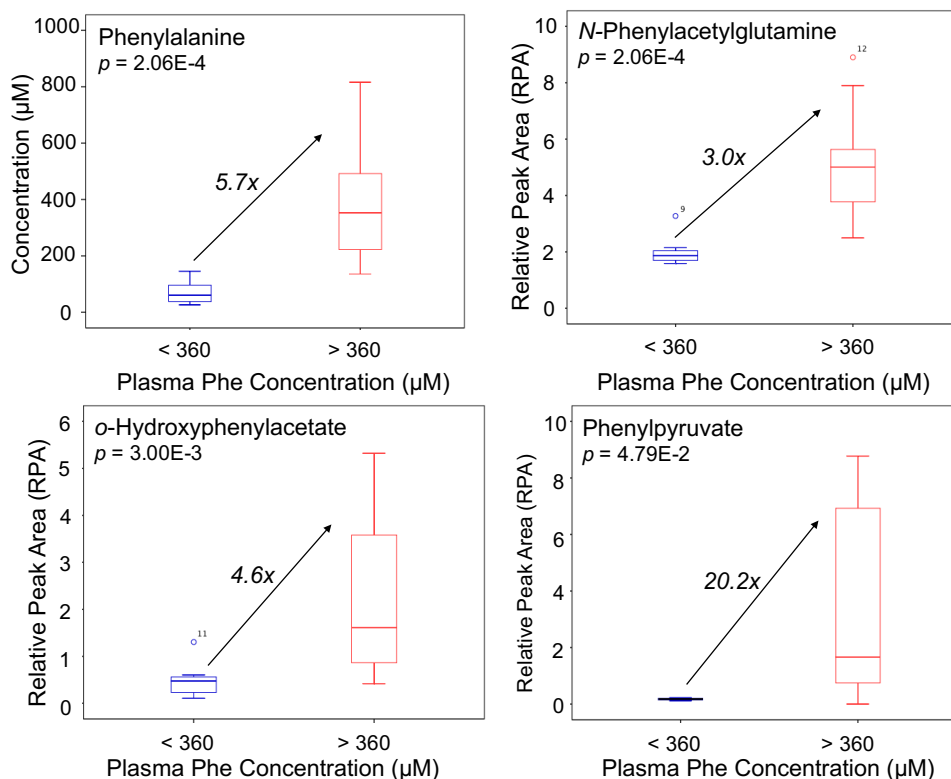


Figure 2.11. Box-and-whisker plots showing median fold-change and p -values for urinary Phe, *N*-phenylacetylglutamine, *o*-hydroxyphenylacetate, and phenylpyruvate when grouped by plasma Phe concentrations of 360 μM as a cut-off to signify likely dietary compliance of PKU patients to ensure optimal therapeutic outcomes.

These results are consistent with previous studies, which have demonstrated a positive correlation of urinary excretion of major Phe catabolites, including phenylpyruvate, with circulating Phe levels.⁷⁷ Michals *et. al.*⁷⁷ demonstrated that individuals with a history of noncompliance to their PKU diet were observed to have higher excretion of these same metabolites. This study suggests that Phe catabolites may differ in individuals with the same blood Phe level due to differences in residual PAH activity and expression of other enzymes that degrade elevated Phe, including co-metabolism by gut microflora. In addition, it has been

shown that phenylpyruvate and phenylacetate inhibit metabolism of ketone bodies⁷⁷ and carnitine synthesis,⁷⁹ respectively, and may contribute to the pathophysiology of the disease spectrum in PKU.⁷⁹ For instance, Xiong *et. al.*⁸⁰ recently demonstrated that phenylpyruvate, phenylacetate, phenyllactate, *o*-hydroxyphenylacetate, and *N*-phenylacetylglutamine are prominent biomarkers of PKU when using GC/MS following pre-column derivatization.⁸⁰ The gold standard of PKU diagnosis remains plasma Phe or the ratio of Phe/Tyr; however, there are some reports indicating that the Phe/Tyr method generates false positives when discriminating PKU from patients with bipterin defects.^{80,81} In contrast, urine sampling is noninvasive in comparison to blood sample collection, and includes a panel of other clinically relevant pathognomonic markers of PKU, offering a more convenient approach for continuous therapeutic monitoring with random single-spot urine specimens during clinical visits.

2.4.4 Nontargeted Metabolite Profiling: Beyond Altered Phe Catabolism

A nontargeted metabolomics approach for the profiling of PKU patients was next carried out to identify metabolites associated with PKU severity and dietary adherence aside from the known markers of PKU, including Phe, Tyr, and related Phe catabolites in urine.

2.4.4.1 Plasma Metabolome Analysis

For nontargeted metabolome analysis of plasma filtrate samples, plasma Phe response was classified as low (Phe < 120 μ M, $n = 4$), medium (120 μ M < Phe <

360 μM , $n = 6$), high (Phe > 360 μM , $n = 5$), or uncontrolled (*i.e.*, not taking formula and poor/uncontrolled diet, $n = 3$). A summary of classic PKU patients within each class is listed in **Table 2.5**. Repeat plasma filtrate samples were not included in this analysis since they were only collected from infants/children who receive clinical testing on a weekly or monthly basis. A nontargeted metabolomic approach was used to elucidate whether there were markers of dietary intake (*i.e.*, protein) in individuals with sub-optimum Phe levels (*i.e.*, high/uncontrolled) above the recommended therapeutic range, which may be used as a more objective approach to monitor for dietary compliance. Multivariate data analysis was carried out to visualize metabolomic differences between PKU patients with elevated Phe (*i.e.*, above the therapeutic cut-off) in comparison to individuals with low/moderate plasma Phe and individuals not consuming a specialized amino acid formula or likely not following a protein-restricted diet. A 2D scores plot from a PLS-DA is shown in **Figure 2.12**. PKU patients with uncontrolled diets were discriminated by high levels of Phe and low levels of propionylcarnitine (C3), phosphoric acid, histidine (His), Tyr, citric acid, and creatine. Nonparametric univariate analysis (Mann-Whitney U tests) with nontransformed RPAs between PKU patients with low/moderate plasma Phe levels and PKU patients on uncontrolled diets confirmed these trends in addition to lower levels of asymmetric dimethylarginine (ADMA) and elevated levels of glycine (Gly) ($p < 0.05$). PKU patients not following a controlled diet were also not consuming a specialized amino acid formula; as a result, differences in plasma concentrations

Table 2.5. Summary of PKU patients within each class examined for nontargeted plasma metabolome analysis.

<i>Class</i>		Low < 120 μM <i>n</i> = 4	Medium 120-360 μM <i>n</i> = 6	High > 360 μM <i>n</i> = 5	Uncontrolled > 800 μM <i>n</i> = 3
<i>Phe</i>	<i>Range</i>	39-108 μM	163-295 μM	383-663 μM	899-1548 μM
	<i>Median</i>	85 μM	238 μM	450 μM	1082 μM
<i>Age</i>	<i>Range (Med.)</i>	2-6 (3.4) y	0.2-50 (8) y	9-24 (11) y	30-43 (37) y
<i>Sex</i>	<i>% Male</i>	75%	50%	60%	66%
<i>Kuvan</i>	<i>%</i>	0%	50%	20%	0%

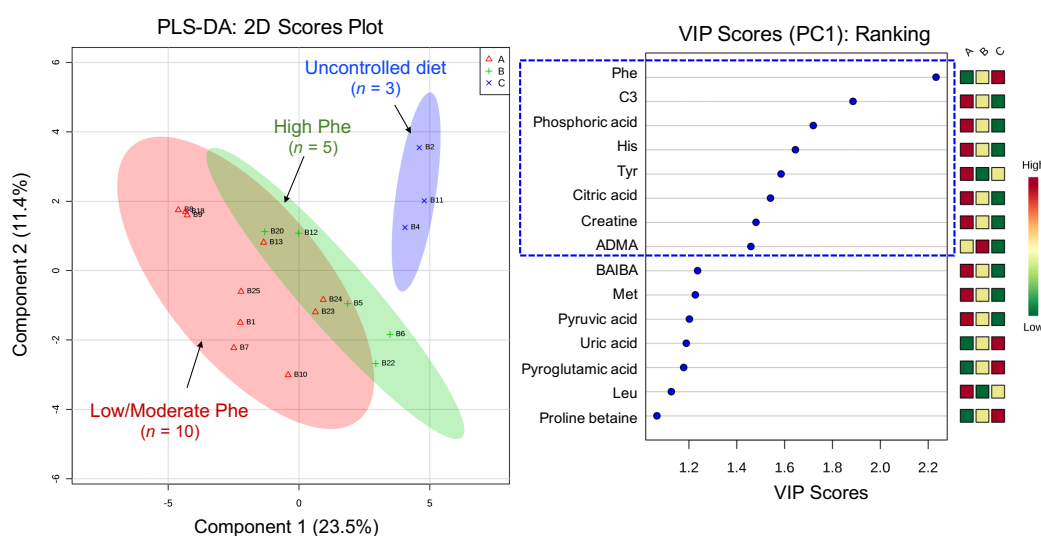


Figure 2.12. Separation between PKU patients with low/moderate plasma Phe (*A*, Phe < 360 μM , *n* = 9), high plasma Phe (*B*, Phe > 360 μM , *n* = 5), and patients on an uncontrolled diet not taking specialized amino acid formula (*C*, *n* = 3) as depicted in a 2D scores plot when using PLS-DA with cross-validation ($R^2 = 0.998$, $Q^2 = 0.299$). All data was *log*-transformed, and autoscaled, with VIP used to assign top-ranked plasma metabolites associated with Phe response in classic PKU. Patients with high Phe (> 360 μM) are predominantly discriminated by top-ranking metabolites with VIP scores > 1.5, including Phe, propionylcarnitine (C3), phosphoric acid, His, and Tyr.

of amino acids and amino acid metabolites are expected considering differences in intake. We were interested in examining differences in individuals following a Phe-restricted diet in order to better understand metabolic differences contributing to Phe response. Nonparametric univariate analysis (Kruskal-Wallis H tests) comparing PKU patients with low, moderate, and high plasma Phe concentrations

showed inverse correlations with α -aminoadipic acid, serine (Ser), leucine (Leu), and isoleucine (Ile) and a positive correlation with creatinine ($p < 0.05$), which were all significantly different between groups (**Table 2.6**). Creatinine is a biomarker of meat intake; however, no additional trends or significant differences were observed for other markers of meat and protein intake (*i.e.*, 3-methylhistidine and carnosine), aside from creatine (**Figure 2.13**).^{82,83} In addition, creatine was determined to be negatively correlated with plasma Phe (Spearman's rank test, $r_s = -0.693$, $p < 0.005$). The opposing trends seen in creatine and creatinine is likely a result of differences in age and/or muscle mass between assigned classes. Overall, analysis of plasma samples of patients with classic PKU does not give significant insight on adherence to a low protein diet through the examination of dietary biomarkers within individuals taking amino acid supplement formulas. Lower levels of amino acids present in the formula (*i.e.*, Leu, Ile, and Ser) as well as their breakdown products (**Figure 2.13**), such as

Table 2.6. Significant metabolites when comparing PKU patients with low, moderate, and high plasma Phe concentrations as determined by Kruskal-Wallis H tests. Fold-change (FC) is based on median RPAs for high Phe/low Phe. Correlation (r_s) with Phe was carried out by a Spearman's rank correlation test. PKU patients following an uncontrolled diet were excluded from this comparison in order to better understand phenotypic differences between individuals taking a specialized amino acid formula and following a Phe-free diet.

Metabolite	<i>m/z</i> :RMT:mode	<i>p</i> -value	Effect size	FC	r_s (<i>p</i> -value)
Phe	166.0863:0.913:p	2.06E-3	0.357	6.415	—
Leu	132.1019:0.835:p	3.20E-2	0.357	0.519	-0.554 ($p < 0.05$)
Ile	132.1019:0.823:p	2.14E-2	0.322	0.465	-0.593 ($p < 0.05$)
Creatinine	114.0662:0.565:p	2.06E-2	0.357	1.854	0.775 ($p < 0.01$)
α -aminoadipic acid	162.0761:0.914:p	1.30E-2	0.357	0.258	-0.639 ($p < 0.05$)
Ser	106.0499:0.825:p	1.09E-2	0.357	0.540	-0.725 ($p < 0.05$)

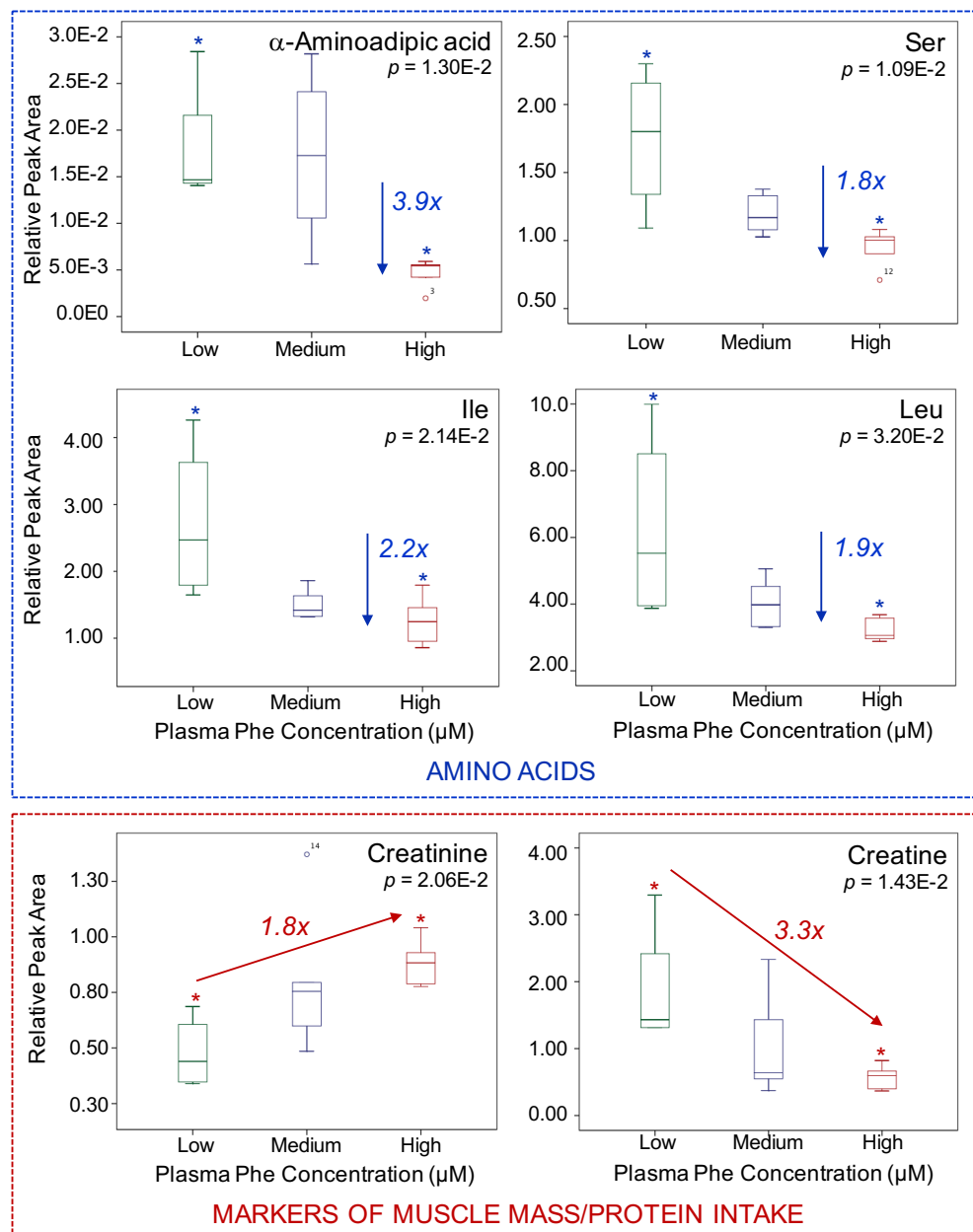


Figure 2.13. Box plots for plasma metabolites determined to be significantly different when grouped by plasma Phe concentrations. Fold-changes are based on median RPAs for high Phe/low Phe, where high Phe > 360 μ M and low Phe < 120 μ M. The amino acids Ser, Ile, and Leu, in addition to Lys breakdown intermediate, α -amino adipic acid, are all decreased with high Phe, suggesting reduced dietary intake (*i.e.*, formula).

α -amino adipic acid, a metabolic intermediate of lysine metabolism, however, may suggest that these individuals are not consuming the prescribed amount of formula consistently or there are metabolic alterations in pathways associated with protein synthesis and central metabolism as reported by Blasco *et. al.*⁵⁸ It is also likely that there are differences in the time of day in which individuals take their formula in addition to meal timing prior to a blood sample collection (*i.e.*, non-fasting state), which would affect concentrations of plasma Phe and circulating amino acids.⁸⁴

In contrast to a recent nontargeted metabolomics analysis of adult PKU patients not following restricted diets using GC/MS, NMR, and an amino acid analyzer,⁵⁸ our study focuses on the metabolome of patients following a Phe-restricted diet and consuming amino acid formulas. In the multi-platform pilot study performed by Blasco *et. al.*,⁵⁸ the analysis of urine and blood plasma samples from 10 adult patients with classic PKU ($n = 6$), mild PKU ($n = 3$), and mild HPA ($n = 1$) showed metabolic alterations in Glu, succinate, Arg, and α -aminobutyric acid, highlighting major changes in amino acid metabolism, which is expected with grossly elevated levels of Phe (*i.e.*, Phe > 1 mM). Our analysis of plasma samples from 3 PKU patients not following a Phe-restricted diet, however, did not show the same trends observed by Blasco *et. al.*, which is likely a result of small sample size in both studies. Similarly, our study focused on a small subset of PKU patients; however, our study demonstrates subtle metabolic differences between individuals with variable Phe responses who are following a restricted

diet rather than the severe metabolic phenotype of PKU on an unrestricted diet compared to healthy individuals. This highlights important factors that may provide better understanding of PKU disease progression, which is highly relevant for PKU treatment especially among adult patients.

2.4.4.2 Urine Metabolome Analysis

A primary goal of this project was to evaluate the metabolic phenotype of a diverse cohort of classic PKU patients recommended to follow a Phe-restricted diet beyond monitoring for circulating Phe concentrations, including recently diagnosed infants, children/adolescents, and adults. Defined urinary Phe reference concentrations in PKU patients based on disease severity and dietary adherence have not been established since it is not routinely measured in a clinical setting. Urinary Phe response for classic PKU patients was classified based on correlation with matching plasma Phe response. Low/moderate urinary Phe (Phe < 200 μM , $n = 7$) excretion was defined as plasma Phe concentrations under 360 μM , whereas high Phe excretion was defined by urinary Phe exceeding 200 μM (*i.e.*, plasma Phe > 360 μM , $n = 4$). PKU patients on an uncontrolled diet who were not consuming a Phe-free amino acid formula were included as a positive control ($n = 5$). Urinary Phe excretion was variable for these patients (*i.e.*, 208-816 μM) despite matched plasma Phe levels > 800 μM for 3 of these patients. A summary of classic PKU patients included within each class is listed in **Table 2.7**. In order to better visualize the metabolic phenotype difference among classic PKU patients

Table 2.7. Summary of classic PKU patients examined for nontargeted urinary metabolome studies with low/moderate urinary Phe excretion (< 200 μM , $n = 7$), high urinary Phe excretion (> 200 μM , $n = 4$), and PKU patients not taking an amino acid supplement with a poor/uncontrolled diet ($n = 5$).

Class	Low/Moderate	High	Uncontrolled
Urinary Phe	< 200 μM $n = 7$	> 200 μM $n = 4$	208-816 μM $n = 5$
Plasma Phe Range (median)	163-530 (253) μM	382-662 (450) μM	899-1548 (1082) μM^*
Age Range (median)	0.2-50 (9.0) y	9-14 (12) y	23-43 (30) y
Sex % Male	60%	50%	40%
Kuvan %	43%	25%	0%

* Matched plasma samples were collected for 3 of 5 PKU patients not consuming a specialized amino acid formula.

likely following Phe-restricted diets based on urinary Phe excretion, a 2D scores plot from a PLS-DA was constructed based on PQN-corrected, *log*-transformed, and autoscaled data (**Figure 2.14**). In this case, low/moderate and high Phe excretion in urine were largely discriminated from PKU patients not taking an amino acid formula or following a restricted diet by 11 top-ranked metabolites with VIP scores > 1.5, including *N*-phenylacetylglutamine, Phe, phenylpyruvate, *N*-methylnicotinamide, Gly, and 3-methylhistidine. To evaluate differences in the metabolic phenotype of PKU patients not taking a specialized amino acid supplement with poor dietary adherence (*i.e.*, uncontrolled group) and PKU patients following a Phe-restricted diet with urinary Phe excretion that is consistent with plasma Phe levels under/within the recommended therapeutic range (*i.e.* low/moderate urinary Phe group), nonparametric univariate statistical analysis was carried out with Mann-Whitney U tests. In this case, *N*-methylnicotinamide ($p = 2.5\text{E-}3$), urocanic acid ($p = 1.8\text{E-}2$), carnitine ($p = 3.0\text{E-}2$), choline ($p = 3.0\text{E-}2$), and pantothenic acid ($p = 3.4\text{E-}2$) were lower in the

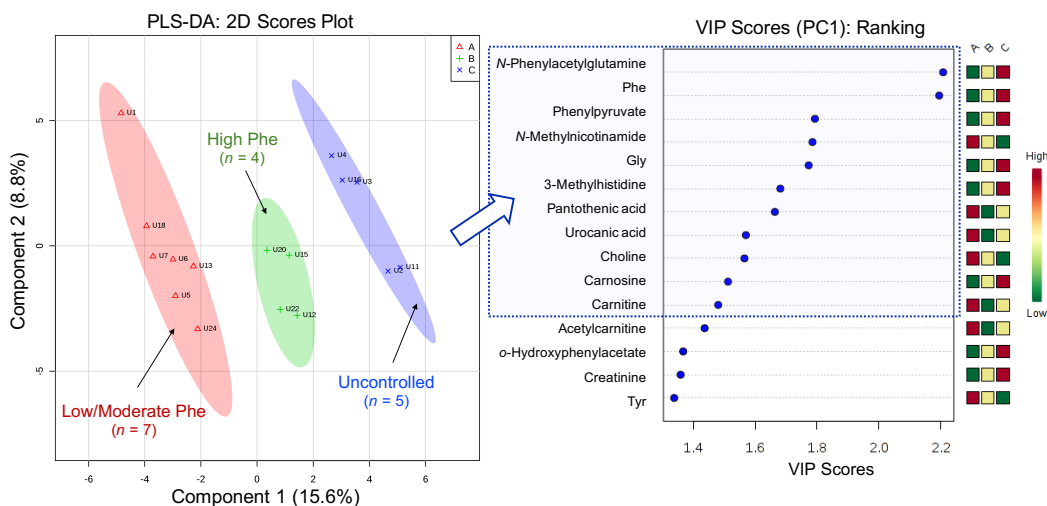


Figure 2.14. Separation between PKU patients with low/moderate (*A*, $n = 7$) and high Phe excretion in urine (*B*, $n = 4$) and PKU patients not taking a specialized amino acid formula who were not following a Phe-restricted diet (*C*, $n = 5$) as depicted in a 2D scores plot when using PLS-DA with cross-validation ($R^2 = 0.997$, $Q^2 = 0.631$). All data was corrected with PQN, \log -transformed, and autoscaled. Multivariate analysis of PQN-corrected RPAs was used for selection of top-ranked urinary metabolites related to Phe excretion in PKU.

uncontrolled group, whereas markers of protein intake,^{82,83} including 3-methylhistidine ($p = 1.0E-2$), carnosine ($p = 3.0E-2$), and creatinine ($p = 4.8E-2$), were elevated significantly. Choline and pantothenic acid (vitamin B5) are both essential nutrients/vitamins present in PKU amino acid formulas that are deficient in the PKU diet, whereas *N*-methylnicotinamide is a urinary metabolite of niacin, which is also present in the PKU amino acid formula.⁸⁵ Furthermore, low dietary intake of carnitine, choline, vitamin B5, and niacin are reported in PKU patients following a restricted diet.⁸⁶

To better visualize group separation between PKU patients consuming amino acid formula likely following Phe-restricted diets with low/moderate and high Phe excretion in urine, a second 2D scores plot from a PLS-DA was constructed

(**Figure 2.15**). High Phe excretion in urine was largely discriminated from low/moderate Phe excretion by 11 metabolites with VIP scores > 1.5 , which included Phe, C0, C2, and His metabolites (*i.e.*, urocanic acid, imidazoleacetic acid, imidazolelactic acid). Additionally, a comparison of metabolites in urine samples from individuals with low/moderate and high Phe excretion was performed using nonparametric univariate statistical analysis. **Table 2.8** summarizes the most significant metabolites based on PQN-corrected RPAs when using a Mann-Whitney U test, including p -values, effect size, and median fold-change (FC).

Imidazoleacetic acid (m/z :RMT 127.0502:0.674) was found to be significantly elevated in PKU patients with high urinary Phe excretion. Imidazoleacetic acid and imidazolelactic acid (m/z :RMT 157.0609:0.745), were identified following an untargeted search of a pooled QC when using a dilution trend filter by MSI-CE-MS. These molecular features were determined to be singly charged ions (MH)⁺ based on their ESI⁺ mass spectrum (**Supplementary Figure S2.1**) and tentatively identified based on their likely molecular formula and Metlin search. PQN-normalized urinary imidazolelactic acid and imidazoleacetic acid excretion were also observed to be strongly positively correlated with urinary Phe concentrations with Spearman's rank correlation coefficients of 0.883 ($p = 4.8E-10$) and 0.846 ($p = 5.2E-4$), whereas only imidazolelactic acid was positively correlated with circulating plasma Phe concentrations ($r_s = 0.818$, $p = 0.002$, $n = 12$). Indeed, imidazolelactic acid and

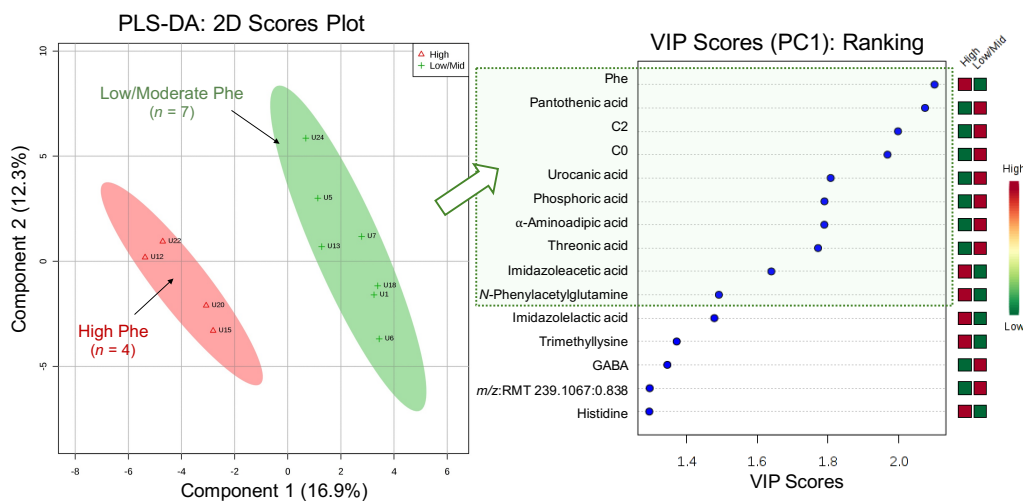


Figure 2.15. Group separation between PKU patients consuming a specialized amino acid formula and following a Phe-restricted diet with low/moderate ($n = 7$) and high ($n = 4$) Phe excretion in urine shown in a 2D scores plot by PLS-DA with cross-validation ($R^2 = 0.974$, $Q^2 = 0.361$). All data was corrected with PQN, \log -transformed, and autoscaled. Multivariate analysis of PQN-corrected RPAs was used for the selection of top-ranked urinary metabolites associated with Phe excretion in PKU.

Table 2.8. Significant metabolites when comparing PQN-normalized urine with low/moderate and high Phe excretion as determined by Mann-Whitney U tests. Fold-change (FC) is based on median RPAs for high Phe relative to low/moderate Phe.

Metabolite	m/z :RMT:mode	p -value	Effect size	FC
Imidazoleacetic acid ^a	127.0502:0.674:p	1.10E-2	0.302	2.21
Valerylcarnitine (C5)	246.1705:0.812:p	1.40E-2	0.292	0.20
Acetylcarnitine (C2)	204.1230:0.724:p	1.70E-2	0.282	0.20
Carnitine (C0)	162.1123:0.713:p	1.70E-2	0.282	0.19
His	156.0768:0.624:p	2.70E-2	0.262	1.62
Phe	166.0863:0.913:p	4.20E-2	0.242	3.80
N-Phenylacetylglutamine	263.1037:0.801:n	4.20E-2	0.242	2.64

^a Imidazoleacetic acid was tentatively identified by mass match using the ESI+ mass spectrum and Molecular Formula Generator (MFG).

imidazoleacetic acid were both determined to be significantly different with Phe excretion when analyzing samples grouped by low ($n = 4$), moderate ($n = 3$), and high ($n = 4$) urinary Phe (Figure 2.16).

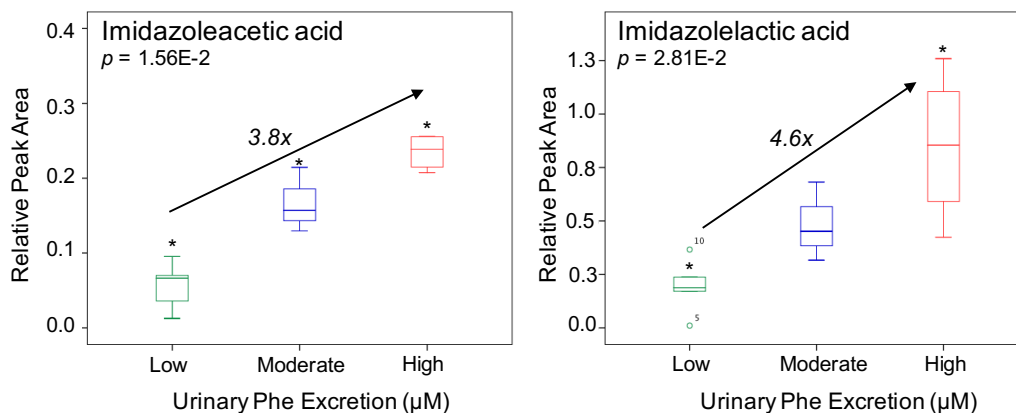


Figure 2.16. Box plots showing differences in urinary excretion of two histidine catabolites, imidazoleacetic acid and imidazolelactic acid, when classified as low ($< 75 \mu\text{M}$, $n = 4$), moderate ($75 \mu\text{M} < \text{Phe} < 200 \mu\text{M}$, $n = 3$), or high ($\text{Phe} > 200 \mu\text{M}$, $n = 4$) urinary Phe. Fold-changes (FC) are based on median RPAs for high Phe/low Phe.

Imidazolelactic acid and imidazoleacetic acid are by-products of histidine catabolism in mammals and are known components of human urine.⁸⁷ Histidine degradation occurs along two pathways; the major pathway involves the deamination of histidine via histidase to urocanic acid, followed by further breakdown to glutamic acid. However, an alternative histidine pathway involves the enzyme histidine-pyruvate aminotransferase to produce imidazolepyruvic acid (not detected in urine), imidazoleacetic acid, and imidazolelactic acid (**Figure 2.17**).⁸⁸ Imidazolelactic acid has also been reported to be elevated in patients with liver cirrhosis, along with histidine and urocanic acid, a major product of histidine catabolism.⁸⁹ In liver cirrhosis, enzymatic conversion of histidine to glutamate is blocked due to folic acid deficiency, which results in the increased excretion of formiminoglutamic acid and its precursor urocanic acid.⁹⁰ The enzymes histidase and histidine-pyruvate aminotransferase are also differentially induced as a result

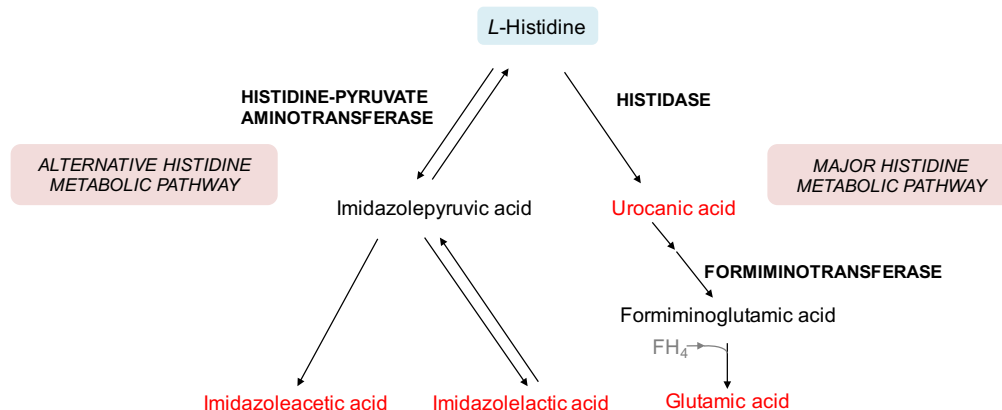


Figure 2.17. Histidine metabolism in mammals occurs through two pathways.⁸⁷ The major pathway leads to the formation of glutamic acid, whereas alternative histidine metabolism produces imidazoleacetic acid and imidazolelactic acid. Urinary metabolites detected by MSI-CE-MS are highlighted in red.

of dietary and hormonal influences.⁸⁸ For example, histidase activity is induced with consumption of a high protein diet or due to high cortisol levels and reduced with a low protein diet, whereas histidine-pyruvate aminotransferase activity increases with high glucagon levels. Alternatively, lower levels of imidazoleacetic acid and imidazolelactic acid may indicate the deficiency of folic acid and/or vitamin B12, as tetrahydrofolic acid is a required co-factor for the conversion of formiminoglutamic acid to glutamic acid.^{91,92} High dietary intake of folic acid is reported for PKU patients consuming amino acid supplements and protein substitutes and is often reported to be higher than the reference range of healthy adults.⁹³ Another study indicated that, when examining PKU patients taking specialized amino acid formulas, 94% of children ($n = 34$) and 73% of adult patients ($n = 22$) were consuming folic acid levels well above recommended daily intake. A strict PKU diet low in protein contains few natural sources of both folic acid and vitamin B12, and intake from these sources is minor in comparison to

that obtained from amino acid supplements.^{93,94} As a result, the increased excretion of imidazolelactic acid and imidazoleacetic acid may suggest a deficiency in folic acid and/or vitamin B12, which may provide a way to assess adherence of formula intake, including the need to monitor for adequate vitamin sufficiency in classic PKU patients following lifelong Phe-restricted diets.

Lower urinary excretion of C0 and short- and medium-chain acylcarnitines, C2 and C5, was also observed in individuals with high Phe and PKU patients not taking specialized amino acid formula or following a restricted diet (**Figure 2.18**), which were all negatively correlated with urinary Phe ($r_s = -0.653, -0.679, \text{ and } -0.683$, respectively, with $p < 0.01$). Carnitine facilitates the transport of long-chain fatty acids for mitochondrial β -oxidation and is both acquired from dietary intake as well as produced endogenously from its precursor *N*-trimethyllysine.^{79,95} Carnitine deficiency has been observed in patients with PKU as a result of minimal intake of red meats and dairy products, deficiencies in carnitine synthesis, and inhibition by Phe degradation products.⁷⁹ *N*-trimethyllysine, was determined to be a discriminating feature in the PLS-DA model (**Figure 2.15**), however had a VIP score under 1.5 and univariate analysis did not show a significant difference between low/moderate Phe excretion and high Phe excretion. Furthermore, PKU patients with high Phe are at a higher risk of carnitine deficiency due to the accumulation of phenylacetate as an intermediate by-product of Phe catabolism, which acts as an inhibitor of carnitine biosynthesis due to the formation of *O*-phenylacetyl-*L*-carnitine.⁷⁹ The negative correlation of

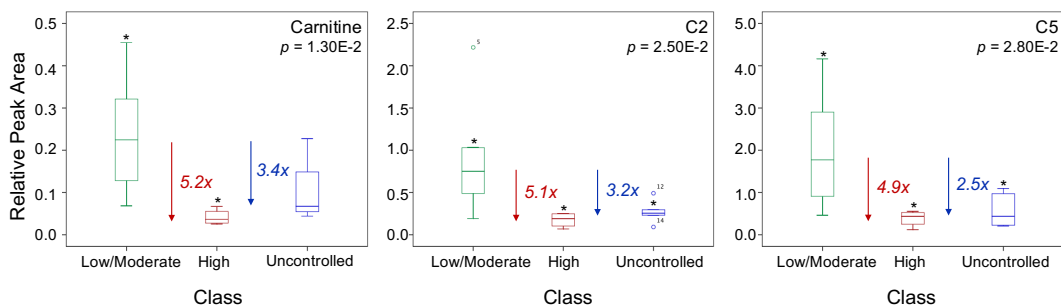


Figure 2.18. Box plots showing differential urinary excretion of carnitine (C0) and acylcarnitines (C2 and C5) based on urinary Phe, grouped by low/moderate ($< 200 \mu\text{M}$, $n = 7$) or high (Phe $> 200 \mu\text{M}$, $n = 4$) excretion, with PKU patients not consuming a specialized amino acid formula or following a restricted diet as a control ($n = 5$). Fold-changes (FC) are based on median RPAs for low/moderate:high Phe or low/moderate Phe:uncontrolled.

free carnitine and other short- and medium-chain acylcarnitines with urinary Phe in classic PKU patients is thus a consequence of both increased phenylacetate and lower dietary carnitine intake, which is consistent with lower carnitine bioavailability that may contribute to greater mitochondrial stress if a Phe-restricted diet is not adhered consistently.

2.4.5 Evaluation of Metabolome Variation in Children with PKU

Infants and young children with PKU are monitored frequently (weekly to monthly) to ensure blood Phe levels stay within an adequate range.²⁶ **Figure 2.19** shows a control chart of blood Phe concentrations throughout sample collection for three PKU patients (ages 2 mo to 2 y at time of recruitment). The concentrations show random variations over several months, where two children (**A** and **B**) had one sample with blood Phe outside the therapeutic range. These fluctuations may be a result of supplement and meal timing.⁸⁴ Fluctuations of Phe

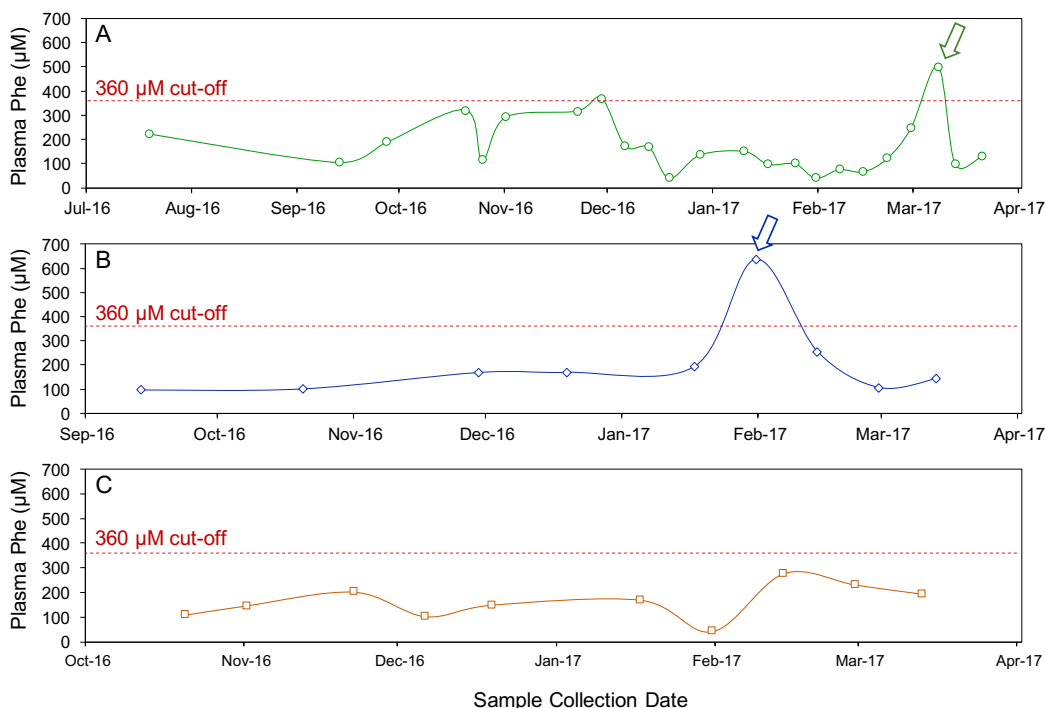


Figure 2.19. Plasma Phe concentrations throughout sample collection for three infants recently diagnosed with classic PKU under 2 y. Patient 1 (2 mo, **A**) showed variable levels of Phe throughout sample collection, patients 8 and 10 (2 y, **B** and **C**, respectively) had consistent Phe levels, aside from two time points where Phe exceeded the recommended therapeutic range, which are indicated by arrows.

within 24 h is noted for individuals with PKU, with periods of fasting (*i.e.*, overnight) resulting in higher levels of Phe. Timing of consumption of the amino acid formula also affects fluctuation in plasma Phe concentrations, with increased blood Phe occurring 90 min after a meal. Day-to-day concentrations in blood Phe for adults considered to have good control over their PKU may vary by up to 400%, as a result of diet, growth rate, and general health. For older children, Phe levels appear to be relatively stable, however this is likely a result of the combination of parental control as well as the previous determination of appropriate Phe allowance and/or the child/family becoming accustomed to

catering to this specialized diet. Overall, it is shown that plasma Phe concentrations are well maintained within therapeutic guidelines (*i.e.*, $< 360 \mu\text{M}$), with intermittent fluctuations likely to be a result of meal timing. There were only two cases with plasma Phe $> 360 \mu\text{M}$, however there is no evidence of higher Phe/protein intake (*i.e.*, no elevations in biomarkers of protein intake). Spearman's rank correlation analysis of repeat plasma samples from children with PKU demonstrated moderate negative correlations of plasma Phe with alanine (Ala; $r_s = -0.534$, $p < 0.005$), His ($r_s = -0.422$, $p < 0.005$), and threonine (Thr; $r_s = -0.399$, $p < 0.005$), which may suggest reduced formula intake and substandard dietary intake. As a result, repeat analysis of plasma samples from recently diagnosed infants with classic PKU demonstrate a far greater consistency of maintaining Phe levels within an optimal therapeutic range due to better dietary compliance with formula feeding as compared to the adult PKU patients in our study who were more likely to have Phe concentrations over the $360 \mu\text{M}$ cut-off.

2.5 Conclusion

It has been demonstrated that MSI-CE-MS offers a reliable yet high-throughput platform for the diagnosis and therapeutic monitoring of PKU patients, which were consistent with previously validated UPLC-UV methods performed within a clinical laboratory setting with low bias ($< 20\%$) and acceptable long-term technical precision ($CV < 15\%$). Additionally, MSI-CE-MS allows for nontargeted and broad-spectrum screening of a diverse number of

polar/ionic metabolites present in human biofluids, including plasma and urine. Plasma Phe concentrations were observed to be highly variable among a cohort of classic PKU patients, with the majority of cases having plasma Phe concentrations within the recommended therapeutic range of 120 μM to 360 μM . Similar to previous studies, higher plasma Phe concentrations were typically observed in older PKU patients who tend to struggle more with dietary adherence. A targeted analysis of known Phe catabolites associated with PKU, including Tyr and various Phe catabolites, was carried out to explore the potential of urine as a biospecimen for therapeutic monitoring of PKU patients as an alternative to blood collection, which is highly invasive. It was shown that urinary excretion of Phe is strongly correlated with circulating blood Phe. Furthermore, Phe catabolites (*N*-phenylacetylglutamine, phenylsulfate, phenylpyruvate, and *o*-hydroxyphenylacetate) were shown to have strong, positive correlations with urinary Phe excretion and circulating plasma Phe concentrations. In particular, phenylpyruvate showed median fold-change responses that were approximately 4-fold greater than that of urinary Phe for individuals with grossly elevated levels of plasma Phe. This may represent a better way to discriminate PKU patients from non-PKU patients, while providing detailed information regarding disease status that is dependent on dietary habits. Nontargeted metabolomic studies were also performed in conjunction with multivariate and univariate data analysis of plasma filtrate samples, which showed a significant elevation in the plasma creatinine/creatinine ratio with decreased levels of α -amino adipic acid, Ser, Ile, and

Leu among classic PKU patients as a function of their plasma Phe concentrations. Individuals not following a restricted diet or consuming an amino acid formula had increased levels of several plasma markers of protein/meat intake, such as carnosine, creatinine, and 3-methylhistidine. Multivariate and univariate analysis of single-spot urine samples after PQN normalization classified by low/moderate or high Phe excretion showed significant decreases in carnitine and two acylcarnitines (C2 and C5), which is consistent with lower carnitine intake in the PKU diet, in addition to a greater risk for mitochondrial stress caused by high levels of Phe and phenylacetate. Similarly, significant elevations in urinary imidazolelactic acid and imidazoleacetic acid excretion were also observed, which were strongly correlated with Phe excretion. Imidazolelactic acid and imidazoleacetic acid are catabolites of His that are excreted in urine with His loading, which may be caused by hepatic stress as a result of poor dietary compliance in terms of low protein intake and/or a deficiency in folic acid or vitamin B12. Overall, this study demonstrated the high variability in the metabolic phenotype of classic PKU patients as reflected by distinctive metabolic perturbations measured in both plasma and urine. Limitations of this study include poor standardization of food records that relied on patient/parental recall accompanying biospecimen collection, which made interpretation of dietary status difficult. Future work will aim to better elucidate the differences in metabolic/nutritional status of PKU patients, which will require the control of diet and interventions. For example, in order to better study the relationship of diet

with circulating and excreted Phe concentrations, a standardized dietary intake (*i.e.*, meal plan) for all PKU patients is needed in order to overcome the limitations introduced by food records. Further, to study the effect of individuals with mediocre or poor dietary adherence, the introduction of foods higher in Phe-content would allow us to study potential dietary markers and metabolic perturbations with a direct correlation to their intake.

2.6 References

1. Muntau, A.C.; Leandro, J.; Staudigl, M.; Mayer, F.; Gersting, S.W. Innovative strategies to treat protein misfolding in inborn errors of metabolism: pharmacological chaperones and proteostasis regulators. *J. Inherit. Metab. Dis.* 2014, **37**: 505-523.
2. Gregerson, N.; Bross, P.; Vang, S.; Christensen, J.H. Protein misfolding and human disease. *J. Inherit. Metab. Dis.* 2006, **29**: 456-470.
3. Kim, Y.E.; Hipp, M.S.; Bracher, A.; Hayer-Hartl, M.; Hartl, F.U. Molecular chaperone functions in protein folding and proteostasis. *Annu. Rev. Biochem.* 2013, **82**: 323-355.
4. Muntau, A.C.; Gersting, S.W. Phenylketonuria as a model for protein misfolding diseases and for the development of next generation orphan drugs for patients with inborn errors of metabolism. *J. Inherit. Metab. Dis.* 2010, **33**: 649-658.
5. Aebi, H.E. Inborn errors of metabolism. *Annu. Rev. Biochem.* 1967, **36**: 271-306.
6. Guthrie, R.; Susi, A. A simple phenylalanine method for detecting phenylketonuria in large populations of newborn infants. *Pediatrics* 1963, **32**: 338-343.
7. Bonham, J.R. Impact of new screening technologies: should we screen and does phenotype influence this decision? *J. Inherit. Metab. Dis.* 2013, **36**: 681-686.
8. Chalcraft, K.R.; Britz-McKibbin, P. Newborn screening of inborn errors of metabolism by capillary electrophoresis-electrospray ionization-mass spectrometry: a second-tier method with improved specificity and sensitivity. *Anal. Chem.* 2009, **81**: 307-314.
9. Cipriano, L.E.; Rugar, C.A.; Zaric, G.S. The cost-effectiveness of expanding newborn screening for up to 21 inherited metabolic disorders using tandem

- mass spectrometry: results from a decision-analytic model. *Value Health* 2007, **10**: 83-97.
10. Wilcken, B. Recent advances in newborn screening. *J. Inherit. Metab. Dis.* 2007, **30**: 129-133.
 11. Williams, R.A.; Mamotte, C.D.S.; Burnett, J.R. Phenylketonuria: An inborn error of phenylalanine metabolism. *Clin. Biochem. Rev.* 2008, **29**: 31-41.
 12. National Institute of Health (NIH). Phenylketonuria: Screening and Management. *NIH Consensus Statement Online* 2000, **17**: 1-27
 13. DeGraw, J.I.; Cory, M.; Skinner, W.A.; Theisen, M.C.; Mitoma, C. Experimentally induced phenylketonuria. I. Inhibitors of phenylalanine hydroxylase. *J. Med. Chem.* 1967, **10**: 64-66.
 14. Fusetti, F.; Erlandsen, H.; Flatmark, T.; Stevens, R.C. Structure of tetrameric human phenylalanine hydroxylase and its implications for phenylketonuria. *J. Biol. Chem.* 1998, **273**: 16962-16967.
 15. Gersting, S.W.; Staudigl, M.; Truger, M.S.; Messing, D.D.; Danecka, M.K.; Sommerhoff, C.P.; Kemter, K.F.; Muntau, A.C. Activation of phenylalanine hydroxylase induces positive cooperativity toward the natural cofactor. *J. Biol. Chem.* 2010, **285**: 30686-30697.
 16. Heintz, C.; Cotton, R.G.H.; Blau, N. Tetrahydrobiopterin, its mode of action on phenylalanine hydroxylase, and importance of genotypes for pharmacological therapy of phenylketonuria. *Hum. Mutat.* 2013, **34**: 927-936.
 17. Flydal, M.I.; Martinez, A. Phenylalanine hydroxylase: Function, structure, and regulation. *IUBMB Life* 2013, **65**: 341-349.
 18. Imperlini, E.; Orrù, S.; Corbo, C.; Daniele, A.; Salvatore, F. Altered brain protein expression profiles are associated with molecular neurological dysfunction in the PKU mouse model. *J. Neurochem.* 2014, **129**: 1002-1012.
 19. Narravula, A.; Garber, K.B.; Askree, S.H.; Hegde, M.; Hall, P.L. Variants of uncertain significance in newborn screening disorders: Implications for large-scale genomic sequencing. *Genet. Med.* 2016, **19**: 77-82.
 20. Guldberg, P.; Rey, F.; Zschocke, J.; Romano, V.; François, B.; Michiels, L.; Ullrich, K.; Hoffman, G.F.; Burgard, P.; Schmidt, H.; Meli, C.; Riva, E.; Dianzani, I.; Ponzzone, A.; Rey, J.; Güttler, F. A European multicenter study of phenylalanine hydroxylase deficiency: Classification of 105 mutations and a general system for genotype-based prediction of metabolic phenotype. *Am. J. Hum. Genet.* 1998, **63**: 71-79.
 21. Scriver, C.R.; Hurtubise, M.; Konecki, D.; Phommavanh, M.; Prevost, L.; Erlandsen, H.; Stevens, R.; Water, P.J.; Ryan, S.; McDonald, D.; Sarkissian, C. PAHdb 2003: What a locus-specific knowledgebase can do. *Hum. Mutat.* 2003, **21**: 333-344.
 22. Phenylalanine Hydroxylase Locus Knowledgebase (PAHdb). Available: <http://www.pahdb.mcgill.ca/> [Accessed 23 August 2017].
 23. Jennings, I.G.; Cotton, R.G.H.; Kobe, B. Structural interpretation of mutations in phenylalanine hydroxylase protein aids in identifying genotype-

- phenotype correlations in phenylketonuria. *Eur. J. Hum. Genet.* 2000, **8**: 683-696.
24. Trunzo, R.; Santacroce, R.; D'Andrea, G.; Longo, V.; De Girolamo, G.; Dimatteo, C.; Leccese, A.; Bafunno, V.; Lillo, V.; Papadia, F.; Margaglione, M. Phenylalanine hydroxylase deficiency in south Italy: Genotype-phenotype correlations, identification of a novel mutant PAH allele and prediction of BH₄ responsiveness. *Clin. Chim. Acta* 2015, **450**: 51-55.
 25. Dworniczak, B.; Aulehla-Scholz, C.; Kalaydjieva, L.; Bartholome, K.; Grudda, K.; Horst, J. Aberrant splicing of phenylalanine hydroxylase mRNA: The major cause for phenylketonuria in parts of southern Europe. *Genomics* 1991, **11**: 242-246.
 26. Erlandsen, H.; Pey, A.L.; Gámez, A.; Pérez, B.; Desviat, L.R.; Aguado, C.; Koch, R.; Surendran, S.; Tying, S.; Matalon, R.; Scriver, C.R.; Ugarte, M. Martinez, A.; Stevens, R.C. Correction of kinetic and stability defects by tetrahydrobiopterin in phenylketonuria patients with certain phenylalanine hydroxylase mutations. *PNAS* 2004, **101**: 16903-16908.
 27. Enns, G.M.; Martinez, D.R.; Kuzmin, A.I.; Koch, R.; Wakeem, C.K.; Woo, S.L.C.; Eisensmith, R.C.; Packman, S. Molecular correlations in phenylketonuria: Mutation patterns and corresponding biochemical and clinical phenotypes in a heterogeneous California population. *Pediatr. Res.* 1999, **46**: 594.
 28. Dipple, K.M.; McCabe, E.R.B. Phenotypes of patients with "simple" Mendelian disorders are complex traits: Thresholds, modifiers, and systems dynamics. *Am. J. Hum. Genet.* 2000, **66**: 1729-1735.
 29. Vockley, J.; Andersson, H.C.; Antshel, K.M.; Braverman, N.E.; Burton, B.K.; Frazier, D.M.; Mitchell, J.; Smith, W.E.; Thompson, B.H.; Berry, S.A. Phenylalanine hydroxylase deficiency: diagnosis and management guideline. *Genet. Med.* 2014, **16**: 188-200.
 30. McHugh, D.M.S.; Cameron, C.A.; Abedenur, J.E.; Abdulrahman, M.; Adair, O.; *et. al.* Clinical validation of cutoff target ranges in newborn screening of metabolic disorders by tandem mass spectrometry: A worldwide collaborative project. *Genet. Med.* 2011, **13**: 230-254.
 31. Blau, N.; Hennermann, J.B.; Langenbeck, U.; Lichter-Konecki, U. Diagnosis, classification, and genetics of phenylketonuria and tetrahydrobiopterin (BH₄) deficiencies. *Molec. Genet. Metab.* 2011, **104**: S2-S9.
 32. Hanley, W.B. Newborn screening in Canada — Are we out of step? *Paediatr. Child Health* 2005, **10**: 203-207.
 33. Farishian, R.A.; Whittaker, J.R. Phenylalanine lowers melanin synthesis in mammalian melanocytes by reducing tyrosine uptake: Implications for pigment reduction in phenylketonuria. *J. Invest. Dermatol.* 1980, **74**: 85-89.
 34. Berry, S.A.; Brown, C.; Grant, M.; Greene, C.L.; Jurecki, E.; Koch, J.; Mosely, K.; Suter, R.; van Calcar, S.C.; Wiles, J.; Cederbaum, S. Newborn screening 50 years later: access issues faced by adults with PKU. *Genet. Med.* 2013, **15**: 591-599.

35. Schuck, P.F.; Malgarin, F.; Cararo, J.H.; Cardoso, F.; Streck, E.L.; Ferreira, G.C. Phenylketonuria pathophysiology: on the role of metabolic alterations. *Aging Dis.* 2015, **6**: 390-399.
36. Rocha, J.C.; Martel, F. Large neutral amino acids supplementation in phenylketonuric patients. *J. Inherit. Metab. Dis.* 2009, **32**: 472-480.
37. Harding, C.O.; Winn, S.R.; Gibson, K.M.; Arning, E.; Bottiglieri, T.; Grompe, M. Pharmacologic inhibition of L-tyrosine degradation ameliorates cerebral dopamine deficiency in murine phenylketonuria (PKU). *J. Inherit. Metab. Dis.* 2014, **37**: 735-743.
38. Shulkin, B.L.; Betz, A.L.; Koeppe, R.A.; Agranoff, B.W. Inhibition of neutral amino acid transport across the human blood-brain barrier by phenylalanine. *J. Neurochem.* 1995, **64**: 1252-1257.
39. de Groot, M.J.; Hoeksma, M.; Blau, N.; Reijngoud, D.J.; van Spronsen, F.J. Pathogenesis of cognitive dysfunction in phenylketonuria: Review of hypotheses. *Mol. Genet. Metab.* 2010, **99**: S86-S89.
40. Cerone, R.; Andria, G.; Giovannini, M.; Leuzzi, V.; Riva, E.; Burlina, A. Testing for tetrahydrobiopterin responsiveness in patients with hyperphenylalaninemia due to phenylalanine hydroxylase deficiency. *Adv. Ther.* 2013, **30**: 212-228.
41. Lachmann, R. Sapropterin hydrochloride: enzyme enhancement therapy for phenylketonuria. *Ther. Adv. Endocrinol. Metab.* 2011, **2**: 127-133.
42. Gramer, G.; Burgard, P.; Garbade, S.F.; Lindner, M. Effects and clinical significance of tetrahydrobiopterin supplementation in phenylalanine hydroxylase-deficient hyperphenylalaninemia. *J. Inherit. Metab. Dis.* 2007, **30**: 556-562.
43. Sarkissian, C.N.; Kang, T.S.; Gámez, A.; Scriver, C.R.; Stevens, R.C. Evaluation of orally administered PEGylated phenylalanine ammonia lyase in mice for the treatment of phenylketonuria. *Mol. Genet. Metab.* 2011, **104**: 249-254.
44. Longo, N.; Harding, C.O.; Burton, B.K.; Grange, D.K.; Vockley, J.; Wasserstein, M.; Rice, G.M.; Dorenbaum, A.; Neuenburg, J.K.; Musson, D.G.; Gu, Z.; Sile, S. Single-dose, subcutaneous recombinant phenylalanine ammonia lyase conjugated with polyethylene glycol in adult patients with phenylketonuria: an open-label, multicentre, phase 1 dose-escalation trial. *Lancet* 2014, **84**: 37-44.
45. Bell, S.M.; Wendt, D.J.; Zhang, Y.; Taylor, T.W.; Long, S.; Tsuruda, L.; Zhao, B.; Laipis, P.; Fitzpatrick, P.A. Formulation and PEGylation optimization of the therapeutic PEGylated phenylalanine ammonia lyase for the treatment of phenylketonuria. *PLoS ONE* 2017, **12**: e0173269.
46. MacDonald, A.; Rocha, J.C.; van Rijn, M.; Feillet, F. Nutrition in phenylketonuria. *Mol. Genet. Metab.* 2011, **104**: S10-S18.
47. Marcason, W. Is there a standard meal plan for phenylketonuria (PKU)? *J. Acad. Nutr. Diet.* 2013, **113**: 1124.

48. Schindeler, S.; Ghosh-Jerath, S.; Thompson, S.; Rocca, A.; Joy, P.; Kemp, A.; Rae, C.; Green, K.; Wilcken, B.; Christodoulou, J. The effects of large neutral amino acid supplements in PKU: An MRS and neuropsychological study. *Molec. Genet. Metab.* 2007, **91**: 48-54.
49. Ney, D.M.; Blank, R.D.; Hansen, K.E. Advances in the nutritional and pharmacological management of phenylketonuria. *Curr. Opin. Clin. Nutr. Metab. Care* 2014, **17**: 61-68.
50. Daly, A.; Evans, S.; Chahal, S.; Santra, S.; MacDonald, A. Glycomacropeptide in children with phenylketonuria: does its phenylalanine content affect blood phenylalanine control? *J. Hum. Nutr. Diet.* 2017, **30**: 515-523.
51. Pinto, A.; Almeida, M.F.; Ramos, P.C.; Rocha, S.; Guimas, A.; Ribeiro, R.; Martins, E.; Bandeira, A.; MacDonald, A.; Rocha, J.C. Nutritional status in patients with phenylketonuria using glycomacropeptide as their major protein source. *Eur. J. Clin. Nutr.* 2017, Epub ahead of print, doi: 10.1038/ejcn.2017.38.
52. Zaki, O.K.; El-Wakeel, L.; Ebeid, Y.; Ez Elarab, H.S.; Moustaga, A.; Abdulazim, N.; Karara, H.; Elghawaby, A. The use of glycomacropeptide in dietary management of phenylketonuria. *J. Nutr. Metab.* 2016, **2016**: 2453027.
53. Brown, C.S.; Lichter-Konecki, U. Phenylketonuria (PKU): A problem solved? *Mol. Genet. Metab. Reports* 2016, **6**: 8-12.
54. Johnson, C.H.; Ivanisevic, J.; Siuzdak, G. Metabolomics: beyond biomarkers and towards mechanisms. *Nat. Rev. Mol. Cell Biol.* 2016, **17**: 451-459.
55. DiBattista, A.; McIntosh, N.; Lamoreaux, M.; Al-Dirbashi, O.; Chakraborty, P.; Britz-McKibbin, P. Temporal signal pattern recognition in mass spectrometry: A method for rapid identification and accurate quantification of biomarkers for inborn errors of metabolism with quality assurance. *Anal. Chem.* 2017, **89**, 8112-8121.
56. Miller, M.J.; Kennedy, A.D.; Eckhart, A.D.; Burrage, L.C.; Wulff, J.E.; Miller, L.A.D.; Milburn, M.V.; Ryals, J.A.; Beaudet, A.L.; Sun, Q.; Sutton, V.R.; Elsea, S.H. Untargeted metabolomic analysis for the clinical screening of inborn errors of metabolism. *J. Inherit. Metab. Dis.* 2015, **38**: 1029-1039.
57. Mütze, U.; Beblo, S.; Kortz, L.; Matthies, C.; Koletzko, B.; Bruegel, M.; Rohde, C.; Thiery, J.; Kiess, W.; Ceglarek, U. Metabolomics of dietary fatty acid restriction in patients with phenylketonuria. *PLoS ONE* 2012, **7**: e43021.
58. Blasco, H.; Veyrat-Durebex, C.; Bertrand, M.; Patin, F.; Labarthe, F.; Henique, H.; Emond, P.; Andres, C.R.; Antar, C.; Landon, C.; Nadal-Desbarats, L.; Maillot, F. A multiplatform metabolomics approach to characterize plasma levels of phenylalanine and tyrosine in phenylketonuria. *JIMD Reports* 2017. **32**: 69-79.
59. Ney, D.M.; Murali, S.G.; Stroup, B.M.; Nair, N.; Sawin, E.A.; Rohr, F.; Levy, H.L. Metabolomic changes demonstrate reduced bioavailability of tyrosine and altered metabolism of tryptophan via the kynurenine pathway

- with ingestion of medical foods in phenylketonuria. *Mol. Genet. Metab.* 2017, **121**: 96-103.
60. Kuehnbaum, N.L.; Kormendi, A.; Britz-McKibbin, P. Multisegment injection-capillary electrophoresis-mass spectrometry: A high-throughput platform for metabolomics with high data fidelity. *Anal. Chem.* 2013, **85**: 10664-10669.
 61. Kuehnbaum, N.L.; Gillen, J.B.; Kormendi, A.; Lam, K.P.; DiBattista, A.; Gibala, M.J.; Britz-McKibbin, P. Multiplexed separations for biomarker discovery in metabolomics: Elucidating adaptive responses to exercise training. *Electrophoresis* 2015, **36**: 2226-2236.
 62. Roux, A.; Thévenot, E.A.; Seguin, F.; Olivier, M.F.; Junot, C. Impact of collection conditions of the metabolite content of human urine samples as analyzed by liquid chromatography coupled to mass spectrometry and nuclear resonance spectroscopy. *Metabolomics* 2015, **11**: 1095-1105.
 63. Dieterle, F.; Ross, A.; Schlotterbeck, G.; Senn, H. Probabilistic quotient normalization as robust method to account for dilution of complex biological mixtures. Application in ¹H NMR metabolomics. *Anal. Chem.* 2006, **78**: 4281-4290.
 64. Walter, J.H.; White, F.J. Blood phenylalanine control in adolescents with phenylketonuria. *Int. J. Adolesc. Med. Health* 2004, **16**: 41-45.
 65. Benneyan, J.C. Use and interpretation of statistical quality control charts. *Int. J. Qual. Health Care* 1998, **10**: 69-73.
 66. Jurecki, E.R.; Cederbaum, S.; Kopesky, J.; Perry, K.; Rohr, F.; Sanchez-Valle, A.; Viau, K.S.; Sheinin, M.Y.; Cohen-Pfeffer, J.L. Adherence to clinic recommendations among patients with phenylketonuria in the United States. *Mol. Genet. Metab.* 2017, **120**: 190-197.
 67. van Spronsen, F.J.; van Rijn, M.; van Dijk, T.; Smit, G.P.A.; Reijngoud, D.J.; Berger, R.; Heymans, H.S.A. Plasma phenylalanine and tyrosine responses to different nutritional conditions (fasting/postprandial) in patients with phenylketonuria: Effect of sample timing. *Pediatrics* 1993, **92**: 570-573.
 68. van Spronsen, F.J.; van Wegberg, A.M.; Ahring, K.; Bélanger-Quintana, A.; Blau, N.; Bosch, A.M.; Burlina, A.; Campistol, J.; Feillet, F.; Gizewska, M.; Huijbregts, S.C.; Kearney, S.; Leuzzi, V.; Maillot, F.; Muntau, A.C.; Trefz, F.K.; van Rijn, M.; Walter, J.H.; MacDonald, A. Key European guidelines for the diagnosis and management of patients with phenylketonuria. *Lancet Diabetes Endocrinol.* 2017, DOI: [dx.doi.org/10.1016/S2213-8587\(16\)30320-5](https://doi.org/10.1016/S2213-8587(16)30320-5).
 69. Hoeksma, M.; Reijngoud, D.J.; Pruijm, J.; de Valk, H.W.; Paans, A.M.; van Spronsen, F.J. Phenylketonuria: high plasma phenylalanine decreases cerebral protein synthesis. *Mol. Genet. Metab.* 2009, **96**: 177-182
 70. Sanayama, Y.; Nagasaka, H.; Takayanagi, M.; Ohura, T.; Sakamoto, O.; Ito, T.; Ishige-Wada, M.; Usui, H.; Yoshino, M.; Ohtake, A.; Yorifuji, T.; Tsukahara, H.; Hirayama, S.; Miida, T.; Fukui, M.; Okano, Y. Experimental evidence that phenylalanine is strongly associated to oxidative stress in

- adolescents and adults with phenylketonuria. *Mol. Genet. Metab.* 2011, **103**: 220-225
71. Wagner, B.D.; Accurso, F.J.; Laguna, T.A. The applicability of urinary creatinine as a method of specimen normalization in the cystic fibrosis population. *J. Cyst. Fibros.* 2010, **9**: 212-216.
 72. Tang, K.W.A.; Toh, Q.C.; Teo, B.W. Normalisation of urinary biomarkers to creatinine for clinical practice and research – when and why. *Singapore Med. J.* 2015, **56**, 7-10.
 73. Neubert, A.; Remer, T. The impact of dietary protein intake on urinary creatinine excretion in a healthy pediatric population. *J. Pediatrics* 1998, **133**: 655-659.
 74. Barr, D.B.; Wilder, L.C.; Caudill, S.P.; Gonzalez, A.J.; Needham, L.L.; Pirkle, J.L. Urinary creatinine concentrations in the U.S. population: Implications for urinary biologic monitoring measurements. *Environ. Health Perspect.* 2005, **113**: 192-200.
 75. Sarkissian, C.N.; Scriver, C.R.; Mamer, O.A. Measurement of phenyllactate, phenylacetate, and phenylpyruvate by negative ion chemical ionization-gas chromatography/mass spectrometry in brain of mouse. Genetic models of phenylketonuria and non-phenylketonuria hyperphenylalaninemia. *Anal. Biochem.* 2000, **280**: 242-249.
 76. Haley, C.J.; Harper, A.E. The importance of transamination and decarboxylation in phenylalanine metabolism *in vivo* in the rat. *Arch. Biochem. Biophys.* 1978, **189**: 524-530.
 77. Michals, K.; Lopus, M.; Matalon, R. Phenylalanine metabolites as indicators of dietary compliance in children with phenylketonuria. *Biochem. Med. Metab. Bio.* 1988, **39**: 18-23.
 78. Wikoff, W.R.; Anfora, A.T.; Liu, J.; Schultz, P.G.; Lesley, S.A.; Peters, E.C.; Siuzdak, G. Metabolomics analysis reveals large effects of gut microflora on mammalian blood metabolites. *PNAS* 2009, **106**: 3698-3703.
 79. Weigel, C.; Kiener, C.; Meier, N.; Schmid, P.; Rauh, M.; Rascher, W.; Knerr, I. Carnitine status in early-treated children, adolescents and young adults with phenylketonuria on low phenylalanine diets. *Ann. Nutr. Metab.* 2008, **53**: 91-95.
 80. Xiong, X.; Sheng, X.; Liu, D.; Zeng, T.; Peng, Y.; Wang, Y. A GC/MS-based metabolomic approach for reliable diagnosis of phenylketonuria. *Anal. Bioanal. Chem.* 2015, **407**: 8825-8833.
 81. Reilly, A.A.; Bellisario, R.; Pass, K. Multivariate discrimination for phenylketonuria (PKU) and non-PKU hyperphenylalaninemia after analysis of newborns' dried blood-spot specimens for six amino acids by ion-exchange chromatography. *Clin. Chem.* 1998, **44**: 2317-2326.
 82. O'Gorman, A.; Gibbons, H.; Brennan, L. Metabolomics in the identification of biomarkers of dietary intake. *Comput. Struct. Biotechnol. J.* 2013, **4**: e201301004.

83. Mayersohn, M.; Conrad, K.A.; Achari, R. The influence of a cooked meat meal on creatinine plasma concentration and creatinine clearance. *Br. J. Clin. Pharmacol.* 1983, **15**: 227-230.
84. Cleary, M.; Trefz, F.; Muntau, A.C.; Feillet, F.; van Spronsen, F.J.; Burlina, A.; Bélanger-Quintana, A.; Gizewska, M.; Gasteyger, C.; Bettiol, E.; Blau, N.; MacDonald, A. Fluctuations in phenylalanine concentrations in phenylketonuria: A review of possible relationships with outcomes. *Molec. Genet. Metab.* 2013, **110**: 418-423.
85. Dezortová, M.; Hejčmanová, L.; Hájek, M. Decreasing choline signal—a marker of phenylketonuria? *MAGMA* 1996, **4**: 181-186.
86. Wilson, K.M.; Clayton, B.E. Importance of choline during growth, with particular reference to synthetic diets in phenylketonuria. *Arch. Dis. Child* 1962, **37**: 565-577.
87. Smith, I.; Rider, L.J. Imidazole lactic acid—a component of normal human urine. *Proc. Soc. Exp. Biol. Med.* 1967, **124**: 233-235.
88. Morris, M.L.; Lee, S.C.; Harper, A.E. Influence of differential induction of histidine catabolic enzymes on histidine degradation *in vivo*. *J. Biol. Chem.* 1972, **247**: 5793-5804.
89. Dubovský, J.; Dubovská, E. Urinary imidazolelactic acid in normal subjects and in liver cirrhosis. *Clin. Chim. Acta* 1965, **12**: 360-362.
90. Carter, F.C.; Heller, P.; Schaffner, G.; Korn, R.J. Formiminoglutamic acid (FIGLU) excretion in hepatic cirrhosis. *JAMA Int. Med.* 1961, **108**: 41-46.
91. Cooperman, J.M.; Lopez, R. The role of histidine in the anemia of folate deficiency. *Exp. Biol. Med. (Maywood)* 2002, **227**: 998-1000.
92. van Roon-Djordjević, B.; Cerfontain-van, S. Urinary excretion of histidine metabolites as an indication for folic acid and vitamin B 12 deficiency. *Clin. Chim. Acta* 1972, **41**: 55-65.
93. Stølen, L.H.; Lije, R.; Jørgensen, J.V.; Blikrud, Y.T.; Almaas, R. High dietary folic acid and high plasma folate in children and adults with phenylketonuria. *JIMD Rep.* 2014, **13**: 83-90.
94. Procházková, D.; Jarkovský, J.; Haňková, Z.; Konečná, P.; Benáková, H.; Vinohradská, H.; Mikušková, A. Long-term treatment for hyperphenylalaninemia and phenylketonuria: a risk for nutritional vitamin B12 deficiency? *J. Pediatr. Endocrinol. Metab.* 2015, **28**: 1327-1332.
95. Fischer, G.M.; Nemeti, B.; Farkas, V.; Debreceni, B.; Laszlo, A.; Schaffer, Z.; Somogyi, C.; Sandor, A. Metabolism of carnitine in phenylacetic acid-treated rats and in patients with phenylketonuria. *Biochim. Biophys. Acta* 2000, **1501**: 200-210.

2.7 Supplementary Tables and Figures

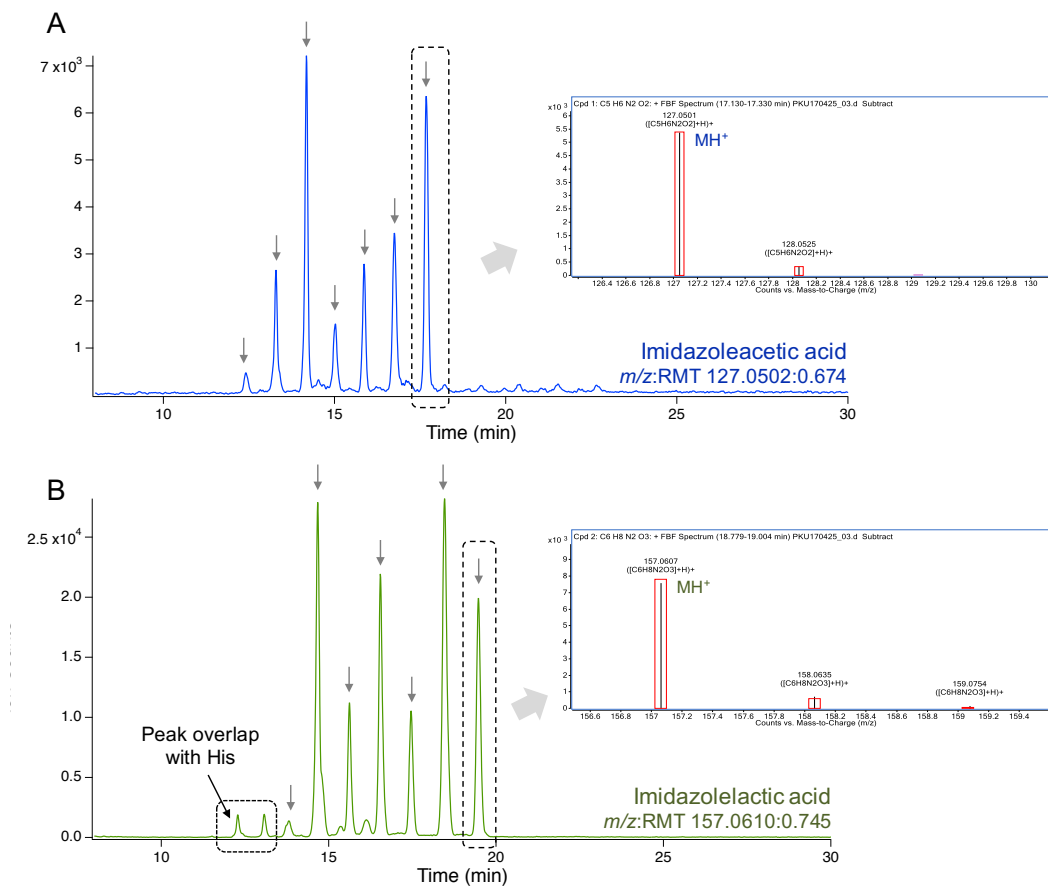


Figure S2.1. Extracted ion electropherogram and ESI+ mass spectrum for imidazoleacetic acid and imidazolelactic acid in urine. These molecular features were determined to be singly charged due to isotope spacing of ~ 1 ppm. Molecular Formula Generator (Qualitative Analysis) and a database search (Metlin) were used to tentatively identify these compounds.

Table S2.1. Clinical characteristics of PKU patients.

Patient	Age	Sex	Type of PKU	Plasma Phe (μM)	Plasma Tyr (μM)	Drug Therapy	Formula	Dietary Adherence
1	0.2	M	Classic	223	70		Nutricia/Periflex Infant	Excellent
2	30	M	Classic	1548	45			Poor
3	28	F	Classic	N/A	N/A			Adequate
4	43	F	Classic	899	37			Poor
5	9	M	Classic	410	39	Kuvan	Abbott/Phenex-2	Adequate
6	24	F	Classic	530	36		Nutricia/Duocal	Poor
7	11	F	Classic	166	45	Kuvan	Nutricia/PhenylAde 60	Excellent
8	2	M	Classic	97	110		Nutricia/Periflex	Excellent
9	5	M	Classic	75	91		Abbott/Phenex-2	Excellent
10	2	F	Classic	108	40		Nutricia/Periflex Jr. Plus	Excellent
11	37	F	Classic	1082	43		Abbott/Phenex-2	Poor
12	14	F	Classic	662	60		Nutricia/Periflex Jr. Plus	Adequate
13	8	M	Classic	295	140		Abbott/Phenex 2	Adequate
14	21	F	HPA	N/A	N/A			None
15	13	F	Classic	N/A	N/A		Cambrooke/Camino Pro	Excellent
16	23	M	Classic	N/A	N/A		Nutricia/PhenylAde Essential	Poor
17	25	M	Classic	N/A	N/A			Poor
18	6	M	Classic	39	100		Nutricia/PhenylAde Essential	Excellent
19	29	F	Classic	N/A	N/A			Adequate
20	11	M	Classic	450	66	Kuvan	Abbott/Phenex-2	N/A
21	25	M	Mild/HPA	113	50	Kuvan	Abbott/Phenex-2	None
22	9	M	Classic	382	30		Nutricia/Periflex Jr.	Adequate
23	3	M	Classic	163	44		Nutricia/PhenylAde Essential	Excellent
24	50	F	Classic	253	91	Kuvan	Periflex Advance	Excellent
25	8	F	Classic	254	98	Kuvan		Excellent

CHAPTER III.

EVALUATING THE IMPACT OF ELECTRONIC CIGARETTE SMOKE EXPOSURE ON THE PLACENTAL METABOLOME

3.1 Abstract

Electronic cigarettes (e-cigarettes) are popularly marketed as a healthier alternative to conventional cigarettes, with use in young adults skyrocketing over the past five years. The general perception that e-cigarettes are low-risk is of concern to public health, notably among individuals who are dependent on smoking cessation during critical periods of their lives, such as women during pregnancy. Indeed, tobacco smoke and nicotine exposure during pregnancy has been associated with deleterious birth outcomes due to impairments in placenta development and nutrient exchange; however, current research on the health impacts of e-cigarette exposure is sparse. Herein, we evaluated the effects of e-cigarette smoke exposure on the metabolome of placental cells as a model system when using multisegment injection-capillary electrophoresis-mass spectrometry (MSI-CE-MS) and headspace-gas chromatography-mass spectrometry (HS-GC/MS). MSI-CE-MS was applied for nontargeted profiling of polar/ionic metabolites from cell extracts in order to derive better mechanistic insights into the potential harmful effects of various components of e-cigarette smoke, including nicotine dosage and a wide range of flavour agents and undocumented chemical additives. We first evaluated the effects of e-cigarette vapour following exposure to first and third trimester placental cells, which confirmed that the first trimester placental cell line was more susceptible to chemical exposures. Next, we evaluated the effects of unflavoured and flavoured e-cigarette formulations as a

function of nicotine dosage. As expected, flavoured e-cigarette vapours containing nicotine led to more pronounced changes in placental metabolism relative to analogous flavourless products and nicotine-free controls, including changes in neutral amino acids, acylcarnitines, γ -aminobutyric acid, and an intermediate in thymine metabolism, suggesting altered metabolic pathways associated with protein and neurotransmitter synthesis which are critical for placental development and function. This timely study supports the hypothesis that flavoured e-cigarette vapour poses a higher risk to placental function than unflavoured vapour that is relevant to fetal health and development. Overall, elucidating the risk flavoured e-cigarette vapours pose on placental health will aid in the development of public policy regarding the regulation and marketing of an expanding array of e-cigarette products aimed primarily at young adults and women.

3.2 Introduction

3.2.1 Cigarette and Tobacco Usage

Tobacco use is the leading cause of preventable death worldwide, causing over 6 million deaths annually with 10% of these deaths being the result of second-hand smoke.^{1,2} Exposure to tobacco smoke is associated with the development of many chronic diseases, such as throat and lung cancer, cardiovascular disease (CVD), and chronic obstructive pulmonary disease.³ Furthermore, tobacco smoke exposure leads to oxidative stress, dysregulation of

cellular metabolism, and cytotoxicity.^{4,5} Tobacco smoke is composed of over 6,000 chemicals, of which 93 have been identified by the United States Food and Drug Administration (FDA) as harmful or potentially harmful constituents (HPHCs) that are inhaled, ingested, or absorbed into the body and cause direct or indirect harm to users of tobacco products.⁶ The HPHCs are classified on the basis of being possible carcinogens, having adverse respiratory/cardiac effects, being reproductive/developmental toxicants, or being psychostimulants prone to abuse and addiction. Along with nicotine, which accounts for 95% of alkaloid content in tobacco, several minor tobacco alkaloids, such as anabasine, *N*-nitrosonornicotine (NNN), and nornicotine are listed as addictive, reproductive and developmental toxicants, and/or cardiovascular toxicants.^{6,7}

Nicotine is primarily responsible for tobacco dependence and addiction.⁸ Upon inhalation and introduction of nicotine into the lungs, it is rapidly absorbed into circulation and reaches the brain where it binds to nicotinic cholinergic receptors.⁹ Nicotinic acetylcholine receptors (nAChRs) are ligand-gated ion channels distributed throughout the central nervous system (CNS) that are responsible for modulating neuron excitability and synaptic communication.^{10,11} Binding of nicotine or the endogenous substrate acetylcholine opens the channel, allowing entry of sodium and calcium ions, which results in neurotransmitter release.^{10,12} The release of dopamine induces a pleasurable sensation, which promotes the ‘reward’ of nicotine.^{10,11} Additionally, nicotine results in the release of glutamate, a facilitator of dopamine release, and γ -aminobutyric acid (GABA),

an inhibitor of dopamine release. Long-term exposure and tolerance to nicotine results in desensitization of nAChRs (ligand-induced closure and unresponsiveness) and neuroadaptation.¹¹ Neuroadaptation occurs when the body begins to compensate for nicotine so that it can continue to function normally, leading to nicotine tolerance and dependence. Inhibition by GABA is diminished with nAChR desensitization; however, glutamate still facilitates the release of dopamine, which leads to an enhanced responsiveness to nicotine. Anxiety and stress-related symptoms of nicotine withdrawal occur when the receptors become sensitized again, whereas nicotine binding alleviates these symptoms. Similarly, maintaining plasma nicotine levels and receptor desensitization prevents withdrawal symptoms.¹³

3.2.2 Electronic Cigarettes ('E-Cigarettes')

While nicotine is the primary determinant of addiction to tobacco products, the majority of tobacco-related diseases are associated with repeated exposure to other chemicals, additives, and combustion by-products in smoke.⁸ Efforts to limit tobacco-related death and disease have focused on harm reduction by use of non-combustible, less toxic, nicotine-containing products instead of conventional cigarettes. Tobacco harm reduction is a public health framework that focuses on reducing the deleterious consequences of tobacco smoke exposure.¹⁴ Nicotine replacement therapies (NRTs) are a form of tobacco harm reduction and are considered medicinal products for smoking cessation, but not as long-term smoking substitutes. An ideal NRT provides nicotine at incrementally lower

dosages over time to prevent withdrawal symptoms while minimizing additional health risks.¹⁵

Electronic nicotine delivery systems (ENDS) and electronic non-nicotine delivery systems (ENNDS) are handheld devices, including electronic cigarettes (e-cigarettes), that deliver an aerosol to the user to mimic the behavioural rituals and sensory properties of smoking.^{16,17} The first e-cigarette was introduced in China in 2003 as a device to aid in smoking cessation.¹⁸ The popularity of e-cigarettes has since greatly expanded, with Canada and the United States being the predominant markets involved in their manufacture and sale.¹⁹ E-cigarettes are now advertised as a healthier alternative to smoking conventional cigarettes, as a smoking cessation aid, for use where smoking is not allowed, and for use in social settings.^{18,20} While there are several generations of e-cigarette devices, the common components include a mouthpiece, flow sensor, heating coil (atomizer), a battery source, and solution storage cartridge (**Figure 3.1**).¹⁷ Commercial e-cigarette devices allow the user to fill the cartridge with an e-cigarette liquid (e-liquid) of their choice. The e-liquids contain a solvent (vegetable glycerin/glycerol with propylene glycol), natural and artificial flavourings, and nicotine at concentrations ranging from 0 to 24 mg/mL.²¹ The atomizer contains a heating coil that heats and vaporizes the e-liquid. Vaporization is activated by pressing a button on the device that heats the e-liquid to 70-100°C.^{22,23} The vaporized liquid then cools and condenses to an aerosol that can be inhaled through the mouthpiece. The composition of the e-cigarette aerosol is dependent

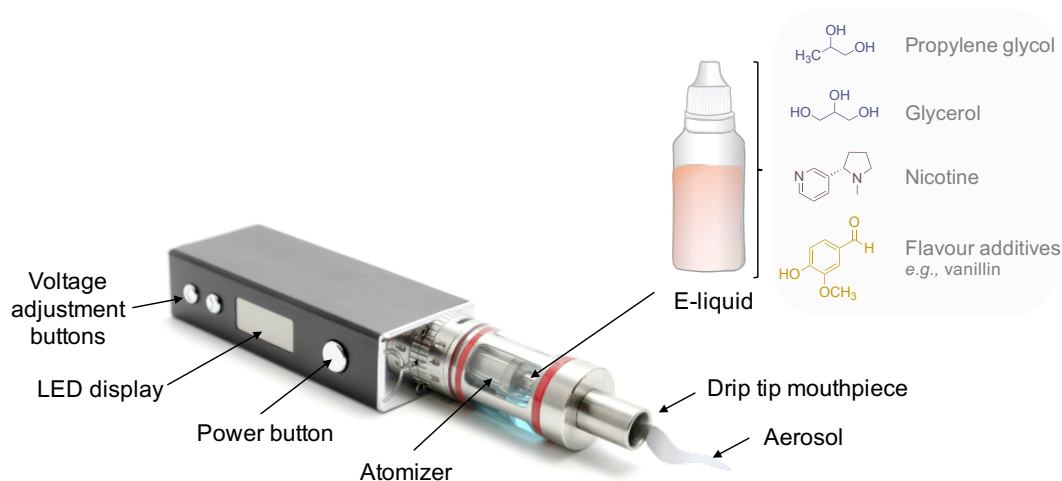


Figure 3.1. Third-generation e-cigarette. The e-cigarette device contains a tank for the e-liquid, a vaporization chamber with a heating element (atomizer), power/voltage control, and battery.

on the ingredients of the e-liquid, the electrical characteristics of the heating source, and the temperature the e-liquid reaches.²¹ Regular e-cigarette users have been reported to ‘vape’ 3 to 4 mL of e-liquid per day, which corresponds to a dosage of up to 96 mg of nicotine for e-liquids with higher nicotine content (*i.e.*, 24 mg/mL formulations),^{24,25} however, only one quarter to one third of this nicotine is vaporized and absorbed into the bloodstream, which occurs at a much slower rate in comparison to tobacco cigarettes.²⁶ Trends among e-cigarette users suggests that, in terms of number of puffs and nicotine content, 2 to 3 mL e-liquid is approximately equivalent to a pack of cigarettes.

3.2.3 E-Cigarette Liquid Formulations and Product Regulations

E-cigarettes are considered to be less harmful than conventional cigarettes since e-liquids contain fewer chemical components than processed tobacco and involve vaporization (70-100°C) instead of combustion at much higher

temperatures (400-900°C).^{23,27} Additionally, the concentrations of toxic compounds found in cigarette smoke, such as acrolein, are significantly reduced (92-99% lower) in e-cigarette aerosol.^{28,29} Compounds measured in e-cigarette aerosol include the major constituents, including nicotine, propylene glycol, and glycerol.³⁰ Known nicotine-related impurities and thermal decomposition products of propylene glycol and glycerol have also been detected. Glycerol, propylene glycol, and many of the flavouring additives are listed as ‘food grade’ and/or have a ‘generally recognized as safe’ (GRAS) designation by the Flavor and Extracts Manufacturing Association (FEMA) and the U.S. Food and Drug Administration (FDA).²⁹ FEMA states that GRAS certification applies only to oral intake of these additives and not exposure via inhalation. Moreover, e-cigarette manufacturers are recommended to refrain from claiming that flavour ingredients used in e-liquid products are safe because they have this classification.³¹ Furthermore, the safety of the long-term inhalation of these substances is not known or thoroughly investigated. E-cigarettes and their aerosols have also commonly been reported to contain a variety of other components that are not listed on the label, such as acetone, acrolein, 1,3-butadiene, formaldehyde, ethanol, and tobacco alkaloids.²⁹ Acrolein is a dehydration product of glycerol, and exposure has been observed to cause irritation, lung damage, and CVD in cigarette smokers.³² E-liquids are available in a plethora of flavours, including tobacco, confectionary, and fruity flavourings.²⁹ Sweet-flavoured e-liquids often contain diacetyl and/or acetyl propionyl.³¹

Diacetyl (2,3-butanedione) is a food-grade flavour additive used in butter flavourings and chronic inhalation of diacetyl vapours has been reported to cause bronchiolitis obliterans (‘popcorn lung’) — a disease that obstructs the bronchioles of the lung as a result of damage and inflammation.^{33,34} Also, cinnamon flavoured products often contain cinnamaldehyde and 2-methoxycinnamaldehyde, which are unstable upon heating and associated with cellular toxicity.³⁵⁻³⁷ The diverse number of popular e-liquid flavourings is highly concerning as it may make e-cigarette products more attractive to youth.²⁹ In addition, they may be unsafe when inhaled despite a GRAS classification and may produce toxic degradation products even during vaporization. Currently, there are no systematic studies evaluating the long-term safety of e-cigarette use, notably among a growing number of adolescents and young adults who are the main demographic users of these products.

Self-reported use of e-cigarettes in addition to e-cigarette sales has significantly increased since 2011, with the global e-cigarette market expected to exceed \$10 billion USD by the end of 2017.^{38,39} Presently, e-cigarette products are not regulated by the Canadian government. Provincial regulations ban the sale of nicotine-containing e-cigarette products as they are regulated as drugs and/or drug delivery devices, however they are still widely available for purchase at most commercial ‘vape’ retailers.^{40,41} An amendment to the *Tobacco Act*—Bill S-5 *Tobacco and Vaping Products Act*—will introduce new legislation for the manufacturing, sale, labelling, and advertising of e-cigarette products, which will

likely come into effect in 2018.⁴² In August 2017, Health Canada began a three month consultation period to gather input from stakeholders, consumers, health professionals, and the general public regarding e-cigarette regulations.⁴³ The Electronic Cigarette Trade Association (ECTA) of Canada was founded in 2011 by e-cigarette vendors with the objective to build and maintain a set of safety standards for e-cigarette products to protect manufacturers and consumers.⁴⁴ ECTA standards include proper documentation for hardware, blind e-liquid testing, and labelling requirements. It is not a legal requirement for businesses involved in the manufacturing and sale of e-cigarette products to join the ECTA; there are only 26 e-cigarette manufacturers within Canada currently registered as members. Standards for members of the ECTA require nicotine concentrations to be within 10% of the concentration reported on the label and to be under threshold levels of harmful compounds such as diethylene glycol and diacetyl (**Table 3.1**).⁴⁵

Table 3.1. E-liquid manufacturing and ingredient standards set by the Electronic Cigarette Trade Association (ECTA) of Canada.⁴⁵

<i>Component/Element</i>	<i>Protocol</i>	<i>LOD</i>	<i>Tolerance</i>
Nicotine concentration	GC/FID	0.1 mg/mL	± 10%
Diethylene glycol	GC/FID	< 20 µg/mL	< 100 µg/mL
Acetaldehyde	HPLC/UV	< 1 µg/mL	< 100 µg/mL
Acetoin	HPLC/UV	< 1 µg/mL	None (informational)
Diacetyl	HPLC/UV	< 1 µg/mL	Non-detection goal > 100 µg/mL – fail
Formaldehyde	HPLC/UV	< 1 µg/mL	< 30 µg/mL
Acetyl propionyl	HPLC/UV	< 1 µg/mL	Non-detection goal > 100 µg/mL – fail
pH level, % Water	Karl Fischer analysis		Target pH: 5.0-8.5
% Propylene glycol			± 10%
% Vegetable glycerin			± 10%

3.2.4 Biological Effects of E-Cigarettes

It has been demonstrated that a number of e-liquid products lead to cytotoxicity and decreased cell viability *in vitro*, with the majority of toxicity being attributed to flavour additives.³⁵ To date, only one study has utilized metabolomics as a systematic screening tool to evaluate e-cigarette liquid toxicity and its mechanism of action. Aug *et. al.*⁴⁶ used metabolomics to study the effects of e-cigarette liquids directly on human bronchial epithelial cells in comparison to cigarette smoke condensate using LC-MS. Treatment of bronchial cells with an unflavoured e-cigarette liquid led to significant increases in glutamate, glutamine, proline, arginine, histidine, and xanthine, which indicated an increase in protein turnover and/or reduction in protein biosynthesis, which is comparable to adverse effects seen with cigarette smoke exposure. The authors also showed that treatment with antioxidants (*e.g.*, *N*-acetyl-cysteine) attenuated these metabolic changes induced by e-cigarette liquid exposure, implicating a mechanistic role to oxidative stress. Exposure to e-cigarette liquids has also been shown to initiate inflammatory responses and oxidative stress in a variety of cell types.^{47,48-50} qPCR analysis of e-cigarette liquid exposure has shown induced expression of genes related to oxidative stress response in human bronchial cells, including increases in expression of genes that catalyze the production of antioxidant glutathione (GSH) and glutathione peroxidases, which are the primary antioxidant enzymes required for detoxifying hydrogen peroxide.⁴⁷ A recent study by Hwang *et. al.*⁴⁸ demonstrated that there was a significant increase in pro-inflammatory mediators

after exposure of normal human lung fibroblast cells to specific flavours of e-liquid solutions. In this case, an inflammatory response was evident with exposure to cinnamon flavours, but not tobacco/grape flavoured e-liquids or propylene glycol and/or glycerol alone. Furthermore, pro-inflammatory mediators IL-6, IL-1 α , IL-13, and MCP-1 were increased in the lungs of mice exposed to tobacco flavoured e-cigarette aerosol in comparison to a control. Other studies note that e-cigarette smoke exposure reduced antimicrobial activity of alveolar macrophages, decreased activity of human leukocytes, and increased oxidative stress response.^{48,49} The impaired ability of macrophages, neutrophils, and epithelial cells to kill bacteria is detrimental to normal host defence function and can increase susceptibility to bacterial infections. Several studies have indicated cytotoxic effects in epithelial lung cells and human keratinocytes with flavoured e-cigarette liquids.^{48,50} Relative to tobacco smoke, e-cigarette aerosol led to significantly lower cytotoxicity *in vitro* in various cell models; however, the long-term biological effects with exposure to flavoured and flavourless e-cigarette vapour are still quite sparse in the literature.⁵⁰⁻⁵¹

Currently, there is inadequate evidence to promote the safe use of e-cigarettes as a smoking cessation aid since it also risks increasing nicotine usage among young adults. One of the issues with current research regarding e-cigarettes is the lack of a standardized research protocol that allows the comparison of e-cigarette aerosol among studies and to tobacco smoke. Most studies to date have examined exposure of the concentrated or diluted e-liquid solution directly, without

studying the generated aerosol under relevant conditions to human exposure. Furthermore, research efforts have so far focused on cell viability and cellular stress responses, with only one study conducting a nontargeted metabolomics analysis on bronchial cells. Importantly, risk assessment of e-cigarette vapour exposure on placental tissues have yet to be investigated in the context of elucidating potential deleterious impacts on fetal development during pregnancy.

3.2.5 E-Cigarette Use in Canada

In 2015, the prevalence of Canadians over 15 who have reported trying an e-cigarette increased by 4% since 2013 to approximately 3.9 million Canadians (or 13% of population), comprising about 26% of youth (ages 15 to 19 y) and 30% of young adults between 20 to 24 y (**Figure 3.2**).⁵² E-cigarette use is highest among youth, women, and current smokers looking to use e-cigarettes as a smoking cessation aid.^{20,52} The reason behind current and former smokers using e-cigarettes is predominantly to aid them in reducing cigarette smoking or to alleviate cravings, as they are perceived to be less harmful, less addictive, and more socially acceptable than cigarettes.²⁰ Fruit flavoured e-cigarette liquids are most popular among youth and young adults (44% and 39%, respectively).⁵² The use of flavouring promotes youth initiation for tobacco products as it reduces the harsh taste of tobacco and increases appeal of use by marketing.⁵³⁻⁵⁴ E-cigarette liquid packaging and advertising is also a factor in youth initiation, as a number of brands offer candy-like flavours (*e.g.*, soft drinks, cotton candy), which have appealing tastes and smells.⁵⁴ Also, the general consensus that e-cigarettes are a

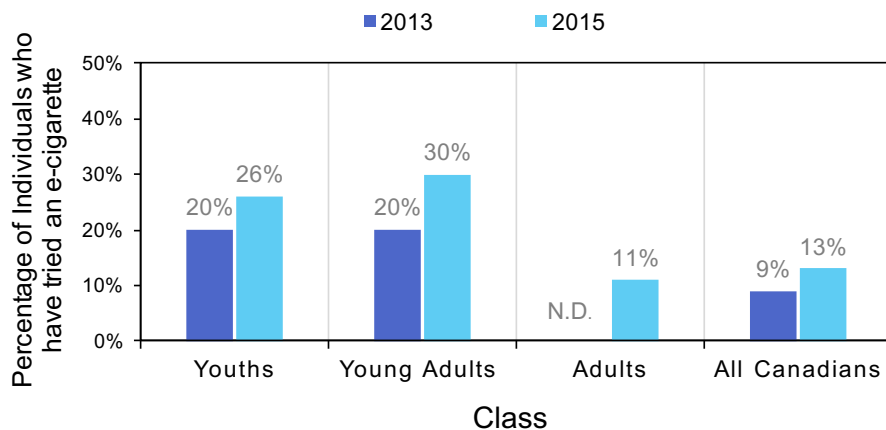


Figure 3.2. The prevalence of Canadians who have used e-cigarettes has increased significantly since 2013, with usage being highest among youth (ages 15-19) and young adults (ages 20-24).⁵²

healthier alternative to cigarettes is concerning for individuals who are dependent on smoking cessation during critical stages of their life, such as pregnancy.^{18,55}

Among pregnant women, 74% believe they are less harmful than conventional cigarettes and 72% believe they will help smoking cessation; the increased acceptance of e-cigarettes and lack of knowledge regarding their potential harm has inadvertently led to lower stigma surrounding their use during pregnancy.^{55,56}

For instance, of 100 pregnant women surveyed (2016), 23% indicated that they were current e-cigarette users, which accounts for almost half of women e-cigarette users in the study ($n = 49$).⁵⁷ It is known that cigarette smoking and nicotine exposure during pregnancy has detrimental effects on both the mother and fetus; nevertheless, despite this, 66% of women continue to smoke during pregnancy, which corresponds to approximately 14% of pregnant women in Canada.^{58,59,60} Presently, there is no available research on the consequences of e-cigarette use on maternal reproductive health or its effects on the developing

fetus.⁶¹ As a result, there is an urgent need to fully investigate the potential toxic health effects of e-cigarettes given the perception among pregnant women that they are safer than tobacco products, before recommending their use as a smoking cessation aid.⁶²

3.2.6 Role of the Placenta in Pregnancy

Proper fetal development and growth depends on the selective transport of nutrients and waste products by the placenta, which serves as a key interface between the maternal circulatory system and the fetus.⁶³ The placenta develops during pregnancy to produce hormones and growth factors, including fetal growth hormone (GH) and insulin-like growth factor 1 (IGF-1).^{63,64} Likewise, placental hormones secreted into maternal circulation act as signals to induce changes in maternal metabolism, whereas growth factors modulate placental function and fetal growth.⁶⁴ The placenta is formed within the trophoctoderm of the blastocyst after invasion into the maternal endometrium. The blastocyst eventually forms the embryo, and the outer layer of the blastocyst—the trophoblast—combines with the maternal endometrium to form the placenta.^{64,65} In early pregnancy, the placenta develops a vascular network for circulation between the mother and fetus.⁶⁶ In addition to mediating implantation and establishing maternal-fetal nutrient exchange, the placenta initiates maternal recognition of pregnancy and modulates growth and maternal metabolism by secreting growth factors and cytokines.^{66,67} It is also responsible for providing antioxidant capacity to protect the embryo from oxidative stress within the placenta.⁶⁸ Later in pregnancy, the

placenta begins to compete with the fetus for maternal substrates such as glucose and oxygen, and its role shifts to support the exponential growth of the fetus. Placental development and function can be altered significantly by environmental factors, leading to detrimental effects such as restricted growth.⁶⁷ Conditions with altered placental and fetal growth, such as maternal nutrient deprivation and environmental stress, are associated with reduced placental blood flow, fetal oxygenation, and nutrient uptake.⁶⁹ The placenta during the first trimester of pregnancy is particularly vulnerable to oxidative stress as the early placenta develops in a low oxygen environment.⁷⁰

In vitro studies of environmental stress on the placenta can be carried out by examining human trophoblast cell lines. For instance, the HTR-8/SVneo and BeWo choriocarcinoma trophoblast cell lines are representative models for first and third trimester placental cells, respectively.⁷¹ Trophoblast cells are important for the development of fetal-maternal nutrient exchange; changes in transporters, hormones, and metabolites within these cells as a result of exposure to environmental stress will give valuable insight on effects on human placental growth and development. Harmful effects on BeWo cells are indicative of impaired growth of the placenta, whereas effects on HTR-8/SVneo cells would indicate improper blastocyst implantation and placentation *in vivo*.⁷¹ Impaired placenta growth can disrupt the maintenance of key physiological pathways, which alter the transfer of nutrients.^{69,71} For example, disruption of the maintenance of vascular endothelial growth factors (VEGF) through oxidative

stress can lead to impaired vascular development and a reduced supply of nutrients to the fetus.⁷² The Wnt signalling pathway plays a role in regulating embryo development, cell fate, proliferation, migration, and cell homeostasis; disruptions in Wnt signalling is thought to alter the transcription of genes critical for placental cell differentiation, migration, and proliferation.⁷³

3.2.7 Smoking and Nicotine Exposure During Pregnancy

Tobacco smoking during pregnancy is associated with intrauterine growth restriction (IUGR), pre-term delivery, and neonatal apnea.^{74,75} Nicotine from tobacco smoke is absorbed into the bloodstream through the oral cavity and lungs, crosses the placenta to the embryo, and accumulates in fetal blood and amniotic fluid where it binds to nAChRs.⁷⁶ The nAChRs are expressed throughout the fetal nervous system, are elevated during critical developmental periods, and regulate fetal brain maturation.⁷⁵ Prenatal nicotine exposure leads to over-exposure to maternal glucocorticoids, increased blood glucose, and increased decomposition of lipids and proteins.⁷⁶ Other tobacco derived metabolites have also been shown to be transported into the placenta.⁷⁷ Abnormalities in maternal circulation as a result of tobacco exposure has been shown to negatively impact fetal development. Frequently reported consequences of tobacco smoking include increased oxidative stress, deregulation of DNA methylation, and altered gene expression.^{77,78} Recently, Rolle-Kampczyk *et. al.*⁷⁷ used a targeted metabolomics approach using LC-MS/MS after phenylisothiocyanate-derivatization to examine the impact of prenatal tobacco smoke exposure on maternal serum and fetal cord

blood. This study is the first examination of the impact of tobacco smoke on human fetal metabolism and assessed 163 metabolites including amino acids, acylcarnitines, and phosphatidylcholines. Significant changes in diacyl- and acyl-ether phospholipids, acylcarnitines, and amino acids were observed in fetal cord blood with maternal tobacco smoking in comparison to no exposure.⁷⁷ A reduction in acylcarnitines was linked with reduced energy consumption, as the fetus primarily uses fatty acid oxidation for energy metabolism, as reflected by lower birth weight outcomes in newborns of maternal smokers. While this study represents the first analysis of tobacco exposure on the fetal metabolome, it is limited in its targeted approach, variability of tobacco smoke exposure between maternal smokers, and collection of samples, as maternal serum was collected at the 34th week of pregnancy and fetal samples were collected on day of birth. In all, there is sufficient evidence suggesting that prenatal tobacco smoke exposure leads to significant changes in energy metabolism within the fetus; however, there is little evidence of the potential harmful effects of e-cigarette vapour on maternal and fetal health. Also, based on the importance of placental function during pregnancy and its role in nutrient/waste transport at the maternal-fetal interface, it represents an excellent model for studying the impact of tobacco smoking and e-cigarette vapour exposure on both maternal health and fetal growth/development.

Nontargeted metabolomics is a valuable approach for evaluating the impact of e-cigarette use, which may provide insight into its potential mechanism of action. Metabolomics analysis of placental cells/tissues has so far focused on

studying the effects of hypoxic stress and the development of preeclampsia using UPLC-MS, GC/MS, and NMR.⁷⁹ MSI-CE-MS is a high-throughput approach that is able to analyze a broad range of polar/ionic metabolites from mass limited samples, such as murine placental tissue and cell extracts.⁸⁰⁻⁸² In MSI-CE-MS, serial sample injections enables the analysis of seven samples within a single run, which offers an accelerated data workflow for biomarker discovery with quality assurance based on temporal signal pattern recognition.⁸² Previous studies examining e-cigarette exposure have been limited by focusing on phenotypic changes such as cell viability and cytotoxicity and/or targeting specific genes within oxidative stress pathways. It is hypothesized that the vapours from flavoured e-cigarette formulations have a more pronounced effect on the placental metabolome than flavourless formulations, as has been previously demonstrated in lung fibroblast cells and human keratinocytes.^{48,50} Metabolomics plays a critical role in deciphering the mechanistic action of environmental exposures on the metabolic phenotype especially when detecting evidence of sub-acute toxicity on a susceptible model.⁸³⁻⁸⁶ As a result, identifying subtle changes in the metabolic phenotype of placental cells will allow us to reveal the impact of e-cigarette vapour exposure relevant to fetal development. Furthermore, the effects of e-cigarette vapour are likely to be very complex with synergistic contributions from both nicotine and various flavouring additives.

In this study, first and third trimester trophoblast cells were exposed to flavoured and nonflavoured e-cigarette vapours at two different nicotine dosages.

Characterization of the e-liquids was first performed by MSI-CE-MS and HS-GC/MS as complementary methods to profile a chemically diverse range of polar/ionic and volatile organic compounds, including nicotine and nicotine-related metabolites, flavour additives, and breakdown products of propylene glycol and glycerol. Metabolomic studies were also performed on placental cell extracts using MSI-CE-MS after 48 h exposure to diluted e-cigarette vapour with and without nicotine. First trimester placental cells were determined to be more susceptible to e-cigarette exposures as reflected by major perturbations in amino acid metabolism in comparison to third trimester cells. Overall, this pilot study aimed to evaluate the potential sub-acute toxicity of exposure to e-cigarette vapours on placental function using a metabolomics approach in order to better understand the potential harm e-cigarettes pose to maternal and fetal health.

3.3 Materials and Methods

3.3.1 Chemicals and Reagents

All chemicals were obtained from Sigma-Aldrich Inc. (St. Louis, MO, USA). E-liquids (Blacklisted, Blue Balls) were purchased from a local e-cigarette/e-liquid retailer (Oakville, ON, CA). All aqueous buffers and stock solutions were prepared with deionized water (dH₂O) using a Thermo Scientific Barnstead EasyPure II LF ultrapure water system and stored in plastic, transport tubes. Standard calibrant solutions, e-liquids, and internal standards were stored at 4°C.

3.3.2 Instrumentation: CE-MS and GC/MS

MSI-CE-MS experiments were performed using an Agilent G7100A CE system interfaced with a coaxial sheath liquid Jet Stream electrospray ion (ESI) source with heated gas to an Agilent 6230 time-of-flight-mass-spectrometer (TOF-MS). The nebulizer gas in the ESI source and the drying gas for MS were nitrogen gas, and the damping/collision gas was helium gas. The sheath liquid for positive ion mode was 60:40 MeOH:H₂O with 0.1% formic acid supplied at a flow rate of 10 μ L/min, whereas 1:1 MeOH:H₂O was used for negative ion mode conditions. Purine and HP-921 were added into the sheath liquid (0.02%) for reference mass calibration (m/z 121.050873 and m/z 922.009798, respectively). The instrument was run in 2GHz extended dynamic range (EDR) mode. CE separations were performed using uncoated fused-silica capillaries (Polymicro Technologies, AZ, USA) with an internal diameter of 50 μ m and total capillary length of 120 cm. All separations were performed with an applied voltage of 30 kV at a constant capillary temperature of 25°C. The background electrolyte (BGE) for positive ion mode detection was 1 M formic acid, 15% *v* acetonitrile, pH 1.8, whereas the BGE for negative ion mode detection for resolving anionic metabolites was 50 mM ammonium bicarbonate, pH 8.5. For MSI, samples were injected hydrodynamically (100 mbar, 5 s) alternating between spacer segments of BGE (100 mbar, 40 s) for a total injection of seven samples within a single run, with an injection time of about 5 min and total run time of 50 min. A QC sample was injected in a randomized position within the seven sample plug serial

injection sequence in MSI-CE-MS. The CE capillary was first conditioned by flushing with MeOH, 1 M NaOH, H₂O, and BGE at high pressure for 30 min each, whereas between runs, the capillary was flushed with BGE for 10 min. For cell culture media and e-liquids, the capillary was flushed with 1 M NaOH and BGE for 15 min at the beginning of each day of runs. At the beginning of each day, an amino acid standard mixture and QC run (6 QC samples including a dH₂O blank) were performed to assess instrument performance prior to analysis of diluted e-liquid solutions, culture media, or randomized placental cell extracts as samples. Capillaries were then rinsed with dH₂O (10 min) and air (10 min) for overnight storage.

Headspace (HS)-GC/MS was used for the analysis of volatile/neutral organic compounds present in e-liquid solutions that were not readily analyzed by MSI-CE-MS. HS-GC/MS analyses were performed using an Agilent 6890 N gas chromatograph, equipped with a DB-17ht column (30 m × 0.25 mm i.d. × 0.15 μm film, J & W Scientific) and a retention gap (deactivated fused silica, 5 m × 0.53 mm i.d.), and coupled to an Agilent 5973 MSD single quadrupole mass spectrometer. In a crimp seal vial, 2 mL of the e-cigarette liquid was heated at 80°C for 10 min, and 200 μL of the headspace was analyzed in splitless mode. The injector temperature was 250°C and carrier gas (helium) flow was 0.8 mL/min with constant flow. The transfer line was 280°C and the MS source temperature was 230°C. The column temperature was set at 40°C, raised to 300°C at 15°C/min, and held at 300°C for 1 min. Mass spectra were acquired using

electron ionization (EI) using full scan from m/z 35 to 800. Data processing was performed by Agilent Enhanced Data Analysis MSD ChemStation D.03.00.611, Bruker DataAnalysis 4.0 SP4, and AMDIS 2.71. Compounds were identified through library searches using NIST/EPA/NIH Mass Spectral Library 2008 (NIST 2008, Gaithersburg, MD, USA). Compounds with scores over 80 which were detected in at least 2 of the 3 replicates for each e-liquid were included in the final compound list.

3.3.3 Culture and Preparation of Exposed Placental Cell Extracts

E-cigarette vapour was produced using a third-generation e-cigarette device (EVOD KangerTech, Shenzhen, Guangdong, China), which had a refillable chamber for e-liquids.⁸⁷ The mouthpiece of the e-cigarette was connected to 5/16" PVC Nalgene tubing. The tubing inserted into the bottom of a 250 mL Erlenmeyer flask (at the level of cell culture) through a rubber stopper. A 4 mm stopcock was inserted before the first flask to control flow (a 1/4 opening was used for media preparation). Outflow from the first flask was connected to a second Erlenmeyer flask via 5/16" PVC Nalgene tubing. The second flask was connected to a vacuum pump (GAST, Benton Harbor, MI, USA) with an in-line HEPA-VENT filter (GE Healthcare, Little Chalfont, Buckinghamshire, UK). E-liquids (Blacklisted and Blue Balls) contained either 0 or 12 mg/mL nicotine (Blacklisted with 0 mg/mL nicotine = BL0; Blacklisted with 12 mg/mL nicotine = BL12; Blue Balls with 0 mg/mL nicotine = BB0; Blue Balls with 12 mg/mL nicotine = BB12). E-liquid volume was selected based on the average daily use reported by

e-cigarette users. To prepare the F-12K and RPMI vape-conditioned media stock, 3 mL of e-liquid was vaporized by simultaneous activation of e-cigarette and vacuum pump for 10 s into 30 mL of Ham's F-12K Nutrient Mixture (Kaighn's Modification, Corning, Manassas, VA, US) or Roswell Park Memorial Institute (RPMI)-1640 medium (Buffalo, NY, US), followed by 3 s rest period.

Two different placental cell lines were used as models for e-cigarette vapour exposure studies in this work, namely first trimester HTR-8/SVneo trophoblast cells and third trimester BeWo choriocarcinoma cells (Cedarlane, Burlington, ON, CA). The HTR-8/SVneo cells (1.3×10^5 cells/well) and BeWo cells (4.7×10^5 cells/well) were plated on 6-well plates (Falcon, Corning, NY, US) and grown in RPMI or F-12K medium with 1% *L*-glutamine. After reaching 80% confluency, cells were split and incubated in F-12K or RPMI control maintenance media or media with 1% or 10% *v/v* vape-conditioned media stock for 48 h. BeWo cells were exposed to 10% *v/v* conditioned media stock for BL0 ($n = 3$), BL12 ($n = 3$), BB0 ($n = 3$), BB12 ($n = 3$), in addition to control cells ($n = 3$) which were exposed to a control maintenance F-12K media without e-cigarette vapour, whereas HTR-8/SVneo cells were exposed to 1% or 10% *v/v* conditioned media stocks for BL0 ($n = 5$), BL12 ($n = 5$), BB0 ($n = 5$), BB12 ($n = 5$), in addition to control cells ($n = 10$), which were exposed to a control maintenance RPMI media without e-cigarette vapour. Metabolite extraction for metabolomics analysis was adapted from a method by Sapcariu *et. al.*⁸⁸ for adherent cells. Post-growth medium was also collected for analysis of residual nutrients and/or secreted

metabolites. Cells were then washed three times with 1 mL aliquots of 0.9% NaCl solution to avoid potential MS spectral interferences from phosphate buffered saline solution.⁸⁸ In our work, cellular metabolism was quenched by the addition of 250 μL 1:1 MeOH:H₂O pre-chilled at -20°C. Wells were then scraped with a 1.8 cm cell scraper and cell extracts from three wells (750 μL total volume) were transferred together into a 1.5 mL centrifuge microtube, flash frozen with liquid N₂, and then stored at -80°C prior to cell extraction and analysis.

3.3.4 Metabolite Extraction and Sample Preparation

BeWo cells ($\sim 1.4 \times 10^6$) and HTR-8/SVneo cells ($\sim 3.9 \times 10^5$) were subjected to two repeated freeze-thaw cycles, vortexed for 30 s, and centrifuged at $14,000 \times g$ for 10 min. 5 μL of each extract was diluted 2-fold in dH₂O. Successive freeze-thaw cycles were not found to further enhance metabolite recovery from cell extracts. Placental cell extracts were filtered using a 3 kDa MWCO Nanosep centrifugal device (Pall Life Sciences, Washington, NY, US) at $14,500 \times g$ for 15 min to remove cellular proteins. Placental cell filtrates were spiked with recovery standards (RS), including 25 μM 4-fluorophenylalanine (F-Phe) and 50 μM HEPES, and then dried for 3 h using a Vacufuge Concentrator (Eppendorf, Westbury, NY, US) with a cold trap attachment using a slurry of dry ice and isopropanol. Extracts were then reconstituted in 60 μL dH₂O with internal standards (IS), namely 25 μM 3-chlorotyrosine (Cl-Tyr) and 50 μM sodium-2-naphthalene sulfonate (NMS). Technical replicates ($n = 3$, BeWo and HTR-

8/SVneo cells) were used for method optimization in order to maximize the overall recovery of metabolites from placental cell extracts.

3.3.5 Data Processing

Nontargeted metabolite profiling by MSI-CE-MS was performed using Molecular Feature Extractor (MFE) and Molecular Formula Generator (MFG) when using Mass Hunter Workstation Qualitative Analysis software (Agilent Technologies Inc.). A dilution trend filter based on a serial seven plug sample injection of a pooled placental cell extract and a blank was performed by MSI-CE-MS as a simple strategy to identify reproducible yet authentic molecular features, while also allowing for the rejection of spurious signals and exclusion of redundant responses derived from same metabolites, including in-source fragments, isotopes, and salt adducts.⁸⁰ BeWo and HTR-8SV/neo cells were run separately from e-cigarette liquids at various dilutions (10- to 1000-fold) in dH₂O spiked with 25 μ M Cl-Tyr and 50 μ M NMS as IS. Samples were then analyzed by MSI-CE-MS in randomly assigned injection positions with a pooled QC analyzed in one of the seven injection positions with each run. Samples were run in positive and negative ion mode conditions over a period of 1 week as described previously.⁸⁹ Molecular features were tentatively identified based on a compiled personal database and/or searching online MS/MS metabolite databases, including METLIN and Human Metabolome Database in cases when authentic standards were not available. In BeWo and HTR-8/SVneo cells, 40 cationic and 9 anionic

metabolites were reliably detected (**Supplementary Table S3.1**) with adequate precision in the QC samples ($CV < 40\%$, $n = 9$) and consistently measured in $> 75\%$ of individual placental cell extract samples of the same cell type. Molecular features (MH^+ or $M-H^-$) for known and unknown metabolites were extracted based on their characteristic accurate mass and relative migration time (m/z :RMT) based on a targeted list determined from a dilution trend filter in profile mode using a 10 ppm mass window. Peaks were smoothed (Savitzky-Golay quadratic/cubic function, 15 points), integrated, and ion responses were normalized relative to an IS (*i.e.*, Cl-Tyr and NMS for positive ion mode and negative ion mode detection, respectively) to improve method precision.

3.3.6 External Calibration Curve and Nicotine Quantification

Calibration standards for nicotine (m/z 163.1230) at seven concentrations (5 to 200 μ M) were prepared in deionized water using 25 μ M Cl-Tyr and F-Phe as IS. External calibration curves were each performed in triplicate using a 7-sample injection format in MSI-CE-MS in order to compare nicotine concentrations with reported e-cigarette nicotine dosage in formulation, as well as confirm nicotine in vaped media prior to placental cell exposure. Linear least-squares regression was used to calculate the calibration equations for nicotine in dH_2O ($y = 0.119x + 0.539$). Good linearity ($R^2 > 0.995$) was observed over a 40-fold dynamic range. The limit of detection ($LOD = 0.28 \mu$ M) and limit of quantification ($LOQ = 0.93 \mu$ M) for nicotine were calculated from the regression line: $C_{LOD} = 3s_{y/x} \div b$ and

$C_{LOQ} = 10s_{y/x} \div b$, where $s_{y/x}$ is the standard deviation of the response and b is the slope of the regression line, with confirmation by measuring the average S/N for the lowest calibrant solution.⁹⁰

3.3.7 Statistical Data Analysis

Extracted ion electropherograms were prepared in Igor Pro 5.0 (Wavemetrics Inc., Lake Oswego, OR, USA), whereas linear regression for calibration curves was performed in Excel 2007 (Microsoft Inc., Redmond, WA, USA). SPSS Statistics (IBM, v. 23) and MetaboAnalyst 3.0 (McGill University) were used for univariate and multivariate statistical tests, respectively. Missing values (*i.e.*, no signal integrated) were estimated by half of the minimum relative peak area (RPA). HTR-8/SVneo cells were received in two batches due to the requirement of additional replicates. A large difference was observed in RPAs of samples received in different batches. Placental cell metabolites were corrected using probabilistic quotient normalization (PQN)⁹¹ to correct for differences in sample preparation and cell culture conditions. PQN calculates a probable normalization factor for each sample from the median distribution of quotients of sample responses to a QC response within each MSI-CE-MS run as a reference for each feature. Before PQN correction, the overall technical variation was adequate (median CV of QC samples = 24%, $n = 9$), in comparison to biological variation within control samples prior to correction (median CV = 83%, $n = 49$). Correction with PQN reduced the biological variation by 2-fold (median CV of PQN-

corrected controls = 36%, $n = 49$). Normality of metabolite responses was assessed using the Shapiro-Wilk test. Metabolites that were not normally distributed were *log*-transformed prior to univariate and multivariate statistical analysis. Group differences between normally distributed metabolites were assessed using *t*-tests and one-way ANOVA, whereas skewed data was assessed using Mann-Whitney U and Kruskal-Wallis H tests. For multivariate analysis, data was *log*-transformed, mean-centered, and scaled by dividing by the standard deviation of each variable (*i.e.*, auto-scaling). Partial least squares-discriminant analysis (PLS-DA) was used to select features that discriminate treatment response between groups with metabolite ranking determined by variable importance in projection (VIP) scores above a minimum threshold (VIP > 1.5)

3.4 Results and Discussion

3.4.1 Nicotine Dosage and Alkaloid Impurities in E-Cigarette Liquids

MSI-CE-MS is well suited for the analysis of polar and ionic compounds from volume-restricted biological samples, such as placental cell extracts. Importantly, multiplexed separations greatly increase sample throughput while allowing for novel data workflows for biomarker discovery with quality assurance. Currently, e-cigarette liquids are not regulated by the Canadian government and thus there is a great deal of batch variability between commercial e-cigarette products based on manufacturing protocols and purity/grade of major constituents, such as propylene glycol, glycerol, and nicotine.⁹² In addition, the

nicotine content in some e-cigarette liquids show high disparity from what is reported on its label, with some cases of nicotine being detected in e-cigarette liquids advertised to contain no nicotine. As a result, quantification of nicotine concentrations and nicotine-related impurities and degradation products was performed in representative e-cigarette liquids using MSI-CE-MS. Dilution of e-cigarette liquids in deionized water (from 10- to 1000-fold) was required due to their high viscosities, while also ensuring that measured nicotine ion responses were within the upper linear dynamic range of the calibration curve (**Supplementary Figure S3.1**).

As expected, nicotine was not detected in the Blacklisted (unflavoured) or Blue Balls (blue-raspberry flavoured) e-cigarette liquids that were labelled to contain 0 mg/mL nicotine (BL0 and BB0), as shown in extracted ion electropherogram overlays in **Figure 3.3**. Therefore, nicotine concentrations were below 3.0 μ M or 450 ng/mL based on an effective detection limit following a 10-fold dilution for e-liquid solutions. For the formulations of Blacklisted (BL12) and Blue Balls (BB12) advertised to contain 12 mg/mL of nicotine, the concentrations differed from reported amounts by 13.8% (10.35 ± 0.77 mg/mL) and 10.4% (13.25 ± 0.79 mg/mL), respectively. Although deviations in reported nicotine concentrations are quite reasonable in comparison to previous studies reporting differences ranging from 45 to 131%, the ECTA's quality control protocols require nicotine concentrations to be within 10% of the concentration

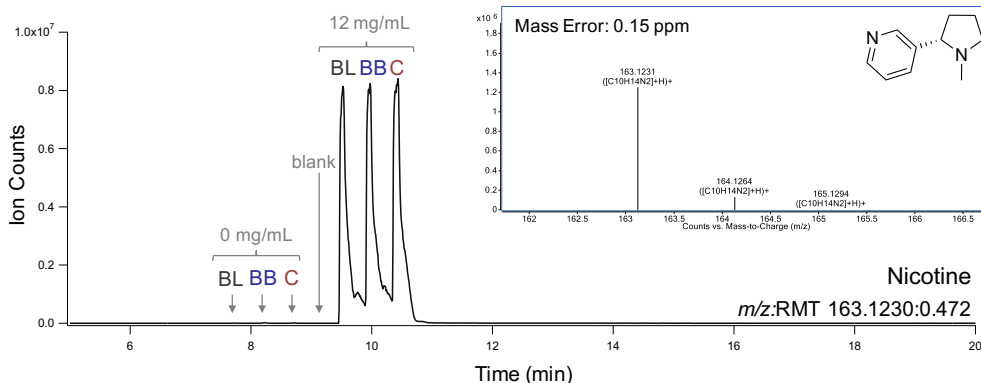


Figure 3.3. Extracted ion electropherogram of nicotine (163.1230:0.472) for a representative MSI-CE-MS run of e-cigarette liquids containing 0 and 12 mg/mL nicotine with an injection order of 0 mg/mL Blacklisted (BL0), Blue Balls (BB0), CinJacks (C0, not discussed), blank, 12 mg/mL Blacklisted (BL12), Blue Balls (BB12), and CinJacks (C12, not discussed). The TOF-MS spectra for nicotine showing its molecular ion (MH^+) and isotope pattern with calculated mass error is shown as an inset.

reported on the label.⁹³ Also, the current lack of government regulation of e-cigarette products and manufacturing practices has led to a large number of tested products (43%) claiming to contain 0 mg/mL actually containing residual amounts of nicotine.⁹⁴

MSI-CE-MS detected several nicotine-related compounds/impurities in the 12 mg/mL e-cigarette liquid formulations, which were not detected in the equivalent nicotine-free brands (**Table 3.2**), including alkaloids derived from tobacco plants, such as nornicotine, anatabine, and cotinine. Furthermore, two unknown compounds (m/z :RMT), including a faster migrating isobar of cotinine (177.1022:0732) and an unknown cation (189.1598:0.781), were likely nicotine alkaloids since they were only detected in the 12 mg/mL nicotine formulations and have similar mobilities to other nicotine alkaloids. Nicotine impurities and degradation products are commonly detected in e-cigarette liquids.⁹⁵ The nicotine

Table 3.2. Nicotine degradation products and minor tobacco alkaloids detected in e-liquid formulations with 12 mg/mL nicotine by MSI-CE-MS in positive ion mode. The total percent abundance of known tobacco/nicotine-related compounds was in Blacklisted and Blue Balls was 1.85% and 1.63%, respectively.

Compound ^a	Formula	<i>m/z</i> :RMT	Mass Error	Type of Impurity	% Abundance ^b	
					BL12	BB12
Nicotine	C ₁₀ H ₁₄ N ₂	163.1230:0.526	0.15 ppm	—	—	—
Anatabine	C ₁₀ H ₁₂ N ₂	161.1070:0.547	2.02 ppm	Tobacco alkaloid	1.04%	0.59%
2'-Hydroxynicotine	C ₁₀ H ₁₄ N ₂ O	179.1179:0.556	0.06 ppm	Degradation	0.52%	0.58%
Nicotine <i>N</i> '-oxide	C ₁₀ H ₁₄ N ₂ O	179.1179:0.566	0.50 ppm	Tobacco alkaloid	0.23%	0.39%
Cotinine	C ₁₀ H ₁₂ N ₂ O	177.1022:0.757	1.47 ppm	Tobacco alkaloid	0.05%	0.06%
Nicotyrine	C ₁₀ H ₁₀ N ₂	159.0917:0.722	1.73 ppm	Tobacco alkaloid	0.03%	0.01%

^a All metabolites were tentatively identified by mass match using the ESI+ mass spectrum and Molecular Formula Generator (MFG), with confirmation performed by high resolution, accurate MS/MS.

^b % abundance relative to major alkaloid, nicotine, assuming similar ionization efficiency (*n* = 3).

that is used in e-cigarette liquids is extracted from tobacco and its purity varies depending on the manufacturer and grade. For example, according to the European Pharmacopoeia, pharmaceutical grade nicotine can contain up to 0.3% of nicotine impurities, comprising minor tobacco alkaloids and degradation products.⁹² Anatabine was the most abundant minor alkaloid detected in both Blacklisted and Blue Balls e-cigarette liquids, corresponding to about 0.6% to 1.0% of total nicotine content; similarly, anatabine and nornicotine are the most abundant minor tobacco alkaloids in most tobacco strains and in tobacco products.⁹⁶ In addition, several minor tobacco alkaloids arise as a result of oxidation during tobacco processing, including cotinine, nicotyrine, and nicotine *N*'-oxide (NNO). Collectively, the relative abundance of nicotine impurities detected in the Blacklisted and Blue Balls e-cigarette liquids examined was about 1.8% and 1.6%, respectively, which suggests that a poorer grade of nicotine was used for these products. Further, the presence of high quantities of nicotine

impurities suggest oxidative degradation occurred during manufacturing or as a result of interactions with packaging and handling/storage (*i.e.*, temperature/light).⁹²

3.4.2 Characterization of Volatile Organics in E-Cigarette Liquids

All e-cigarette liquids examined in this work listed propylene glycol, glycerol, nicotine (12 mg/mL formulations only), and “artificial/natural flavourings” on their labels. MSI-CE-MS was not optimal for the analysis of e-cigarette liquids for volatile organics other than nicotine and its alkaloid impurities or degradation products. As shown in **Table 3.3**, MSI-CE-MS analysis of 10-fold diluted e-cigarette liquids revealed only a small list of compounds that were not reported on the label. In addition to glycerol, propylene glycol, and their degradation products (*i.e.*, acrolein and propionaldehyde), 4 features that were only detected in the Blue Balls e-liquids were tentatively identified as flavour compounds, including benzaldehyde (bitter almond/cherry).⁹⁷ Total characterization of e-cigarette liquid solutions by MSI-CE-MS was not possible given that the majority of flavour additives are nonpolar/uncharged. Also, the majority of features identified in positive ion mode detection were neutral compounds, such as propylene glycol and ethyl maltol, and thus co-migrate with the EOF and are prone to ionization suppression/enhancement effects.

The chemical profile of the e-liquid aerosol is more relevant to the vaping process in terms of assessing the impact of human exposure than the profile of the liquid components.²⁸ In addition, many flavour additives are neutral organic

Table 3.3. List of compounds detected by MSI-CE-MS in Blacklisted and Blue Balls e-cigarette liquids. Analysis was repeated in triplicate.

Compound ^a	Formula	<i>m/z</i> :RMT:mode	Mass Error	Abundance ^b	
				BL	BB
Glycerol	C ₃ H ₈ O ₃	93.0546:1.527:p	0.22 ppm	—	—
Unknown ^c	—	215.0533:1.527:p	—	—	45.2%
Unknown	C ₈ H ₈ O ₃	151.0407:0.958:n	4.85 ppm	3.4%	41.6%
Propionaldehyde	C ₃ H ₆ O	59.0491:1.527:p	2.39 ppm	9.4%	9.2%
Acrolein	C ₃ H ₄ O	57.0335:1.523:p	0.15 ppm	3.9%	4.0%
Unknown	C ₈ H ₈ N ₄ O ₂	191.0572:0.845:n	1.90 ppm	—	2.0%
Benzaldehyde	C ₇ H ₆ O	107.0495:1.527:p	0.55 ppm	—	1.8%
Ethyl maltol	C ₇ H ₈ O ₃	141.0546:1.527:p	3.40 ppm	0.7%	1.7%
Propylene glycol	C ₃ H ₈ O ₂	77.0599:1.526:p	2.10 ppm	1.4%	1.4%
Unknown	C ₅ H ₁₀ O ₂	101.0608:0.993:n	0.03 ppm	—	0.2%

^a All metabolites were tentatively identified by mass match using the ESI+ mass spectrum and Molecular Formula Generator (MFG).

^b % abundance relative to major constituent, glycerol (vegetable glycerin), that were measured in triplicate.

^c Formula could not be determined by MFG or database search.

compounds that are not resolved under the buffer conditions for separations in MSI-CE-MS. As a result, headspace (HS)-GC/MS was used as a complementary method that is ideal for characterizing volatile organic mixtures as required for environmental, flavour, and fragrance analysis.⁹⁸ Temperatures for aerosol generation within e-cigarettes generally range from 40°C to 100°C, with many e-cigarette manufacturers limiting operating temperatures to under 100°C to avoid the production of toxic degradation products derived from glycerol or propylene glycol.⁹⁹ **Table 3.4** lists compounds identified in the flavourless (Blacklisted) and blue-raspberry flavoured (Blue Balls) e-liquids by HS-GC/MS (*n* = 3) after equilibration and sampling headspace of e-liquid solutions with heating at 80°C. Argon, propylene glycol, and butyl isovalerate were detected in all e-liquids analyzed. Argon is often used to flush oxygen-sensitive pharmaceutical products,

Table 3.4. List of compounds detected by HS-GC/MS in Blacklisted and Blue Balls e-cigarette liquids with nicotine concentrations of 0 and 12 mg/mL. HS-GC/MS analysis was completed in triplicate and compounds appearing in at least two repeat samples with mass spectral library match scores > 80% are listed. Propylene glycol and butyl isovalerate were detected in all e-liquid formulations, whereas nicotine was detected only in the 12 mg/mL formulations of Blacklisted and Blue Balls.

Compound	Molecular Formula	M (m/z)	RT (min)	NIST Score	Relative Abundance ^b	Flavour
Propylene glycol ^a	C ₃ H ₈ O ₂	76	3.341	97.0	—	—
Benzyl acetate	C ₉ H ₁₀ O ₂	150	7.276	92.8	28.8%	Fruit ⁹⁷
Isoamyl acetate	C ₇ H ₁₄ O ₂	130	3.798	90.5	28.1%	Apple/banana ⁹⁷
Ethyl acetate	C ₄ H ₈ O ₂	88	2.741	92.2	25.8%	Citrus ¹⁰⁶
β-Damascenone	C ₁₃ H ₁₈ O	190	8.944	94.2	21.9%	Apple ¹⁰⁷
Ethanol	C ₂ H ₆ O	46	2.561	91.5	17.4%	—
Ethyl butyrate	C ₆ H ₁₂ O ₂	116	3.363	91.4	17.4%	Strawberry/apple ¹⁰⁸
Isoamyl butyrate	C ₉ H ₁₈ O ₂	158	5.209	95.5	12.0%	Fruit ⁹⁷
Butyl isovalerate ^a	C ₉ H ₁₈ O ₂	158	5.092	81.5	0.3%, 11.2%	Fruity ⁹⁷
Ethyl isovalerate	C ₇ H ₁₄ O ₂	130	3.611	86.8	11.2%	Apple/fruit ⁹⁷
Hexyl acetate	C ₈ H ₁₆ O ₂	144	4.889	88.2	9.3%	Apple/banana ⁹⁷
Benzyl alcohol	C ₇ H ₈ O	108	6.057	90.6	9.2%	Boiled cherries ⁹⁷
Nicotine ^c	C ₁₀ H ₁₄ N ₂	163	8.921	95.0	7.4%, 1.5%	—
Linalool	C ₁₀ H ₁₈ O	154	5.727	94.2	6.0%	Floral/lemon ⁹⁷

^a Detected consistently in all Blacklisted and Blue Balls e-liquid formulations analyzed in this study.

^b % Abundance of volatile organic compounds relative to propylene glycol, that were measured in triplicate (n = 3).

^c Detected only in e-liquids containing 12 mg/mL nicotine.

such as nicotine, before closure and long-term storage.¹⁰⁰ Butyl isovalerate is a flavouring additive contributing a fruity flavour that has ‘Generally Recognized as Safe’ (GRAS) approval by the FDA.⁹⁷ Further, there were significant levels of siloxanes detected in the aerosol of all of the e-liquids analyzed. Polysiloxanes are used as plastic additives and have been previously detected in a variety of e-liquid aerosols, however its presence is attributed to background impurities presented by the analytical method (*i.e.*, GC column).¹⁰¹⁻¹⁰³ The Blue Balls e-liquid contained ethanol, which is typically used as a solvent for flavourants,¹⁰⁴ and ethyl acetate,

which is also used as an extraction solvent.¹⁰⁵ The Blue Balls e-liquid also contained ten known fruit-based flavour additives (*i.e.*, apple, banana, citrus) which were not found in the unflavoured e-liquid. The majority of these compounds are esters (*i.e.*, isoamyl acetate) and alcohols (*i.e.*, linalool). As expected, the Blue Balls e-liquid vapour was much more complex than the unflavoured e-liquids (Blacklisted), which is evident when comparing the total ion chromatogram traces for both nicotine-free formulations (**Figure 3.4**).

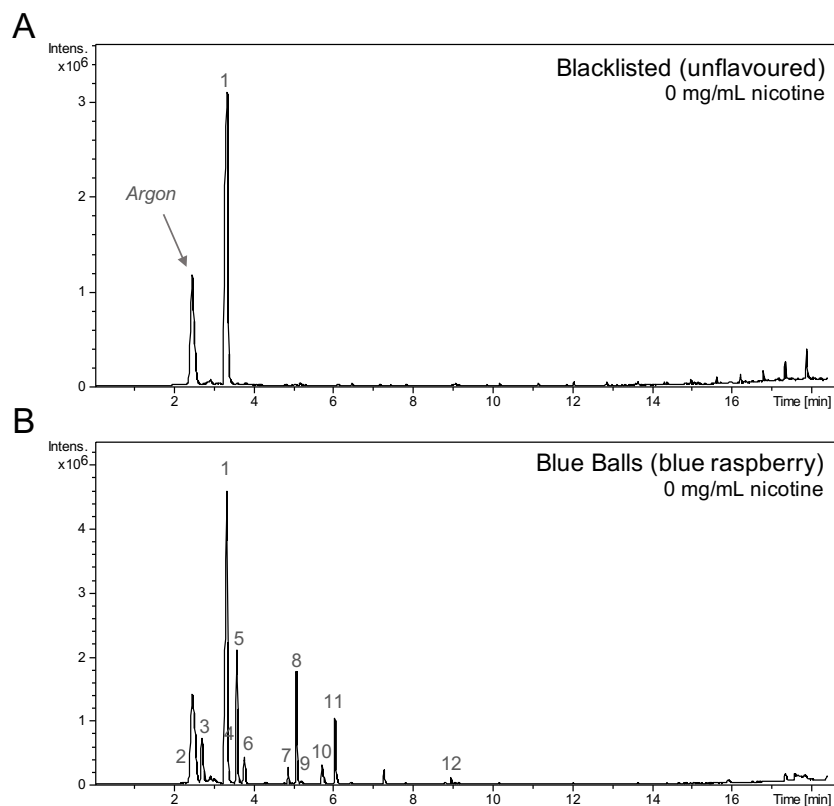


Figure 3.4. Total ion chromatograms when using HS-GC/MS comparing the chemical profile of (A) Blacklisted and (B) Blue Balls e-cigarette liquid formulations with 0 mg/mL nicotine. Peaks are identified as 1 = propylene glycol, 2 = ethanol, 3 = ethyl acetate, 4 = ethyl butyrate, 5 = ethyl isovalerate, 6 = isoamylacetate, 7 = hexyl acetate, 8 = butyl isovalerate, 9 = isoamyl butyrate, 10 = linalool, 11 = benzyl alcohol, 12 = β -damascenone.

3.4.3 Preparation and Validation of E-Cigarette Vapour Media

In order to evaluate the effects of e-cigarettes on human placental cells in a manner relevant to human exposures (*i.e.*, inhalation of vapours), cell growth media were prepared following their direct exposure to e-cigarette vapours as described in the experimental section. Placental cells were then subsequently exposed to 1% and 10% *v/v* dilutions of e-cigarette vapour-exposed cell growth media for 48 h. The higher dose 10% *v/v* vapour media was first evaluated to assess whether exposure elicited an observable change in either first and third trimester placental cellular metabolism, whereas exposure to the 1% *v/v* vapour media was used to mimic low level exposures that would be more relevant to model impact on humans after e-cigarette vapour inhalation based on known blood nicotine concentrations in cigarette smokers.¹⁰⁹ Nicotine concentrations in the undiluted BL12 and BB12 vape-conditioned media stocks (*i.e.*, cell growth media exposed to e-cigarette vapour from 3 mL of e-liquid) corresponded to about 1% of nicotine content in Blacklisted and Blue Balls e-liquids (10.35 and 13.25 mg/mL) as summarized in **Table 3.5**. Nicotine content in the BB12 vape-conditioned F-12K media stock prepared for exposure of third trimester placental cells was 4-fold lower than the other stocks, which was likely caused by an error in the vaping process since nicotine content in the Blue Balls e-liquid is largely consistent with its label concentration. Furthermore, the concentrations in the 10% *v/v* vape-conditioned media corresponded to about 15-20% or on average 23 $\mu\text{g/mL}$ of nicotine in the stock solutions ($\sim 125 \mu\text{g/mL}$). 1% *v/v* vape-conditioned

Table 3.5. Nicotine content in original growth media (undiluted stock), as well as 10% and 1% v/v vape-conditioned media prepared for treatment of first and third trimester placental cells. 1% v/v vape-conditioned media was not prepared for F-12K media. Concentrations for the 1% v/v vape-conditioned media were estimated since concentrations levels were below the method LOD.

Vape Stock Solution and Labeled Nicotine Dosage	Nicotine Dosage for Placental Cell Exposure		
	Conditioned Growth Media	10% v/v Diluted Media	1% v/v Diluted Media
F-12K Blacklisted (12 mg/mL)	129 ± 19.4 µg/mL	23 ± 3 µg/mL	—
F-12K Blue Balls (12 mg/mL)	29 ± 4.0 µg/mL	4.5 ± 0.1 µg/mL	—
RPMI Blacklisted (12 mg/mL)	130 ± 20.7 µg/mL	25 ± 3 µg/mL	2.5 µg/mL
RPMI Blue Balls (12 mg/mL)	115 ± 6.0 µg/mL	21 ± 1 µg/mL	2.1 µg/mL

media were prepared only for Blacklisted and Blue Balls in the RPMI media for treatment of first trimester placental cells. Nicotine concentrations in the 1% vapour stocks were below the method LOD following dilution and could not be measured directly, however they were estimated based on the 10% v/v vapour media concentrations (~2.3 µg/mL) as listed in **Table 3.5**. In addition, nicotine-related impurities (*i.e.*, tobacco alkaloids and degradation products) were detected in e-cigarette liquids, but were not detected in any of the conditioned media due to their much lower abundances (< 1% of nicotine). Nicotine concentrations were measured explicitly for two reasons—firstly, to evaluate the consistency of the method when preparing media exposed to e-cigarette vapours, which demonstrated that nicotine concentrations were, for the most part, consistent across both media types and flavours, and, secondly, to provide verification that nicotine and other components of the e-liquids were integrated into media for placental cell exposure.

3.4.4 Placental Cell Exposure to E-Cigarette Vapour

To evaluate the effects of e-cigarette vapours on placental cells, first trimester (HTR-8/SVneo) and third trimester (BeWo) trophoblast cells were treated in media exposed to Blacklisted (unflavoured) or Blue Balls (blue-raspberry flavour) e-cigarette vapour. After cells were grown to 80% confluency (about 1.3×10^5 and 4.7×10^5 cells/well for HTR-8/SVneo and BeWo cells, respectively), they were incubated in either 1% or 10% v/v vape-conditioned media (BL0, BL12, BB0, BB12) or control maintenance media for 48 h. Metabolism was then quenched with 1:1 MeOH:H₂O and cells were extracted prior to metabolomic analysis using MSI-CE-MS. The quenching/extraction procedure was optimized for maximizing metabolite extraction efficiency while using a minimum number of wells to achieve adequate sensitivity and metabolome coverage by MSI-CE-MS. MSI-CE-MS was performed under acidic (positive ion mode) and alkaline (negative ion mode) conditions for the detection of cationic and anionic metabolites derived from placental cell extracts, respectively. For washing of placental cells, 0.9% NaCl and a minimal volume (250 μ L) of 1:1 MeOH:H₂O pre-chilled to -20°C was used as an extraction solution during cell scraping.⁷⁰ The pooling of placental cells derived from 3 wells of a 6-well plate (approximately 3.9×10^5 and 1.4×10^6 cells total for HTR-8/SVneo and BeWo cell lines) and use of two consecutive freeze-thaw cycles were found to provide optimal metabolite recovery and coverage in this work. Overall, this optimized extraction procedure demonstrated good technical

precision ($n = 3$) for non-exposed HTR-8/SVneo cell extracts with a median CV = 7% (ranging from 0.8% to 31.4%) for 49 polar/ionic metabolites consistently measured in the majority of placental cells that also satisfied selection criteria when performing a dilution trend filter (**Supplementary Table S3.1**).⁸⁰ Only 10 anionic metabolites were consistently detected in placental cells, which is likely a result of lower sensitivity when using negative ion mode in addition to inadequate cell densities.¹¹⁰ Of these 49 metabolites, 12% were unknown and were annotated based on their characteristic m/z :RMT. Among the known compounds, the majority were amino acids (44%), acylcarnitines (10%), and various amino acid derivatives (8%).

The analysis of placental cells treated with BL0, BL12, BB0, and BB12 vape-conditioned media and control maintenance media with MSI-CE-MS was first evaluated with a current trace overlay (**Figure 3.5**) for a total of 42 runs in (A) positive ion mode using an acidic BGE and (B) negative ion mode using an alkaline BGE. The current trace provides a way to monitor instrument stability and robustness during data acquisition.¹¹¹ Overall, there was good reproducibility throughout runs with CV < 2.5% for positive and ion mode; however, in negative ion mode, a number of runs were discarded due to current drops and/or current variability outside cut-off limits exceeding $\pm 3SD$. In addition, quality assurance protocols were also carried out by monitoring a recovery standard (F-Phe, 25 μ M) within all samples analyzed ($n = 78$), including pooled QC samples (**Figure 3.6**),

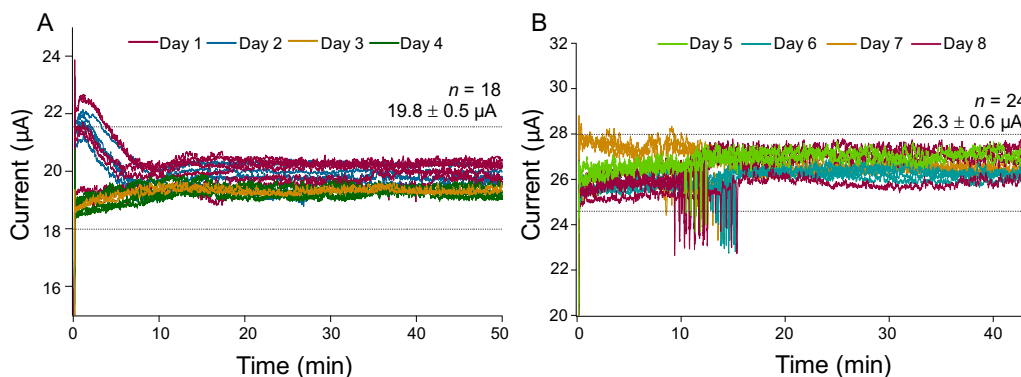


Figure 3.5. An overlay of CE current traces from 42 runs performed over 8 days of analysis in positive and negative ion mode. Excellent reproducibility was observed in positive and negative ion mode (CV = 2.5% and 2.3%, respectively), however a number of runs in negative ion mode were discarded due to significant variation in the current and/or current drops/crashes. Upper and lower limits of agreement are denoted by dotted grey lines ($\pm 3SD$).

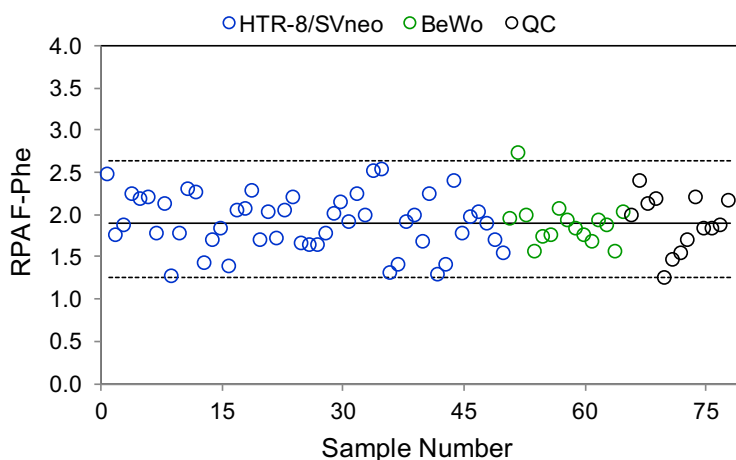


Figure 3.6. Control chart depicting relative peak area (RPA) of recovery standard 4-fluorophenylalanine (F-Phe) over 50 HTR-8SV/neo cells (blue), 15 BeWo cells (green), and 13 pooled QCs (black) in positive ion mode. The solid line represents the average RPA and the dotted lines represent the upper/lower control limits ($\pm 3SD$). BeWo and HTR-8/SVneo cells were analyzed by MSI-CE-MS on different dates.

which gave an indicator of long-term precision of both cellular extraction and MSI-CE-MS performance for both cell types with only 1 outlier (BeWo) exceeding agreement limits ($\pm 3SD$). The apparent ion response ratio for F-Phe

measured in positive (CV = 16.3%) and negative (CV = 20.2%) ion mode displayed acceptable random variation.

BeWo and HTR-8/SVneo cells were treated with 10% v/v BL0, BL12, BB0, and BB12 vape-conditioned media to evaluate whether the presence of vaped e-cigarette additives led to changes in placental cell metabolism in comparison to control cells which were not exposed to e-cigarette vapour. To determine the susceptibility of first and third trimester cells to e-cigarette exposure, we examined metabolite profiles without e-cigarette exposure (*i.e.*, control) in comparison to cells treated with the e-cigarette vapour we hypothesized would have the greatest effect on placental metabolism. There were no significant differences in metabolite profiles with treatment of 10% v/v BB12 ($n = 3$) in comparison to controls ($n = 3$) observed in BeWo cells (Mann-Whitney U test, $p > 0.05$), which suggests that the concentrations of nicotine and other e-cigarette liquid components in the diluted vape-conditioned media did not produce a significant effect and/or the treatment was too short in duration (48 h) to elicit a measurable change in cellular metabolism. This was confirmed by comparing control BeWo cells with the other e-liquid vape-conditioned media (BL0, BL12, and BB0) using Mann-Whitney U tests, which demonstrated no significant differences between groups. In contrast, first trimester HTR-8/SVneo cells treated with control maintenance media ($n = 10$) and 10% BB12 ($n = 5$) showed major differences in responses for several metabolite classes, including amino acids and acylcarnitines. A more pronounced effect on the first trimester cell line is

consistent with current knowledge regarding placental development and susceptibility to stressors.⁸⁹ First trimester placental cells are known to be more susceptible to chemical influences as a result of active differentiation and chemical/environmental stressors that can cause significant detrimental effects on DNA methylation and gene expression.^{89,112} In addition, maternal smoking has been observed to be less harmful at the end of pregnancy than in early pregnancy, as third trimester trophoblast cells are highly differentiated with higher resistance to chemical exposures. In the first trimester, the placenta develops in a hypoxic environment and is more vulnerable to oxidative stress.⁷⁰ For this reason, first trimester HTR-8/SVneo cells were further investigated when using a lower dose exposure/sub-acute toxicity study when using nontargeted metabolite profiling by MSI-CE-MS.

HTR-8/SVneo cells treated with 1% and 10% *v/v* e-cigarette vape-conditioned media were received in two batches due to the requirement of additional replicates. A large difference was observed in ion responses of the same cell lines received in two different batches that were prepared over a time period spanning 6 months, which is depicted in the 2D scores plot of a principal components analysis (PCA) that provides an overview of the total data variance (**Figure 3.7**). As the QC samples measured over the two batches were consistent, the likely source of batch differences is changes in sample preparation and/or cell culture conditions, and was not a result of instrumental issues. To correct for the observed batch differences between samples, probabilistic quotient normalization

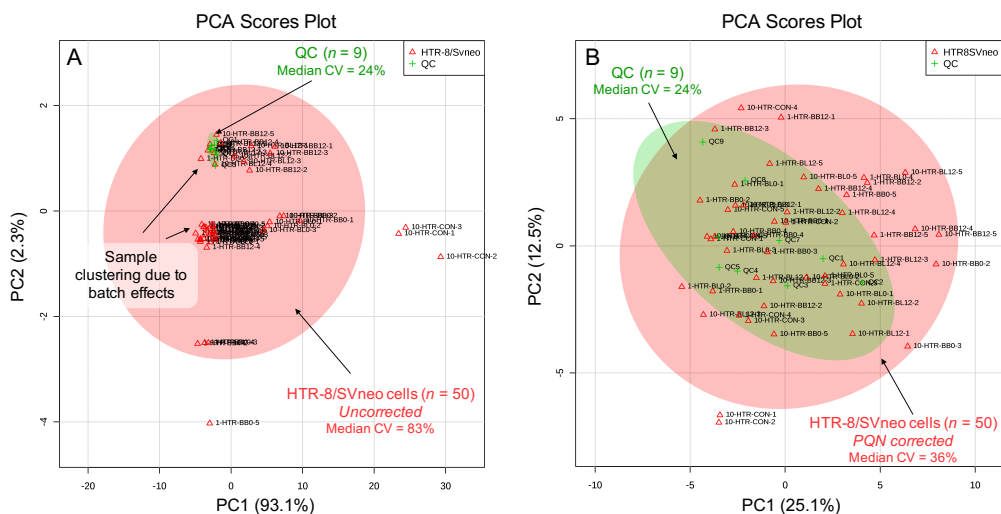


Figure 3.7. 2D scores plot from principal component analysis (PCA) of 49 cationic and anionic metabolites detected in first trimester HTR-8/SVneo cells showing (A) uncorrected data and (B) PQN-corrected data in comparison to the adequate technical variation within the QC samples analyzed within each run. PQN correction reduced the total biological variation from 83% to 36% (median CV). All data was *log*-transformed and autoscaled.

(PQN)⁹¹ was applied using a pooled QC as a reference for normalization purposes, which reduced the total biological variation in treated/control cells as reflected by a median CV for all placental cell metabolites being reduced from 83% (uncorrected, A) to 36% (B). Furthermore, PCA also shows the adequate technical variation with the overall clustering of the QC group in comparison to the total biological variation; in this case, the median CV for all features within the data set was 24.0% ($n = 49$ over 9 runs). An overview of the overall data structure for treated HTR-8/SVneo cells is shown in the 2D heat map with hierarchical cluster analysis (HCA) (Figure 3.8) based on 49 cationic and anionic metabolites which were consistently measured in all placental cell extracts. To visualize differences as a result of exposure to e-cigarette vapour, a 2D scores plot from a partial least squares-discriminant analysis (PLS-DA) was next applied

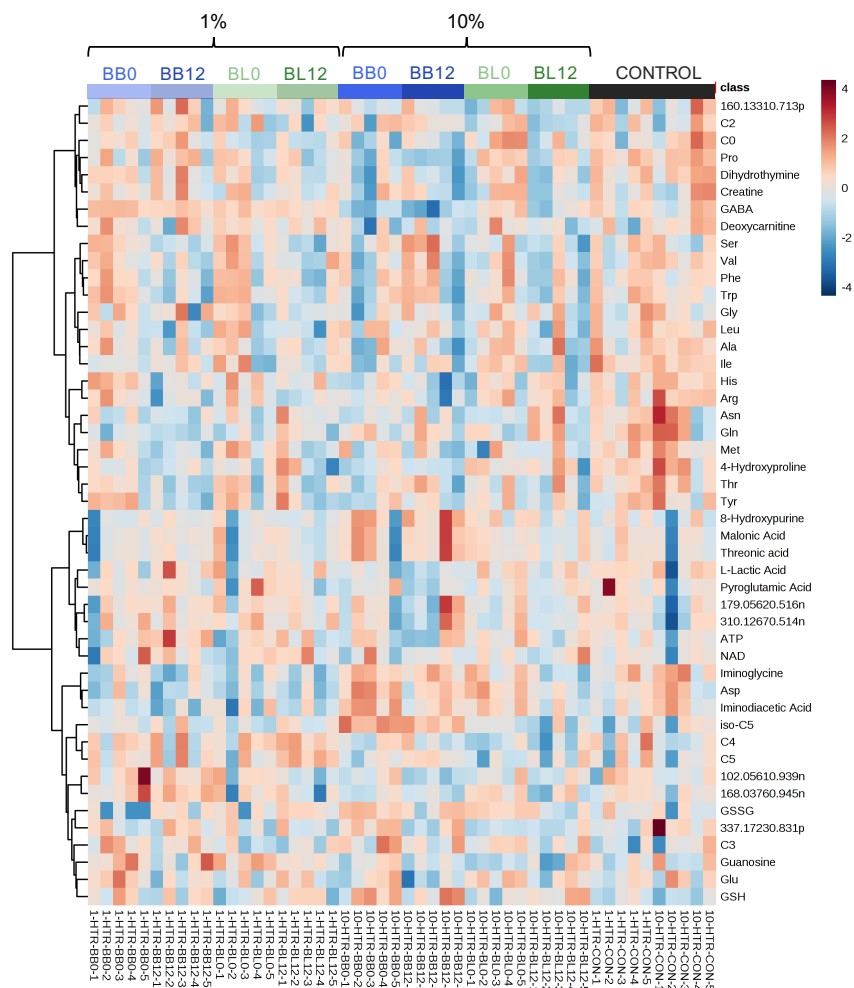


Figure 3.8. Hierarchical cluster analysis (HCA) 2D heatmap of PQN-corrected, autoscaled, and *log*-transformed metabolomic data showing the overall data structure for HTR-8/SVneo cells treated with 1% and 10% *v/v* e-cigarette vapour conditioned media ($n = 5$ in each group) and control maintenance media ($n = 10$).

based on PQN-corrected, *log*-transformed, and autoscaled data for (A) 10% *v/v* and (B) 1% *v/v* e-cigarette vape- conditioned media (Figure 3.9). In this supervised PLS-DA model, cells treated with 10% *v/v* vape-conditioned media had clear separation of the flavour-exposed cells (BB12 and BB0), which cannot be seen with treatment with the 1% *v/v* vape-conditioned media under otherwise identical conditions. As seen in the VIP scores ranking for exposed cells, several

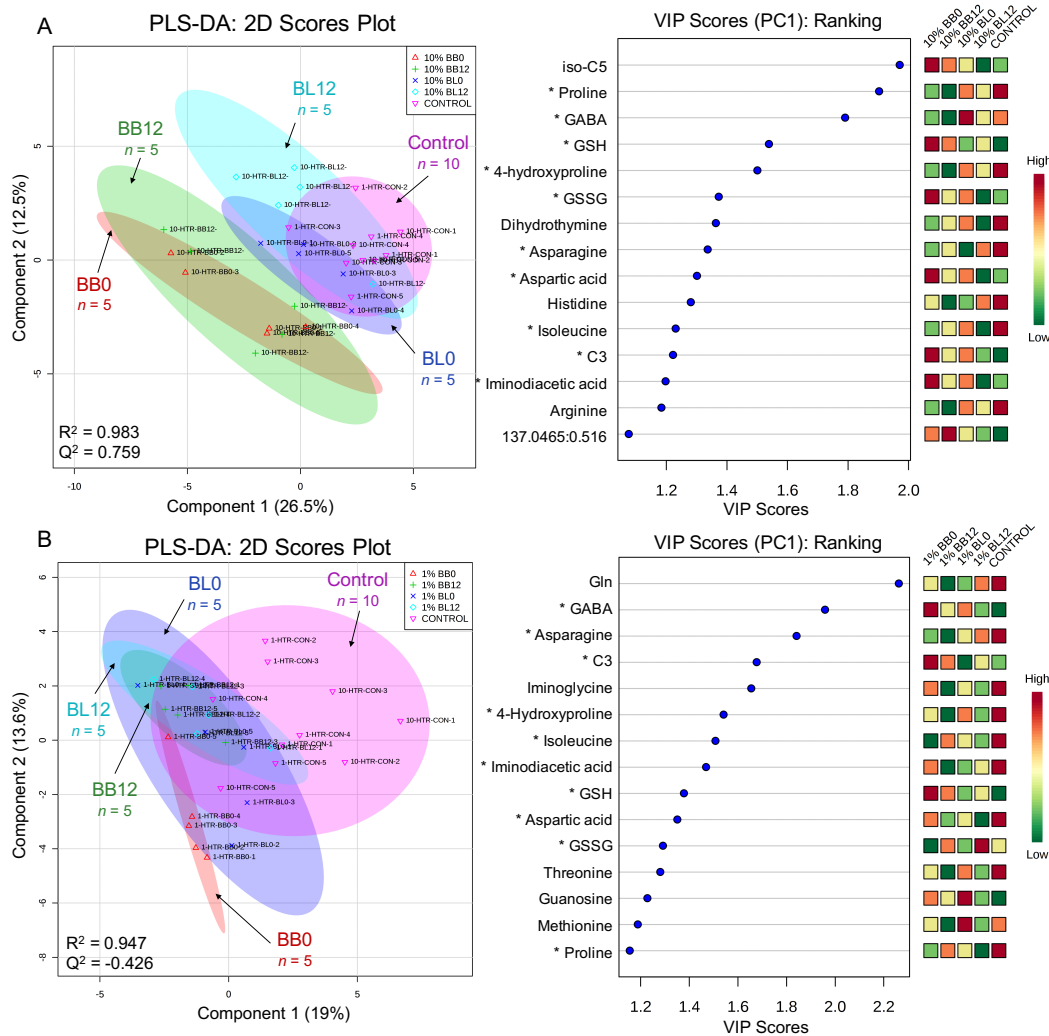


Figure 3.9. PLS-DA 2D scores plot for HTR-8/SVneo cells exposed to (A) 10% v/v and (B) 1% v/v e-cigarette vape-conditioned media. All data was corrected with PQN, log-transformed, and autoscaled. Multivariate analysis of PQN-corrected RPAs was used for the selection of top-ranked placental metabolites responsible for group separation. Top-ranked metabolites that were consistently altered for both exposures are indicated by an asterisk.

metabolites were consistently associated with differences observed between groups, namely GABA, asparagine (Asp), 4-hydroxyproline, isoleucine (Ile), and propionylcarnitine (C3). The separation of the BB0 and BB12 groups in the 10% v/v e-cigarette vape-conditioned media group agree with our original hypothesis

that the exposure of flavored e-liquids at higher doses have a stronger perturbation on placental metabolism for susceptible first trimester cell lines.

3.4.4.1 First Trimester Placental Cell Exposure to Unflavoured E-Cigarette Vapour

The chemical composition of the unflavoured Blacklisted e-cigarette liquids was much simpler than the flavoured Blue Balls e-liquid, containing propylene glycol and glycerol as its main constituents in addition to some breakdown products and other minor additives as presented in **Table 3.3** and **Table 3.4**. As research regarding the biological effects of e-cigarette exposure is limited and many studies fail to include unflavored, nicotine-free e-liquid vapours as a control, the first objective in this work was to evaluate the effect of the basic e-liquid constituents (*i.e.*, propylene glycol, glycerol, and breakdown products) on first trimester placental cells using univariate statistical tests. Relative peak area (RPA) responses for metabolites were not normally distributed, as determined by Shapiro-Wilk tests (p value < 0.001 , $n = 49$). As a result, nonparametric univariate analysis (Kruskal-Wallis H) was performed on non-transformed, PQN-corrected data to compare cells treated with control maintenance media ($n = 10$), 1% v/v BL0 vape-conditioned media ($n = 5$), and 10% v/v BL0 vape-conditioned media ($n = 5$) in order to evaluate the effect of major solutes in nicotine-free and flavourless e-cigarette vapours. Overall, there were no significant differences observed between control cells and cells exposed to BL0 vape-conditioned media at either dosage. Cell exposure to BL0 shows metabolite profiles similar to the

control cells, which suggests that the basic constituents of the e-cigarette vapour do not have a measurable effect on placental cell metabolism and survival at these concentrations. Toxicological studies have demonstrated that the aerosols of the two humectants used as the e-cigarette liquid base, propylene glycol and glycerol, do not cause cell toxicity *in vitro*¹¹³ or *in vivo*¹¹⁴⁻¹¹⁶; however, a recent study by Scheffler and *et. al.*¹¹⁷ demonstrated that human bronchial epithelial cells exposed to vapours from 99.5% pure propylene glycol and glycerol experienced reduced cell viability and higher oxidative stress in comparison to cells exposed to clean air.¹¹⁷ This study, however, assessed exposure to concentrated propylene glycol and glycerol independently, whereas e-cigarette liquids are usually composed of mixtures of the two humectants, and so assessing them independently is not a proper control for the major constituents of e-cigarette liquids.

Previous work has shown that nicotine is easily absorbed into the bloodstream with smoking, where it crosses the placenta and accumulates in fetal blood and amniotic fluid.⁷⁶ Next, the impact of nicotine dosage in unflavoured e-cigarette vapours was evaluated with Kruskal-Wallis H tests comparing control cells ($n = 10$), cells treated with 1% *v/v* BL12 vape-conditioned media ($n = 5$), and cells treated with 10% *v/v* BL12 vape-conditioned media ($n = 5$), which corresponded to exposure to 25 $\mu\text{g/mL}$ and 2.5 $\mu\text{g/mL}$ nicotine, respectively. As expected, in first trimester placental cells treated with 1% *v/v* or 10% *v/v* BL12 vape-conditioned media, there were significant decreases in several amino acids in comparison to control/unexposed cells (**Table 3.6**). Three neutral amino acids,

Table 3.6. Significant metabolites altered in first trimester placental cells when comparing unexposed control cells, 1% v/v BL12 vape-conditioned media, and 10% v/v BL12 vape conditioned media as determined by Kruskal-Wallis H tests in order to evaluate the effect of nicotine on placental cells. Fold-change (FC) is based on median RPAs and the FCs reported are for 10% or 1% v/v BL12/control. All data was corrected with PQN.

Metabolite	m/z:RMT:mode	p-value	Effect size	Fold-change	
				1% v/v	10% v/v
Isoleucine	132.1019:0.865:p	1.10E-2	0.385	0.564	0.692
Dihydrothymine	129.0658:0.754:p	1.50E-2	0.192	0.676	0.780
Iminoglycine ^a	74.0237:0.981:p	1.60E-2	0.332	0.630	0.627
Proline	116.0706:0.925:p	1.60E-2	0.332	0.718	0.740
Methionine	150.0589:0.915:p	3.00E-2	0.315	0.787	0.756

^a Significantly different from 10% v/v BL0 vape-conditioned media.

namely Ile, proline (Pro), and methionine (Met), were expressed at significantly lower concentrations in placental cells exposed to vape-conditioned media at both dosage levels (1% and 10% v/v) in comparison to unexposed control cells as depicted in box plots comparing PQN-corrected data (**Figure 3.10**), with median fold-changes (FC) in responses ranging from 1.3-fold to 1.8-fold. Comparing cells exposed to 1% v/v BL12 vape-conditioned media to cells exposed to 1% v/v BL0 vape-conditioned media showed no significant differences, whereas a significant decrease in iminoglycine was observed for cells treated with 10% v/v BL12 in comparison to BL0 vape-conditioned media. While there are no significant differences between treatment with 1% and 10% v/v BL12 vape-conditioned media, box plots for Ile and Pro highlight that there may be a dose-dependent effect, with larger FC differences for 10% v/v treatment groups. These results are consistent with prenatal nicotine exposure studies in fetal blood plasma of rats,⁷⁶ which showed decreases in Ile and Met with nicotine exposure, as well as second

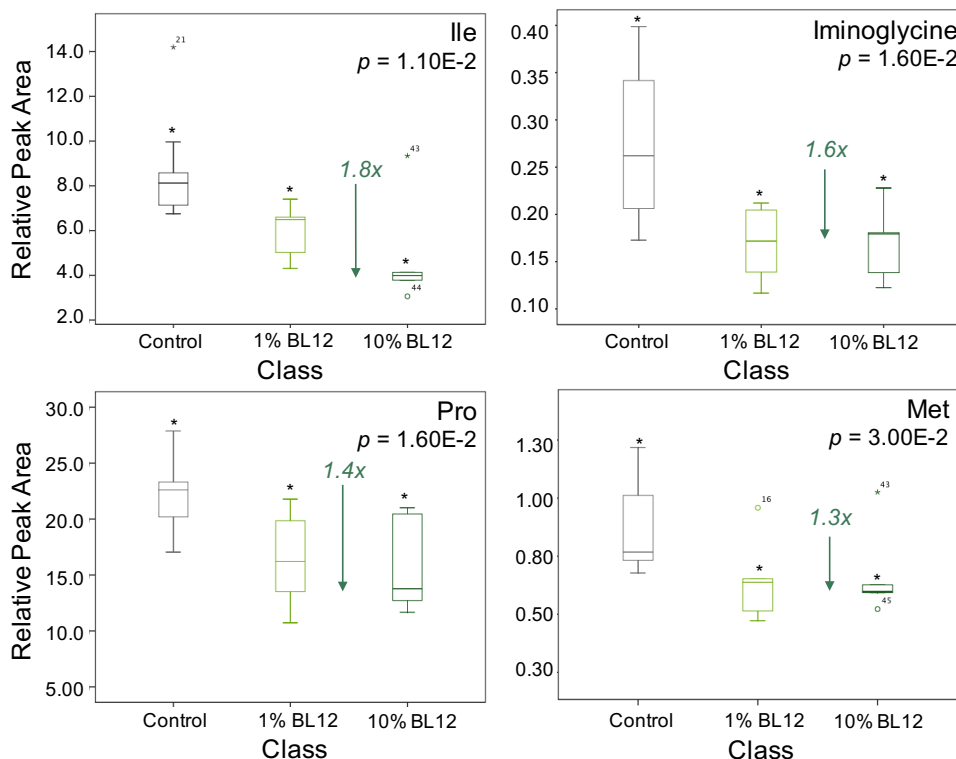


Figure 3.10. Box plots showing the effect of treatment with 1% ($n = 5$) and 10% ($n = 5$) v/v BL12 vape-conditioned media in comparison to control cells ($n = 10$). Groups that were significantly different are marked with an asterisk. Fold-changes (FC) are based on median RPAs for the 10% v/v BL12 treatment group and control cells. Data shown is corrected with PQN.

trimester amniotic fluid in humans,¹¹⁸ which showed dysregulation of Pro and Met metabolism. Iminoglycine is an oxidation product of glycine (Gly) and the iminoglycine transport system is involved in the intracellular transport of uptake of glycine, proline, and hydroxyproline, which may further implicate nicotine in the inhibition of amino acid transport.^{118,119} Large biological variation was observed within the 1% v/v BL0 vape-conditioned media treatment group, which may be the reason for not detecting a significant effect with 1% v/v BL12 vape-conditioned media. While decreases in Ile and Pro were observed in comparison to 10% v/v BL0 vape-conditioned media, the FCs were smaller and differences

were not as significant. This may also suggest that the basic constituents of the e-cigarette liquids do indeed have a minor impact on placental cellular metabolism despite not being statistically significant due to the small sample size in this pilot study.

3.4.3.2 First Trimester Placental Cell Exposure to Flavoured E-Cigarette Vapour

The major concern in regard to e-cigarette usage is the unknown effects of flavour additives present in e-cigarette liquids and, although they are generally safe for human consumption, long-term exposure studies on susceptible cell models have been sparsely reported in the literature. Several flavoured e-liquids have been demonstrated to be cytotoxic to a number of cell types (*e.g.*, human bronchial epithelial cells) but, for the most part, these effects have been observed with high levels of exposure involving direct exposure of cells to the viscous e-liquid solution. In contrast, we evaluate the effect of low-dosage e-cigarette vapour exposure on placental cells with biologically relevant dosage levels of nicotine upon subsequent dilution. Since metabolite ion responses were not normally distributed, as determined by Shapiro-Wilk tests ($p < 0.001$, $n = 49$), Mann-Whitney U tests were performed to assess the impact of flavouring additives on first trimester placental cell metabolism through treatment with BB0 vape-conditioned media. As it has been demonstrated that cells treated with 1% and 10% *v/v* BL0 had metabolic signatures similar to the controls, cells treated with 10% *v/v* BL0 vape-conditioned media were used as a ‘vape control’ to

account for exposure to the major e-liquid constituents and to increase certainty that any metabolic perturbations detected are likely caused by the complex array of flavour compounds within vape-exposed media. No significant differences were observed in cells treated with low dosage of 1% v/v BB0 vape-conditioned media (PQN normalized data) in comparison to unexposed control cells. In contrast, significant decreases in GABA, Ile, Pro, and dihydrothymine in addition to an elevation in iso-C5 were measured in cells treated with 10% v/v BB0 vape-conditioned media in comparison to unexposed cells (**Figure 3.11**). Decreases in GABA and iso-C5 were also significant in comparison to the ‘vape’-control, 10% v/v BL0 (**Table 3.7**). Overall, placental cells treated with the high dose of the flavoured e-liquid vapour (10% v/v BB12) showed the largest difference between control cells or were similar to trends observed in cells treated with 10% v/v BB0 vape-conditioned media, as observed in the PLS-DA 2D scores plot presented in **Figure 3.9**, which confirmed our original hypothesis that the combination of nicotine and flavour additives would lead to synergistic effects and a stronger perturbation on placental cell metabolism. Multivariate analysis with PLS-DA highlighted iso-C5, proline, and GABA as the major discriminating features with VIP scores > 1.5 for group separation between unexposed control cells, cells exposed to 10% v/v BL0 and BL12, and, importantly, cells exposed to 10% v/v BB0 and BB12, which was consistent with outcomes from univariate analysis with nontransformed data. Additionally, the effects of flavoured e-cigarette vapour at the higher dose (10% v/v) clearly differs from that of the unflavoured e-

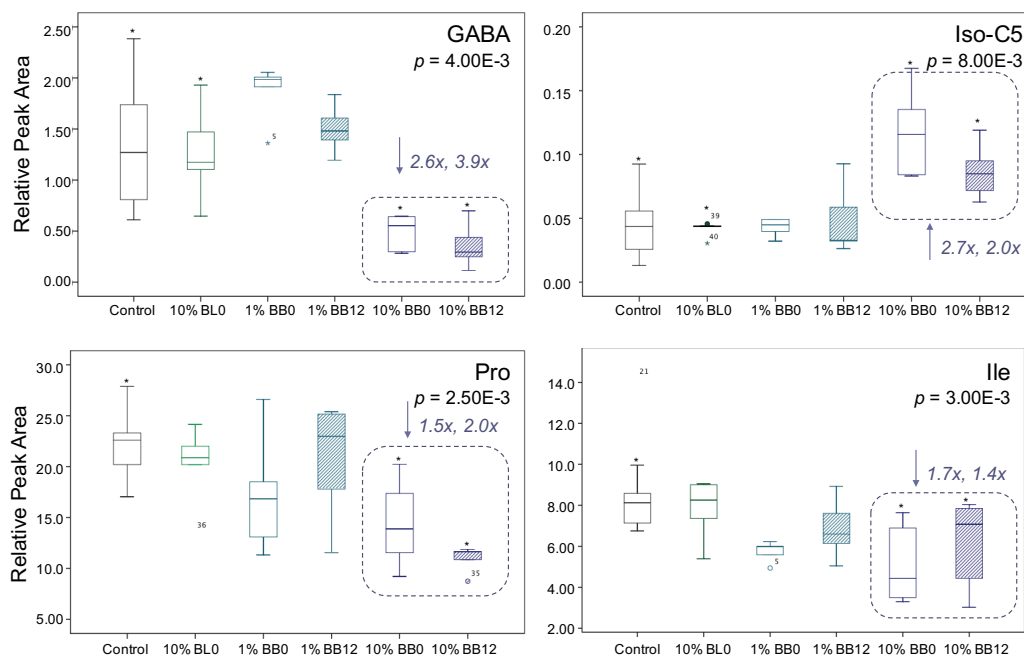


Figure 3.11. Box plots showing the effects of flavoured e-cigarette vapour at 1% and 10% *v/v* on GABA, Ile, Pro, and iso-C5 in comparison to control cells. In general, dose-dependent effects are observed for all metabolites shown, with cells treated with 10% *v/v* vapour exposed media had a more significant effect on metabolite levels. The addition of nicotine (*i.e.*, BB12) showed the same trend. Data shown is corrected with PQN.

Table 3.7. Significant metabolites when comparing cells treated with control maintenance media and 10% *v/v* BB0 vape-conditioned media as determined by Mann-Whitney U tests in order to compare the effects of flavouring agents in nicotine-free e-cigarette vapours. Fold-change is based on median RPAs for PQN-corrected data.

Metabolite	m/z:RMT:mode	<i>p</i> -value	Effect size	Fold-change
Proline	116.0706:0.925:p	2.50E-3	0.367	0.651
Isoleucine	132.1019:0.865:p	3.00E-3	0.349	0.598
Dihydrothymine	129.0658:0.754:p	3.80E-3	0.332	0.699
GABA ^a	104.0706:0.647:p	4.00E-3	0.367	0.378
Iso-C5 ^a	246.1700:0.826:p	8.00E-3	0.402	2.657

^a Significant difference was also observed between cells exposed to 10% *v/v* BL0 and 10% *v/v* BB0 vape-conditioned media.

cigarette vapour. With exposure to BB0 and BB12 in 10% *v/v* vape-conditioned media, a 2- to 2.7-fold increase was observed in iso-C5. Valerylcarnitine (C5)

also demonstrated the same trend, however was only significant when comparing cells treated with 10% v/v BL0 and BB0 vape-conditioned media, whereas responses of other measured acylcarnitines (C2-C4) and carnitine (C0) were similar to that of the control.

Importantly, significant decreases in GABA (2.6- to 3.9-fold change) were observed with exposure to both 10% v/v BB0 and BB12 as compared to lower dosage (1% v/v) and controls. GABA is synthesized from glutamate via glutamate decarboxylase and is the primary inhibitory neurotransmitter in the central nervous system (CNS).¹²⁰ In the CNS, glutamate decarboxylase is activated to synthesize GABA as a response to stress. GABA and its receptors are present in peripheral tissues, such as the ovaries and placenta, although its function in these tissues has not been fully explored;¹²¹ however, there is evidence that GABA plays a role in cellular apoptosis in trophoblast cells, which is involved in normal placental development. An impairment in GABA synthesis and/or its receptors could lead to imbalances in normal placental function, growth, and transport.^{121,122} Further, decreases in the amino acids Ile and Pro and an intermediate of thymine metabolism, dihydrothymine, were observed in cells treated with 10% v/v BL12, BB0, and BB12, which suggests that both nicotine and flavour additives present in the Blue Balls vapour have a cumulative effect on DNA synthesis and/or metabolism. Nicotine exposure has been shown to interfere with DNA synthesis and proliferation. For example, acute nicotine administration led to reduced synthesis of DNA in brain regions in neonatal rats.¹²³ Also, a study by Ginzkey *et*.

*al.*¹²⁴ demonstrated that exposure of human bronchial cells to nicotine led to significant DNA damage likely as a result of oxidative stress. Changes in amino acid metabolism can have serious implications on protein synthesis and cellular metabolism, which is essential for the normal growth and development of a fetus during pregnancy. While changes in placental metabolism have been shown to be induced by the presence of flavouring additives in e-cigarette vapour, it is essential to validate these small yet measurable effects on protein/gene expression and cell phenotype/function in order to better link the mode of action of these bioactive compounds. Collaborative work studying the effect of Blacklisted vape-conditioned media exposure on trophoblast viability and function demonstrated that HTR-8/SVneo trophoblast angiogenesis was significantly altered ($p < 0.05$) by decreasing distinct tube arrangements.¹²⁵ This work shows that, although a change was not seen on the metabolite level with treatment with 1% v/v BL0, early placental development could be affected by exposure to even the basic e-liquid constituents. Furthermore, BeWo cells treated with unflavoured (Blacklisted) and flavoured (Blue Balls) e-cigarette vape-conditioned media were found to have evidence of altered growth and development.⁸⁷ For example, 10% v/v flavoured e-cigarette vapour was shown to reduce vascular endothelial growth factor A (VEGF) expression in BeWo cells. Combined with the metabolomics data presented, it is suggested that the Blue Balls e-cigarette vapour may have more potent effect on placental cell development and function that would

contribute to a risk to normal fetal growth and development for women e-cigarette smokers during pregnancy.

E-cigarette liquids are very complex mixtures, as demonstrated by MSI-CE-MS and HS-GC/MS analysis of polar/ionic (*i.e.*, nicotine impurities) and volatile organic compounds (*i.e.*, flavour additives), which identified 28 compounds altogether. Placental trophoblast cells were exposed to two concentrations of flavourless and flavoured e-cigarette vapours at levels that did not induce cytotoxicity in order to evaluate potential acute effects on placental development, function, and metabolism. Exposure of HTR-8/SVneo cells to e-cigarette vapour with nicotine and flavour additives led to subtle changes in amino acid metabolism in addition to other cellular metabolites. To better evaluate the size effect of these differences, lead compounds need to first be verified with MS/MS and/or by spiking standards into the cell matrix, in addition to quantification with external calibration curves. While this study was limited by small sample sizes ($n = 5$) for each treatment group in addition to the lack of a standardized method to correct for cell content (*e.g.*, protein or DNA concentrations), cumulative differences in the presence of flavour and nicotine (*i.e.*, comparison of BB0 and BB12 treatments) suggest that a number of components have an impact on placental metabolism and, potentially, development/function. While the mechanism of these changes and the potential harm e-cigarettes pose on maternal health cannot be concluded directly from this study, it is demonstrated that there are metabolic perturbations as a result of e-cigarette exposure, particularly to the

flavoured and nicotine-containing e-cigarette liquids. Examining only one flavour greatly limits the scope of this work and, in order to have a better understanding of e-cigarette vapour exposure, a larger study involving placental cells treated with various flavours of e-cigarette vapours is warranted. Also, exposure studies to individual flavour additives that have been vaporized under the same conditions will allow better assessment of the safety of certain e-cigarette flavours as a whole, with the potential of improving pending regulation of e-cigarette products.

3.5 Conclusion

E-cigarette liquids are complex matrices consisting of a base solution made up of a combination of propylene glycol and glycerol, nicotine at different dosages, and various natural and artificial flavourings. A comparative analysis of flavourless and blue raspberry-flavoured e-liquid formulations with MSI-CE-MS and headspace-GC/MS confirmed the complexity of these consumer products popular among young adults, and it was demonstrated that these e-liquids contain more constituents than listed on their labels (*i.e.*, at least 13 compounds not including various flavour additives). Nicotine-containing e-liquids were also shown to contain a significant amount of tobacco impurities and related nicotine degradation products. As expected, the blue-raspberry flavoured e-liquid contained a significantly larger number of flavour compounds, which possess GRAS designation by the FDA and FEMA.

This work was a pilot study to explore the putative effects of e-cigarette vapour on placental metabolism using first trimester and third trimester trophoblast cells. Placental cells represent a relevant *in vitro* model of pregnancy when studying effects of chemical/environmental exposures, as placental dysfunction will negatively affect maternal health and fetal development.¹²⁶ No significant changes at the metabolite level were observed in third trimester cells in comparison to altered metabolite profiles measured in first trimester cells. This result was not surprising as first trimester placental cells are known to be more susceptible to chemical influences.¹²⁷ This is consistent with maternal smoking, which has been shown to be less harmful at the end of pregnancy as third trimester trophoblast cells have a higher resistance to chemical influences. No effect was observed in first trimester cells exposed to an unflavoured e-cigarette liquid vapour matrix without nicotine and metabolite profiles were similar to control cells. It was determined that the flavourless and blue raspberry flavoured e-cigarette liquids advertised as 0 mg/mL nicotine did not contain nicotine above a detection threshold (LOD) of 0.3 μ M. In low dose exposure studies, the e-cigarette liquid base components (*i.e.*, propylene glycol and glycerol) do not have a measurable perturbation on cellular metabolism, which allowed us to evaluate the effects of flavoured and nicotine-containing e-liquids with some confidence since the observed changes were a direct result of flavour additives and/or nicotine and nicotine impurities. Similarly, synergistic effects were observed with exposure to the more complex e-cigarette liquid vapours in the presence of

nicotine. The inclusion of nicotine led to alterations in amino acids (Ile, Met, Pro) which was observed at both exposures of vapour explored (1% and 10% v/v) and is consistent with studies involving prenatal nicotine exposure leading to alterations in Pro and Met metabolism.¹¹⁸ The presence of flavouring in the e-cigarette vapour matrix led to subtle changes in normal trophoblast amino acid metabolism, which was not observed in the presence of the base e-liquid. This supports the hypothesis that the flavour compounds added to e-cigarette liquids to increase their desirability can contribute to alterations in placental metabolism, which may in turn have a deleterious impact on maternal and fetal health with chronic long-term e-cigarette exposure. This study demonstrates that the ‘safe’ designation given to flavour additives in regard to ingestion may not apply when the route of exposure is inhalation. Additionally, there is a critical need to evaluate the safety of these additives for the general population and high-risk individuals, such as pregnant women and their developing fetus.

3.6 References

1. World Health Organization, WHO Report on the Global Tobacco Epidemic, 2011. Geneva: World Health Organization, 2011 [accessed 2017 April 13].
2. World Health Organization, Tobacco Fact Sheet. Geneva: World Health Organization, 2016 [accessed 2017 April 13].
3. Office of the Surgeon General (US); Office on Smoking and Health (US). The Health Consequences of Smoking: A Report of the Surgeon General. Atlanta (GA): Centers for Disease Control and Prevention (US), 2004.
4. Anderson, C.; Majeste, A.; Hanus, J.; Wang, S. E-cigarette aerosol exposure induces reactive oxygen species, DNA damage, and cell death in vascular endothelial cells. *Tox. Sci.* 2016, **154**: 332-340.

5. Messner, B.; Bernhard, D. Smoking and cardiovascular disease: Mechanisms of endothelial dysfunction and early atherogenesis. *Arterioscler. Thromb. Vasc. Biol.* 2014, **34**: 509-515.
6. U.S. Food and Drug Administration (FDA), Harmful and Potentially Harmful Constituents in Tobacco Products and Tobacco Smoke; Established List, 2012. <http://www.fda.gov/TobaccoProducts/GuidanceComplianceRegulatoryInformation/ucm297786.htm> [Accessed 2017 April 13].
7. Lisko, J.G.; Stanfill, S.B.; Duncan, B.W.; Watson, C.H. Application of GC-MS/MS for the analysis of tobacco alkaloids in cigarette filler and various tobacco species. *Anal. Chem.* 2013, **85**: 3380-3384.
8. Le Houezec, J.; McNeill, A.; Britton, J. Tobacco, nicotine and harm reduction. *Drug Alcohol Rev.* 2011, **30**: 119-123.
9. Benowitz, N.L. Nicotine addiction. *N. Engl. J. Med.* 2010, **362**: 2295-2303.
10. Dajas-Bailador, F.; Wonnacott, S. Nicotinic acetylcholine receptors and the regulation of neuronal signalling. *Trends Pharmacol. Sci.* 2004, **25**: 317-324.
11. Dana, J.A.; De Biasi, M. Cellular mechanisms of nicotine addiction. *Pharmacol. Biochem. Behav.* 2001, **70**: 439-446.
12. D'Souza, M.S.; Markou, A. Neuronal mechanisms underlying development of nicotine dependence: Implications for novel smoking-cessation treatments. *Addict. Sci. Clin. Pract.* 2011, **6**: 4-16.
13. Brody, A.L.; Mandelkern, M.A.; London, E.D.; Olmstead, R.E.; Farahi, J.; Scheibal, D.; Jou, J.; Allen, V.; Tionsgon, E.; Chefer, S.I.; Koren, A.O.; Mukhin, A.G. Cigarette smoking saturates brain alpha 4 beta 2 nicotinic acetylcholine receptors. *Arch. Gen. Psychiatry* 2006, **63**: 907-915.
14. Cahn, Z.; Siegel, M. Electronic cigarettes as a harm reduction strategy for tobacco control: A step forward or a repeat of past mistakes? *J. Public Health Policy* 2011, **12**: 16-31.
15. Henningfield, J.E. Drug therapy: nicotine medications for smoking cessation. *N. Engl. J. Med.* 1995, **333**: 1196-1203.
16. El Dib, R.; Suzumura, E.A.; Akl, E.A.; Gomaa, H.; Agarwal, A.; Chang, Y.; Prasad, M.; Ashoorion, V.; Heels-Ansdell, D.; Maziak, W.; Guyatt, G. Electronic nicotine delivery systems and/or electronic non-nicotine delivery systems for tobacco smoking cessation or reduction: a systematic review and meta-analysis. *BMJ Open* 2017, **7**: e012680.
17. American Academy of Pediatrics. Policy Statement, Electronic Nicotine Delivery Systems: Section on Tobacco Control. *Pediatrics* 2015, **136**; doi: 10.1542/peds.2015-3222.
18. Grana, R.; Benowitz, N.; Glantz, S.A. E-Cigarettes: A Scientific Review. *Circulation* 2008, **129**: 1972-1986.
19. Beige Market Intelligence. Global Vape Market (e-Cigarette and Vaporizer) – Strategic Assessment and Forecast – Till 2021, 2015. <http://www.beigemarketintelligence.com/reports/research-report-consumer-and-retail->

- [market/vape-ecigarette-vaporizer-market-research-report/](#) [Accessed 2017 April 14].
20. Berg, C.J. Preferred flavors and reasons for e-cigarette use and discontinued use among never, current and former smokers. *Int. J. Public Health* 2016, **61**: 225-236.
 21. Dinakar, C.; O'Connor, G.T. The health effects of electronic cigarettes. *N. Engl. J. Med.* 2016, **375**: 1372-1381.
 22. Farsalinos, K.E.; Romagna, G.; Tsiapras, D.; Kyrzopoulos, S.; Spyrou, A.; Voudris, V. Impact of flavour variability on electronic cigarette use experience: an internet survey. *Int. J. Environ. Res. Public Health* 2013, **10**: 7272-7282.
 23. Hutzler, C.; Paschke, M.; Kruschinski, S.; Henkler, F.; Hahn, J.; Luch, A. Chemical hazards present in liquids and vapors of electronic cigarettes. *Arch. Toxicol.* 2014, **88**: 1295-1308.
 24. Farsalinos, K.E.; Romagna, G.; Tsiapras, D.; Kyrzopoulos, S.; Voudris, V. Evaluation of electronic cigarette use (vaping) topography and estimation of liquid consumption: implications for research protocol standards definition and for public health authorities' regulation. *Int. J. Environ. Res. Public Health* 2013, **10**: 2500-2514.
 25. Trehly, M.L.; Ye, W.; Hadwiger, M.E.; Moore, T.W.; Allgire, J.F.; Woodruff, J.T.; Ahadi, S.S.; Black, J.C.; Westenberger, B.J. Analysis of electronic cigarette cartridges, refill solutions, and smoke for nicotine and nicotine related impurities. *J. Liq. Chromatogr. Relat. Technol.* 2011, **34**: 1442-1458.
 26. Farsalinos, K.E.; Spyrou, A.; Tsimopoulou, K.; Stefopoulos, C.; Romagna, G.; Voudris, V. Nicotine absorption from electronic cigarette use: comparison between first and new-generation devices. *Sci. Rep.* 2014, **4**: 4133.
 27. Baker, R.R. Product formation mechanisms inside a burning cigarette. *Prog. Energ. Combust.* 1981, **7**: 135-153.
 28. Goniewicz, M.L.; Gawron, M.; Smith, D.M.; Peng, M.; Jacob, P., 3rd; Benowitz, N.L. Exposure to nicotine and selected toxicants in cigarette smokers who switched to electronic cigarettes: a longitudinal within-subjects observational study. *Nicotine Tob. Res.* 2017, **19**: 160-167.
 29. Tierney, P.A.; Karpinski, C.D.; Brown, J.E.; Luo, W.; Pankow, J.F. Flavour chemicals in electronic cigarette fluids. *Tob. Control* 2016, **25**: e10-e15.
 30. Azzopardi, D.; Patel, K.; Jaunky, T.; Santopietro, S.; Camacho, O.M.; McAughey, J.; Gaça, M. Electronic cigarette aerosol induces significantly less cytotoxicity than tobacco smoke. *Toxicol. Mech. Methods* 2016, **26**: 477-491.
 31. Flavor and Extract Manufacturers Association (FEMA). Safety assessment and regulatory authority to use flavors—focus on electronic nicotine delivery systems and flavored tobacco products, 2016. <https://www.femaflavor.org/safety-assessment-and-regulatory-authority-use->

- [flavors-focus-electronic-nicotine-delivery-systems](#) [Accessed 2017, April 14].
32. Goniewicz, M.L.; Knysak, J.; Gawron, M.; Kosmider, L.; Sobczak, A.; Kurek, J.; Prokopowicz, A.; Jablonska-Czapla, M.; Rosik-Dulewska, C.; Havel, C.; Jacob, P., III.; Benowitz, N. Levels of selected carcinogens and toxicants in vapor from electronic cigarettes. *Tob. Control* 2014, **23**: 133-139.
 33. Barrington-Trimis, J.L.; Samet, J.M.; McConnell, R. Flavorings in electronic cigarettes: an unrecognized health hazard? *JAMA* 2014, **312**: 2493-2494.
 34. Allen, J.G.; Flanigan, S.S.; LeBlanc, M.; Vallarino, J.; MacNaughton, P.; Stewart, J.H.; Christiani, D.C. Flavoring chemicals in e-cigarettes: Diacetyl, 2,3-pentanedione, and acetoin in a sample of 51 products, including fruit-, candy-, and cocktail-flavoured e-cigarettes. *Environ. Health Perspect.* 2016, **124**: 733-739.
 35. Lerner, C.A.; Sundar, I.K.; Yao, H.; Gerloff, J.; Ossip, D.J.; McIntosh, S.; Robinson, R.; Rahman, I. Vapors produced by electronic cigarettes and e-juices with flavorings induce toxicity, oxidative stress, and inflammatory response in lung epithelial cells and in mouse lung. *PLoS ONE* 2015, **10**: e0116732.
 36. El. Golli, N.; Dkhili, H.; Dallagi, Y.; Rahali, D.; Lasram, M.; Bini-Dhouib, I.; Lebret, M.; Rose, J.P.; El Fazaa, S.; Asmi, M.A. Comparison between electronic cigarette refill liquid and nicotine on metabolic parameters in rats. *Life Sci.* 2016, **146**: 131-138.
 37. Farsalinos, K.E.; Romagna, G.; Alliffranchini, E.; Ripamonti, E.; Bocchietto, E.; Todeschi, S.; Tsiapras, D.; Kyrzopoulos, S.; Voudris, V. Comparison of the cytotoxic potential of cigarette smoke and electronic cigarette vapor extract on cultured myocardial cells. *Int. J. Environ. Res. Public Health* 2013, **10**: 5146-5162.
 38. Marynak, K.L.; Gammon, D.G.; King, B.A.; Loomis, B.R.; Fulmer, E.B.; Wang, T.W.; Rogers, T. National and state trends in sales of cigarettes and e-cigarettes, U.S., 2011-2015. *Am. J. Prev. Med.* 2017, **53**: 96-101.
 39. Shiplo, S.; Czoli, C.D.; Hammond, D. E-cigarette use in Canada: prevalence and patterns of use in a regulated market. *BMJ Open* 2015, **5**: e007971.
 40. Hon Dipika, D. (Associate Minister of Health and Long-Term Care). Bill 45, Making Healthier Choices Act, 2015. http://www.ontla.on.ca/bills/bills-files/41_Parliament/Session1/b045ra.pdf [Accessed 2017 April 15].
 41. Health Canada. Notice—To All Persons Interested in Importing, Advertising or Selling Electronic Smoking Products in Canada. Health Canada file number 09-108446-55, March 27, 2009. http://www.hc-sc.gc.ca/dhp-mps/prodpharma/applic-demande/pol/notice_avis_e-cig-eng.php [Accessed 2017 April 15].
 42. Senate of Canada. Bill S-5 (First Reading), November 22, 2016. <http://www.parl.gc.ca/HousePublications/Publication.aspx?Language=E&Mode=1&DocId=8616193> [Accessed 2017 April 15].

43. Health Canada. Consultation on proposals for the regulation of vaping products, August 25, 2017. <https://www.canada.ca/en/health-canada/programs/consultation-regulation-vaping-products.html> [Accessed 2017 August 30].
44. Electronic Cigarette Trade Association. About ECTA, 2016. <http://ectaofcanada.com/about/> [Accessed 2017 April 15].
45. Electronic Cigarette Trade Association. Why Juice Should Be Tested, September 18, 2014. <http://ectaofcanada.com/why-juice-should-be-tested/> [Accessed 2017, April 15].
46. Aug, A.; Altraja, S.; Kilk, K.; Porosk, R.; Soomets, U.; Altraja, A. E-cigarette effects the metabolome of primary normal human bronchial epithelial cells. *PLoS One* 2015, **10**: e0142053.
47. Solleti, S.K.; Bhattacharya, S.; Ahmad, A.; Wang, Q.; Mereness, J.; Rangasamy, T.; Mariani, T.J. MicroRNA expression profiling defines the impact of electronic cigarettes on human airway epithelial cells. *Sci. Rep.* 2017, **7**: 1081-1091.
48. Hwang, J.H.; Lyes, M.; Sladewski, K.; Enany, S.; McEachern, E.; Mathew, D.P.; Das, S.; Moshensky, A.; Bapat, S.; Pride, D.T.; Ongkeko, W.M.; Crotty Alexander, L.E. Electronic cigarette inhalation alters innate immunity and airway cytokines while increasing the virulence of colonizing bacteria. *J. Mol. Med.* 2016, **94**: 667-679.
49. Rubenstein, D.A.; Hom, S.; Ghebrehiwet, B.; Yin, W. Tobacco and e-cigarette products initiate Kupffer cell inflammatory responses. *Molec. Immunol.* 2015, **67**: 652-660.
50. Cervellati, F.; Muresan, X.M.; Sticozzi, C.; Gambari, R.; Montagner, G.; Forman, H.J.; Torricelli, C.; Maioli, E.; Valacchi, G. Comparative effects between electronic cigarettes and cigarette smoke in human keratinocytes and epithelial lung cells. *Toxicol. In Vitro* 2014, **28**: 999-1005.
51. Orr, M.S. Electronic cigarettes in the USA: a summary of available toxicology data and suggestions for the future. *Tob. Control* 2014, **23**: ii18-ii22.
52. Government of Canada. Canadian Tobacco Alcohol and Drugs (CTADS): 2015 summary. <https://www.canada.ca/en/health-canada/services/canadian-tobacco-alcohol-drugs-survey/2015-summary.html> [Accessed 2017 April 15].
53. Carpenter, C.M.; Wayne, G.F.; Pauly, J.L.; Koh, H.K.; Connolly, G.N. New cigarette brands with flavors that appeal to youth: tobacco marketing strategies. *Health Aff. (Millwood)* 2005, **224**: 1601-1610.
54. Villanti, A.C.; Richardson, A.; Vallone, D.M.; Rath, J.M. Flavored tobacco product use among U.S. young adults. *Am. J. Prev. Med.* 2013, **44**: 388-391.
55. Kahr, M.K.; Padgett, S.; Shope, C.D.; Griffin, E.N.; Xie, S.S.; Gonzalez, P.J.; Levison, J.; Mastrobattista, J.; Abramovici, A.R.; Northrup, T.F.; Stotts, A.L.; Aagaard, K.M.; Suter, M.A. A qualitative assessment of the perceived

- risks of electronic cigarette and hookah use in pregnancy. *BMC Public Health* 2015, **15**: 1273-1280.
56. Mark, K.S.; Farquhar, B.; Chisolm, M.S.; Coleman-Cowger, V.H.; Terplan, M. Knowledge, attitudes, and practice of electronic cigarette use among pregnant women. *J. Addict. Med.* 2015, **9**: 266-272.
 57. Ashford, K.; Wiggins, A.; Butler, K.; Ickes, M.; Rayens, M.K.; Hahn, E. e-Cigarette use and perceived harm among women of childbearing age who reported tobacco use during the past year. *Nurs. Res.* 2016, **65**: 408-414.
 58. Paterson, J.M.; Neimanis, I.M.; Bain, E. Stopping smoking during pregnancy: are we on the right track? *Can. J. Public Health* 2003, **94**: 297-299.
 59. Al-Sahab, B.; Saqib, M.; Hauser, G.; Tamim, H. Prevalence of smoking during pregnancy and associated risk factors among Canadian women: a national survey. *BMC Pregnancy Childbirth* 2010, **10**: 24.
 60. Kuntz, B.; Lampert, T. Social disparities in maternal smoking during pregnancy. *Geburtshilfe Frauenheilkd.* 2016, **76**: 239-247.
 61. Suter, M.A.; Mastrobattista, J.; Sachs, M.; Aagaard, K. Is there evidence for potential harm of electronic cigarette use in pregnancy? *Birth Defects Res. Part A* 2014, **103**: 186-195.
 62. Baeza-Loya, S.; Viswanath, H.; Carter, A.; Molfese, D.L.; Velasquez, K.M.; Baldwin, P.R.; Thompson-Lake, D.G.Y.; Sharp, C.; Fowler, J.C.; De La Garza, R., 2nd; Salas, R. Perceptions about e-cigarette safety may lead to e-smoking during pregnancy. *Bull. Menninger. Clin.* 2014, **78**: 243-252.
 63. Bauer, M.K.; Harding, J.E.; Bassett, N.S.; Breier, B.H.; Oliver, M.H.; Gallaher, B.H.; Evans, P.C.; Woodall, S.M.; Gluckman, P.D. Fetal growth and placental function. *Molec. Cell. Endocrinol.* 1998, **140**: 115-120.
 64. Garnica, A.D.; Chan, W.Y. The role of the placenta in fetal nutrition and growth. *J. Am. Coll. Nutr.* 1996, **15**: 206-222.
 65. James, J.L.; Stone, P.R.; Chamley, L.W. Cytotrophoblast differentiation in the first trimester of pregnancy: evidence for separate progenitors of extravillous trophoblasts and syncytiotrophoblast. *Reproduction* 2005, **130**: 95-103.
 66. Robinson, J.; Chidzanja, S.; Kind, K.; Lok, F.; Owens, P.; Owens, J. Placental control of fetal growth. *Reprod. Fertil. Dev.* 1995, **7**: 333-344.
 67. Cross, J.C. Placental function in development and disease. *Reprod. Fertil. Dev.* 2006, **18**: 71-76.
 68. Wu, F.; Tian, F.-J.; Lin, Y.; Xu, W.-M. Oxidative stress: Placental function and dysfunction. *Am. J. Reprod. Immunol.* 2016, **76**: 258-271.
 69. Reynolds, L.P.; Caton, J.S.; Redmer, D.A.; Grazul-Bilska, A.T.; Vonnahme, K.A.; Borowicz, P.P.; Luther, J.S.; Wallace, J.M.; Wu, G.; Spencer, T.E. Evidence for altered placental blood flow and vascularity in compromised pregnancies. *J. Physiol.* 2006, **572**: 51-58.

70. Koklanaris, N.; Nwachukwu, J.C.; Huang, S.J.; Guller, S.; Karpisheva, K.; Garabedian, M.; Lee, M.J. First-trimester trophoblast cell model gene response to hypoxia. *Am. J. Obstet. Gynecol.* 2006, **194**: 687-693.
71. Mannelli, C.; Ietta, F.; Avanzati, A.M.; Skarzynski, D.; Paulesu, L. Biological tools to study the effects of environmental contaminants at the feto-maternal interface. *Dose-Resp.* 2015, **13**: 1-11.
72. Mayhew, T.M.; Charnock-Jones, D.S.; Kaufmann, P. Aspects of human fetoplacental vasculogenesis and angiogenesis. III. Changes in complicated pregnancies. *Placenta* 2004, **25**: 127-139.
73. Nayeem, S.B.; Arfuso, F.; Dharmarajan, A.; Keelan, J.A. Role of Wnt signalling in early pregnancy. *Reprod. Fertil. Dev.* 2016, **28**: 525-544.
74. Shisler, S.; Eiden, R.D.; Molnar, D.S.; Schuetze, P.; Huestis, M.; Homish, G. Smoking in pregnancy and fetal growth: the case for more intensive assessment. *Nicotine Tob. Res.* 2017, **19**: 525-531.
75. England, L.J.; Bunnell, R.E.; Pechacek, T.F.; Tong, V.T.; McAfee, T.A. Nicotine and the developing human: a neglected element in the electronic cigarette debate. *Am. J. Prev. Med.* 2015, **49**: 286-293.
76. Feng, J.; Yan, Y.; Liang, G.; Liu, Y.; Li, X.; Zhang, B.; Chen, L.; Yu, H.; He, X.; Wang, H. Maternal and fetal metabonomic alterations in prenatal nicotine exposure-induced rat intrauterine growth restriction. *Mol. Cell. Endocrinol.* 2014, **394**: 59-69.
77. Rolle-Kampczyk, U.E.; Krumsiek, J.; Otto, W.; Röder, S.W.; Kohajda, T.; Borte, M.; Theis, F.; Lehmann, I.; von Bergen, M. Metabolomics reveals effects of maternal smoking on endogenous metabolites from lipid metabolism in cord blood of newborns. *Metabolom.* 2016, **12**: 76-87.
78. Suter, M.; Ma, J.; Harris, A.; Patterson, L.; Brown, K.A.; Shope, C.; Showalter, L.; Abramovici, A.; Aagaard-Tillery, K.M. Maternal tobacco use modestly alters correlated epigenome-wide placental DNA methylation and gene expression. *Epigenetics* 2011, **6**: 1284-1294.
79. Fanos, V.; Atzori, L.; Makarenko, K.; Melis, G.B.; Ferrazzi, E. Metabolomics application in maternal-fetal medicine. *Biomed. Res. Int.* 2013, **2013**: 720514.
80. Kuehnbaum, N.L.; Kormendi, A.; Britz-McKibbin, P. Multisegment injection-capillary electrophoresis-mass spectrometry: A high-throughput platform for metabolomics with high data fidelity. *Anal. Chem.* 2013, **85**: 10664-10669.
81. Kuehnbaum, N.L.; Gillen, J.B.; Kormendi, A.; Lam, K.P.; DiBattista, A.; Gibala, M.J.; Britz-McKibbin, P. Multiplexed separations for biomarker discovery in metabolomics: Elucidating adaptive responses to exercise training. *Electrophoresis* 2015, **36**: 2226-2236.
82. DiBattista, A.; McIntosh, N.; Lamoreaux, M.; Al-Dirbashi, O.; Chakraborty, P.; Britz-McKibbin, P. Temporal signal pattern recognition in mass spectrometry: A method for rapid identification and accurate quantification

- of biomarkers for inborn errors of metabolism with quality assurance. *Anal. Chem.* 2017, **89**, 8112-8121.
83. Lankadurai, B.P.; Nagato, E.G.; Simpson, M.J. Environmental metabolomics: an emerging approach to study organism responses to environmental stressors. *Environ. Rev.* 2013, **21**: 180-205.
84. Ch, R.; Singh, A.M.; Pandey, P.; Saxena, P.N.; Mudiam, M.K.R. Identifying the metabolic perturbations in earthworm induced by cypermethrin using gas chromatography-mass spectrometry based metabolomics. *Sci. Rep.* 2015, **5**: 15674.
85. Fernando, S.; Shaw, L.; Shaw, D.; Gallea, M.; VandenEnden, L.; House, R.; Verma, D.K.; Britz-McKibbin, P.; McCarry, B.E. Evaluation of firefighter exposure to wood smoke during training exercises at burn houses. *Environ. Sci. Technol.* 2016, **50**: 1536-1543.
86. Zaitso, K.; Hayashi, Y.; Kusano, M.; Tsuchihashi, H.; Ishii, A. Application of metabolomics to toxicology of drugs of abuse: A mini review of metabolomics approach to acute and chronic toxicity studies. *Drug Metab. Pharmacokinet.* 2016, **31**: 21-26.
87. Kleiboer, S.; Holloway, A. *The effects of electronic cigarette vapour on placenta growth and development.* Unpublished Undergraduate Thesis. McMaster University, 2017.
88. Sapcariu, S.C.; Kanashova, T.; Weindl, D.; Ghelfi, J.; Dittmar, G.; Hiller, K. Simultaneous extraction of proteins and metabolites from cells in culture. *MethodsX* 2014, **1**: 74-80.
89. de Macedo, A.N.; Mathiaparanam, S.; Brick, L.; Keenan, K.; Gonska, T.; Pedder, L.; Hill, S.; Britz-McKibbin, P. The sweat metabolome of screen-positive Cystic Fibrosis infants: revealing mechanisms beyond impaired chloride transport. *ACS Cent. Sci.* 2017, **3**: 904-913.
90. Miller, J.M. Basic statistical methods for analytical chemistry. Part 2. Calibration and regression methods. A review. *Analyst.* 1991, **116**: 3-14.
91. Dieterle, F.; Ross, A.; Schlotterbeck, G.; Senn, H. Probabilistic quotient normalization as robust method to account for dilution of complex biological mixtures. Application in 1H NMR metabolomics. *Anal. Chem.* 2006, **78**: 4281-4290.
92. Etter, J.F.; Zäther, E.; Svensson, S. Analysis of refill liquids for electronic cigarettes. *Addiction* 2013, **108**: 1671-1679.
93. Peace, M.R.; Baird, T.R.; Smith, N.; Wolf, C.E.; Poklis, J.L.; Poklis, A. Concentration of nicotine and glycols in 27 electronic cigarette formulations. *J. Anal. Toxicol.* 2016, **40**: 403-407.
94. Buettner-Schmidt, K.; Miller, D.R.; Balasubramanian, N. Electronic cigarette refill liquids: Child-resistant packaging, nicotine content, and sales to minors. *J. Pediatr. Nurs.* 2016, **31**: 373-379.
95. Flora, J.W.; Wilkinson, C.T.; Sink, K.M.; McKinney, D.L.; Miller, J.H. Nicotine-related impurities in e-cigarette cartridges and refill e-liquids. *J. Liq. Chromatogr. Relat. Tech.* 2016, **39**: 821-829.

96. Benowitz, N.L.; Hukkanen, J.; Jacob, P., 3rd. Nicotine chemistry, metabolism, kinetics and biomarkers. *Handb. Exp. Pharmacol.* 2009, **192**: 29-60.
97. Flavor & Extract Manufacturers Association (FEMA), FEMA Flavor Ingredient Library, 2017. Available <https://www.femaflavor.org/flavor> [accessed 2017 August 8].
98. Snow, N.H.; Slack, G.C. Head-space analysis in modern gas chromatography. *Trends Anal. Chem.* 2002, **21**: 608-617.
99. Bertholon, J.F.; Becquemin, M.H.; Annesi-Maesano, I.; Dautzenberg, B. Electronic cigarettes: A short review. *Respiration* 2013, **86**: 433-438.
100. Aulton, M.E.; Taylor, K.M.G. Aulton's Pharmaceutics: The Design and Manufacture of Medicines. 5th ed. Elsevier Health Sciences, 2018.
101. Marco, E.; Grimalt, J.O. A rapid method for the chromatographic analysis of volatile organic compounds in exhaled breath of tobacco cigarette and electronic cigarette smokers. *J. Chromatogr. A* 2015, **1410**: 51-59.
102. Herrington, J.S.; Myers, C. Electronic cigarette solutions and resultant aerosol profiles. *J. Chromatogr. A* 2015, **1418**: 192-199.
103. Lim, H.H.; Shin, H.S. Determination of volatile organic compounds including alcohols in refill fluids and cartridges of electronic cigarettes by headspace solid-phase micro extraction and gas chromatography-mass spectrometry. *Anal. Bioanal. Chem.* 2017, **409**: 1247-1256.
104. Poklis, J.L.; Wolf, C.E., 2nd; Peace, M.R. Ethanol concentration in 56 refillable electronic cigarettes liquid formulations determined by headspace gas chromatography with flame ionization detection (HS-GC-FID). *Drug Test. Analysis* 2017, doi: 10.1002/dta.2193 [Epub ahead of print].
105. Jiménez-Salcedo, M.; Tena, M.T. Determination of cinnamaldehyde, carvacrol and thymol in feedstuff additives by pressurized liquid extraction followed by gas chromatography-mass spectrometry. *J. Chromatogr. A* 2017, **1487**: 14-21.
106. Nisperos-Carriedo, M.O.; Shaw, P.E. Comparison of volatile flavor components in fresh and processed orange juices. *J. Agric. Food Chem.* 1990, **38**: 1048-1052.
107. Kelley, L.E.; Cadwallader, K.R. Identification and quantification of potent odorants in spearmint oils. *J. Agric. Food Chem.* 2017, doi: 10.1021/acs.jafc.6b04852 [Epub ahead of print].
108. Wang, X.; Xie, K.; Zhuang, H.; Ye, R.; Fang, Z.; Feng, T. Volatile flavor compounds, total polyphenolic contents and antioxidant activities of a China ginkgo wine. *Food Chem.* 2015, **182**: 41-46.
109. Russell, M.A.; Jarvis, M.; Iyer, R.; Feyerabend, C. Relation of nicotine yield of cigarettes to blood nicotine concentrations in smokers. *Br. Med. J.* 1980, **280**: 972-976.
110. Ramautar, R.; Sastre Toraño, J.; Somsen, G.W.; de Jong, G.W. Evaluation of CE methods for global metabolic profiling of urine. *Electrophoresis* 2010, **31**: 2319-2327.

111. Yamamoto, M.; Ly, R.; Gill, B.; Zhu, Y.; Moran-Mirabel, J.; Britz-McKibbin, P. Robust and high-throughput method for anionic metabolite profiling: Preventing polyimide aminolysis and capillary breakages under alkaline conditions in capillary electrophoresis-mass spectrometry. *Anal. Chem.* 2016, **88**: 10710-10719.
112. Maccani, J.Z.J.; Maccani, M.A. Altered placental DNA methylation patterns associated with maternal smoking: Current perspectives. *Adv. Genome Genet.* 2015, **2015**: 205-214.
113. Bahl, V.; Lin, S.; Xu, N.; Davis, B.; Wang, Y.; Talbot, P. Comparison of electronic cigarette refill fluid cytotoxicity using embryonic and adult models. *Reprod. Toxicol.* 2012, **34**: 529-537.
114. Robertson, O.H.; Loosli, C.G.; Puck, T.T.; Wise, H.; Lemon, H.M.; Lester, W. Tests for the chronic toxicity of propylene glycol and triethylene glycol on monkeys and rats by vapor inhalation and oral administration. *J. Pharmacol. Exp. Therap.* 1947, **91**: 52-76.
115. Werley, M.S.; McDonald, P.; Lilly, P.; Kirkpatrick, D.; Wallery, J.; Byron, P.; Venitz, J. Non-clinical safety and pharmacokinetic evaluations of propylene glycol aerosol in Sprague-Dawley rats and Beagle dogs. *Toxicol.* 2011, **287**: 76-90.
116. Farsalinos, K.E.; Polosa, R. Safety evaluation and risk assessment of electronic cigarettes as tobacco cigarette substitutes: a systematic review. *Ther. Adv. Drug Saf.* 2014, **5**: 67-86.
117. Scheffler, S.; Dieken, H.; Krischenowski, O.; Förster, C.; Branscheid, D.; Aufderheide, M. Evaluation of e-cigarette liquid vapor and mainstream cigarette smoke after direct exposure of primary human bronchial epithelial cells. *Int. J. Environ. Public Health* 2015, **12**: 3915-3925.
118. Fischer, S.T.; Lili, L.N.; Li, S.; Tran, V.T.; Stewart, K.B.; Schwartz, C.E.; Jones, D.P.; Sherman, S.L.; Fridovich-Keil, J.L. Low-level maternal exposure to nicotine associates with significant metabolic perturbations in second-trimester amniotic fluid. *Environ. Internat.* 2017, **107**: 227-234.
119. Revsin, B.; Morrow, G., 3rd. Imino acid transport in human diploid fibroblasts. *Exper. Cell Res.* 1979, **119**: 55-61.
120. Shelp, B.J.; Bown, A.W.; McLean, M.D. Metabolism and functions of gamma-aminobutyric acid. *Trends Plant Sci. Rev.* 1999, **4**: 446-452.
121. Lu, J.; Zhang, Q.; Tan, D.; Luo, W.; Zhao, H.; Ma, J.; Liang, H.; Tan, Y. GABA A receptor π subunit promotes apoptosis of HTR-8/SVneo trophoblastic cells: Implications in preeclampsia. *Int. J. Mol. Med.* 2016, **38**: 105-112.
122. Zhang, S.; Regnault, T.R.H.; Barker, P.L.; Botting, K.J.; McMillen, I.C.; Roberts, C.T.; Morrison, J.L. Placental adaptations in growth restriction. *Nutrients* 2015, **7**: 360-389.
123. McFarland, B.J.; Seidler, F.J.; Slotkin, T.A. Inhibition of DNA synthesis in neonatal rat brain regions caused by acute nicotine administration. *Development. Brain Res.* 1991, **58**: 223-229.

124. Ginzkey, C.; Stueber, T.; Friehs, G.; Koehler, C.; Hackenberg, S.; Richter, E.; Hagen, R.; Kleinsasser, N.H. Analysis of nicotine-induced DNA damage in cells of the human respiratory tract. *Toxicol. Lett.* 2012, **208**: 23-29.
125. Raez Villanueva, S.; Ma, C.; Kleiboer, S.; Holloway, A. The effects of electronic cigarette vapour on placental Htr-8/SVneo trophoblast cells. 2017, McMaster University.
126. Mannelli, C.; Ietta, F.; Avanzati, A.M.; Skarzynski, D.; Paulesu, L. Biological tools to study the effects of environmental contaminants at the feto-maternal interface. *Dose Resp.* 2015, **13**: 1-11.
127. Gruslin, A.; Qiu, Q.; Tsang, B.K. Influence of maternal smoking on trophoblast apoptosis throughout development: Possible involvement of Xiap regulation. *Biol. Reprod.* 2001, **65**: 1164-1169.

3.7 Supplementary Tables and Figures

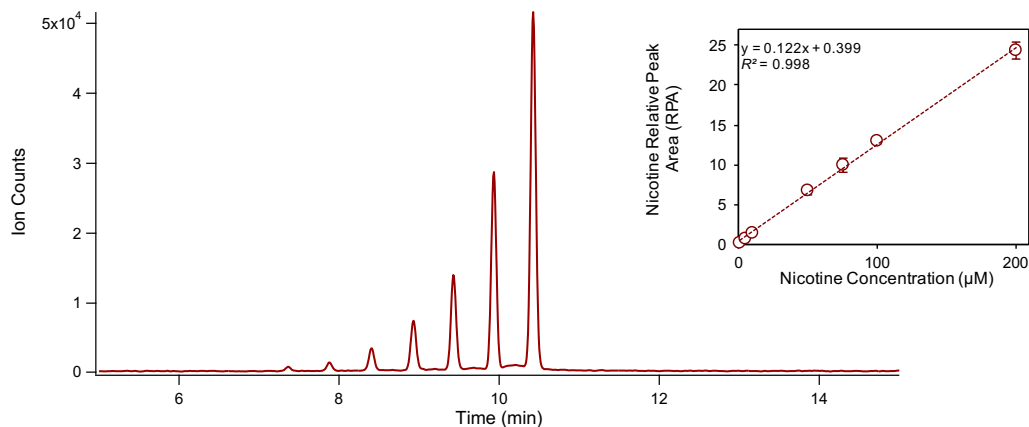


Figure S3.1. Extracted ion electropherogram for nicotine calibration standards with concentrations ranging from 0.5 to 200 μM in dH₂O. The nicotine calibration curve is shown, with the line of best fit is represented as a dotted line. Error bars show the standard deviation ($n = 3$).

Table S3.1. Summary of 49 metabolites consistently detected in first trimester HTR-8/SVneo cells, including *m/z*, RMT, ionization mode (p = ESI+, n = ESI-), molecular formula, and compound ID.

<i>m/z</i> :RMT:mode	Formula	Mass Error	Compound ID	Classification
74.0237:0.981:p	C ₂ H ₃ NO ₂	3.83 ppm	Iminoglycine	Amino acid derivative
76.0393:0.738:p	C ₂ H ₅ NO ₂	4.20 ppm	Glycine	Amino acid
90.0550:0.614:p	C ₃ H ₇ NO ₂	2.72 ppm	<i>Unknown</i>	Unknown
90.0550:0.783:p	C ₃ H ₇ NO ₂	1.61 ppm	Alanine	Amino acid
104.0706:0.647:p	C ₄ H ₉ NO ₂	0.05 ppm	γ -amino-butyric acid	Amino acid derivative
104.1070:0.557:p	C ₅ H ₁₃ NO	1.05 ppm	Choline	Quaternary ammonium salt
106.0499:0.868:p	C ₃ H ₇ NO ₃	3.12 ppm	Serine	Amino acid
116.0706:0.925:p	C ₅ H ₉ NO ₂	2.54 ppm	Proline	Amino acid
118.0863:0.858:p	C ₅ H ₁₁ NO ₂	0.47 ppm	Valine	Amino acid
120.0655:0.907:p	C ₄ H ₉ NO ₃	1.00 ppm	Threonine	Amino acid
129.0658:0.754:p	C ₅ H ₈ N ₂ O ₂	2.74 ppm	Dihydrothymine	Ureide
132.0655:1.021:p	C ₅ H ₉ NO ₃	0.15 ppm	4-Hydroxyproline	Amino acid derivative
132.0767:0.770:p	C ₄ H ₉ N ₃ O ₂	4.14 ppm	Creatine	Amino acid
132.1019:0.865:p	C ₆ H ₁₃ NO ₂	0.04 ppm	Isoleucine	Amino acid
132.1019:0.874:p	C ₆ H ₁₃ NO ₂	0.72 ppm	Leucine	Amino acid
133.0608:0.905:p	C ₄ H ₈ N ₂ O ₃	1.74 ppm	Asparagine	Amino acid
133.0972:0.578:p	C ₅ H ₁₂ N ₂ O ₂	0.72 ppm	Ornithine	Amino acid
134.0448:0.982:p	C ₄ H ₇ NO ₄	0.63 ppm	Aspartic acid	Amino acid
147.0764:0.926:p	C ₅ H ₁₀ N ₂ O ₃	1.23 ppm	Glutamine	Amino acid
147.1128:0.595:p	C ₆ H ₁₄ N ₂ O ₂	2.07 ppm	Lysine	Amino acid
148.0604:0.936:p	C ₅ H ₉ NO ₄	0.23 ppm	Glutamic acid	Amino acid
150.0589:0.915:p	C ₅ H ₁₁ NO ₂ S	0.49 ppm	Methionine	Amino acid
156.0768:0.635:p	C ₆ H ₉ N ₃ O ₂	0.94 ppm	Histidine	Amino acid
160.1331:0.713:p	C ₈ H ₁₇ NO ₂	1.84 ppm	<i>Unknown</i>	Unknown
162.1124:0.726:p	C ₇ H ₁₅ NO ₃	1.42 ppm	Carnitine (C0)	Amino acid derivative
166.0863:0.935:p	C ₉ H ₁₁ NO ₂	0.93 ppm	Phenylalanine	Amino acid
175.1190:0.626:p	C ₆ H ₁₄ N ₄ O ₂	0.27 ppm	Arginine	Amino acid
182.0812:0.965:p	C ₉ H ₁₁ NO ₃	2.91 ppm	Tyrosine	Amino acid

202.1809:0.804:p	C ₁₁ H ₂₃ NO ₂	0.72 ppm	Unknown	Unknown
204.1231:0.772:p	C ₉ H ₁₇ NO ₄	1.15 ppm	Acetylcarnitine (C2)	Acyl carnitine
205.0972:0.935:p	C ₁₁ H ₁₂ N ₂ O ₂	1.73 ppm	Tryptophan	Amino acid
218.1387:0.803:p	C ₁₀ H ₁₉ NO ₄	0.07 ppm	Propionylcarnitine (C3)	Acyl carnitine
232.1543:0.814:p	C ₁₁ H ₂₁ NO ₄	0.15 ppm	Butyrylcarnitine (C4)	Acyl carnitine
246.1700:0.826:p	C ₁₂ H ₂₃ NO ₄	0.06 ppm	iso-valerylcarnitine (iso-C5)	Acyl carnitine
246.1700:0.831:p	C ₁₂ H ₂₃ NO ₄	3.59 ppm	Valerylcarnitine (C5)	Acyl carnitine
284.0984:1.128:p	C ₁₀ H ₁₃ N ₅ O ₅	3.33 ppm	Guanosine	Purine nucleoside
307.0833:1.027:p	C ₂₀ H ₃₂ N ₆ O ₁₂ S ₂	0.79 ppm	Glutathione (oxidized)	Peptide
308.0911:1.094:p	C ₁₀ H ₁₇ N ₃ O ₆ S	1.68 ppm	Glutathione (reduced)	Peptide
337.1693:0.831:p	C ₁₆ H ₂₄ N ₄ O ₂ S	0.08 ppm	Unknown	Unknown
89.0244:1.173:n	C ₃ H ₆ O ₃	0.93 ppm	L-Lactic acid	Hydroxy carboxylic acid
102.0561:0.939:n	C ₄ H ₉ NO ₂	4.43 ppm	Unknown	Unknown
128.0353:1.029:n	C ₅ H ₇ NO ₃	4.56 ppm	Oxoproline	Amino acid derivative
132.0302:1.003:n	C ₄ H ₇ NO ₄	0.24 ppm	Iminodiacetic Acid	Amino acid
135.0299:0.516:n	C ₄ H ₈ O ₅	0.02 ppm	Threonic acid	Sugar acid
137.0465:0.516:n	C ₅ H ₆ N ₄ O	2.80 ppm	8-Hydroxypurine	Purinone
179.0562:0.516:n	C ₆ H ₁₂ O ₆	1.74 ppm	Glucose	Hexose
183.0887:0.513:n	C ₇ H ₁₂ N ₄ O ₂	0.27 ppm	Unknown	Unknown
505.9885:1.248:n	C ₁₀ H ₁₆ N ₅ O ₁₃ P ₃	3.10 ppm	ATP	Purine ribonucleoside triphosphate
662.1018:0.639:n	C ₂₁ H ₂₇ N ₇ O ₁₄ P ₂	0.54 ppm	NAD ⁺	(5'→5')-Dinucleotide

^a Most probable formula is presented in the case of unknowns/tentatively identified compounds

^b All metabolites were tentatively identified by mass match using the ESI+/ESI- mass spectrum, Molecular Formula Generator (MFG), and Metlin database search.

CHAPTER IV.

CONCLUSION AND FUTURE DIRECTIONS

4.1 Overview of Major Thesis Contributions

Metabolomics is a powerful tool that can be used to improve upon our understanding of various aspects of human health and assess the impact of different stressors on metabolic networks. In this thesis, two major projects in metabolomics associated with public health and disease management/prevention have been presented. *Chapter I* presents an overview of the role of metabolomics in disease diagnostics and biomarker discovery in addition to exploring the impact of endogenous and exogenous factors on the metabolome of biological systems. Further, it presents the various analytical platforms widely used in metabolomics, with a focus on the platform used in this work: multisegment injection-capillary electrophoresis-mass spectrometry (MSI-CE-MS). Finally, it discusses the data workflow involved in metabolomic analysis, including study design, quality assurance, method validation, and statistical analysis. As presented, metabolomics represents a valuable tool in understanding the pathophysiology of human diseases and targets/mechanisms of various stressors, such as environmental contaminants, on human health.

In *Chapter II*, a nontargeted metabolomics approach was applied to analyze the impact of controlled and relaxed diets within a small set of individuals with phenylketonuria (PKU), a potentially debilitating metabolic disease with compromised phenylalanine (Phe) to tyrosine (Tyr) conversion. Severe accumulation of Phe and Tyr deficiency in PKU leads to irreversible neurological

impairments, which can be readily prevented with immediate dietary restriction of Phe-containing foods (*i.e.*, protein heavy foods) and supplementation with non-Phe amino acids formulas.¹ This work has demonstrated the applicability of MSI-CE-MS for the screening of PKU that is validated against the clinical screening method of ultra-performance liquid chromatography with ultraviolet detection (UPLC-UV) in monitoring biomarkers of PKU (Phe and Tyr) in blood. Furthermore, a number of Phe- and Tyr-derived catabolites were detected in the urine of PKU patients, including *N*-phenylacetylglutamine, phenylsulfate, phenylpyruvate, phenyllactate, and *o*-hydroxyphenylacetate. These Phe catabolites, excluding phenyllactate, were found to have strong and positive correlations with urinary Phe excretion, which demonstrates the potential for the use of urine as a less invasive biospecimen for therapeutic monitoring of PKU patients. Also, the use of MSI-CE-MS can minimize analysis times while maintaining accuracy for reliable quantification of clinically relevant metabolites, as well as a wide range of polar/ionic metabolites that can act as biomarkers of disease status in PKU, providing detailed information regarding the metabolic phenotype of individual patients. Multivariate and univariate analysis of single-spot urine samples from individuals with highly variable concentrations of plasma Phe demonstrated lower levels of carnitine and acylcarnitines (C2 and C5), suggesting an inhibition of fatty acid β -oxidation and mitochondrial stress in PKU patients who do not maintain Phe levels within optimal therapeutic target ranges due to poor dietary compliance. This is consistent with results seen by Weigel *et.*

al.,² who demonstrated reduced carnitine bioavailability as a result of increased levels of phenylacetic acid in individuals with PKU on a diet with zero or minimal intake of red meats and dairy products. Products of alternative histidine metabolism, imidazolelactic acid and imidazoleacetic acid, were also found to be significantly correlated with urinary Phe excretion, suggesting the presence of hormonal changes (*i.e.*, glucagon) as a result of excess Phe or deficiencies of folic acid and/or vitamin B12. There were also significant elevations in creatinine/creatinine ($p < 0.05$) and lower levels of Leu, Ile, α -aminoadipic acid, and Ser in individual PKU patients with plasma Phe concentrations exceeding the therapeutic target range of 360 μM set by the American College of Medical Genetics and Genomics (ACMGG). The purpose of this work was to evaluate markers of dietary intake in individuals with levels of Phe greater than the recommended clinical concentration as a way of monitoring dietary compliance. Creatinine is a marker of meat intake and an elevation may suggest the increased consumption of meat products and/or protein; however, no significant elevations in other markers of protein intake (*e.g.*, 3-methylhistidine and carnosine) were observed.^{3,4} For nontargeted analysis, only individuals supplementing their diet with a Phe-free amino acid formula were included in order to minimize variability of response. Lower levels of amino acids present in these formulas (Leu, Ile, and Ser) may indicate that individuals with higher levels of Phe are not consuming the prescribed amount of formula consistently or this may be a result of timing of sample collection and/or meals.⁵ Metabolomics studies examining the

pathophysiology of PKU has been limited, with little work focused on the impact of complex interactions of the PKU diet and/or treatment on the metabolome. Overall, this project demonstrates the complexity of the PKU disease spectrum due to confounding factors such as age, dietary compliance, and disease severity.

Chapter III explores the potential deleterious effects of e-cigarette vapour exposure on placental cell function in the first and third trimester. E-cigarettes are generally considered by the public to be a healthier alternative to smoking conventional tobacco cigarettes; however, the biological effects of vaporized flavour additives in popular e-cigarette liquid formulations is largely unknown. Furthermore, e-cigarettes represent a serious public health risk due to unregulated advertising, unawareness, and limited availability of long-term studies assessing their impact. Aside from the listed constituents of propylene glycol, glycerol, nicotine, and flavourings, there is little detail regarding ingredients in e-cigarette liquids that is provided by the manufacturer. Analysis of various e-cigarette liquids (flavourless, blue raspberry) by MSI-CE-MS and headspace-gas chromatography-mass spectrometry (HS-GC/MS) confirmed the chemical complexity of these consumer products. Nicotine-containing e-liquids (12 mg/mL nicotine concentration) also contained many tobacco impurities and nicotine degradation products, such as cotinine, nicotyrine, and 2-hydroxynicotine. Also, the blue raspberry flavoured e-liquid contained 12 known flavour additives which are generally recognized as safe (GRAS) for human ingestion by the Flavor and Extracts Manufacturing Association (FEMA) and the U.S. Food and Drug

Administration (FDA), but have not been evaluated for safety when inhaled.⁶ Exposure to a flavourless e-liquid vapour without nicotine showed no measurable metabolic differences in comparison to first trimester and third trimester control cells. However, first trimester trophoblast cells were determined to be more susceptible to the effects of e-cigarette vapour exposure as no significant metabolic differences were observed in third trimester cells under treatment with flavoured (Blue Balls) and flavourless (Blacklisted) e-liquid vapour media at two dosage levels. This is consistent with reports demonstrating the higher susceptibility of the first trimester to chemical exposures.⁷ Indeed, the presence of flavour additives led to acute, yet significant, changes in amino acid metabolism (Pro, Ile) and importantly, GABA synthesis/transport. This supports the hypothesis that the GRAS designation assigned to flavour compounds may not be applicable with inhalation and that these compounds pose a risk to human health, especially within critical periods of development. Overall, this work provided valuable insight into the potential harm of e-cigarettes on fetal development and provides a basis for future analysis into the effects of specific flavouring agents on placental metabolism.

4.2 Evaluating the Impact of Nutrition on the PKU Metabolome

The study presented in *Chapter II* has a number of uncontrolled variables, which significantly reduces the statistical power of the conclusions made in this thesis. In this study, a small number of individuals with PKU were recruited. The

target study population was 30 PKU patients, with varying disease severities (*i.e.*, non-PKU HPA, mild PKU, and classic PKU), with age grouping distributions of infants/young children ($n = 10$), adolescents/teenagers ($n = 10$), and adults over 18 y ($n = 10$). Patients were recruited by convenience with recruitment occurring during their regularly scheduled appointments at McMaster Children's Hospital. While age distributions were fairly consistent with target subgroups, with the exception of infants/young children under 6 y ($n = 6$), there was a discrepancy between number of plasma samples obtained for individual patients, which was predominantly based on age. Infants are monitored weekly for the first year of life, whereas children between 1 and 12 y are typically monitored biweekly or monthly.⁸ In contrast, adults are only monitored 1-2 times per year. Due to a short recruitment and sample collection period (< 8 months), samples were, for the most part, limited to 1 spot urine and blood plasma sample for teenager/adult patients. One of the major objectives in this study was to monitor dietary compliance; however, the lack of samples corresponding to older PKU patients makes this difficult since adherence to the restrictive PKU diet becomes more irregular with patient age and, in general, the diets of infants and young children are often tightly controlled by parents.⁹ In addition, the study did not recruit healthy individuals for controls, but rather individuals with a non-PKU metabolic disease. Comparison of individuals with PKU with the non-PKU group is, therefore, not representative of the difference between the healthy and diseased state and there is expected to be considerable metabolic variations within the

control group due to the differing diagnoses and treatment plans (*e.g.*, protein-restricted and non-protein restricted diets). For this reason, they were not included in the statistical comparisons. In addition, we could not use individuals with mild PKU or hyperphenylalaninemia (HPA) as a control group for comparison of metabolic differences with disease severity as only two individuals recruited had this diagnosis.

Meal timing in relation to sample collection and the degree of completeness and/or detail with dietary records represented another significant source of variation within this study. Consumption of the amino acid supplement and periods of fasting may be responsible for fluctuations of Phe and other metabolites of interest within and between individuals.⁵ There was no participant requirement prior to sample collection (*e.g.*, 12 h fasting), which adds a significant source of variability between patients and between time points, which makes data analysis and interpretation difficult. Furthermore, diet records were not very detailed or were absent for some individuals recruited. A well-controlled study where the premise of using metabolomics as a way of monitoring dietary compliance could be evaluated will require the use of controlled meal plans and/or detailed diet records. For example, a study with some individuals having full compliance and low Phe/protein intake and others with slightly increased Phe intake, which would result in Phe concentrations that exceed clinical recommendations (360 μM), would allow a better association of diet and Phe response. Analysis of compliance could therefore be evaluated with more

confidence with control over diet. In addition, requirements with meal timing and fasting prior to sample collections will also improve the study design, especially within individuals taking an amino acid supplement and following a controlled diet. Furthermore, a set number of matched plasma and urine samples need to be collected for each study participant for better visualization of the effect of diet over the PKU metabolome within individuals. In addition to extreme variability presented with age, dietary compliance/records, as well as samples collected, the study size is far too small to be considered statistically powerful, especially in terms of biomarker discovery. The study should be repeated, with tighter control as described, with a larger number of individuals of each age grouping in addition to a healthy set of controls.

The observation of a positive correlation of urinary Phe and products of alternative histidine metabolism, imidazolelactic acid and imidazoleacetic acid, requires deeper investigation into changes in hormone levels (*i.e.*, glucagon and cortisol) and vitamin/micronutrient deficiencies (*i.e.*, folic acid and vitamin B12) as a result of adherence or non-adherence to tight dietary regulations and supplementation with amino acids. The identification of these metabolites must be confirmed using MS/MS fragmentation patterns in addition to the use of internal standards for confirmation of fragmentation and relative migration. It has been shown that glucagon stimulates hepatic phenylalanine hydroxylase in rats¹⁰ and amino acid loading (*i.e.*, Arg and Phe) results in the rise of plasma insulin and glucagon in humans.¹¹ Further, increased insulin and glucagon secretion leads to

reduced extracellular concentrations of amino acids, stimulation of amino acid transport for protein synthesis, and activation of enzymes involved in gluconeogenesis and urea synthesis, in addition to tyrosine α -ketoglutarate transaminase and phenylalanine pyruvate transaminase.¹¹ The enzyme phenylalanine pyruvate transaminase also shows specificity towards histidine (*i.e.*, histidine pyruvate transaminase); histidine pyruvate transaminase is the enzyme responsible for the conversion of His to imidazolepyruvic acid and, further, imidazoleacetic acid and imidazolelactic acid.¹² Further investigation into the enzymatic activity of phenylalanine/histidine pyruvate transaminase in addition to hormone secretion in individuals with PKU in comparison to healthy controls upon amino acid and/or increased intake of Phe will give more insight into the complex relationship of diet and metabolism within PKU.

4.3 Targeted Evaluation of Vaporized Flavour Chemicals in E-Cigarettes

The study presented in *Chapter III* is a pilot study for the initial evaluation of the potential toxic health effects of flavoured e-cigarettes vapours. There are a number of limitations to this study, which includes issues with normalization (*i.e.*, PQN *vs.* normalization to protein concentration) and small sample sizes ($n = 5$ for each treatment group). Protein concentrations were determined using the Bradford Assay in order to normalize the data and account for differences in cell growth between treatment groups.^{13,14} Cells were grown in different batches spanning several months apart and protein concentrations were determined at the time of

receiving samples. Sample pretreatment required the concentration and reconstitution of cell extracts, leaving minimal amounts for protein concentration determination. On average, there was a 7-fold difference between protein concentrations measured for different batches under the same exposure conditions. Probabilistic quotient normalization (PQN) was carried out to correct for batch-to-batch differences between protein concentrations as well as to correct for the differences in relative peak area (RPA) responses of metabolites being analyzed. PQN normalization thereby enabled concentration comparison of 1% and 10% *v/v* exposed placental cells by reducing total biological variation from 83% to 36% (median CV of 48 features).

As a pilot study, this work has shown that there is reason to be concerned with the potential effects of e-cigarettes; however, these results must be validated by repeating the study with a larger sample population and more controlled experimental design in order to minimize systematic differences between batches.¹⁵ Sample sizes for each treatment group should be between 10 to 40 in order to increase confidence and significance within the study.¹⁶ Further, the experimental design must be adjusted as to avoid batch effects, with normalization used to correct for unwanted variation that arises as a result of sample preparation, treatment, and instrumental analysis.¹⁷ While normalization using protein concentration is common for metabolomics studies, the presence of buffers and solvents for quenching can result in inaccurate protein measurements. Furthermore, in this study, there was limited cell extract available for reliable

concentration determination using the Bradford Assay. DNA concentration measurements from the sample cell pellet, which is discarded in the sample preparation process, may be a better technique for data normalization as it has been determined to be a more accurate representation of cell number. Further, a method to validate consistency in vapour media preparation and protocol is necessary, especially considering an automatic machine was not utilized. Limitations in the e-cigarette vapour apparatus such as over-use of the e-cigarette and exposing the vapour system to the open environment when refilling the e-cigarette cartomizer may have resulted in inconsistent media exposure to the e-cigarette vapour.¹⁸ Determination of nicotine concentrations in the vapour exposed media (BB12 and BL12) for first trimester trophoblast cells showed similarity in nicotine concentrations, demonstrating consistency in media exposure; however, there is no way to evaluate the integration of the e-cigarette vapour into the media for the e-liquids containing no nicotine.

A limited evaluation of flavoured e-cigarette liquids has been presented due to the nature of this pilot study. The blue raspberry flavoured e-liquid was chosen as it has been demonstrated that women of reproductive age are more likely to choose fruity flavours and this flavour was the most popular at the site of purchase.^{18,19} The thorough examination of only one flavour greatly reduces the strength and scope of this research due to the large variety of flavours available and flavour additives that may pose a risk to human health. In order to determine the agent(s) responsible for changes observed with exposure to flavoured e-

cigarette liquids, it is necessary to perform exposure studies with varying concentrations to monitor potential sub-acute toxicity and cytotoxicity of isolated flavour additives. Further, a more comprehensive analysis of a large variety of flavoured e-cigarette liquids is necessary to better assess the potential risk e-cigarettes pose on human and, in particular, maternal/fetal health.

4.4 Overall Perspective

In summary, this work has presented an application of metabolomics using a unique data workflow based on MSI-CE-MS to evaluate the effects of modifiable lifestyle factors such as disease and smoking on human health with an emphasis on disease prevention and management. Nontargeted metabolomics analysis of the PKU metabolome when considering the complex interactions of diet and treatment with altered metabolism is extremely limited and this thesis strives to improve the understanding of the impact of diet/nutrition on PKU. Also, the effects of e-cigarette vapour *in vitro* and *in vivo* is a relatively new field of research, and this work demonstrates the benefits of a nontargeted metabolomics approach to assessing the sub-acute toxicity of e-cigarette vapour.²⁰ Overall, this thesis has demonstrated the applicability of metabolomics using MSI-CE-MS in the evaluation of the potential toxic health effects of e-cigarette flavouring additives, as well as the important impact of diet compliance and continuous therapeutic monitoring on manageable genetic diseases, such as PKU, for prevention of adverse health outcomes in both children and older adults.

4.5 References

1. Williams, R.A.; Mamotte, C.D.S.; Burnett, J.R. Phenylketonuria: An inborn error of phenylalanine metabolism. *Clin. Biochem. Rev.* 2008, **29**: 31-41.
2. Weigel, C.; Kiener, C.; Meier, N.; Schmid, P.; Rauh, M.; Rascher, W.; Knerr, I. Carnitine status in early-treated children, adolescents and young adults with phenylketonuria on low phenylalanine diets. *Ann. Nutr. Metab.* 2008, **53**: 91-95.
3. O’Gorman, A.; Gibbons, H.; Brennan, L. Metabolomics in the identification of biomarkers of dietary intake. *Comput. Struct. Biotechnol. J.* 2013, **4**: e201301004.
4. Mayersohn, M.; Conrad, K.A.; Achari, R. The influence of a cooked meat meal on creatinine plasma concentration and creatinine clearance. *Br. J. Clin. Pharmacol.* 1983, **15**: 227-230.
5. Cleary, M.; Trefz, F.; Muntau, A.C.; Feillet, F.; van Spronsen, F.J.; Burlina, A.; Bélanger-Quintana, A.; Gizewska, M.; Gasteyger, C.; Bettiol, E.; Blau, N.; MacDonald, A. Fluctuations in phenylalanine concentrations in phenylketonuria: A review of possible relationships with outcomes. *Molec. Genet. Metab.* 2013, **110**: 418-423.
6. Flavor & Extract Manufacturers Association (FEMA), FEMA Flavor Ingredient Library, 2017. Available <https://www.femaflavor.org/flavor> [accessed 2017 August 8].
7. Gruslin, A.; Qiu, Q.; Tsang, B.K. Influence of maternal smoking on trophoblast apoptosis throughout development: Possible involvement of Xiap regulation. *Biol. Reprod.* 2001, **65**: 1164-1169.
8. Vockley, J.; Andersson, H.C.; Antshel, K.M.; Braverman, N.E.; Burton, B.K.; Frazier, D.M.; Mitchell, J.; Smith, W.E.; Thompson, B.H.; Berry, S.A. Phenylalanine hydroxylase deficiency: diagnosis and management guideline. *Genet. Med.* 2014, **16**: 188-200.
9. Jurecki, E.R.; Cederbaum, S.; Kopesky, J.; Perry, K.; Rohr, F.; Sanchez-Valle, A.; Viau, K.S.; Sheinin, M.Y.; Cohen-Pfeffer, J.L. Adherence to clinic recommendations among patients with phenylketonuria in the United States. *Mol. Genet. Metab.* 2017, **120**: 190-197.
10. Beirne, E.; Carty, M.P.; Donlon, J. Effect of glucagon on hepatic phenylalanine hydroxylase in vivo. *Bioscience Reports* 1985, **5**: 463-467.
11. Güttler, F.; Kühl, C.; Pedersen, L.; Påby, P. Effects of oral phenylalanine load on plasma glucagon, insulin, amino acid and glucose concentrations in man. *Scan. J. Clin. Lab. Invest.* 1978, **38**: 255-260.
12. Emes, A.V.; Hassall, H. The degradation of L-histidine in the rat. *Biochem. J.* 1973, **136**: 649-658.
13. Silva, L.P.; Lorenzi, P.L.; Purwaha, P.; Yong, V.; Hawke, D.H.; Weinstein, J.N. Measurement of DNA concentration as a normalization strategy for metabolomic data from adherent cell lines. *Anal. Chem.* 2013, **85**: 9536-9542.

14. Dietmair, S.; Timmins, N.E.; Gray, P.P.; Nielsen, L.K.; Krömer, J.O. Towards quantitative metabolomics of mammalian cells: Development of a metabolite extraction protocol. *Anal. Biochem.* 2010, **404**: 155-164.
15. Mertens, B.J.A. Transformation, normalization and batch effect in the analysis of mass spectrometry data for omics studies. In *Statistical Analysis of Proteomics, Metabolomics, and Lipidomics Data Using Mass Spectrometry*. Eds. Datta, S.; Mertens, B.J.A. Gainesville, FL, USA: Springer International Publishing, 2017: 1-21, doi: 10.1007/978-3-319-45809-0.
16. Hertzog, M.A. Considerations in determining sample size for pilot studies. *Res. Nursing Health* 2008, **31**: 180-191.
17. Silva, L.P.; Lorenzi, P.L.; Purwaha, P.; Yong, V.; Hawke, D.H.; Weinstein, J.N. Measurement of DNA concentration as a normalization strategy for metabolomic data from adherent cell lines. *Anal. Chem.* 2013, **85**: 9536-9542.
18. Kleiboer, S.; Holloway, A. *The effects of electronic cigarette vapour on placenta growth and development*. Unpublished Undergraduate Thesis. McMaster University, 2017.
19. Orton, S.; Bowker, K. Cooper, S.; Naughton, F.; Ussher, M.; Pickett, K.E.; Leonardi-Bee, J.; Sutton, S.; Dhalwani, N.N.; Coleman, T. Longitudinal cohort survey of women's smoking behavior and attitudes in pregnancy: Study methods and baseline data. *BMJ Open* 2014, **4**: e004915.
20. Aug, A.; Altraja, S.; Kilk, K.; Porosk, R.; Soomets, U.; Altraja, A. E-cigarette affects the metabolome of primary normal human bronchial epithelial cells. *PLoS One* 2015, **10**: e0142053.